

Investigations into the mode of action of biologically active molecules

zur Erlangung des Grades
DOCTOR RERUM NATURALIUM

(Dr. rer. nat.)

dem Fachbereich Chemie der

TU-Graz

vorgelegte

DISSERTATION

von

M. Sc.

Jana Rentner



Graz, 01.06.2012

1. Gutachter: Prof. Dr. Rolf Breinbauer
2. Gutachter: Prof. Dr. Ernst Lankmayr

Die vorliegende Doktorarbeit wurde in der Zeit von Januar 2008 bis Mai 2012 im Fachbereich Chemie unter der Betreuung von Prof. Dipl.-Ing. Dr. rer. nat. Rolf Breinbauer am Institut für Organische Chemie der Technischen Universität Graz durchgeführt.

EIDESSTATTLICHE ERKLÄRUNG

Ich erkläre an Eides statt, dass ich die vorliegende Arbeit selbstständig verfasst, andere als die angegebenen Quellen/Hilfsmittel nicht benutzt, und die den benutzten Quellen wörtlich und inhaltlich entnommene Stellen als solche kenntlich gemacht habe.

Graz, am

.....

(Unterschrift)

Danksagung

An dieser Stelle möchte ich mich bei Prof. Rolf Breinbauer für die Überlassung dieser interessanten und interdisziplinären Forschungsthemen, für sein in mich gestecktes Vertrauen, sowie für die Möglichkeit Verantwortung am Institut übernehmen zu können und die Freiheit selbständig forschen zu dürfen, bedanken. Danke Rolfi! ☺

Prof. Dr. Lankmayr danke ich herzlichst für die Übernahme des Zweitgutachtens.

Ein herzliches Dankeschön gebührt Martin Peters und Jakob Pletz für die lustige Zeit im Labor. Desweiteren möchte ich mich beim Arbeitskreis (Hilmar Schröder, Xuepu Yu, Joanna (Asia) Krysiak, Melanie Trobe, Mario Leypold, Jakov Ivkovic und Nicole Mayer) und allen Institutsmitarbeitern für das angenehme Arbeitsklima bedanken. Astrid Nauta, unserer guten Seele am Institut, danke ich für ihre ständige Einsatzbereitschaft, egal was ich benötigte oder welche Fragen ich hatte. Prof. Hansjörg Weber möchte ich für seine engagierte fachliche Unterstützung bei komplexen NMR-Problemstellungen und für die Einführung ins Badmintonspielen danken. Besonderer Dank gilt auch den ACIB-Mitarbeitern, mit denen ich so kollegial zusammen arbeiten konnte, insbesondere Dr. Mandana Gruber und Dr. Gernot Strohmeier. Gernot möchte ich auch herzlichst für seine engagierte Einführung in die "Kunst" der HPLC-Gerätebedienung und seine andauernde Hilfsbereitschaft danken. Ich weiß jetzt, an welchen Schrauben ich drehen muss, damit die Geräte vernünftig funktionieren. Prof. Christian Slugovc danke ich für die Bereitstellung der Metathesekatalysatoren und Prof. Robert Saf für die Messungen der hochaufgelösten Massen.

Meinen Studenten Mathias Pickl, Sebastian Grimm, Lukas Hutter, Anna-Maria Hatzl, Marko Kljajic, Lisa Ramona Offner, Peter Finichiu, Michaela-Christina Melcher, Katharina Plasch und Christian Marco Pichler bin ich für ihre vielen Überstunden, ihre Freude an der Chemie und ihre aufopfernde Mitarbeit an meinen Forschungsthemen zu großem Dank verpflichtet. Danke für diese unvergessliche Zeit.

Bei Dr. Uwe Rix und Prof. Giulio Superti-Furga (CeMM, Wien), bei Dr. Burghard König, Dr. Waander Riethorst, Dr. Ferdinand Zepeck, Dr. Klaus Totschnig und Dr. Barbara Marktl (Sandoz, Kundl in Kooperation mit dem ACIB, Graz) und bei Georg Schneditz und Prof. Ellen Zechner (Uni Graz) möchte ich mich herzlichst für die produktiven Kooperationen und für zahlreiche, fruchtbare Diskussionen bedanken.

Besonders dankbar bin ich auch Uwe Groß für seine Geduld, für gemeinsame Wochenenden im Labor und für zahlreiche erholsame und inspirierende Kakaopausen. Meinen Eltern und meinem Bruder möchte ich für ihre andauernde Unterstützung danken, ohne die diese Dissertation wahrscheinlich nicht möglich gewesen wäre. Bei meinen Freunden und allen, die ich noch nicht namentlich genannt habe, die mich ebenfalls unterstützt haben, bedanke ich mich herzlichst für die schöne Zeit in Graz.

Vielen Dank!

"Das Leben ist zu kostbar, um es dem Schicksal zu überlassen."

-Deus X. Machina-

Walter Moers, *Die 13 ½ Leben des Käpt'n Blaubär*, Eichborn AG, Frankfurt/Main, **1999**, p. 5.

*Diese Arbeit ist
meiner Oma Elfriede und meinem Cousin Christian
gewidmet.*

Zusammenfassung

Oftmals bleiben Nebenwirkungen von Medikamenten lange Zeit unentdeckt. Sind die Nebenwirkungen allerdings zu gravierend, müssen diese Medikamente wieder vom Markt genommen werden. Um dem entgegen zu wirken, wurde in dieser Dissertation in Kooperation mit dem „Research Center for Molecular Medicine“ in Wien die „Compound-Centric Chemical Proteomics“ Methode zur Identifizierung von allen Proteinen, die mit dem Wirkstoff wechselwirken, angewandt. Eine Herausforderung bei der Chemischen Proteomik ist die Immobilisierung der Wirkstoffe an einer festen Phase, welche die Aktivität des Medikaments auf keinen Fall beeinträchtigen darf. Deshalb wurden in dieser Arbeit drei verschiedene Immobilisierungsmethoden von Wirkstoffen inklusive unterschiedlicher Linkersynthesen entwickelt. Chemisches Hauptaugenmerk wurde dabei auf die bio-orthogonale Thiol-En Reaktion und Olefin-Kreuzmetathese sowie die erst vor wenigen Jahren entwickelte oxidative Kreuzkupplung durch doppelte CH-Aktivierung gelegt. Alle drei Reaktionstypen konnten erfolgreich als Verlinkungsmethoden implementiert werden.

Zum Testen unserer entwickelten Immobilisierungsstrategien wurden Thalidomid und die später entwickelten Derivate Pomalidomid und Lenalidomid gewählt, deren molekularer Mechanismus für die Entstehung der Teratogenität selbst nach 50 Jahren immer noch nicht vollständig aufgeklärt ist. Nach der Synthese dieser drei Wirkstoffe in zwei bis sechs Stufen wurde Thalidomid über zwei selbst entwickelte Immobilisierungsmethoden, Pomalidomid und Lenalidomid jeweils über eine Immobilisierungsmethode verlinkt. Das Chemische Proteomik Screening verlief jedoch aufgrund der sensiblen Zellextrakte, die wahrscheinlich denaturiert waren, bisher ohne Erfolg.

Neben den bereits entwickelten Medikamenten finden sich in der Natur immer wieder zahlreiche Naturstoffe mit nutzbarer biologischer Aktivität. Am Institut für Molekulare Biowissenschaften der Universität Graz wurden *Klebsiella oxytoca* Bakterien gefunden, die einen solchen Naturstoff produzieren und anschließend ausscheiden. In dieser Arbeit wurde eine Methode zur Isolierung, Reinigung und Charakterisierung dieses Naturstoffes unter Verwendung modernster Analysemethoden entwickelt und dieser Naturstoff letztendlich als Tilivallin identifiziert.

Summary

Adverse effects of drugs often remained undiscovered for a long time. Severe adverse effects of drugs resulted in costly withdrawals from the market. This thesis, in collaboration with the Research Center for Molecular Medicine in Vienna deals with the application of a compound-centric chemical proteomics method for the identification of a drug's entire protein target spectrum. The main goal of this technique is to acquire a maximum of information on biological activities in order not to oversee negative properties of a certain drug. One of the most challenging issues is the immobilization of drugs onto a solid support without losing their biological activity. Hence, in this thesis three different strategies for drug immobilization and the prerequisite linker syntheses were developed. The chemical focus was put on the bio-orthogonal thiol-ene reaction and olefin cross-metathesis as well as the dehydrogenative cross-coupling via double CH-activation, which had been developed recently. All three reaction types were successfully implemented in the linkage strategies.

For the establishment of the investigated linkage strategies, thalidomide and its promising derivatives pomalidomide and lenalidomide were chosen. Their molecular mechanism, which is responsible for the teratogenicity, remains still unknown, even after 50 years of research. These drugs were synthesized within this thesis via two to six step synthesis sequences. Thalidomide was tethered using two of our linkage strategies, pomalidomide and lenalidomide, both, were tethered via one linkage strategy. Unfortunately, chemical proteomics screening did not provide any conclusive results to date. A reason for that might be the very sensitive cell extracts, which might have been denatured.

Apart from chemically synthesized drugs, nature comes up with numerous natural products, which possess interesting biological activities. At the Institute of Molecular Biosciences at the University of Graz, *Klebsiella oxytoca* bacteria were identified, which produce and subsequently excrete an unknown natural product. In this thesis, a method to isolate, purify and characterize this natural product was developed using modern analysis techniques. Finally, this natural product was identified as tilivalline.

Table of contents

1. INTRODUCTION	1
2. THEORETICAL PART	3
2.1 KLEBSIELLA OXYTOCA.....	3
2.1.1 Pathogenicity island of <i>K. oxytoca</i>	4
2.1.2 Pyrrolbenzodiazepines.....	5
2.2 THALIDOMIDE.....	6
2.2.1 Tragedy	6
2.2.2 Revival.....	7
2.3 COMPOUND-CENTRIC CHEMICAL PROTEOMICS	9
2.3.1 Linker requirements.....	10
2.3.2 Limitations of linker strategies.....	12
2.3.3 Solid support.....	13
2.3.4 Immobilization strategies.....	15
2.3.4.1 Azide-alkyne ligation.....	16
2.3.4.2 Staudinger ligation.....	16
2.3.4.3 Thiol-ene ligation.....	17
2.4 STATE-OF-THE-ART ARYLATION, ALKYLATION AND ALKENYLATION.....	18
2.4.1 Cross-coupling.....	18
2.4.2 Desulfurization.....	23
2.4.3 Olefin cross-metathesis	26
3. AIMS OF THE DISSERTATION	29
4. RESULTS AND DISCUSSION	31
4.1 DRUG SYNTHESSES.....	31
4.1.1 Synthesis of thalidomide (1)	31
4.1.2 Synthesis of pomalidomide (2).....	32
4.1.3 Synthesis of lenalidomide (3)	32

4.2 LINKAGE STRATEGIES	38
4.2.1 Thiol-ene linkage strategy	38
4.2.1.1 Thiol-linker synthesis	39
4.2.1.2 Allylation	40
4.2.1.3 Thiol-ene reaction	41
4.2.1.4 Chemical Proteomics screening	44
4.2.2 Cross-metathesis linkage strategy	45
4.2.2.1 Allyl-linker synthesis.....	46
4.2.2.2 Olefin cross-metathesis screenings	46
4.2.2.3 Optimized olefin cross-metathesis	51
4.2.3 Thiophene-linkage strategy	54
4.2.3.1 Cross-coupling	55
4.2.3.2 Desulfurization	57
4.2.3.3 Synthesis of thiophene derivatives.....	60
4.2.3.4 Optimization and thiophene substrate screening.....	63
4.2.3.5 Screening of heterocyclic substrates in the thiophene linkage	69
4.3 ISOLATION OF AN UNKNOWN CYTOTOXIN	75
4.3.1 Preparation of the culture solution.....	75
4.3.2 Purification	75
4.3.3 Optimization attempts	80
4.3.4 Characterization and identification	80
5. SUMMARY AND OUTLOOK.....	85
5.1 DRUG SYNTHESSES.....	85
5.2 THIOL-ENE LINKAGE	86
5.3 LINKER SYNTHESSES	87
5.4 CROSS-METATHESIS LINKAGE.....	88
5.5 THIOPHENE LINKAGE	89
5.6 ISOLATION OF AN UNKNOWN CYTOTOXIN	92

6. EXPERIMENTAL PART	94
6.1 GENERAL ASPECTS.....	94
6.1.1 Chemicals and solvents.....	94
6.1.2 Materials for chromatography.....	98
6.1.3 Equipment	99
6.1.4 Biological preparations.....	102
6.2 EXPERIMENTAL PROCEDURES.....	103
6.2.1 Drug syntheses.....	103
6.2.2 Linker syntheses.....	118
6.2.3 Drug linkage	130
6.2.4 Thiophene derivatives	139
6.2.5 Other heteroarenes	144
6.2.6 Cross-coupling.....	148
6.2.7 Desulfurization and deprotection.....	161
6.2.8 Isolation and characterisation of a cytotoxin of <i>K. oxytoca</i>	171
7. REFERENCES	173
8. ABBREVIATIONS.....	180
9. APPENDIX	186

1. Introduction

It has always been human's desire to live a longer and healthier life. Looking back over the past 200 years, a tremendous improvement in the treatment of diseases has been accomplished. Healthcare has become increasingly important and lots of research has been done towards the discovery and development of synthetic drugs.^[1] Along with that, the interest in understanding all processes on a molecular level was intensified. One might say that this was the birth of modern natural science. Isolated natural products with special biological effects, i. e. antibiotics, were discovered.^[2] However, because our environment is highly diverse, many natural compounds with interesting properties remain undiscovered even today. Finding those compounds, which possess intrinsic biological activity, and identifying their mechanism of action is a major focus. One example is a recently discovered cytotoxin produced by the intestinal bacteria of *K. oxytoca*, an antibiotic resistant culture.^[3] Working together with the Institute of Molecular Biosciences at the University of Graz, one aim of this dissertation is the identification and characterisation of this unknown cytotoxin, including clarification of its biosynthesis and mode of action.

Over decades, some of these natural products have been commercialized, or alternatively, new classes of synthetic drugs have been created. These emerging drugs were screened for activity and in case of confirmation they were often quickly put onto the market. A drug with dramatic adverse effects, namely Contergan[®], changed our perspective of drug safety.^[4] As a consequence of the tragedy, emerging drugs must be tested *in vitro* and *in vivo* with different animal species. At the end of the development chain, these emerging drugs must pass tests with human beings before being distributed.

This complex testing procedure clearly improved drug safety, but even today important protein targets of certain drugs remain unknown and are identified only many years after the drug has entered the market. Among the most famous examples is Aspirin[®], which was put onto the market at the beginning of the 20th century as analgesic and was later recognized to serve as valuable anticoagulant.^[5] Contergan[®], which was temporarily sold as sedative until birth defects were found, is now administered to patients suffering from erythema nodosum leprosum.^[6] However, the molecular

mechanism of action of Contergan® and some of its promising derivatives and most of the protein targets addressed are still unknown. Therefore, the second very challenging aim of this dissertation is the identification of the protein targets of this class of compounds in collaboration with the Research Center for Molecular Medicine (CeMM) of the Austrian Academy of Science in Vienna.

Still today, there is a strong need to develop a universal method for the identification of a whole drug target spectrum without using living resources such as animals or humans. One modern approach with encouraging potential is compound-centric chemical proteomics.^[7] After tethering drugs via linker to a solid support, all proteins to be tested are added and thereby allowed to interact with the immobilized compound. Then, the binding proteins are identified with modern proteomics techniques. Despite the attractiveness of the concept, compound-centric chemical proteomics will only become a general method when appropriate linkers become available and their influence on the binding of proteins becomes predictable. Therefore, the third topic of this dissertation deals with the development and establishment of innovative linkage methods suitable for small drug-like molecules in chemical proteomics approaches.

2. Theoretical part

2.1 *Klebsiella oxytoca*

Klebsiella oxytoca bacteria belong to the family of Enterobacteriaceae and are non-motile capsules, surrounded by polysaccharide. These gram-negative, rod-shaped bacteria metabolize facultatively anaerobic. With 1.6 % to 9 % of healthy humans carrying *K. oxytoca*,^[8] these opportunistic bacteria are part of the natural intestinal flora. Nevertheless, people with weak immune system can become seriously infected sometimes even with lethal consequences. In neonatal intensive care units in the USA, *K. oxytoca* bacteria belong to the top 4 pathogens that induce infections, such as antibiotic associated hemorrhagic colitis (AAHC).^[3,9] Since *K. oxytoca* bacteria are able to produce an extended-spectrum of β -lactamases, they are resistant to many classes of antibiotics, e. g. penicillins or carbapenems.^[9] Treating an AAHC patient with these antibiotics results in overcolonization of *K. oxytoca* bacteria in the intestinal tract. This was proven in a mouse model.^[10] These mice were treated with ampicillin and indomethacin, allowing fast growth of *K. oxytoca* bacteria. The group of mice, which was infected with *K. oxytoca* AHC-6 wild type bacteria, showed strong symptoms of AAHC. The second group, additionally treated with a mutated variant of *K. oxytoca* ($\Delta npsA$) without cytotoxic activity, remained uninfected.

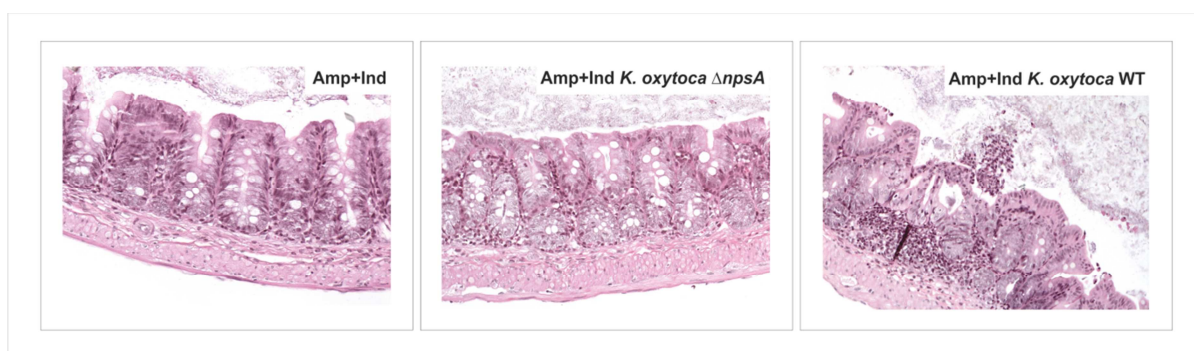


Figure 1. Intestine of mice treated with ampicillin and indometacin (Amp+Ind) alone, Amp+Ind and *K. oxytoca* cytotoxin-negative mutant ($\Delta npsA$) or Amp+Ind and *K. oxytoca* cytotoxin-positive wild type. Samples of the murine colon were stained with hematoxylin and eosine.^[10]

2.1.1 Pathogenicity island of *K. oxytoca*

Recently, the group of Ellen Zechner at the Institute of Molecular Biosciences at the University of Graz identified a pathogenicity island of *K. oxytoca* by transposon mutagenesis and genome sequencing, harboring a biosynthetic gene cluster responsible for the production of a cytotoxin.^[11] This cytotoxin has an unusual low molecular mass (<1 kDa)^[12] and is associated with *K. oxytoca* from patients with AAHC. Sequence comparison revealed a high homology to pyrrolbenzodiazepine-producing gene clusters (figure 2). The identified pathogenicity island shares gene orientation, organization and gene number with other benzodiazepine clusters, which implies a benzodiazepine derivative as product. Hence, this is the first example of gram-negative bacteria containing a pyrrolbenzodiazepine-producing gene cluster. But the chemical structure, its mechanism of action and the clinical relevance of the cytotoxin produced by *K. oxytoca* remain unclear.

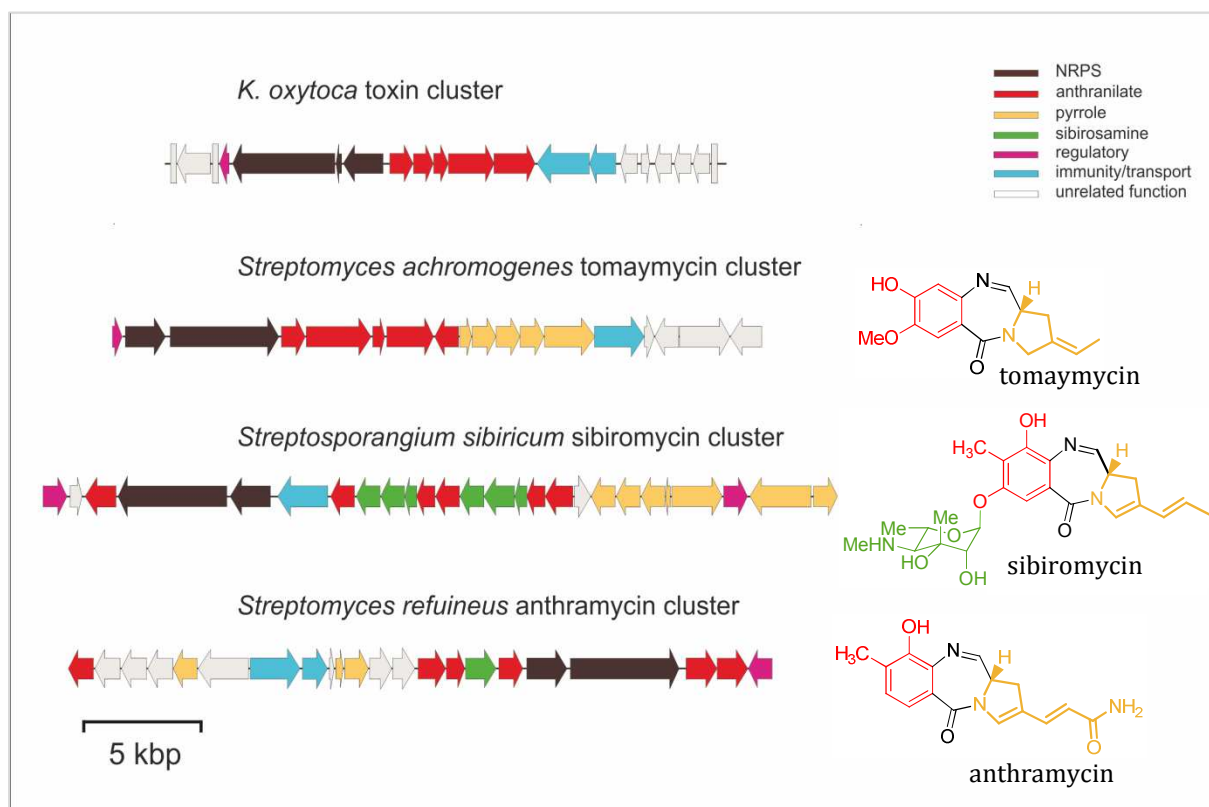


Figure 2. Pathogenicity island of the cytotoxin of *K. oxytoca* compared to related gene clusters and the products they encode for.^[11]

2.1.2 Pyrrolobenzodiazepines

Pyrrolobenzodiazepines (PBDs), known as potent cytostatics, are commonly produced by gram-positive *Actinomycetales*.^[13] A few pyrrolobenzodiazepines were also isolated from *Aspergillus sp.*^[14] From gram-negative *Klebsiella* bacteria only tilivalline is known.^[15] Natural occurring pyrrolobenzodiazepines have the *S*-configuration at the C-11a atom in common, which seems to be required for biological activity. Additionally, pyrrolobenzodiazepines incorporate usually electron donating substituents at the benzene scaffold presumably to enhance biological activity.

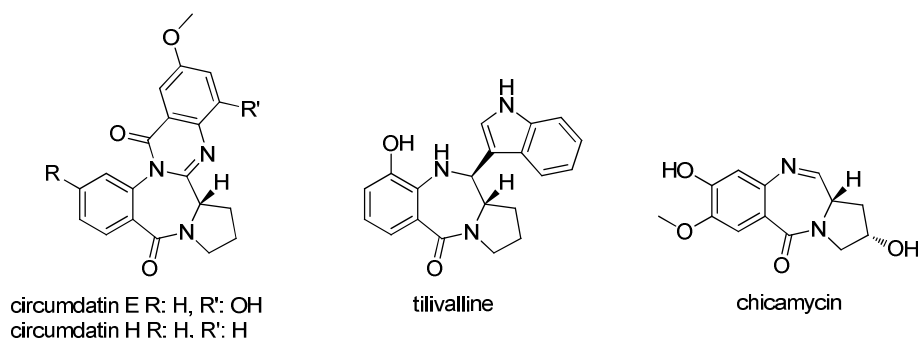
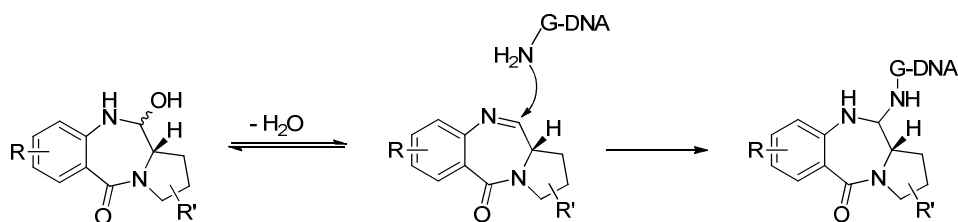


Figure 3. Examples of naturally occurring pyrrolobenzodiazepines.

Pyrrolobenzodiazepines from *Actinomycetales* are classified as DNA-interactive antibiotics because of their imine or carbinolamine structure.^[16] They possess a reactive C-11 atom for binding covalently to guanine at the minor groove of the DNA (scheme 1). Since this DNA part is commonly found in bacterial promoters and origins of replication, these pyrrolobenzodiazepines possess bactericidal activity. Due to this interaction, these pyrrolobenzodiazepines are not only potent antibiotics but also might be applied as antitumor agents. Covalent DNA modification leads to cell cycle arrest, which results in cell death in tumor cell lines.^[16] Additionally, double bonds at the pyrrole scaffold enhance the antitumor activity especially when the C-2 atom is sp^2 -hybridized. Prominent examples are anthramycin, thomaymycin and sibiromycin (figure 2).^[17]



Scheme 1. Formation of a PBD-DNA complex.^[16]

2.2 Thalidomide

2.2.1 Tragedy

The history of thalidomide started in 1957 when it was introduced as a new sedative and anti-hypnotic by Grünenthal onto the market. Compared to the barbiturates, which were frequently used at that time, thalidomide was said to have no adverse effects, to be non-addictive and overdose to be harmless even for pregnant women.^[4] After a few animal tests, thalidomide was distributed globally and in some countries even without prescription. In 1960, over 14.6 tons of thalidomide were sold in 46 countries all over the world.^[4] One year later, the physicians *William McBride* and *Widukind Lenz* noticed, independently from each other, the correlation between the latest increase of birth defects after consumption of thalidomide.

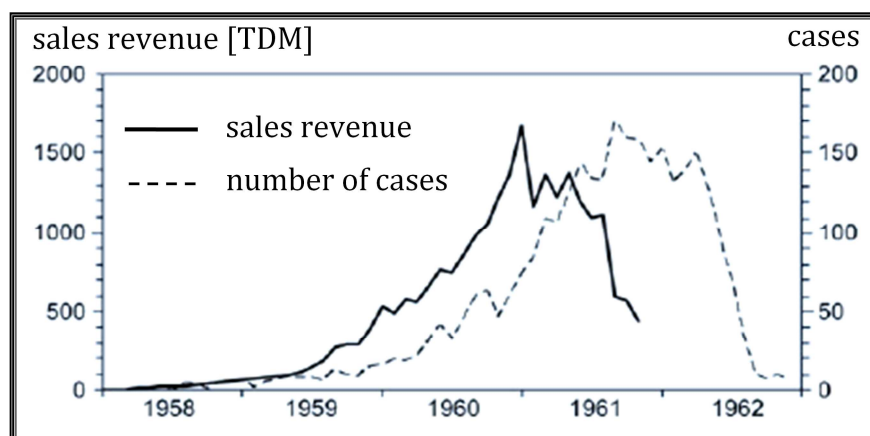


Figure 4. Correlation between the number of cases of birth defects and the net sales revenue of thalidomide.^[4a]

Due to the dramatically increased number of newborns with malformations mainly of limbs or other organ defects, thalidomide was subsequently withdrawn from the market in 1962. Also the infant mortality at that time increased dramatically due to thalidomide's high teratogenicity by ingesting only one pill during pregnancy.^[4] With over 10000 children suffering from birth defects it became the most fatal drug disaster of the 20th century.

2.2.2 Revival

Only two years later, in 1964, the Israeli physician *Jacob Sheskin* discovered a new application of thalidomide by treating an erythema nodosum leprosum patient with thalidomide.^[4] Consequently, research on unravelling its mode of action and the search for new, more potent derivatives revived. Quickly, two promising derivatives, namely pomalidomide and lenalidomide, were identified with increased positive effects but only little decrease of undesired effects.^[18] Investigations to influence the interchange of their enantiomers under physiological conditions are without positive results till today.

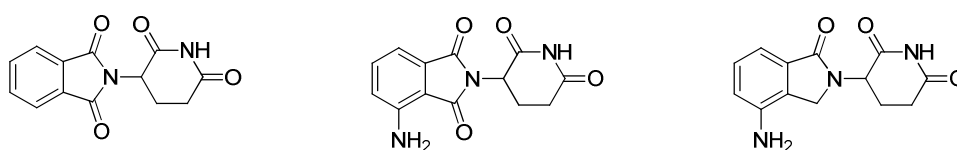


Figure 5. Thalidomide, pomalidomide and lenalidomide.

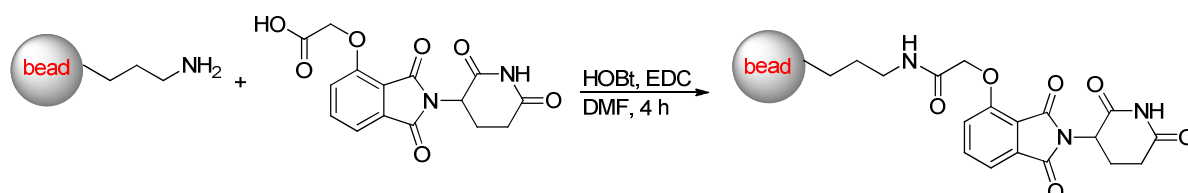
For their mode of action, over 30 hypotheses were postulated as summarized by *Vargesson* in 2009:^[19]

- inhibition of angiogenesis,
- induction of cell death,
- antagonism of integrin / cell adhesion signalling,
- effects on growth factor signalling,
- nerve toxicity,
- intercalation with DNA or
- effects on chondrogenesis.

But till today, more detailed insights into the mode of action of these drugs on a molecular level are pending. The protein targets, responsible for all these effects could not be identified within the last 50 years of research, which indicates a very complex mode of action. However, some information about a few indirect targets of thalidomide is already obtained. It is postulated that oxidative stress and antiangiogenic action play an important role in teratogenicity processes of thalidomide, resulting in the inhibition of several cytokines, mainly tumor necrosis factor α , and some growth factors.^[20] Consequently, apoptosis is induced. A main challenge is the rapid occurrence of

numerous metabolites of thalidomide under physiological conditions, which might have the same protein targets.

In 2010, *Ito* and co-workers identified for the first time cereblon (CRBN) and damage DNA binding protein 1 (DDB 1), two proteins that play an important role in teratogenicity processes of thalidomide.^[21] For the identification of thalidomide's protein targets, *Ito* and co-workers immobilized carboxylic acid modified thalidomide covalently via a short alkyl linker to a magnetic solid support (scheme 2). Using compound-centric chemical proteomics, direct binding cereblon and indirect binding DDB 1 could be enriched from human HeLa cell extracts and were identified by gel electrophoresis and tandem mass spectrometry after proteolytic digest.



Scheme 2. Covalent immobilization of thalidomide by *Ito* and co-workers.

CRBN and DDB 1 are both part of the E3 ubiquitin ligase complex associated with direct polyubiquitination of substrate proteins (figure 6). *Ito* and co-workers proved that inhibition of the E3 complex through direct interaction of thalidomide with cereblon finally results in maldevelopment of limbs.^[21] Hence, this interference causes teratogenicity when ingesting thalidomide during pregnancy. Since oxidative stress, as another teratogenic effect induced by thalidomide, does not originate from CRBN, affecting CRBN alone is not solely responsible for thalidomide's teratogenicity.

Ito and co-workers reached a milestone in resolving the mode of action of thalidomide although they identified only one teratogenic interaction of thalidomide. Nevertheless, in a few countries thalidomide is again sold for the treatment of erythema nodosum leprosum or multiple myeloma. So far, the targets, which explain the favorable anti-cancer properties of thalidomide, have not been identified yet.

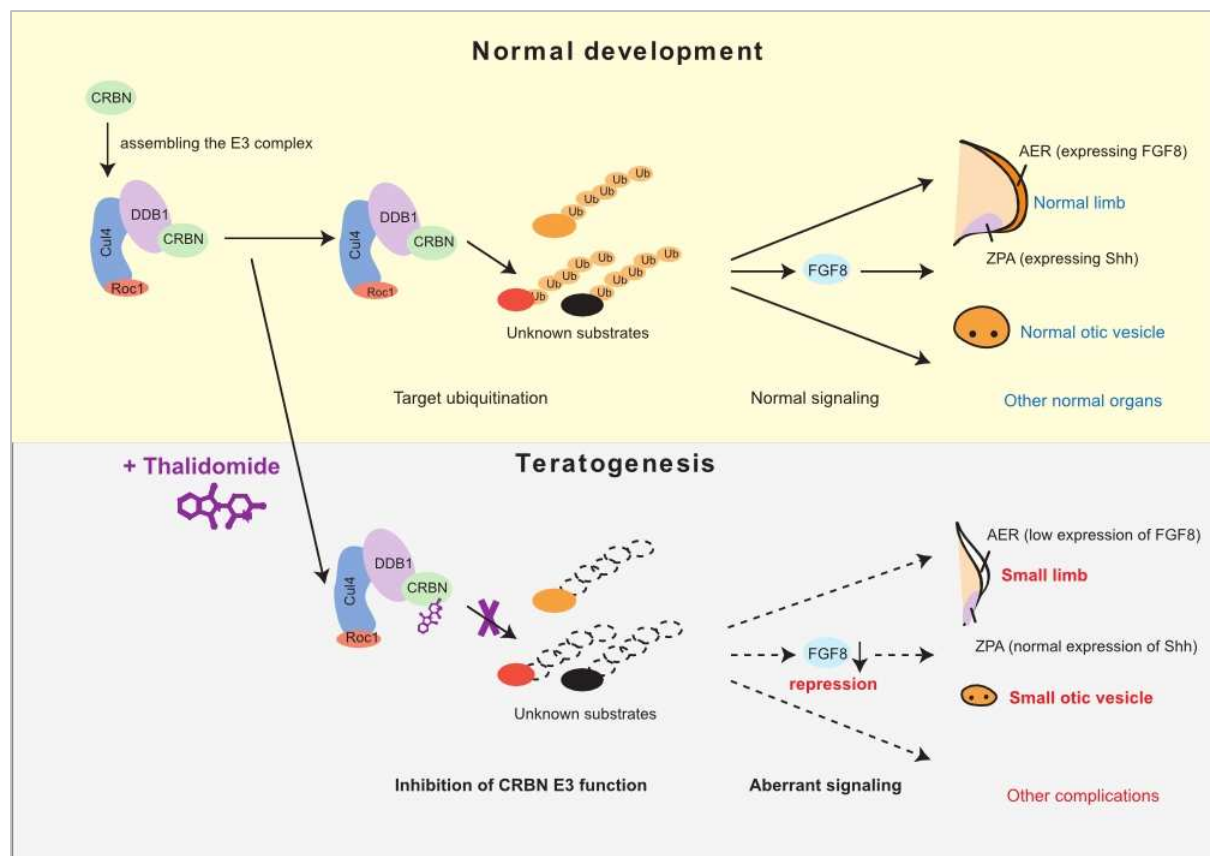


Figure 6. Schematic model for the molecular mechanism of thalidomide's teratogenicity.^[21]

2.3 Compound-centric chemical proteomics

For studying protein targets of small molecules, two main chemical proteomics approaches were established during the last decades (figure 7).^[7,22] In affinity based protein profiling (ABPP), small molecules were marked with a tag and then incubated with proteins of choice. The binding proteins can subsequently be identified and quantified after binding to appropriately attached drugs onto a solid support. This method is very useful to distinguish between binding strength of different small molecules to one particular family of proteins. Screening of a large number of proteins with ABPP is impracticable in contrast to compound-centric chemical proteomics (CCCP).^[22]

Compound-centric chemical proteomics starts with the attachment of a small molecule of interest to a solid support using different types of tethering techniques. The immobilized drug is subsequently incubated with cell lysates or other protein containing

extracts and the non-binding proteins are washed away. All specifically binding proteins that interfered with the tethered drug are subsequently eluted usually by detachment with free drugs. The enriched proteins can be analyzed using 1D or 2D gel electrophoresis, gel-free 'shotgun proteomics' or nano-LC-MS/MS after proteolytic digest. Comparing the obtained data of the peptide mixture with common protein databases enables the identification of the drug's direct protein targets.

An immense strength of CCCP is the possibility to identify natural proteins in their competitive cellular environment including post-translationally modified proteins. CCCP is a general method for qualitative analysis of protein targets proteome wide. The lacking opportunity to identify active metabolites remains as a disadvantage. Identification of target proteins is further limited by the solubility of proteins. Quantification of the received results is still difficult. Furthermore, the drug of interest must be modified chemically for use in CCCP approach, which often leads to complete loss of biological activity.

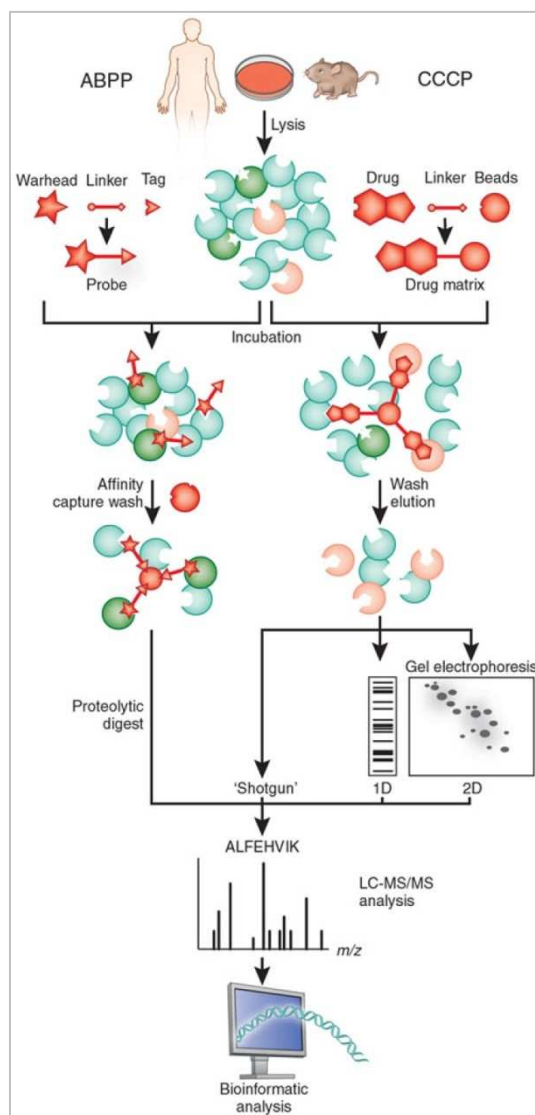


Figure 7. ABPP versus CCCP.[22a]

2.3.1 Linker requirements

Linkers for drug-like molecules that are to be investigated in compound-centric chemical proteomics have to meet some requirements to attach drugs covalently to a solid support. Moreover, different types of linkage methods can be used beside covalent tethering. This thesis focuses exclusively on covalent immobilization strategies as it is

the main type of attachment. Since cleavage of the linker from the drug plays no role in compound-centric chemical proteomics, this topic will not be discussed.

Particular attention has to be paid on positioning the linker on the drug scaffold. It is very important to keep the part of the drug that will reach deepest into the active site of a protein chemically unmodified to retain biological activity. Additionally, a linker should consist of a chain-like molecule with two orthogonal functional groups, one at each end. The functional groups must not interact with the rest of the drug molecule.

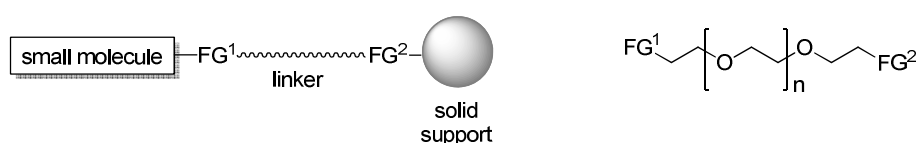


Figure 8. General structure of linkers.

The length of a linker should be well-conceived. It is obvious that a drug will not reach into the active site of the protein when the linker is too short. On the other hand, an oversized linker will increase the background levels in CCCP measurements by stronger interference with high abundant proteins. Based on physical adsorption, proteins such as tubulin or actin will interact non-specifically. Additionally, the polarity of the linker can influence the outcome of the CCCP screening. Polar linkers will increase the solubility of naturally apolar drugs and therefore increase the chance to identify target proteins. On the contrary, polar linkers can again interfere stronger with polar, high-abundant proteins and might decrease the signal-to-noise ratio. For each drug, the position of the linker, its functional groups, its length and polarity have to be selected with caution.

Studies on the influence of non-specific binding proteins to linkers with varying polarity were reported by *Shiyama* and co-workers.^[23] They designed four different linkers with either ethylene glycol or tartaric acid scaffold to immobilize tacrolimus, a natural product from *Streptomyces tsukubaensis* bacteria, which is applied as an immunosuppressive drug (figure 9). In a control experiment tacrolimus was directly immobilized onto a methacrylate type solid support only via hydrophobic spacer. In the presence of immobilized tacrolimus a common lysate of rat brain was screened for specific binding proteins.

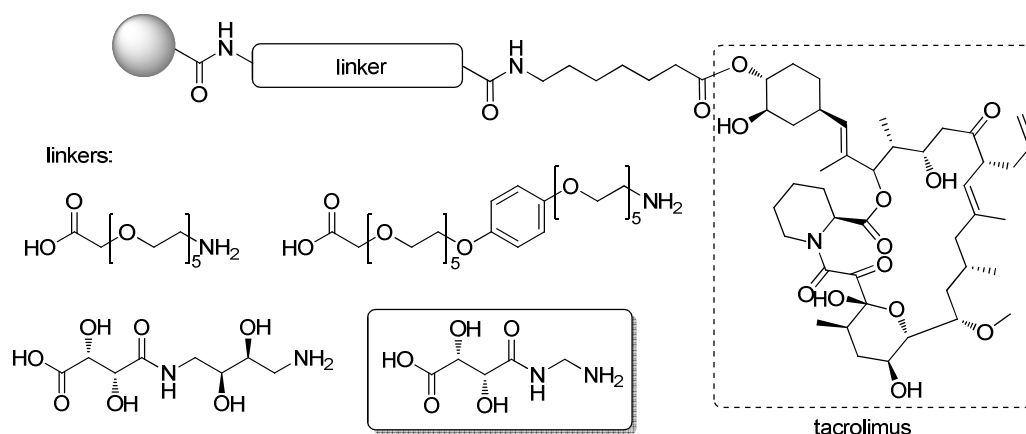
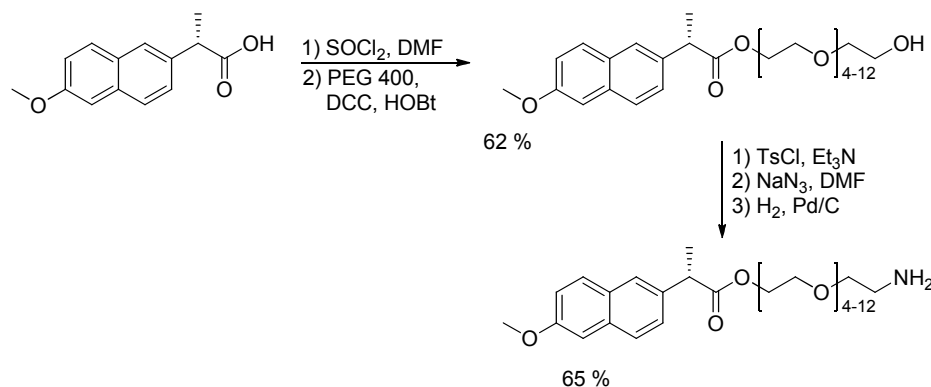


Figure 9. Immobilization of tacrolimus via different linkers.

Interestingly, *Shiyama* and co-workers demonstrated an increased signal-to-noise ratio with tacrolimus tethered via tartaric acid linkers onto a methacrylate type solid support instead of the tested ethylene glycol linkers.^[23] The tartaric acid linkers reduced non-specific binding of the high abundant proteins tubulin and actin up to 90 % over the control experiments. *Shiyama* and co-workers postulate this reductive effect to originate from the hydrophilicity of the tartaric acid linkers.

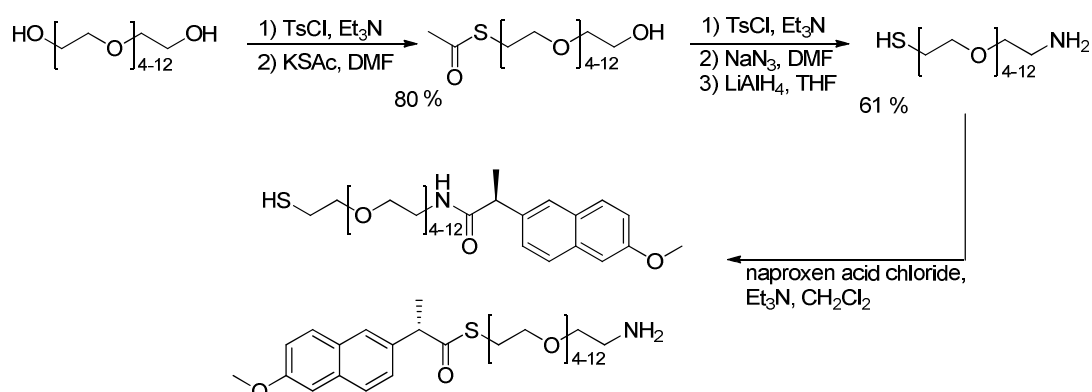
2.3.2 Limitations of linker strategies

In 2008, *Stefanko* and co-workers implemented polyethylene glycol derivatives for the immobilization of naproxen, a non-steroidal anti-inflammatory drug.^[24] For this purpose, they pursued two different synthetic strategies. The first strategy focuses on the linker synthesis starting with naproxen (scheme 3). Herein, the PEG-linker was built up in five steps with a good overall yield of 40 % of the tethered naproxen. Unfavorably, this linear linkage strategy requires the drug from the very first step of the linker synthesis on.



Scheme 3. Immobilization of naproxen by stepwise formation of the linker on the naproxen scaffold.

The second linker strategy of *Stefanko* and co-workers is based on a separate linker synthesis with an excellent overall yield of 49 % followed by tethering of naproxen (scheme 4).^[24] Since the drug is introduced in the last step of the linker strategy, this approach should be preferred. Unfortunately, the chosen functional groups at each end of the linker do not react orthogonally, which results in a mixture of tethered naproxen with either terminal thiol group or terminal amino group. This mixture is inseparable using common purification methods.



Scheme 4. Immobilization of naproxen by separate linker synthesis followed by naproxen tethering.

2.3.3 Solid support

Within the last decades, a broad range of solid supports has been developed for several areas of application. DNA chips and other arrays make mainly use of glass slides, metal or metal oxide surfaces.^[25] If a planar surface is not essential, nanoparticles and functionalized polymers were used to form beads.^[26] With the appropriate selection of materials for the synthesis of beads, various chemical and physical properties can be induced.

Robert Bruce Merrifield invented the solid-phase synthesis of peptides, for what he received the Nobel Prize in chemistry in 1984.^[26] His so called Merrifield resin is formed by co-polymerization of styrene and 1-2 % divinylbenzene, followed by chloromethylation to introduce functional groups. Its general structure is shown in figure 10. Due to a low degree of crosslinking, this polystyrene resin lacks physical stability and can be easily destroyed mechanically. Hydrophobic solvents, which enable

the swelling of resins are accepted. But very polar, protic solvents, required for peptide synthesis, diminish reaction rates due to the poor solvation of the resin.

Advanced polystyrene resins are grafted with polyethylene glycol and co-polymerized to obtain TentaGel (figure 10). Due to the PEG chains, these resins are compatible with both, polar and apolar solvents, which results in enhanced physical robustness and flexibility at the same time.^[26] Bottom up synthesis of peptides on TentaGel resins is feasible. But also the interaction with non-specific binding, polar molecules is increased.

Alternatively, sepharose resins were developed. Sepharose has its name from **S**eparation-**P**harmacia-**A**garose and consists of a polysaccharide polymer. The degree of crosslinkage is variable and can occur on each free hydroxyl group. Due to its galactose building blocks, sepharose is highly polar and has good swelling properties in water. Fortunately, non-specific binding of high abundant proteins is negligible. Higher agarose contents reduce the porosity of sepharose resins resulting in decreased mechanical stability.^[27]

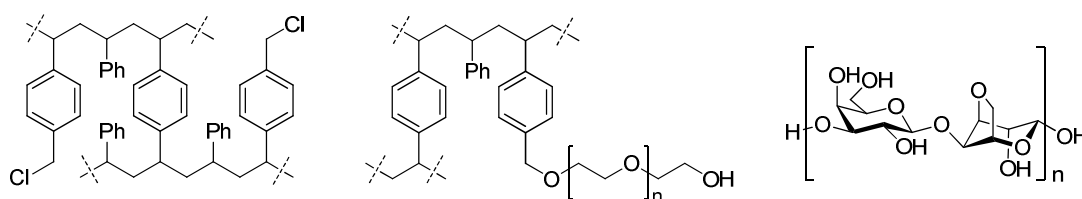


Figure 10. Segments of Merrifield's polystyrene resin (left), TentaGel (middle) and Sepharose resin (right).

To overcome the problem of mechanical instability, magnetic resins have been investigated (figure 11).^[28] They generally consist of a polystyrene or a polyglycidyl methacrylate (GMA) matrix with incorporated ferrite nanoparticles. All steps of the synthesis, isolation and purification with magnetic resins are performed using magnets. The magnetic resins can easily be recovered. Centrifugation for resin collection, which might destroy interacting proteins, is not mandatory. Therefore, magnetic resins can be applied as a gentle alternative, resulting in increased sensitivity and effectiveness.

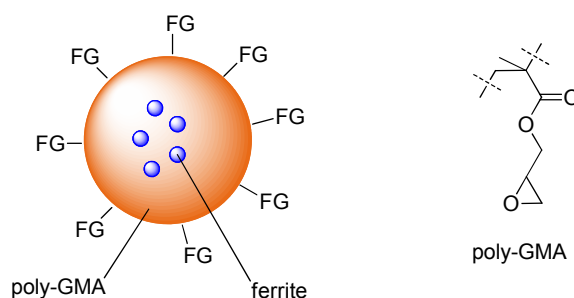
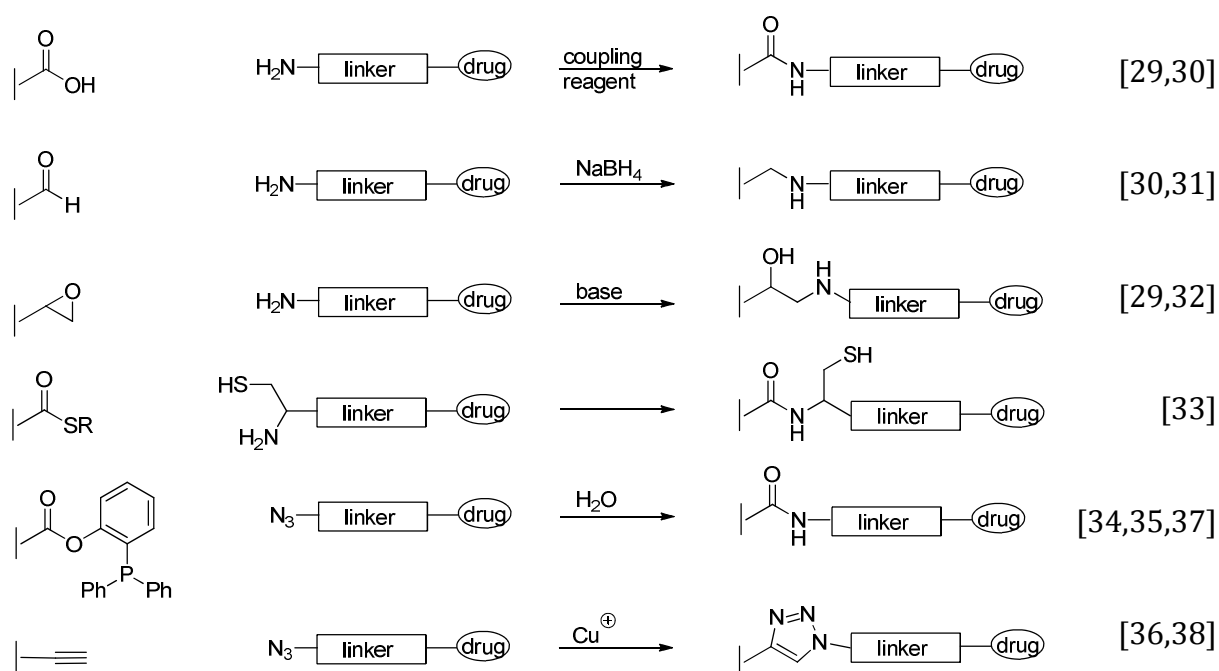
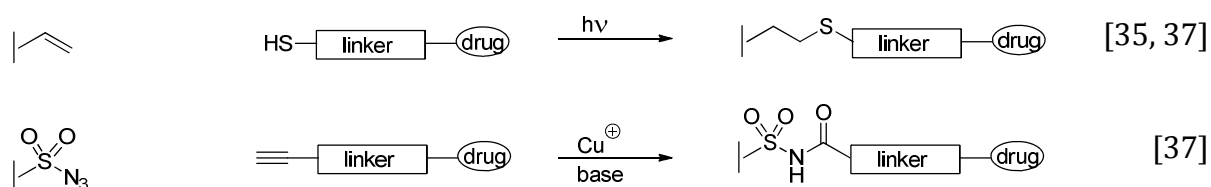


Figure 11. General composition of magnetic beads.

2.3.4 Immobilization strategies

Well explored methods for binding of substrates, especially proteins, to a solid support were developed in the past. Most of these immobilization strategies focus on covalent ligation, in particular the general attachment of functionalized linkers to a solid support. Tethering small molecules of choice was then done individually. Nevertheless, most of these ligation reactions are also valuable for small molecule tethering. Some general covalent linkage methods especially for linkers with a terminal amino group or related, are listed in scheme 5. Theoretically, functional groups of the solid support and the linker can be exchanged. Some important types of reactions for linkage are additionally discussed in the following chapters.

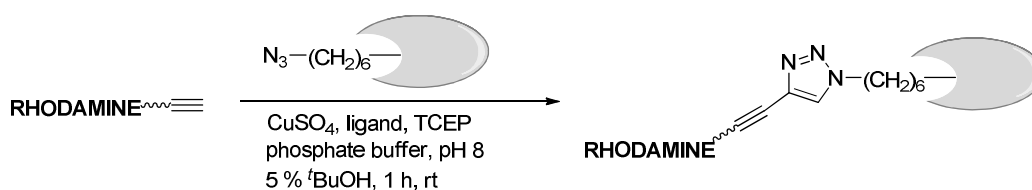




Scheme 5. Overview about common covalent immobilization reactions.

2.3.4.1 Azide-alkyne ligation

The bio-orthogonal [2+3]-cycloaddition between azides and alkynes was established by *Huisgen* and can be performed in the presence of catalytic amounts of Cu(I) salts.^[36] Using this azide-alkyne coupling, *Cravatt* and co-workers attached rhodamine, a fluorescence tag, selectively *in vitro* to an enzyme of a complex mixture within one hour.^[38] Because of the speed and simplicity of coupling this method is well-known as “click chemistry”.



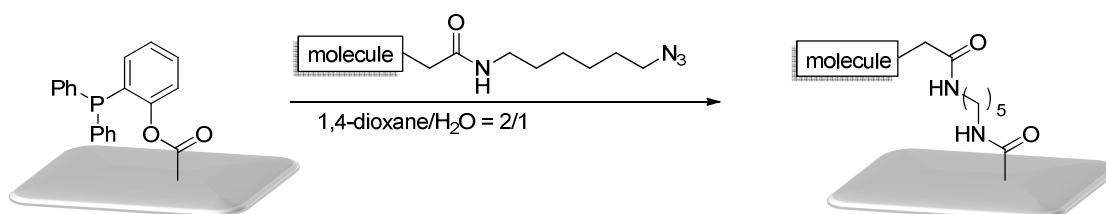
Scheme 6. Labelling of an enzyme via azide-alkyne coupling.

As these Cu(I) salts are cell toxic, a metal-free alternative was developed making use of the considerable ring strain of cyclooctynes.^[36] This stress-induced azide-alkyne coupling can be carried out under physiological conditions.

2.3.4.2 Staudinger ligation

The basis of the Staudinger ligation is the Staudinger reaction of an azide in the presence of triphenylphosphine and water to form the corresponding amine. This reaction was realized by *Hermann Staudinger* and *Jules Meyer* in 1919.^[39] More than 80 years later, *Bertozzi* adapted this reaction, optimized the phosphine reagent and invented the Staudinger ligation for the coupling of peptides.^[40] Within a few years, the field of application increased and the Staudinger ligation is now also used for immobilization of

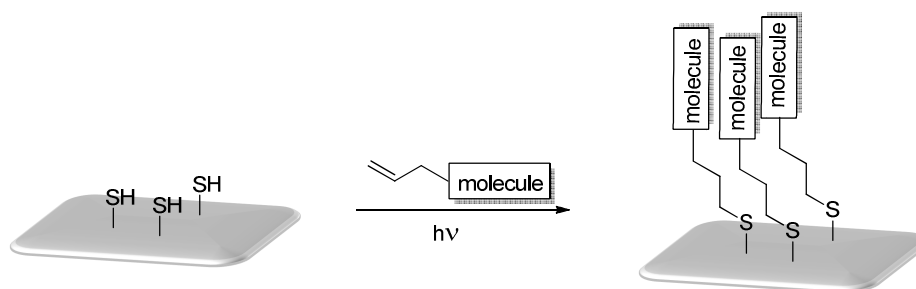
small molecules.^[41] Depending on the applied phosphine, traceless Staudinger ligation is possible resulting in the formation of an amide bond (scheme 7). *Köhn* and co-workers reported a strategy for the functionalization of glass arrays taking advantage of the traceless Staudinger ligation.^[41b]



Scheme 7. Preparation of small-molecule arrays by traceless Staudinger ligation.

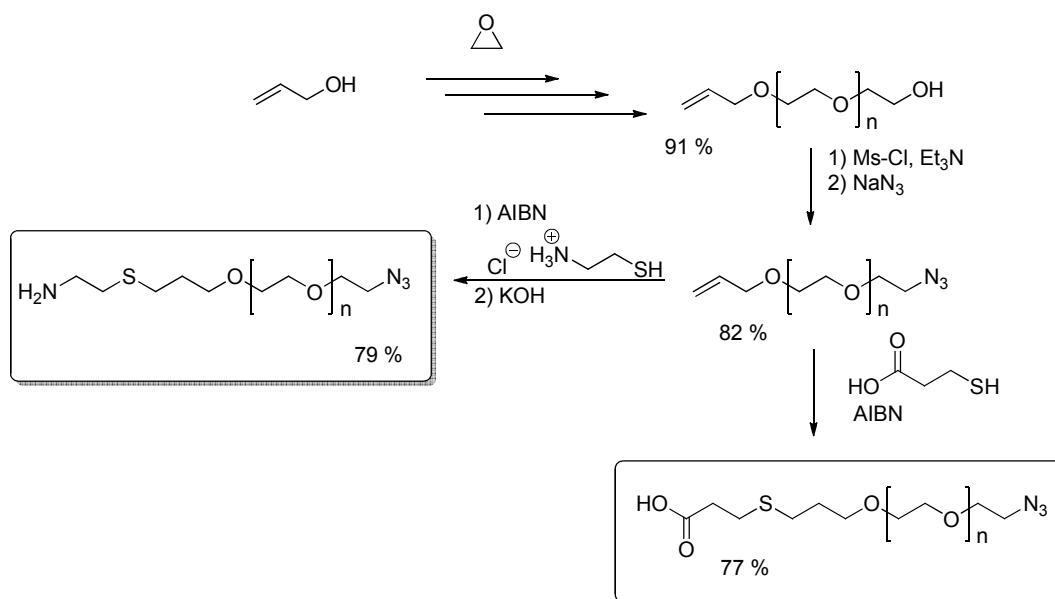
2.3.4.3 Thiol-ene ligation

Radical addition of a thiol to an alkene in the presence of light or an initiator under neutral conditions results in thio ethers. Sometimes this reaction is also called 'click' reaction. Studies about its mechanism and the influence of the alkene on the course of reaction were performed by *Roper* and co-workers.^[42] *Jonkheijm* and co-workers were able to immobilize ene-modified small molecules and peptides on a surface via photoactivation.^[43] The allyl-group itself was used as short linker.



Scheme 8. Compound immobilization by thiol-ene reaction.

Hiki and *Kataoka* applied the thiol-ene reaction in their linker synthesis towards functionalized, linear polyethylene glycol derivatives, which can be tethered to a solid support using standard immobilization strategies.^[44] To start the thiol-ene reaction they used AIBN as initiator.

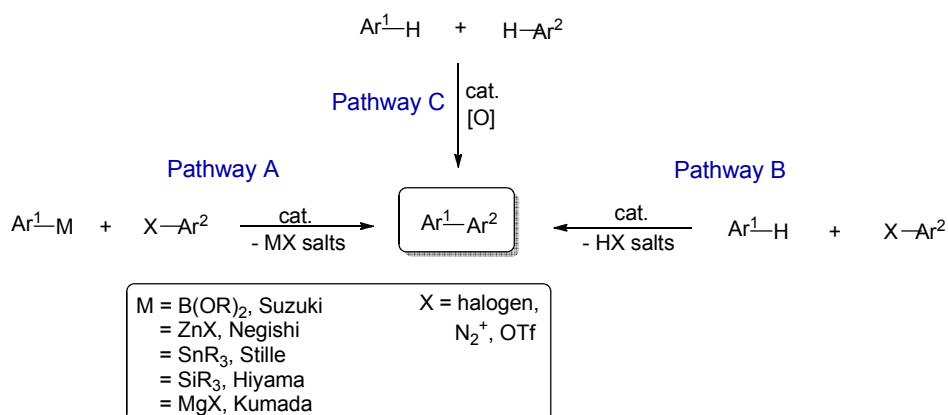


Scheme 9. PEG linker synthesis using thiol-ene reaction.

2.4 State-of-the-art arylation, alkylation and alkenylation

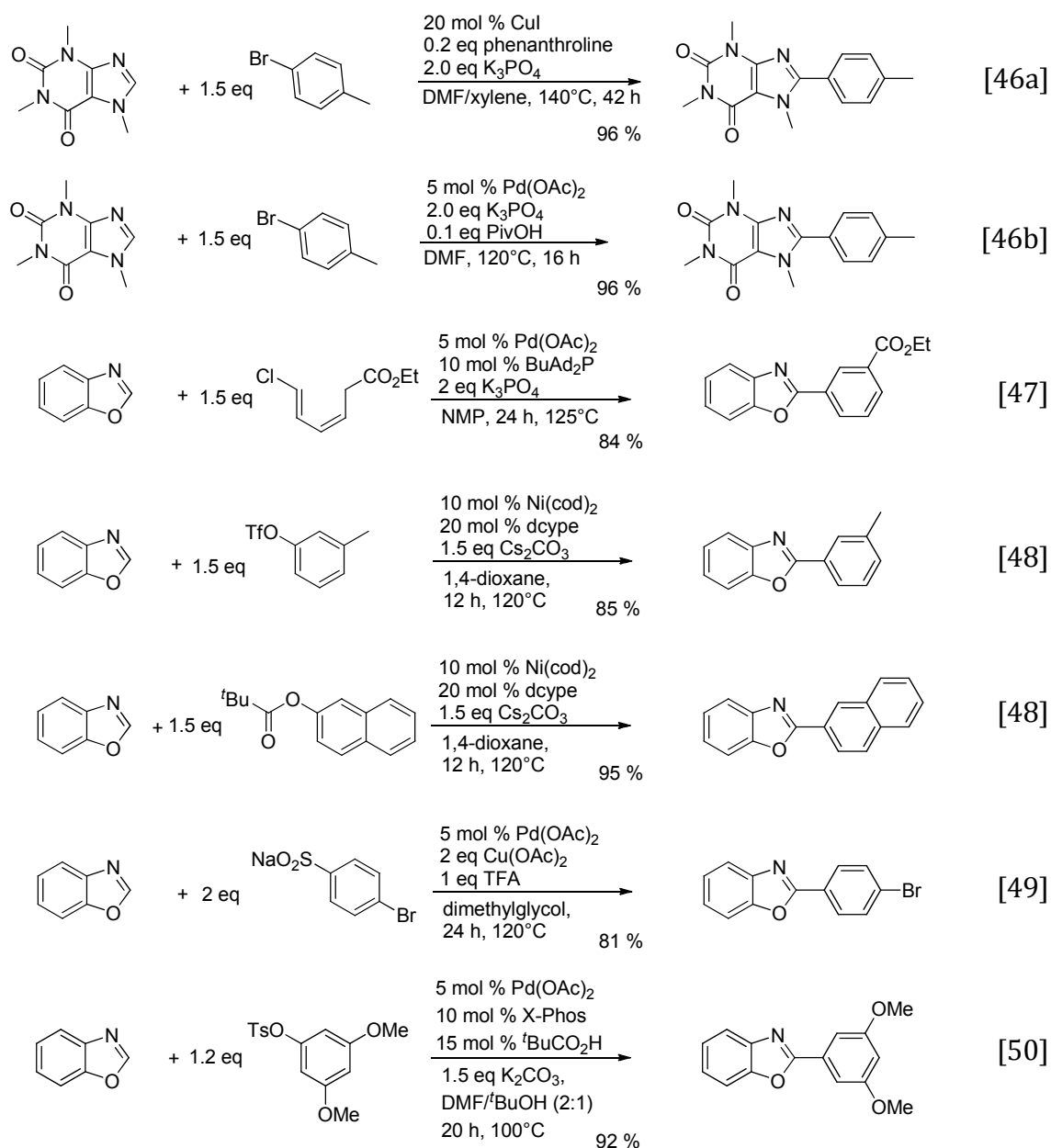
2.4.1 Cross-coupling

Heck, *Negishi* and *Suzuki*, the inventors of the palladium catalyzed cross-coupling, developed a general method for the C(sp²)-C(sp²) bond formation by activating typically carbon-halogen bonds with different metals (scheme 10, pathway A).^[45] On that account they were honored with the Nobel Prize in 2010. Advancements of this metal mediated cross-coupling reaction led to the direct arylation by activation of one aryl-C-H bond (pathway B).



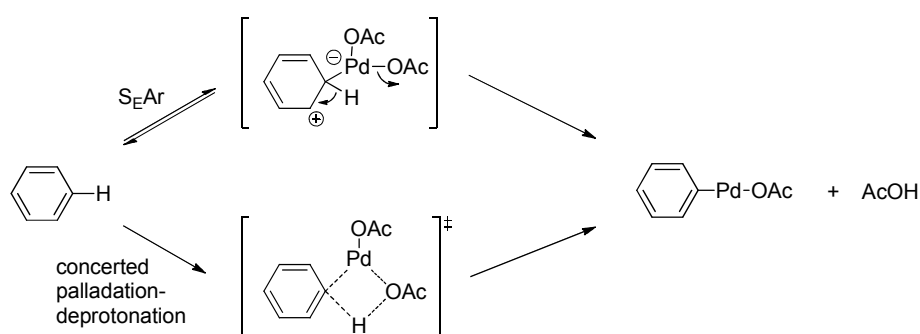
Scheme 10. Possible cross-coupling reactions to form a C(sp²)-C(sp²) bond.

For the direct arylation, several leaving groups (e. g. halogens, triflates, tosylates, sulfonates or pivalic esters) are established (scheme 11). The direct cross-coupling via onefold CH-activation occurs in general metal(II) catalyzed at higher temperatures in the presence of a ligand and under acidic or basic conditions. Interestingly, cross-coupling reactions of a heteroarene with an arene are more frequently reported. The yield of each direct cross-coupling reaction highly depends on the nature of (hetero)arenes used. Little variations in the structure of one (hetero)arene often lead to considerably decreased yields.



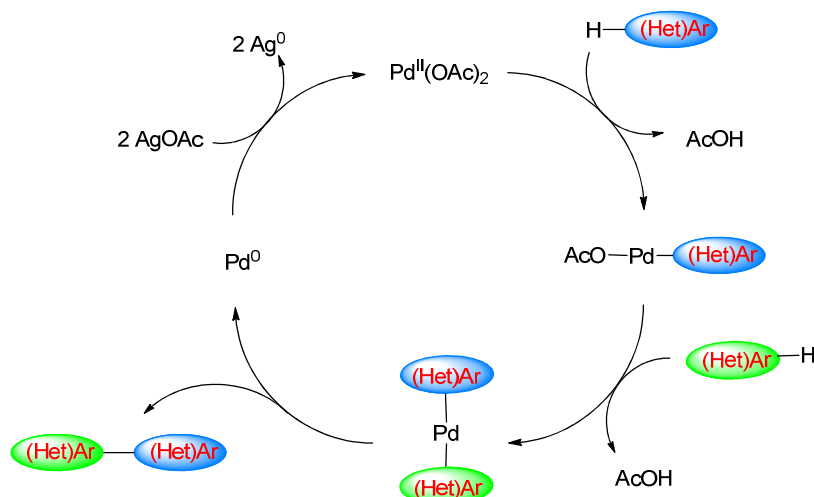
Scheme 11. Cross-coupling of heteroarenes with substituted arenes via direct arylation with different leaving groups and catalytic systems.

Even more interesting is the invention of cross-coupling reactions of two (hetero)aromatic compounds in the absence of functional groups by double CH-activation (scheme 10, pathway C). The catalysis of this reaction is quite challenging since two different (hetero)arenes must react without forming homo-coupling products. This can only be achieved, when the reacting (hetero)arenes differ in electronic and steric properties, respectively, and when they are activated via different modes of action (scheme 12).^[51] The mechanism of the so called dehydrogenative cross-coupling (scheme 13) starts with an electrophilic metallation reaction (S_{EAr}). In most cases a Pd(II) species, i. e. palladium acetate, is used. The new catalytic species reacts selectively with the second (hetero)arene in a concerted palladation-deprotonation reaction step. Therefore, both (hetero)arenes must have an inverse reactivity. Homocoupling products only occur, when the reaction rates of both (hetero)arenes in the palladation pathways equal each other.



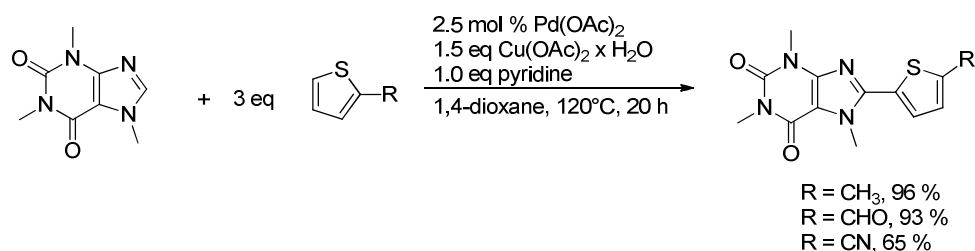
Scheme 12. Mechanism of the electrophilic aromatic palladation (top) versus the concerted palladation-deprotonation (bottom).

Reductive elimination furnishes the cross-coupled product. The Pd-catalyst is regenerated via an oxidizing agent (mainly copper(II) or silver(I) acetate) to restart the catalytic cycle.^[52] Molecular oxygen is also investigated as oxidant in the dehydrogenative cross-coupling.^[52]



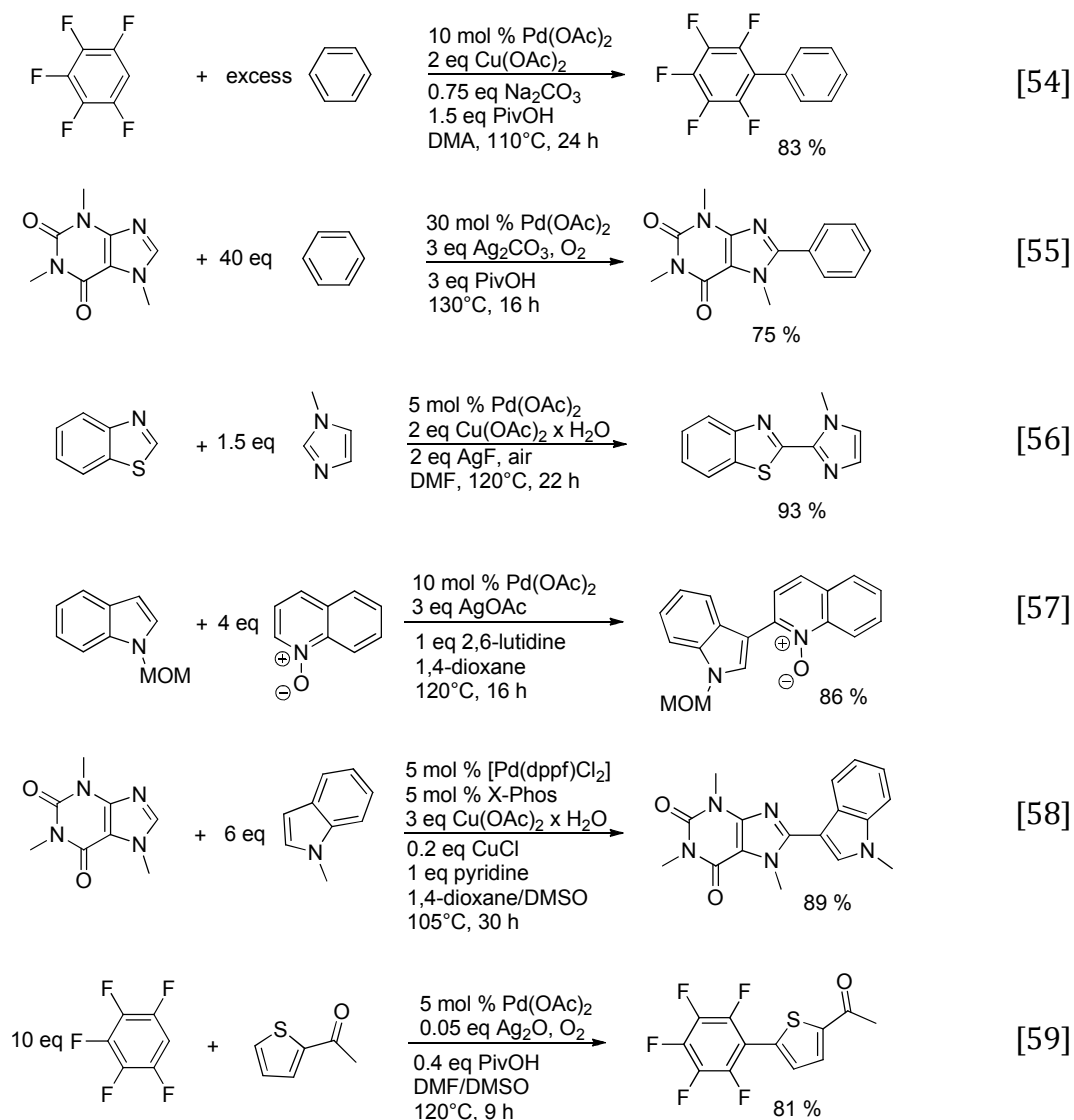
Scheme 13. Catalytic cycle of the dehydrogenative cross-coupling with palladium(II) acetate as catalyst and silver(I) acetate as oxidant.^[53]

In January 2010, *Xi* and co-workers reported the dehydrogenative cross-coupling of caffeine with different thiophene derivatives in excellent yields, using catalytic amounts of palladium acetate and a slight excess of copper acetate as oxidant in the presence of an equimolar amount of pyridine.^[53]



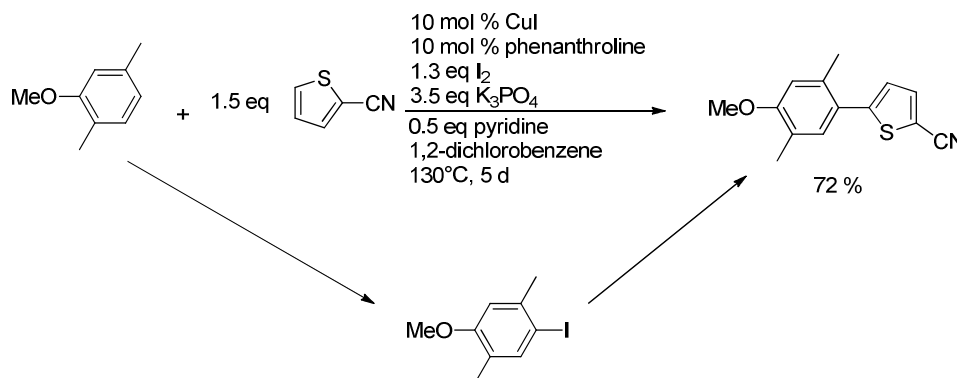
Scheme 14. Dehydrogenative cross-coupling of caffeine with different thiophenes by *Xi* and co-workers.^[53]

From there on, the development of new catalytic systems in the dehydrogenative cross-coupling was intensively investigated. Almost monthly, novel reaction conditions for two arenes, two heteroarenes or one heteroarene with one arene were reported. A few examples of the most important dehydrogenative cross-coupling reactions since December 2010 are listed in scheme 15, varying especially in oxidizing agent, ligands and salt additives. Similar to the direct arylation via onefold CH-activation, little changes in substrate structures may result in dramatically decreased yields. A general method for a broad range of substance classes does not exist so far.



Scheme 15. Overview of novel reaction conditions for the dehydrogenative cross-coupling.

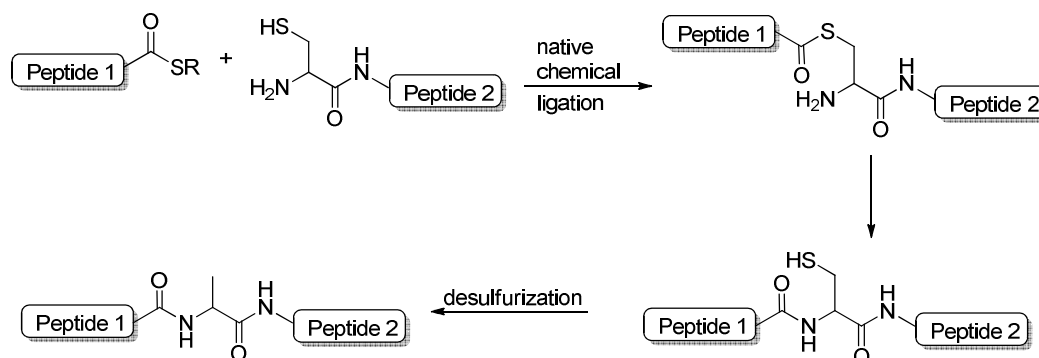
Do and *Daugulis* reported in August 2011 new reaction conditions without using a Pd(II) catalyst.^[60] At the first glance, their reaction looks like a standard dehydrogenative cross-coupling. But actually, it is a two-step reaction, with *in situ* iodination of one arene followed by direct cross-coupling. Instead of the metal(0) catalyst, one arene is oxidized chemo- and regioselectively through iodination. *Do* and *Daugulis* determined this iodination of electron-deficient arenes to proceed at the most acidic C-H bond through a deprotonative halogenation mechanism.^[60] In contrast, electron-rich arenes were iodinated through an electrophilic aromatic substitution.



Scheme 16. Two-step cross-coupling reaction of thiophene-2-carbonitrile by *Do* and *Daugulis*.

2.4.2 Desulfurization

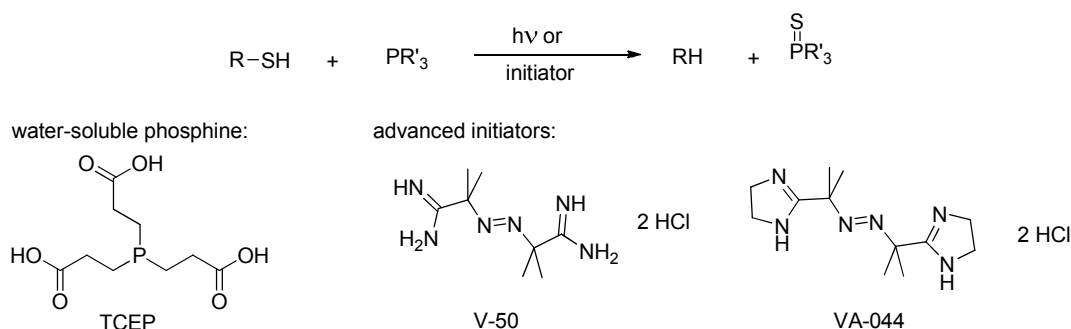
Removal of sulfur to obtain alkanes is interdisciplinarily investigated. Desulfurization reactions or hydrodesulfurizations are applied for example in the purification of fuels^[61] as well as in tailor-made peptides.^[62] These synthetic peptides are often formed using native chemical ligation, in which two smaller peptide fragments are connected via cysteine. When the HS-group of the cysteine residue is undesired, it has to be removed specifically under bio-orthogonal reaction conditions.



Scheme 17. Native chemical ligation of two peptides followed by desulfurization.

This radical desulfurization occurs generally with tributylphosphine or triethylphosphite initiated by light or a radical initiator like AIBN (scheme 18). Since peptides are normally well soluble in water but only poorly soluble in organic solvents, water-soluble phosphines (e. g. TCEP) and initiators (V-50 or VA-044) were developed. To support this metal-free version of desulfurization, catalytic amounts of sulfur containing additives, such as ^tBuSH, EtSH or glutathione, can be added.^[62] These

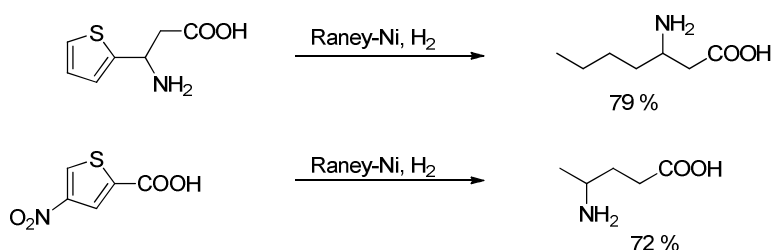
additives will start the radical reaction together with the initiator, when the initiator alone is insufficient. Once sulfur radicals are formed, the reaction will go on smoothly.



Scheme 18. Radical desulfurization of thiols.

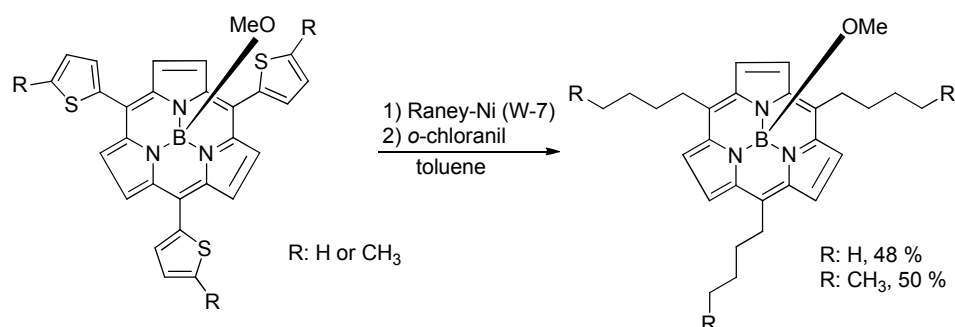
Alternatively, metal-based variants of this desulfurization were reported using palladium on different solid supports, such as alumina, barium sulfate or charcoal,^[63] or Raney Nickel in the presence of hydrogen,^[63] although sulfur is known to be poisonous for these catalysts. Such metal-based hydrogenation catalysts were also required for the hydrodesulfurization of fuels whose sulfur impurities are mainly aromatic compounds like thiophenes.^[61] To receive the corresponding sulfur-free alkyl chain, two reactions are required: hydrogenation and desulfurization. Local-density-functional calculations and *ab initio* simulations of the reactivity of thiophene on Pt (111)^[64] or Ni (110)^[65] indicate direct desulfurization via C-S bond cleavage first, followed by hydrogenation of the double bonds.

Gol'dfarb and co-workers already screened in the late 1950s several thiophene derivatives in the desulfurization reaction, proving the tolerance of amines and carboxylic acids.^[66] Nitro groups were reduced simultaneously under the hydrogenating reaction conditions. The desulfurized products were obtained in good yields.



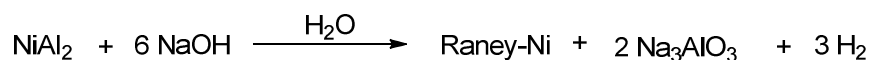
Scheme 19. Desulfurization of functionalized thiophene derivatives by *Gol'dfarb* and co-workers.

Furthermore, *Hayashi* used the desulfurization reaction with Raney Nickel (W-7 type) for the introduction of alkyl chains at subporphyrins yielding 48-50 % of the threefold alkylated products.^[67] Since Raney Nickel also hydrogenates some important double bonds of the subporphyrin, reoxidation to keep the unsaturated scaffold was necessary.



Scheme 20. Threefold desulfurization of subporphyrins by *Hayashi* and co-workers.

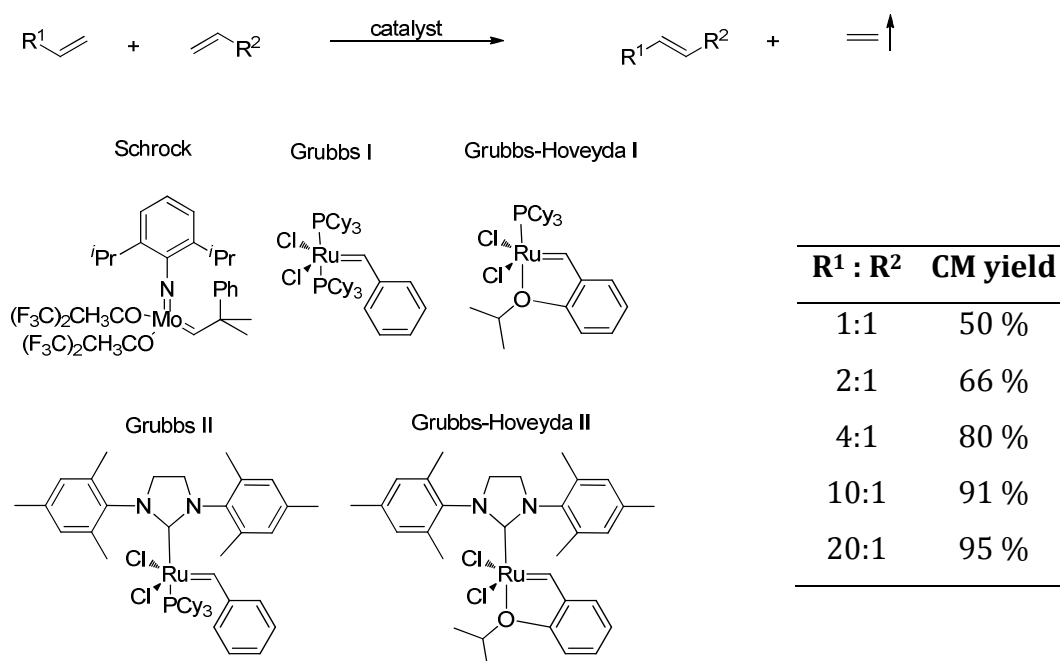
Activated Raney Nickel can be categorized into 7 different generations W-1 up to W-7, all types differing in reaction time for Raney-Ni synthesis and workup conditions.^[68] *Murray Raney* reported the first Raney-Ni catalyst in 1927 without immobilization of the metal on a surface.^[69] W-2 to W-7 type Raney Nickel catalysts are advancements of this first catalyst and show in general increased reactivity mainly to varying functional groups. In parallel, its stability decreases. These catalyst generations must be synthesized shortly before use and cannot be stored over a longer period. Another very important fact is their extremely high inflammability increasing with the catalyst generation. All Raney Nickel catalysts incorporate emerging hydrogen during its synthesis from nickel-aluminium alloy under basic conditions (scheme 21). Due to the highly pyrophoric properties of all Raney Nickel catalysts they were only stored and handled as suspension. Stating the exact amount of catalyst for a reaction is therefore impossible.



Scheme 21. General synthesis of Raney Nickel.

2.4.3 Olefin cross-metathesis

In 2005, *Yves Chauvin, Robert H. Grubbs and Richard R. Schrock* received the Nobel Prize in chemistry for the development of the metathesis reaction as an alternative for metal-mediated coupling reactions.^[70] Apart from polymerisations and ring closing reactions, two alkenes can be coupled via cross-metathesis (CM) using standard catalysts at low loading to yield a new alkene and ethene.^[70] Due to the lack of selectivity, a mixture of homocoupling and cross products can occur. Hence, an excess of one olefin is necessary to reach acceptable yields. A main advantage is the high tolerance of functional groups in the cross-metathesis using Grubbs-type catalysts. Protecting groups are normally not required.



Scheme 22. General cross-metathesis with common catalysts.

Based on a categorization of alkenes by *Chatterjee* and co-workers into four types of olefins makes the olefin cross-metathesis fairly predictable.^[71] Depending on the catalyst used, olefins have to be re-categorized. In table 1 the most important olefins are classified for the use in cross-metathesis with Grubbs II catalyst.

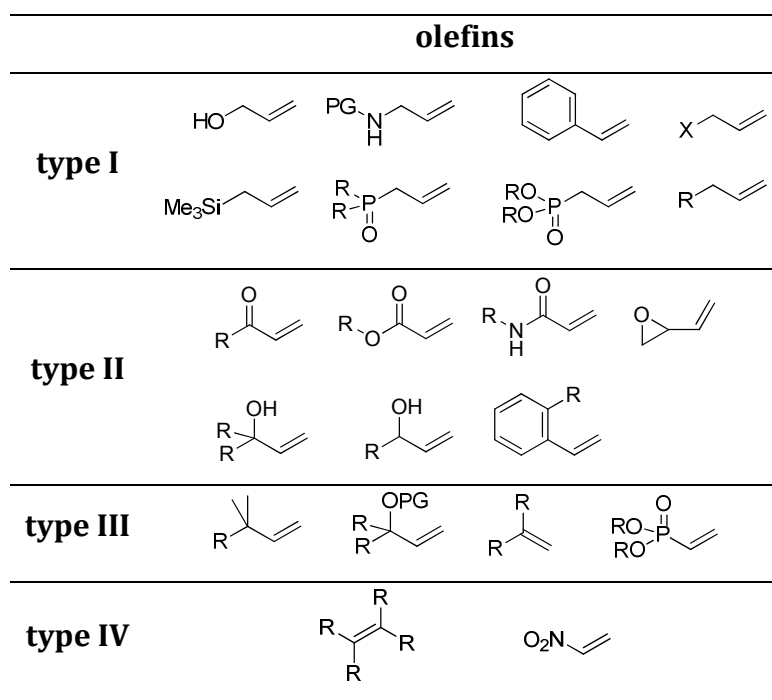


Table 1. Categorization of olefins in cross-metathesis with Grubbs II catalyst. R: alkyl, X: halogen, PG: protecting group.^[71]

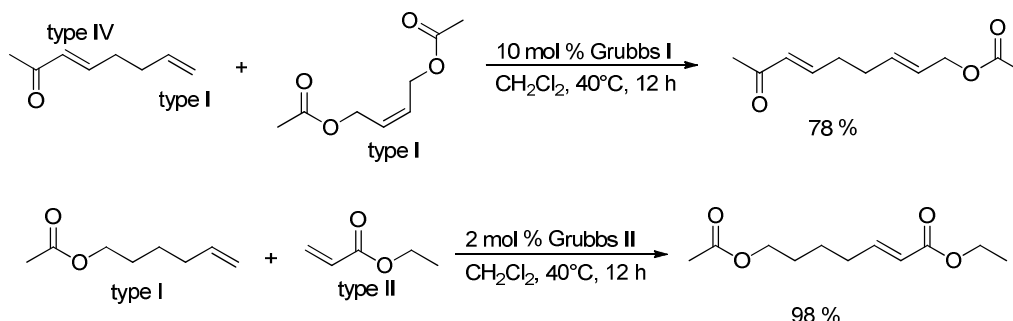
In general, one can conclude that from type I to type IV olefins steric demand increases and electronic density decreases. Along with that order reactivity of olefins in cross-metathesis decreases. Type IV olefins do not interfere with the catalyst, respectively, they do not undergo cross-metathesis with any type of olefin.

Type I olefins are highly reactive and therefore perform rapid homodimerization. When two type I olefins undergo metathesis the product consists of a statistical mixture of all homodimerized and cross products with *cis* and *trans* configuration. Nevertheless, this type of olefins can be used selectively with type II or III olefins by forming the homodimerized product first and allowing it to react with the type II or III alkene in a cross-metathesis reaction. Type II olefins undergo slow cross-metathesis with type III olefins. A *cis/trans* mixture of cross-products will be obtained by letting react two type II or two type III olefins.

	type I	type II	type III	type IV
type I	statistical			
type II	selective CM	non-selective CM		
type III	selective CM	slow CM	non-selective CM	
type IV	no CM	no CM	no CM	no CM

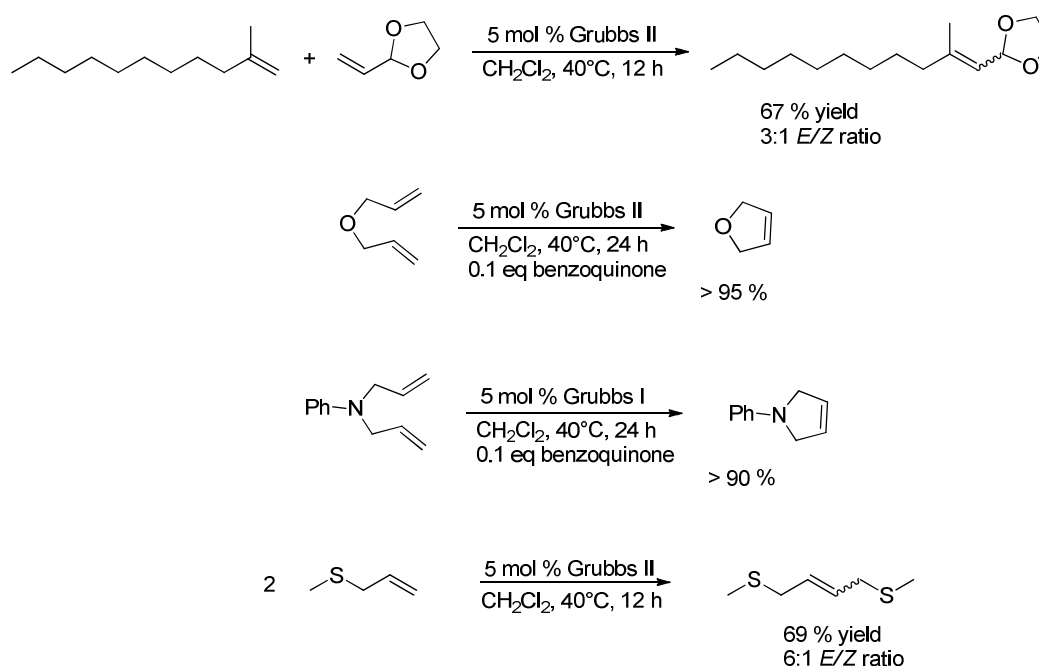
Table 2. Grubb's model of selectivity. ^[71]

Based on this information, olefin cross-metathesis products can be obtained by choosing the right catalyst and suitable olefins.^[71,72] Furthermore, olefins can be modified to change their category and meet the requirements for a selective cross-metathesis.



Scheme 23. Non-selective and selective olefin cross-metathesis.

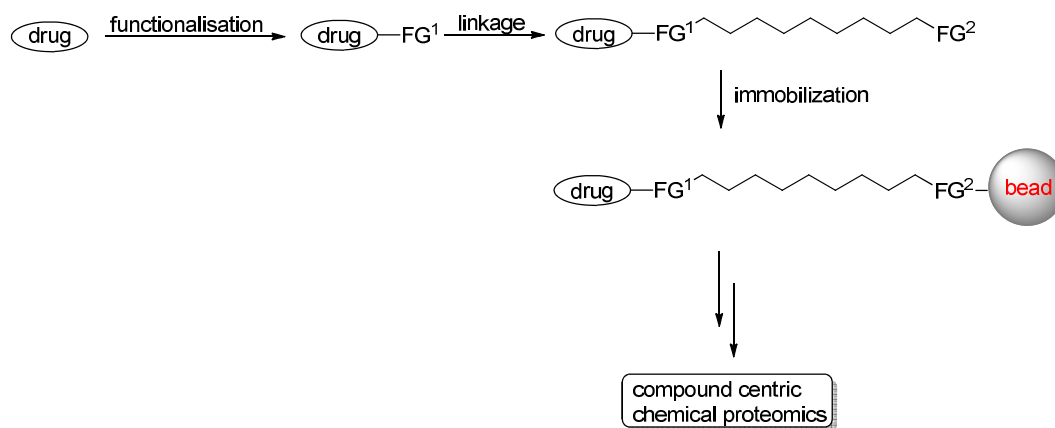
Alkyl chain type alkenes undergo olefin cross-metathesis in high yields under standard conditions.^[72] The high distance of functionalities from the reactive double bond is conspicuous. Cross-metathesis reactions with allylated ethylene glycol derivatives, which are perfect scaffolds for linkers, have not been investigated effectively yet. Nevertheless, a few cross-metathesis or ring closing metathesis reactions were reported containing functional groups related to ethers close to the reactive double bond.^[71,73] These alkenes undergo metathesis smoothly under standard conditions with Grubbs II catalyst.



Scheme 24. Olefin metathesis with heteroatoms close to the reacting double bond.

3. Aims of the dissertation

There is still a great demand for a general methodology to identify all protein targets of a drug without trial-and-error tests with animals and at later stage with human beings. As this is a well-known problem in medicinal chemistry, researchers already developed a possible solution, named compound-centric chemical proteomics. By tethering active molecules via linker to a solid support, ideally all types of binding proteins could be identified. This screening method in combination with state-of-the-art techniques enables an early recognition of off-targets. Additionally, the number of *in vivo* tests of emerging drugs might be decreased. On that account, a general linkage method for tethering small molecules of interest is highly desired. But as this is illusionary, different linkage methods for each compound class have to be evaluated, which is still challenging. One focus of this thesis is devoted to the development and establishment of general covalent linkage methods. Taking advantage of newly developed chemical reactions, i. e. dehydrogenative cross-coupling, linkage without prior functionalization of the drug should be possible.



Scheme 25. Drug tethering for the immobilization of drug compounds onto solid supports.

These linkage methods have to meet the following requirements:

- i) the method has to be as effective as possible including high-yield reactions,
- ii) the last reaction step of the linkage method should enable an easy purification of the linked drugs,
- iii) functionalization and linkage must be orthogonal to all other functional groups of the drugs,

- iv) the drugs have to be linked at a position of the molecule, that will not reach into the active site of the investigated enzyme and
- v) it would be advantageous, if covalent functionalization of the drugs before linkage can be avoided.

In collaboration with CeMM researchers in Vienna who screened the tethered drugs by the compound-centric chemical proteomics approach, we chose thalidomide (**1**), pomalidomide (**2**) and lenalidomide (**3**) as examples for the development of basic drug linkage methods. These drugs are known to possess adverse but also promising and useful biological activities. Since their mode of action still remains undiscovered, identification of the protein targets is of great interest. For that reason, thalidomide (**1**), pomalidomide (**2**) and lenalidomide (**3**) had to be synthesized in this thesis using literature known procedures.

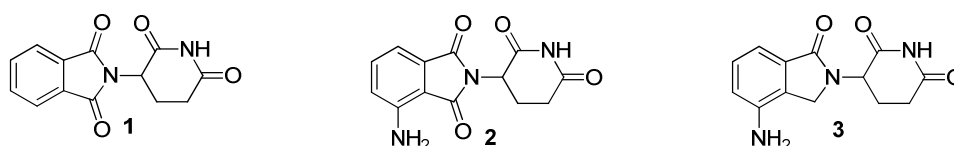


Figure 12. Structures of thalidomide, pomalidomide and lenalidomide.

Furthermore, orthogonally functionalized linkers that react primarily with thalidomide (**1**) and its derivatives **2** and **3** had to be synthesized. Moreover, these linkers are designed in a way to enable a general attachment onto this compound class. The linker synthesis should be flexible and allow choosing any linker length of interest.

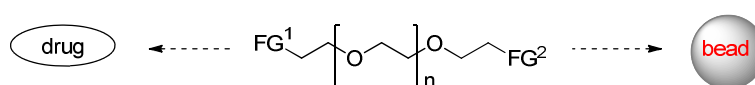


Figure 13. General linker structure.

Additionally, another important aim of this thesis was the isolation and characterisation of a cytotoxin produced by *K. oxytoca* bacteria. As this natural product not only causes gastro-intestinal diseases with sometimes lethal consequences, it is important to identify this cytotoxin, its molecular targets and its mode of action. Biological studies of the isolated cytotoxin were performed in collaboration with the Institute of Molecular Biosciences at the University of Graz.

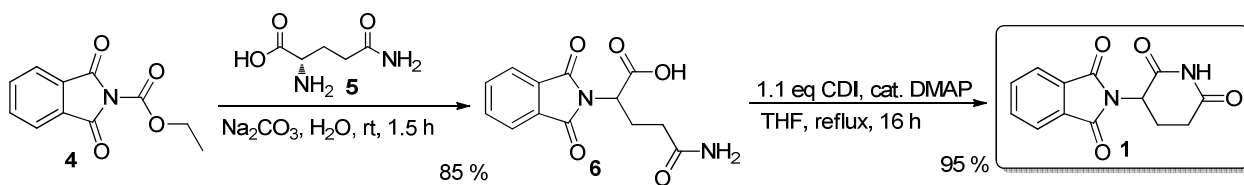
4. Results and discussion

4.1 Drug syntheses

Before we were able to start developing and testing our linkage strategies, we had to synthesize the drugs that should be investigated with chemical proteomics screening. Therefore, we chose thalidomide (**1**) and its promising derivatives pomalidomide (**2**) and lenalidomide (**3**). Even after 50 years of research, these drugs remain of great interest because of their high potential in the treatment of several diseases, although a clarification of their mechanism of action is still pending. The identification of the drug's entire protein targets starts with the synthesis of the drugs itself.

4.1.1 Synthesis of thalidomide (**1**)

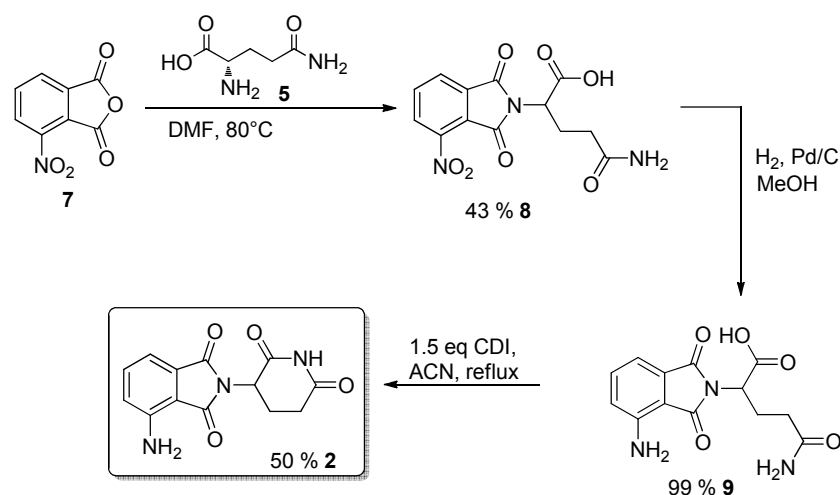
Thalidomide (**1**) can be synthesized quite easily via two steps according to the literature protocol from *Muller et al.*^[74] The reaction of L-glutamine (**5**) with phthalimide derivative **4** under basic conditions yielded 85 % of the product **6** after precipitation under acidic conditions. After activation of the acid **6** with carbonyl diimidazole (CDI), glutamine derivative **6** cyclized intramolecularly to thalidomide (**1**) in 95 % yield, again precipitated from the reaction mixture. Fortunately, we obtained thalidomide (**1**) in an overall yield of 81 % in two steps, following the procedure of *Muller* and co-workers who received an overall yield of only 61 %. Although starting with the enantiomerically pure L-glutamine (**5**), we were not interested in an enantioselective synthesis of thalidomide (**1**), as this has been intensively investigated in the last decades.



Scheme 26. Synthesis of thalidomide (**1**).

4.1.2 Synthesis of pomalidomide (2)

Pomalidomide (**2**) was synthesized according to the patent of *Ge* and co-workers in 2007, who produced pomalidomide (**2**) on a 5 kg scale.^[75] This was achieved in three steps. Coupling of L-glutamine (**5**) with nitro-substituted phthalic anhydride **7** yielded 43 % of precipitate **8**. Hydrogenation of the nitro group to form the amino derivative **9** proceeded quantitatively. The last step, an intramolecular cyclization, is similar to the synthesis of thalidomide (**1**), but yielded only 50 % of pomalidomide (**2**) as a yellow solid. This synthesis step bears potential for optimization, but yields were adequate to test this drug in a chemical proteomics approach.

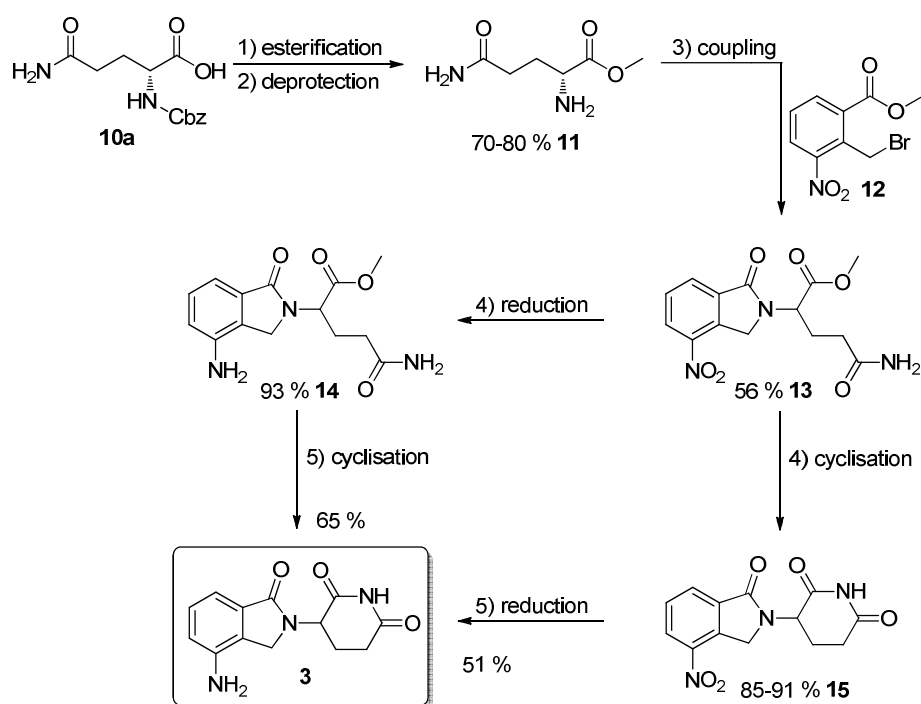


Scheme 27. Synthesis of pomalidomide (**2**).

4.1.3 Synthesis of lenalidomide (3)

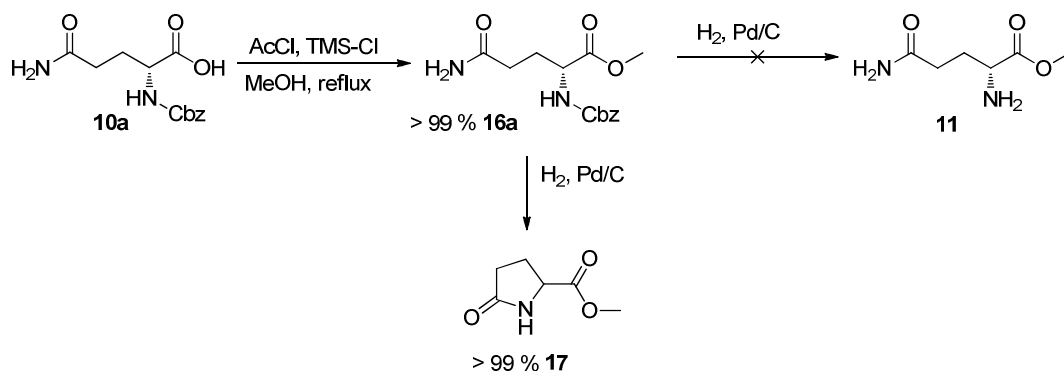
The synthesis of lenalidomide (**3**) was much more challenging. Inspired by a patent from *Muller* and co-workers from 2006, showing a complete synthesis sequence, we decided to test their route (scheme 28).^[76] Starting from *N*-Cbz-glutamine **10a** they methylated the carboxylic acid in 75 % yield. After Cbz-deprotection with 5 % Pd/C under 40 psi hydrogen atmosphere they coupled crude methyl glutamine **11** with benzyl bromide derivative **12** in the presence of triethyl amine to yield 56 %. Finally, two possible ways to lenalidomide (**3**) were mentioned. Hydrogenation of the nitro group followed by intramolecular cyclization or cyclization under basic conditions followed by hydrogenation, were described. Most notably, the coupling of the aromatic building

block **12** with glutamine ester **11** and the last step in both routes are the yield limiting reactions.



Scheme 28. Synthetic route of Muller *et al* toward lenalidomide (**3**).

Analogously to Muller and co-workers, we started with the esterification of *N*-Cbz-glutamine **10a**, using methanol and catalytic amounts of acetyl chloride and trimethylsilyl chloride to obtain the methyl ester **16a** quantitatively. In fact, we were able to improve their reaction yield. Unfortunately, Cbz-deprotection of the amine **16a** never led to glutamine methyl ester **11**. Instead, we always observed an immediate intramolecular cyclization of the free amine to the five-membered cyclic amide **17** under these reaction conditions.



Scheme 29. Spontaneous intramolecular cyclization during Cbz-deprotection.

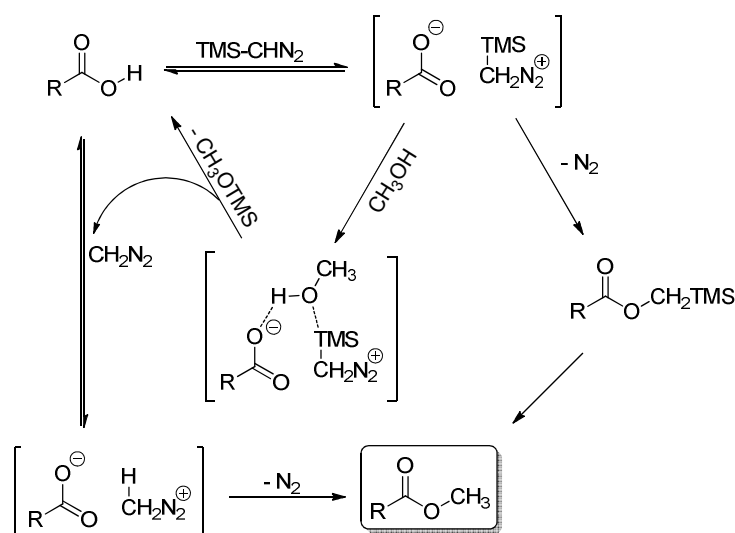
To solve this problem, we decided to change the protecting group from Cbz to Boc. Removal of Boc-protecting group occurs under acidic conditions, under which the resulting free amine will immediately form the corresponding ammonium salt **19**, which is supposed to be inert to this unintended cyclization reaction. Unexpectedly, the esterification of *N*-Boc-glutamine **10b** turned out to be associated with a lot of problems. Under the same reaction conditions as for *N*-Cbz-glutamine **10a**, the conversion of *N*-Boc-glutamine **10b** after 7 days was just 50 %. With sulfuric acid and CaSO₄ in methanol double esterification occurred, meaning that the side chain amide was also converted.



PG	Esterification conditions	Conversion
Cbz	cat. TMSCl, AcCl, MeOH, reflux, 5 h	quantitative
Boc	cat. TMSCl, AcCl, MeOH, reflux, 7d	< 50 %
Boc	H ₂ SO ₄ , CaSO ₄ , MeOH	double esterification
		 18
Boc	TMS-CHN ₂ , Et ₂ O/MeOH 4:1	95 %

Table 3. Methyl ester formation of *N*-protected glutamines **10**.

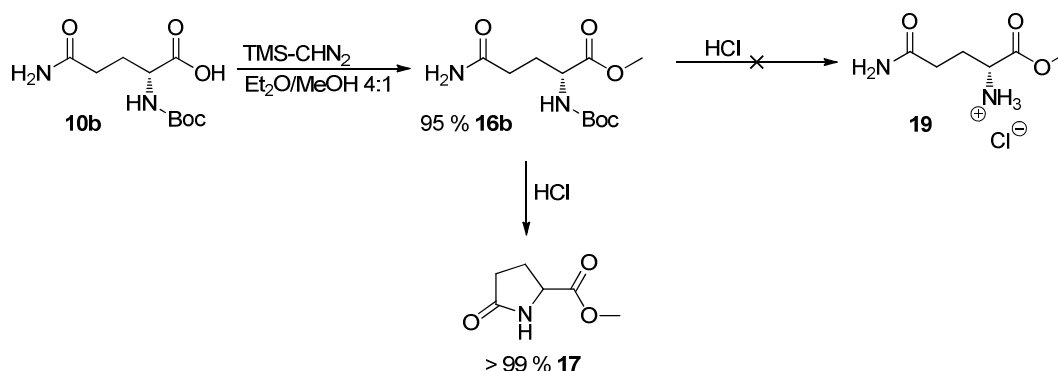
Luckily, *N*-Boc-glutamine **10b** underwent quantitative esterification with TMS-diazomethane in a methanolic solution according to the procedure of *Castonguay* and co-workers.^[77] The mechanism for this esterification was first proposed in 2007 by *Kuehnel* and co-workers.^[78] As TMS-diazomethane (b.p. 96°C) has an increased stability compared to diazomethane (b.p. -23°C), it is less harmful and easier to handle. But due to the mechanism for methyl esterification of acids by TMS-diazomethane, one should be aware of the very toxic and explosive diazomethane being liberated *in situ* anyway.



Scheme 30. Proposed mechanism of the methyl esterification of carboxylic acids with TMS-diazomethane in toluene with 20 % methanol.

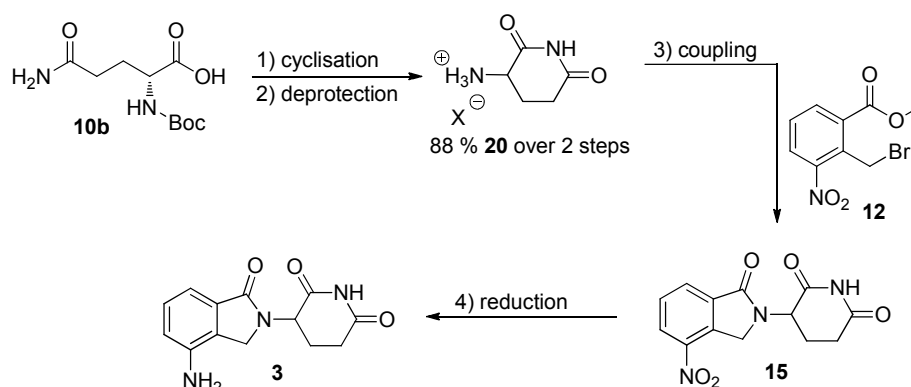
Nevertheless, this method is a rapid transformation toward methyl esters as carboxylic acids immediately react with TMS-diazomethane. The color of this reagent serves as an indicator for the progress of conversion when titrated to the colorless carboxylic acid solution. Full conversion is achieved when the solution stayed yellow, which can also be proved by TLC. Final evaporation of the solvent resulted in pure methyl ester **16b**. Although the esterification with TMS-diazomethane is dangerous and should be handled with utmost care, it is a very smooth reaction.

Unfortunately, the second step, deprotection of the amine **16b**, again resulted in an intramolecular cyclization to the amide **17**, which is in sharp contrast to the description of *Castonguay* and co-workers.^[77] As a consequence, we had to change our synthetic route toward lenalidomide (**3**).



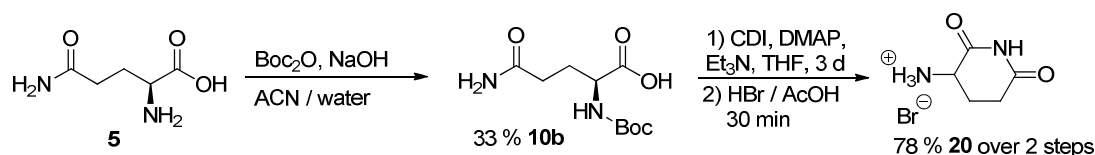
Scheme 31. Intramolecular cyclization during Boc-deprotection.

In 2009, *Nakamura et al* reported the preparation of the saturated building block **20** of lenalidomide (**3**) via a controlled intramolecular cyclization to the six membered ring followed by deprotection of the amine to form the hydrobromide salt **20** in 88 % overall yield.^[79] Already in 2007, *Stewart* and co-workers published the synthesis of this saturated building block **20** in 72 % overall yield as triflate salt.^[80] Fortunately, this strategy avoids the formation of the undesired five membered ring **17**. This saturated building block **20** was then coupled to benzyl bromide derivative **12** by a double substitution at the exocyclic amino group followed by hydrogenation of the nitro group to form lenalidomide (**3**).



Scheme 32. Synthetic route of *Nakamura et al* toward lenalidomide (**3**).^[79]

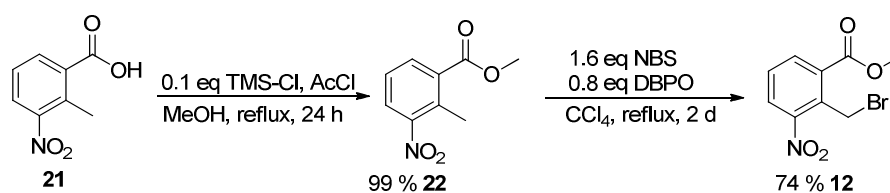
In our synthesis, we introduced the Boc-protecting group into L-glutamine (**5**) under standard conditions following the Organic Syntheses procedure of *Keller* and co-workers to obtain 33 % of *N*-Boc-glutamine **10b**.^[81] The next step was the intramolecular amide formation. After deprotection and precipitation as hydrobromide, the saturated cyclic building block **20** was furnished in 78 % yield over two steps.



Scheme 33. Synthesis of the saturated cyclic building block **20**.

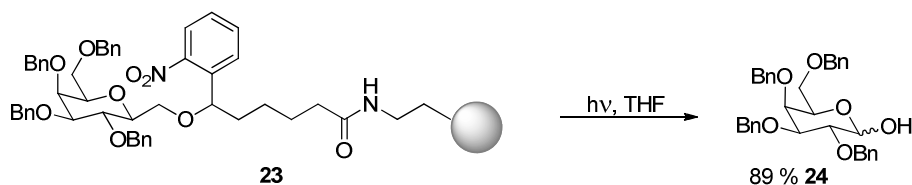
The aromatic building block **12** was synthesized in two steps starting with the esterification of 2-methyl-3-nitro-benzoic acid (**21**). As the first esterification attempt with sulfuric acid in methanol remained incomplete, catalytic amounts of TMSCl and acetyl chloride in methanol were added to the benzoic acid derivative **21** to finally yield the methyl ester **22** in 99 %. Bromination of the *ortho*-methyl group was performed

under standard conditions with NBS and DBPO as initiator to yield the aromatic building block **12** in 74 % yield.



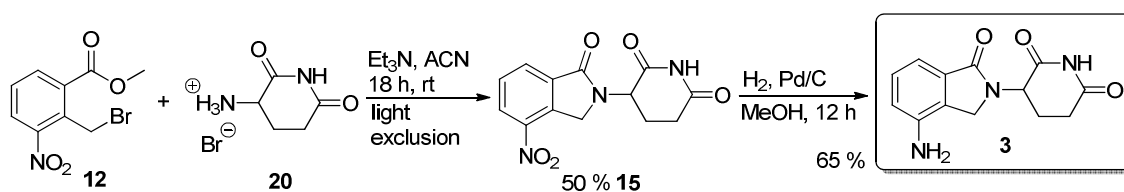
Scheme 34. Synthesis of the aromatic building block **12**.

Coupling of the arene **12** and the saturated cyclic building block **20** by double substitution at the amine group according to the patent of *Devarakonda* and co-workers^[82] required some optimization steps and was found to be only satisfactory under the exclusion of light. In the presence of light, the aromatic building block **12** decomposed. This reactivity is reasonable, since similar motifs are used as photocleavable linkers in organic synthesis. *Rodebaugh* and co-workers, for example, published the cleavage of a galactose derivative **23** via *ortho*-substituted nitrobenzene linker from a solid support in the presence of light yielding 89 % of the free galactose derivative **24**.^[83]



Scheme 35. Photocleavage using a nitrobenzene linker by *Rodebaugh* and co-workers.

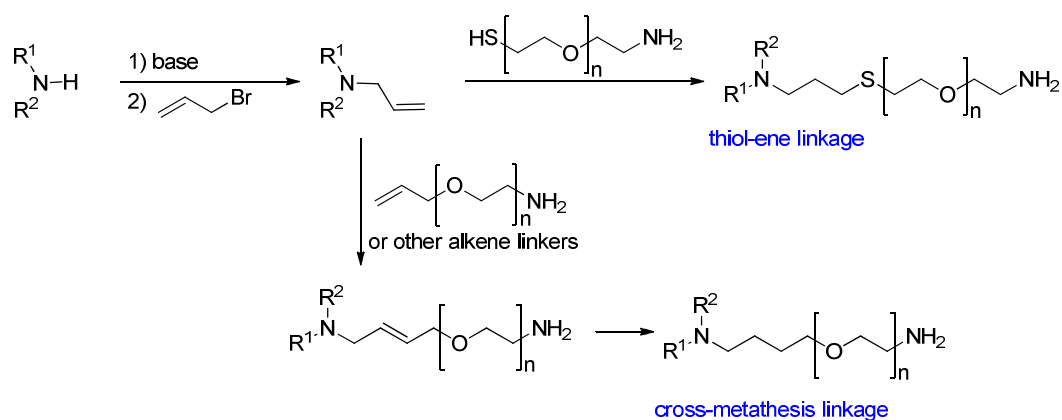
Nevertheless, in the dark we received 50 % of pure product **15**. Final hydrogenation of the nitro-group yielded lenalidomide (**3**) in acceptable 65 % yield as a yellow solid.



Scheme 36. Synthesis of lenalidomide (**3**).

4.2 Linkage strategies

To develop and proof our linkage strategy, we chose the previously synthesized drugs thalidomide (**1**), pomalidomide (**2**) and lenalidomide (**3**) because unravelling their protein targets is still of great interest. If possible, our linkage strategies were tested and optimized with thalidomide (**1**), as this was the easiest derivative to synthesize in larger amounts. Three different linkage points of thalidomide (**1**) were already found to be unsuitable in chemical proteomics screenings by CeMM researchers. We were therefore looking for another immobilization position. Structure activity relation studies of CeMM researchers indicated that the aromatic part of thalidomide (**1**) reaches deepest into the binding pocket of the unknown enzymes. To meet the situation best, we developed two new strategies for the linkage at the saturated cyclic building block using the NH-functionality. These strategies were named thiol-ene linkage approach and cross-metathesis linkage approach. Both methods are supposed to be universal for a wide range of small molecules containing a free functionality for allylation and subsequent linkage.



Scheme 37. Two general linkage strategies based on terminal allyl groups.

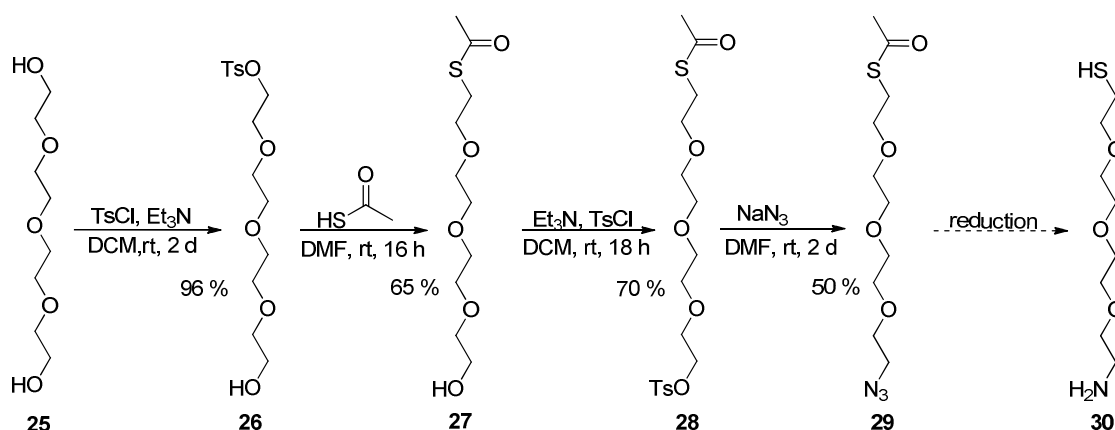
4.2.1 Thiol-ene linkage strategy

In this first linkage approach, the linker is formed in two steps. For introduction of the linker, a reactive functionality is necessary. Our idea was to use an allyl group as it should be easily introduced in NH groups via allylation. As a second step, the addition of a linker type thiol, e. g. cysteamine (**36**), is envisioned. This reaction is expected to lead to a sole product, which facilitates the final purification.

4.2.1.1 Thiol-linker synthesis

To have access to diverse linker lengths, a flexible thiol-linker synthesis is required as only a few bifunctional thiols of interest are commercially available. Furthermore, more polar linkers are preferred, so we chose a thiol-functionalized ethylene glycol chain with an amine at the other end. The ethylene glycol chain can be varied in its length depending on the spatial requirements for drugs to enter the active site of a protein.

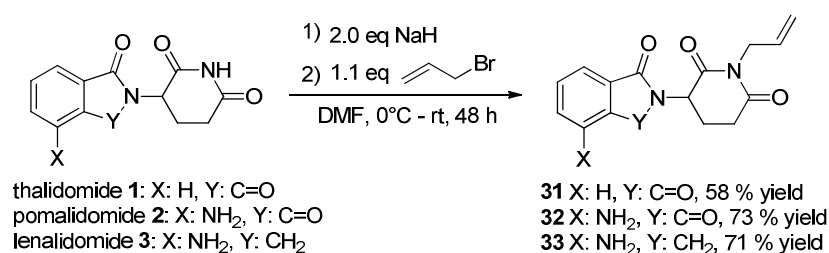
For our linker synthesis, we used the protocol from *Stefanko* and co-workers who investigated a series of tetraethylene up to dodecaethylene glycols.^[24] They obtained their thiol linker in five steps with an overall yield of 49 %. Since we needed a defined linker length, we chose tetraethylene glycol (**25**) as starting material. Selective tosylation of one hydroxy group worked smoothly with a yield of 96 % of monotosylated tetraethylene glycol (**26**). Fortunately, only little double tosylation occurred. The thioacetate **27** could only be obtained in 65 % yield, presumably because of its high volatility that caused a significant loss. As the reaction had to be carried out in DMF, the thioacetate **27** evaporated partly with DMF during workup. Nevertheless, tosylation of the free hydroxy group led to 70 % yield and after nucleophilic substitution with sodium azide 50 % of azide **29** were furnished. Due to air sensitivity of the thiol linker **30**, the last step, the double reduction with LiAlH_4 , is supposed to be performed just before coupling it to the allylated drugs. However, this was not investigated anymore, because the biological studies had in the meanwhile already proofed that our cysteamine linker had an appropriate length. But if a longer linker is needed, this would be an excellent route with the opportunity to vary the length of linkers by selecting different types of ethylene glycols.



Scheme 38. Synthesis of the thiol linker **30** from tetraethylene glycol (**25**).

4.2.1.2 Alkylation

As thalidomide (**1**) has only little solubility in almost all solvents, the alkylation had to be carried out in DMF. Deprotonation of the imide **1** could be monitored by GC-MS after quenching of the basic solution with D₂O. As expected, sodium hydride mediated deprotonation was sufficient regardless whether the 60 % dispersion or the pure, freshly washed, sodium hydride was used. As anticipated, double deprotonation of thalidomide (**1**) was obtained. Deprotonation with sodium *tert*-butoxide was incomplete even in large excess of the base and after several days reaction time.



Scheme 39. *N*-allylation of thalidomide (**1**), pomalidomide (**2**) and lenalidomide (**3**).

Because of the poor solubility of compounds **31-33**, their purification was quite tricky. Normal column chromatography was insufficient as the products **31-33** precipitated on silica gel. Interestingly, preparative TLC in contrast was successful. The crude product **31** could be applied onto the preparative TLC plate as DMF solution, but due to the poor solubility in the eluent, recovery of allyl-thalidomide **31** from the TLC plate was low. Much more effective was the crystallization or precipitation from DMF and cyclohexane, which yielded pure allyl-thalidomide **31** in 58 %.

In analogy, pomalidomide (**2**) and lenalidomide (**3**) were allylated by the same strategy. As crystallization of the substrates **32** and **33** was pretty difficult, we successfully applied preparative thin-layer chromatography (PTLC) to isolate 73 % of allyl-pomalidomide **32**, respectively 71 % of allyl-lenalidomide **33**. Remarkably, both compounds showed fluorescence after excitation with UV-light at 366 nm.

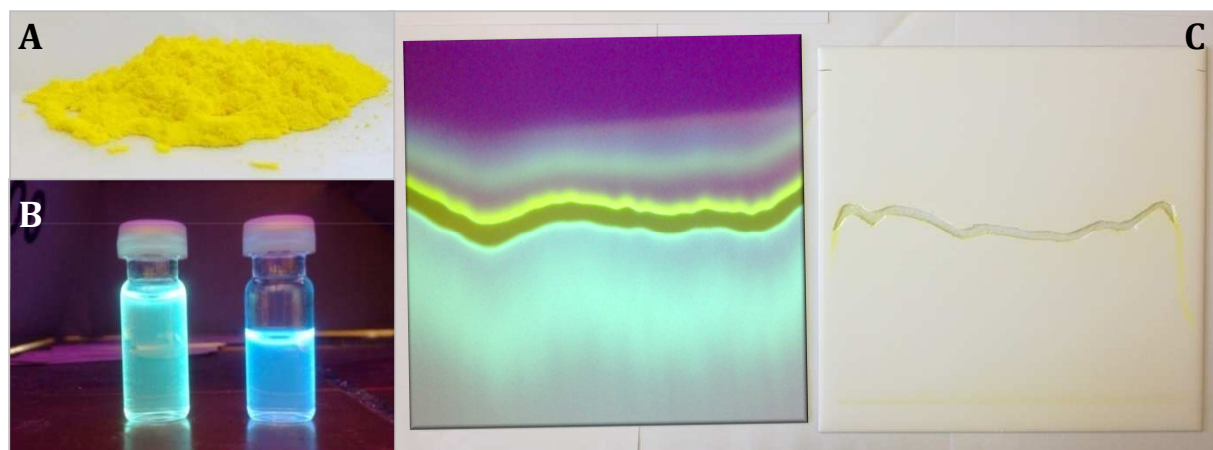
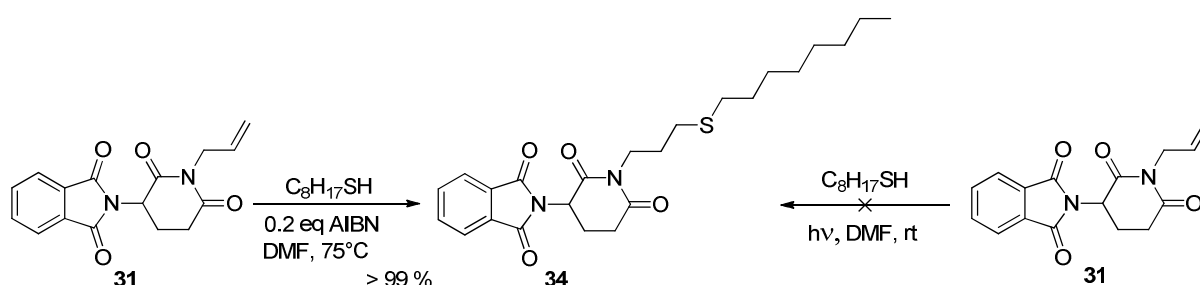


Figure 14. A: Pomalidomide (**2**); B: pomalidomide (**2**) (left) and allyl-pomalidomide **32** (right) dissolved in methanol at 366 nm radiation; C: PTLC-plate of allyl-pomalidomide purification at 366 nm radiation (left) and at visible light (right).

4.2.1.3 Thiol-ene reaction

The second step of this linkage strategy used a thiol-ene reaction to attach the linker to the allyl-functionalized drug **31-33**. For this radical reaction, initiation with light or radical starter AIBN at 75°C was tested using a simplified system containing octanethiol (**87**) as this compound bears no further functional groups that might interfere. Our light source was a standard 150 W Superlux lamp from Philips, which was positioned in a distance of 20 cm to the Schlenk tube to avoid any uncontrolled heating of the reaction mixture originating from the lamp. Nevertheless, the reaction with light as initiator showed no conversion of allyl-thalidomide **31** due to an insufficient activation of the radical thiol-ene reaction. Luckily, with radical starter AIBN under heating, full conversion could be confirmed by TLC monitoring.



Scheme 40. Thiol-ene reaction of allyl-thalidomide **31** with octanethiol (**87**).

As we had now proved our concept, we switched to more useful linkers. Cysteamine (**36**) was our first candidate to build a short linker. However, this amino reagent made

troubles during the reaction. With a pK_a in the range of 8-11, primary aliphatic amines and aliphatic thiols do not differ significantly. Under basic conditions the thiol will be deprotonated and the negatively charged sulfur cannot undergo homolytical radical cleavage, as proposed for the radical mechanism. Comparison of NMR-spectra of cysteamine (**36**) and cysteamine hydrochloride (**35**) in deuterated DMSO indicated that cysteamine (**36**) contains a NH_3^+ -group, visible as broad singlet, but with a different chemical shift as in cysteamine hydrochloride (**35**). We therefore speculated that a thiol-ene reaction with cysteamine (**36**) cannot take place as it is supposed to be an internal salt.

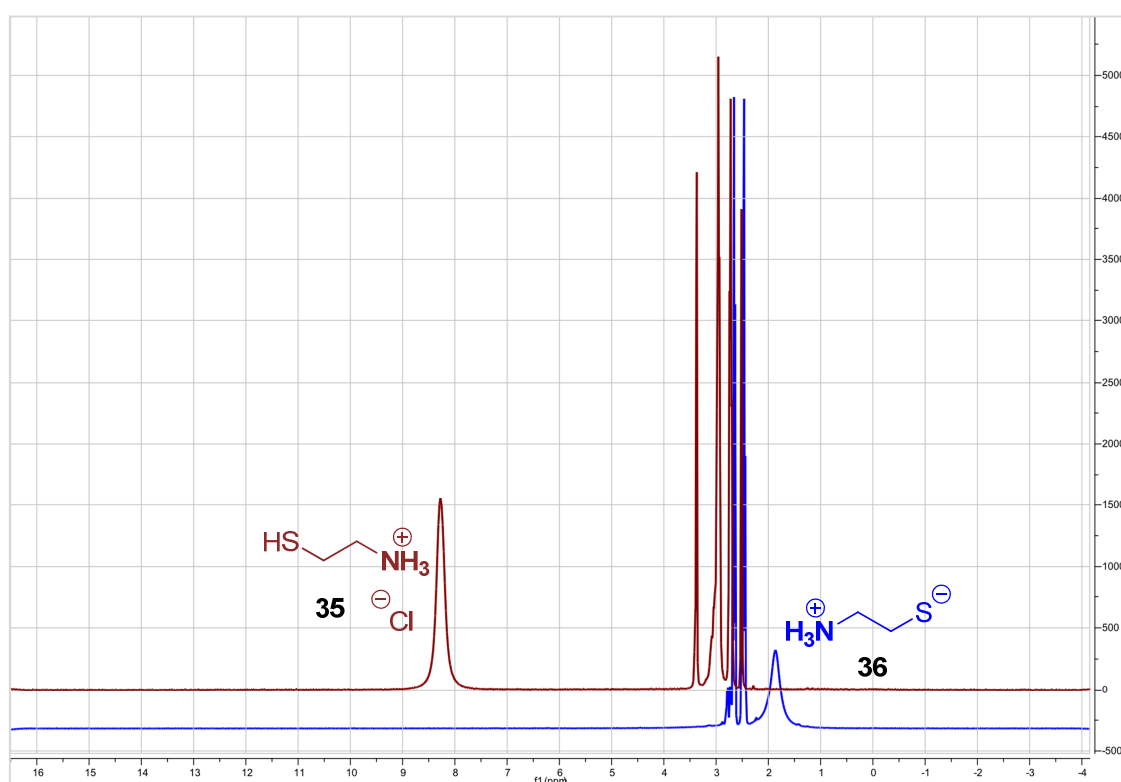
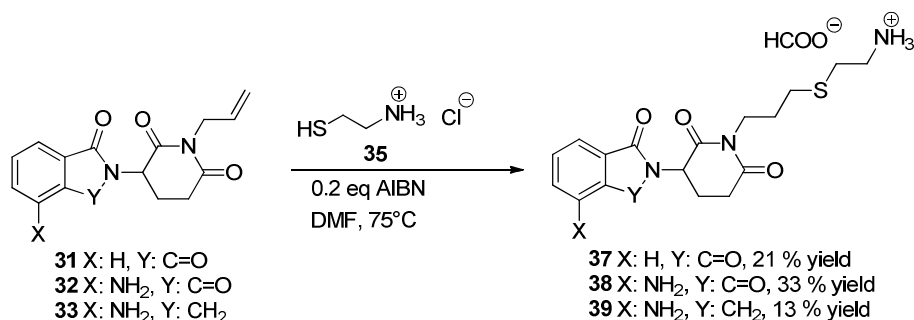


Figure 15. 1H -NMR of cysteamine (**36**) (blue) and cysteamine hydrochloride (**35**) (red) in $DMSO-d_6$.

This theory is supported by our results, where allyl-thalidomide **31** showed absolutely no conversion with cysteamine (**36**) under our optimized reaction conditions. To prevent the amino group from deprotonating the thiol, we applied cysteamine as hydrochloride **35**. With this linker we now received full conversion of allyl-thalidomide **31** and after purification of the crude product by preparative HPLC we could isolate 21 % of pure linked thalidomide **37**. Due to the 0.01 % formic acid buffer used in one of the eluents, the hydrochloride was exchanged by formate. Analogously, to the thiol-ene reaction with allyl-thalidomide **31**, allyl-pomalidomide **32** and allyl-lenalidomide **33**

also underwent this reaction with cysteamine hydrochloride (**35**) to obtain the linked products **38** and **39** with 33 % and 13 % yield.



Scheme 41. Thiol-ene reaction of allyl-thalidomide **31**, allyl-pomalidomide **32** and allyl-lenalidomide **33** with cysteamine hydrochloride (**35**).

Surprisingly, the linked lenalidomide **39** was not stable during purification and oxidized to the very stable linked pomalidomide **38**, as monitored by HPLC-MS (figure 16). This oxidation could not be prevented during the preparative HPLC purification. Interestingly, pure lenalidomide (**3**) and the allylated lenalidomide **33** were stable compounds. A reason for that instability might be a dependence of the oxidation on the pH value. Lenalidomide (**3**) is formed under neutral and allylated under basic conditions. The thiol-ene reaction was conducted under neutral conditions. During HPLC-MS reaction monitoring no pomalidomide derivative **38** could be detected. But the aqueous eluent for preparative HPLC contained 0.01 % formic acid with a pH of 3.40. Possibly, an excess of water could also be responsible for the instability. However, an air-sensitivity of the linked lenalidomide **39** is more likely the reason for the oxidation perhaps even initiated by light. All reactions were carried out under inert conditions except for the purification. Extraction and purification of allyl-lenalidomide **33** by preparative TLC in the presence of air did not result in an oxidation although the silica gel on the TLC plate is slightly acidic. There is no evidence for cysteamine hydrochloride (**35**) to be responsible for the oxidation. Nevertheless, 64 % of the linked pomalidomide **38** were isolated from the thiol-ene reaction of the allylated lenalidomide **33**.

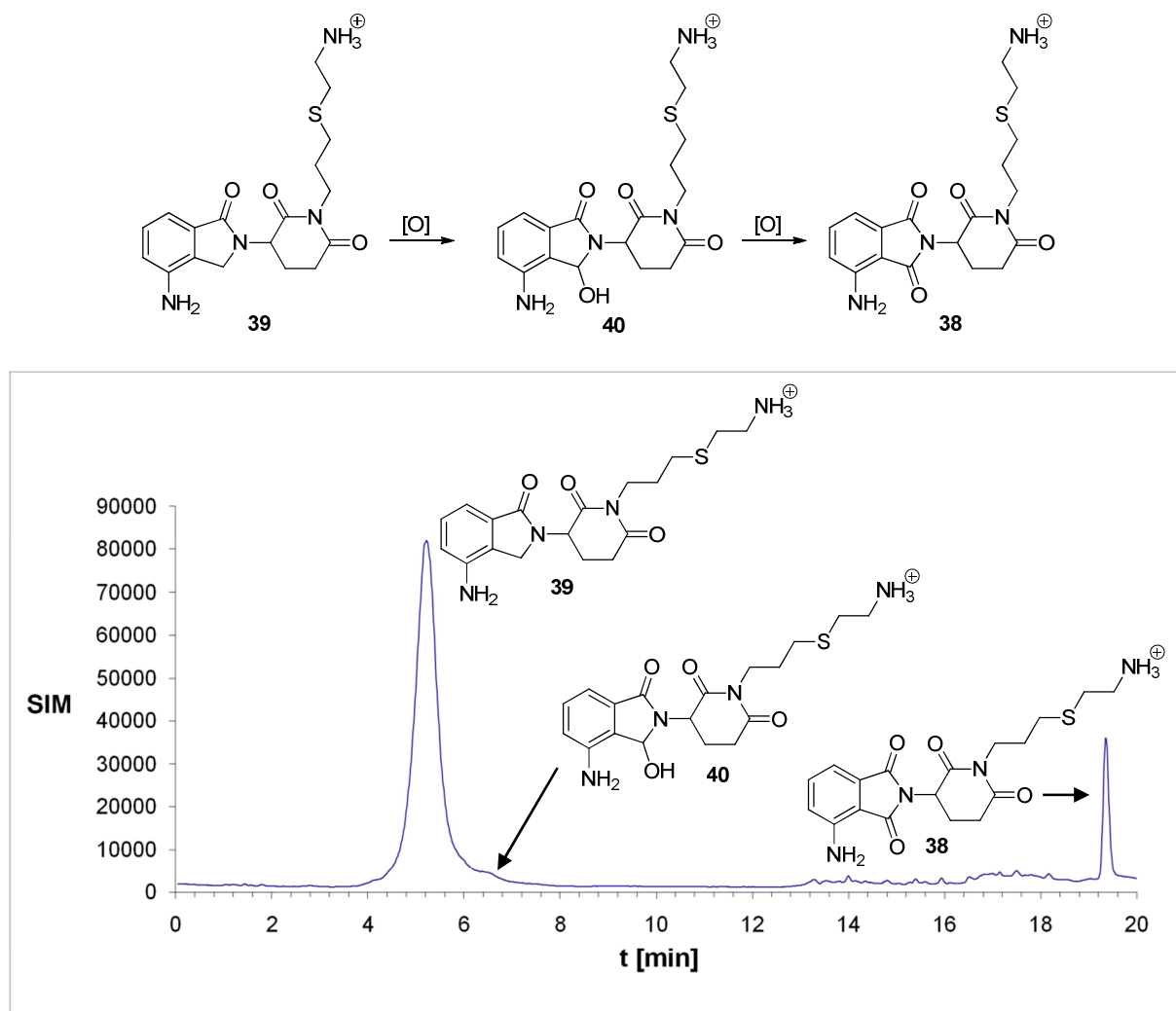


Figure 16. MS-Chromatogram of the linked lenalidomide **39** during oxidation to the linked pomalidomide **38** in two steps. HPLC-method D.

4.2.1.4 Chemical Proteomics screening

All linked drugs **37-39** were screened for protein targets in a compound-centric chemical proteomics approach. For this purpose, specialists at the CeMM in Vienna optimized the incubation time, drug load on the beads and the protein amount and concentration to successfully increase the signal-to-noise ratio. Nine different cell types were tested, that are supposed to be responsible for the myelodysplastic syndrome or multiple myeloma. 14 differently tethered thalidomides, pomalidomides and lenalidomides based on four different linker attachment points were tested. Our three synthesized, linked drugs **37-39** were included in the test series. Two different immobilization strategies were chosen, direct covalent immobilization to an inert matrix

or biotinylation and binding to streptavidin beads. Additionally, two types of negative control (unrelated drug and drug competition) were used in parallel and two buffer systems were tested. Altogether 38 drug affinity purifications were made and analyzed by mass spectrometry or anti-biotin immunoblot and silver stain analysis.

Using our linked drugs **37-39** in this compound-centric chemical proteomics screening, CeMM researchers were able to identify a multiple myeloma cell line (OPM-2), which showed affinity to pomalidomide (**2**) and lenalidomide (**3**), but not to thalidomide (**1**). Our linked drugs **37-39** were suitable for immobilization and drug affinity chromatography but, unfortunately, no protein target could be enriched by any drug in comparison to the negative control.

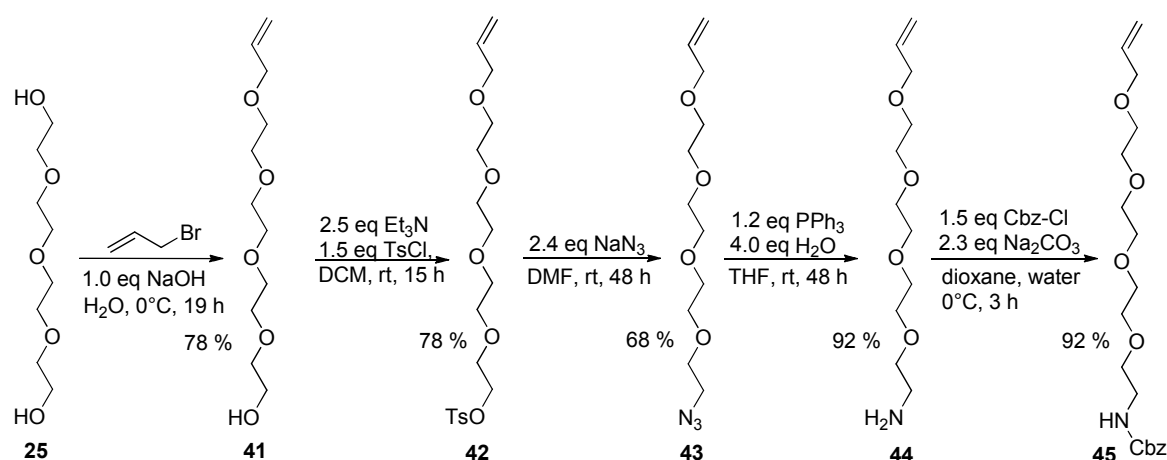
One possible reason for the negative result in the chemical proteomics screening might be that the target of these drugs **1-3** is not a protein but for example a lipid or a nucleic acid. Although CCCP can detect proteins in nanomolar range, possibly proteins were enriched only below its detection limits. The class of thalidomide drugs is known to be chemically and metabolically unstable. Maybe an active metabolite led to a wrong positive result at the beginning. As a consequence, chemical proteomics is possibly the wrong choice for the identification of thalidomide's targets. It is also conceivable that an interference of the linker with the binding of a target protein was present. This undesired target-linker interaction would recede when the drug is much larger than the linker. Furthermore, we assume that the labile cell extracts for chemical proteomics induced the negative result. Regarding the past research on thalidomide (**1**) and its derivatives over the last decades, the aim to identify thalidomide's protein targets remains a tough challenge.

4.2.2 Cross-metathesis linkage strategy

In our second approach, we tried to introduce an allyl-linker in an olefin cross-metathesis reaction. Since the resulting double bond might be hindering for a linked drug as free rotation is constrained, hydrogenation will terminate this reaction sequence. In this linkage strategy we could again use our previously allylated drugs **31-33**. Additionally, we synthesized an allylated tetraethylene glycol linker.

4.2.2.1 Allyl-linker synthesis

The allyl-linker for olefin cross-metathesis was synthesized analogously to the thiol linker **30**. Starting from tetraethylene glycol (**25**), one hydroxyl group was selectively allylated with 78 % yield. Subsequently, the second hydroxyl group was tosylated, substituted by an azide and reduced to the amine in a Staudinger reduction to yield the allyl-linker **44** in 38 % over four steps. Additionally, the terminal amino group was Cbz-protected to yield 92 % of the Cbz-protected allyl-linker **45**.



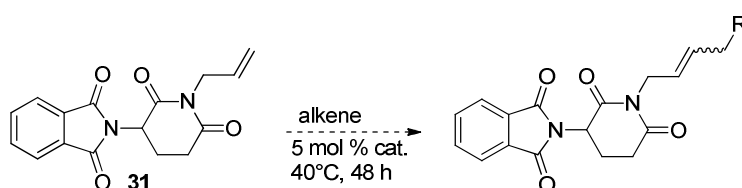
Scheme 42. Synthesis of the allyl-linker **44** from tetraethylene glycol (**25**).

4.2.2.2 Olefin cross-metathesis screenings

As model substrate, we again used our allylated thalidomide **31**. Categorization of allyl-thalidomide **31** analogously to the system by *Chatterjee* and co-workers is difficult. It might be classified as type I olefin but with increased sterical hindrance. Since our allylated linker **44** is linear it might also belong to type I olefins in cross-metathesis reactions with Grubbs II catalyst. If both are type I olefins, the allyl-linker **44** should rapidly but not selectively react with allyl-thalidomide **31**. In that case, homocoupling products might be problematic since they decrease the yield and complicate purification. However resulting *E/Z* mixtures would be acceptable, because they will anyway be reduced to the corresponding alkane in the last step of the linkage strategy. Unfortunately, ethers and allylated imides are hardly described in literature for olefin cross-metathesis and are therefore not yet categorized. For that reason, this olefin cross-

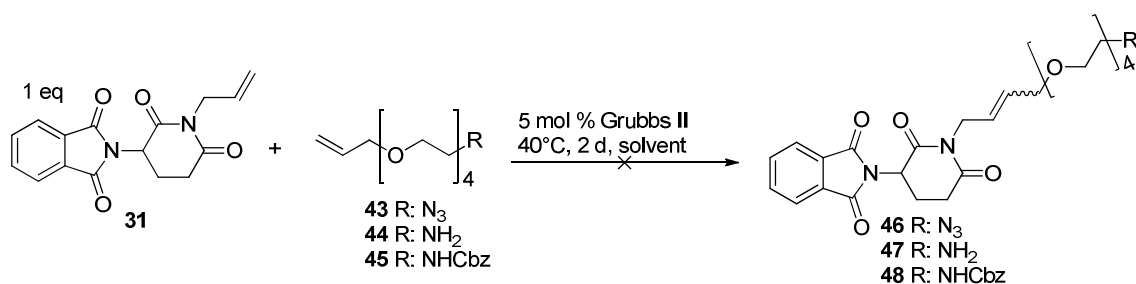
metathesis is not really predictable and we have to determine empirically to which category our olefins **31** and **44** belong.

In the first olefin cross-metathesis screening we used 5 mol % Grubbs II catalyst. Its *N*-heterocyclic carbene ligand is a strong σ -donor and poor π -acceptor. Compared to Grubbs I catalyst, the second generation Grubbs catalyst is more stable and better soluble and therefore allows rougher reaction conditions. All reactions were carried out at 40°C for two days and were monitored by TLC and HPLC-MS.



Scheme 43. Cross-metathesis of allyl-thalidomide **31** with linker-like alkenes.

We started with the screening of four different solvents, namely dichloromethane (DCM) and dichloroethane (DCE) as it is known that yields in olefin cross-metathesis reactions were higher in chlorinated solvents,^[70,71] dimethylformamide (DMF) as our starting material **31** is only in DMF completely soluble and tetrahydrofuran (THF) as alternative. We also tested the dependence of different equivalents of alkenes starting from a 1:1 ratio up to 1:3. Finally we changed our allylated linker. We screened the free amine **44**, the Cbz-protected amine **45** and the azide **43** as the latter ones can be reduced to the amine in an one pot reaction during hydrogenation of the newly formed double bond. Results of this first cross-metathesis screening are shown in table 4.



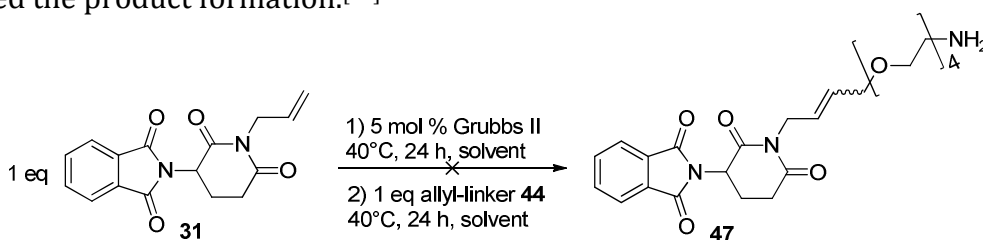
Entry	Linker	Equivalents	Solvent
1	44	3	DCM
2	44	3	DMF
3	44	3	DCE
4	44	3	THF

5	44	2	THF
6	44	2	DCM
7	45	1	DCM
8	45	1	DMF
9	43	1	DCM
10	43	1	DMF

Table 4. First olefin cross-metathesis screening with Grubbs II catalyst.

Unfortunately, no olefin cross-metathesis occurred. This might be due to steric hindrance of the well embedded allyl-group of allyl-thalidomide **31**. Nevertheless, the different reactivity of allyl-thalidomide **31** in these reactions was conspicuous. Interestingly, in DCE and THF no reaction took place neither product formation nor consumption of the starting materials **31** or **43-45**. Homocoupling products could also not be identified. Although in reactions with DCM and DMF no cross-metathesis product **46-48** could be obtained, some other reactions took place. This could be visualized via TLC and HPLC-MS.

So we went on with our screening and changed the order of addition of allylated substrates **31** and **44**. Previously, we had put everything in one portion into a Schlenk tube, but now we did let the allylated thalidomide **31** react with the catalyst for one day and subsequently added the allylic linker **44**. In this reaction setup allyl-thalidomide **31** is supposed to form a homodimer, corresponding to the reactivity of type I olefins, before reacting with the allyl-linker **44**. In some cases this sequence of the reaction increased the product formation.^[71]

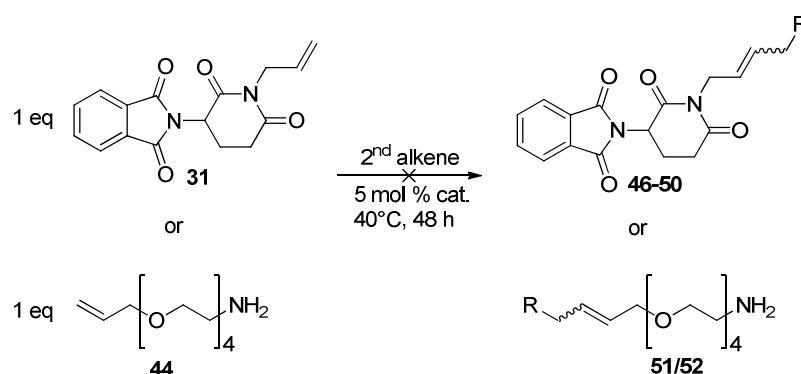


Scheme 44. Solvent screening in the stepwise olefin cross-metathesis with allyl-thalidomide **31** and allyl-linker **44**.

We repeated this reaction with four different solvents (DCM, DCE, DMF and THF), but again no cross-coupling product **47** could be detected. Also homocoupling products were not detectable. Anyway, the order of addition of allyl-thalidomide **31** and linker **44**

did not influence the course of the reaction. Once more, DCM seemed to be the solvent in which any reactivity was detectable.

In the following studies we reduced the number of experiments to those ones with DCM as solvent. We replaced the initial metathesis catalyst by Grubbs-Hoveyda catalyst II, which is even more stable and has an increased activity at once compared to the Grubbs II catalyst. We tested again the amine **44**, the Cbz-protected amine **45** and the azide **43**. Furthermore, we switched to more simple alkenes **53** and **54** that are known to undergo cross-metathesis with a broad range of alkenes^[71] and let them react either with allyl-thalidomide **31** or with the allyl-linker **44**.



Entry	Alkene	2 nd Alkene	Equivalents	Catalyst	Product
1	31	45	3	Grubbs-Hoveyda-II	48
2	31	44	3	Grubbs-Hoveyda-II	47
3	31	43	3	Grubbs-Hoveyda-II	46
4	31	53	1	Grubbs-II	49
5	31	53	3	Grubbs-II	49
6	31	54	1	Grubbs-II	50
7	31	54	4	Grubbs-II	50
8	44	53	1	Grubbs-II	51
9	44	53	4	Grubbs-II	51
10	44	54	1	Grubbs-II	52
11	44	54	4	Grubbs-II	52

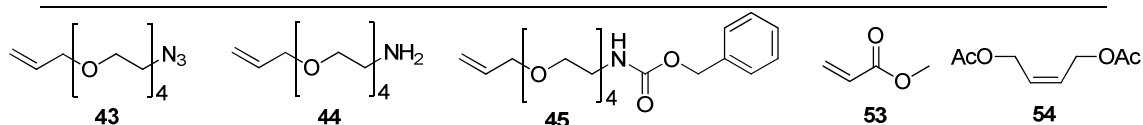
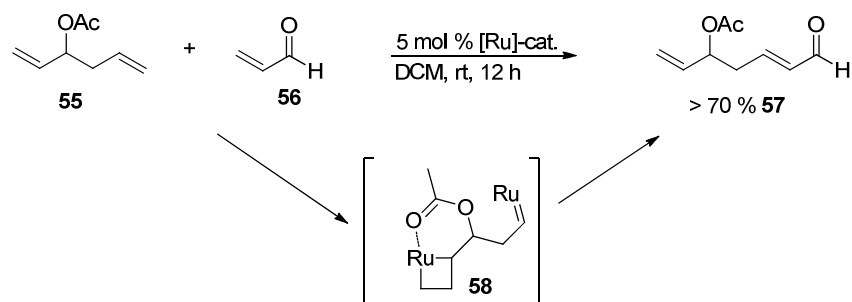


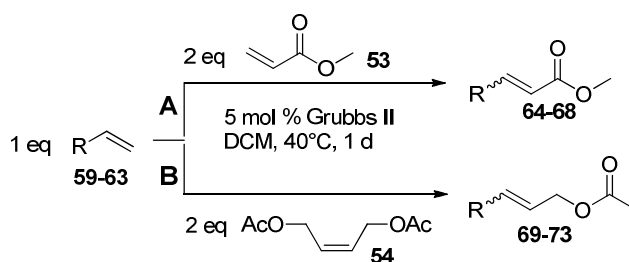
Table 5. Olefin cross-metathesis screening of allyl-thalidomide **31** or allyl-linker **44**.

Again, none of these reaction conditions was successful or showed even a trace of cross-metathesis products **46-52**. Once more, our results indicated steric or electronic influences of our olefins because of several carbonyl and ether groups close to the allyl-functionality. These groups might coordinate to the ruthenium catalyst, which results in inhibition. We found evidence for our hypothesis in a paper of *BouzBouz* and co-workers who made use of this hindrance to distinguish the reactivity of two double bonds (scheme 45).^[84] Under their reaction conditions the Ru catalyst initiated olefin cross-metathesis of hexadiene acetate **55** at both double bonds. But since one double bond was closer to the acetate, its carbonyl group coordinated to the Ru catalyst resulting in its inhibition and loss of reactivity of this double bond. The second double bond of hexadiene acetate **55** then could react smoothly with acrylaldehyde **56** to form the cross-metathesis product **57** in over 70 % yield regioselectively.



Scheme 45. Different reactivity of double bonds in cross-metathesis with Grubbs-Hoveyda II catalyst due to sterical hindrance of carbonyl groups.

If this was really the reason for our decreased reactivity and not our catalytic system, other substrates should undergo olefin cross-metathesis under our conditions smoothly. That is why we went back to less complex substrates (table 6). To prove our reaction conditions A and B (table 6) we chose substrates that are well explored in cross-metathesis reactions.^[71] All conversions were either confirmed by GC-MS or by HPLC-MS. Allylated ethylene glycols **62** and **63**, used in this screening, were synthesized according to the procedure of the allylated tetraethylene glycol linker **44**.



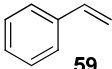
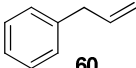
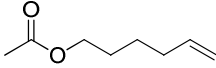
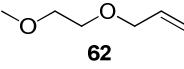
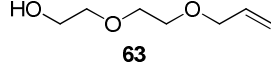
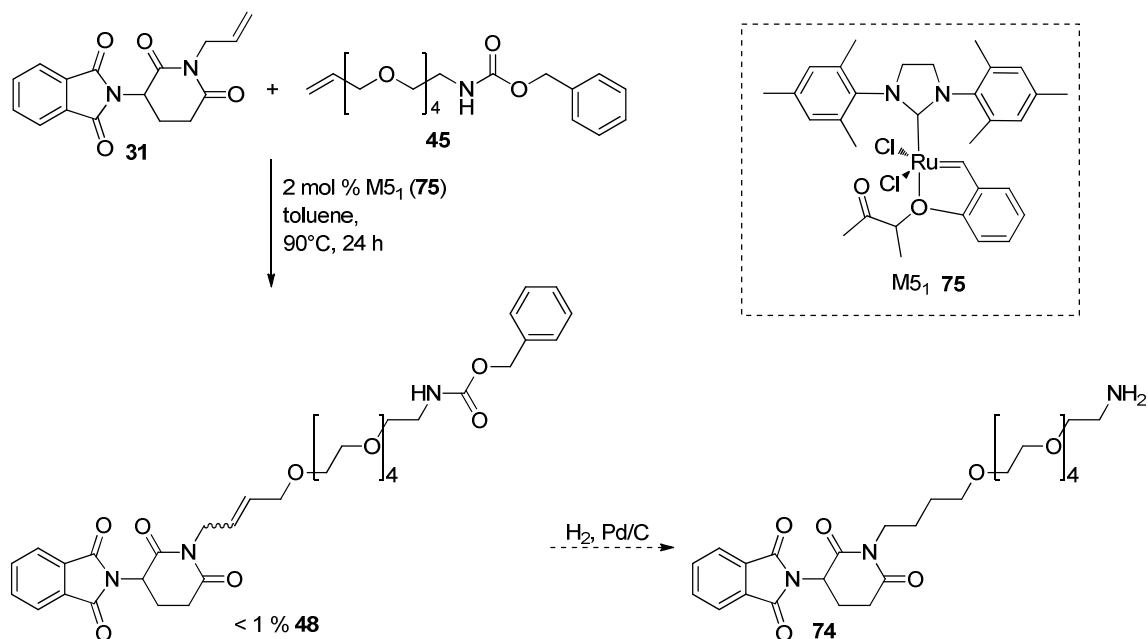
Alkene	Entry	Conversion	Product
 59	A	70 %	64
	B	-*	69
 60	A	40 %	65
	B	5 %	70
 61	A	1 %	66
	B	28 %	71
 62	A	6 %	67
	B	0 %	72
 63	A	0 %	68
	B	0 %	73

Table 6. Screening of alkenes **59-63** in cross-metathesis. Conversion was confirmed via GC-MS or HPLC-MS. *Schlenk tube was broken during the reaction.

Styrene (**59**) and allyl-benzene (**60**) underwent cross-metathesis smoothly. But when we brought one of the alkenes more into line with our linker structure **44**, reactivity decreased dramatically and finally no reaction occurred. This alkene screening showed once more how much the success of cross-metathesis reactions depends on the nature of alkene used. Too many oxygen atoms close to the reacting double bond influence the course of the reaction negatively.

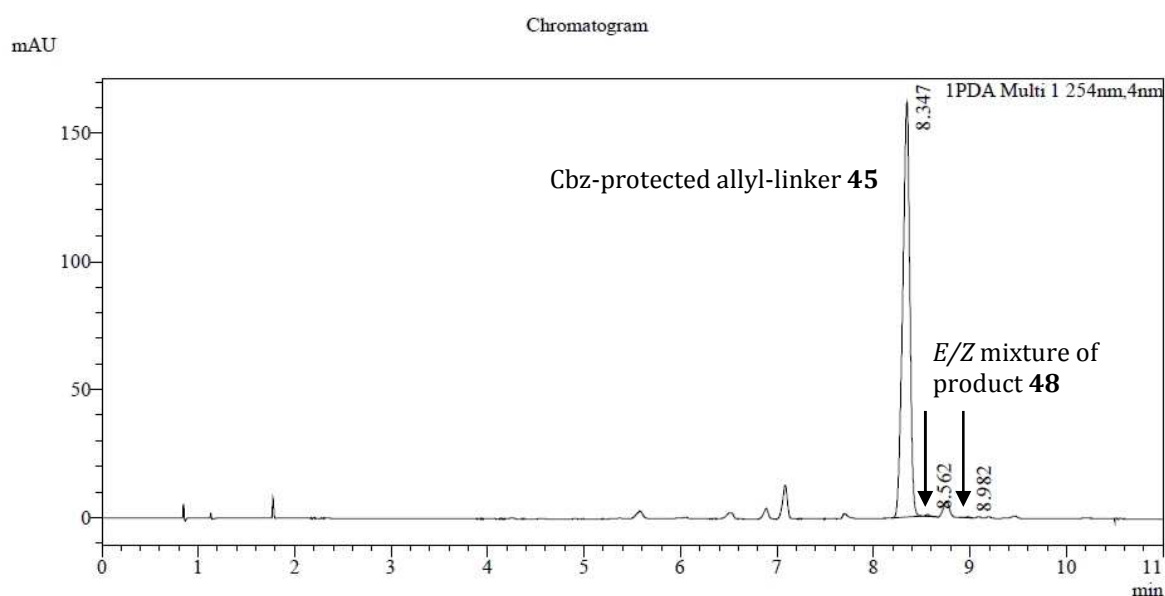
4.2.2.3 Optimized olefin cross-metathesis

As these reaction conditions were not satisfying enough for us, we switched to the more stable and sterically more demanding catalyst M5₁ (**75**). Now we could increase once again the reaction temperature. Because of its strongly coordinating ligands, catalyst inhibition should be prevented or at least dramatically decreased. The reactions were now carried out in toluene or chlorobenzene at 80-90°C. To prevent other side reactions, only the Cbz-protected allyl-linker **45** was tested. To get the equilibrium of the cross-metathesis reaction more to the product side, we tried to get rid of the gaseous ethene by evacuating the Schlenk flask constantly and flushing it with N₂.



Scheme 46. Optimized cross-metathesis linkage of allyl-thalidomide **31** with our allyl-linker **45**.

With these optimized reaction conditions, we were able to detect for the first time the cross-coupling product **48** but the conversion of <math>< 1\%</math> was rather low and could not be improved neither by varying the amount of reactants or catalyst nor by temperature or solvent. Reactions in dichlorobenzene and toluene were identical.



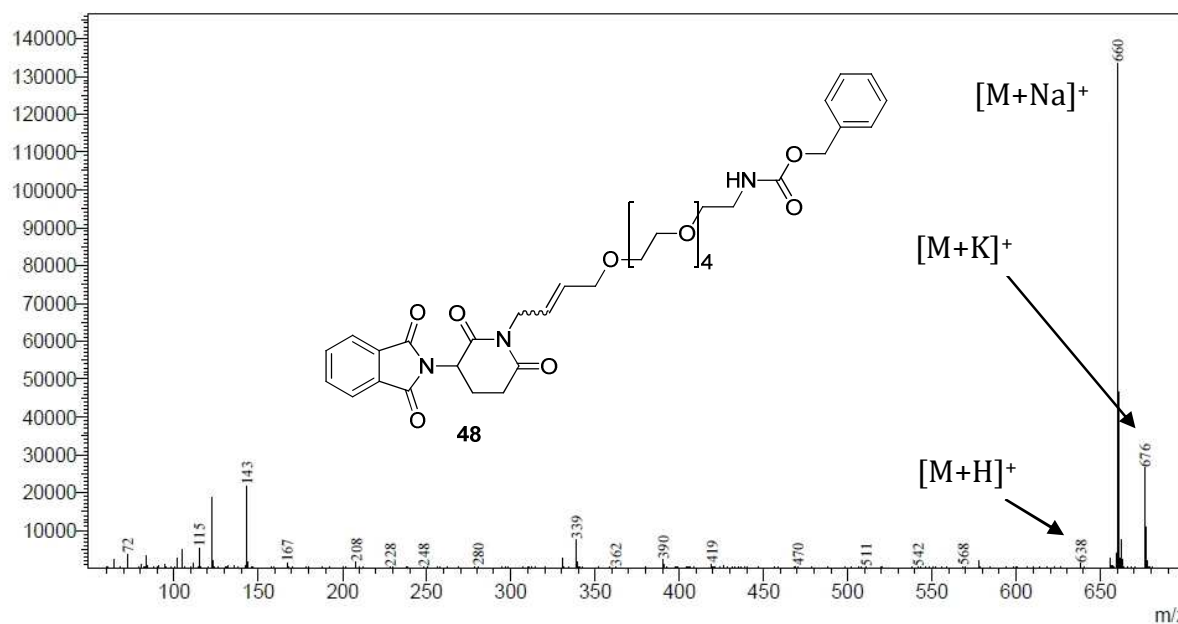
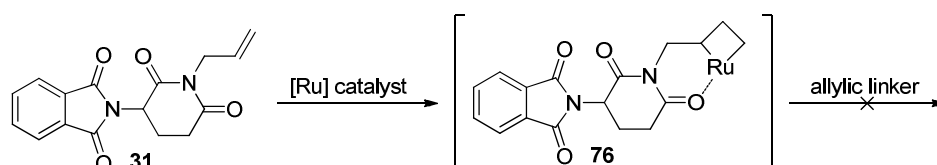


Figure 17. UV-chromatogram and mass spectrum of the cross-metathesis product **48** in the reaction mixture. HPLC-method H, 254 nm.

Nevertheless, we have seen the linked thalidomide **48** via olefin cross-metathesis for the first time. Due to the low reactivity of both alkenes, allyl-linker **45** and allyl-thalidomide **31**, they might be categorized as type II and type III olefins. One of them could alternatively be a type IV olefin, which would not react in the olefin cross-metathesis. Probably this was allyl-thalidomide **31** that additionally inactivated the Ru catalyst upon formation of a stable complex **76** via carbonyl coordination.

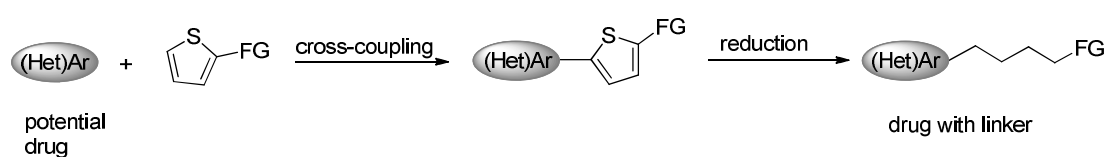


Scheme 47. Possible inactivation of the Ru-catalyst by allyl-thalidomide **31**.

To prove this putative catalyst inhibition, the Ru-allyl-thalidomide complex **76** must be investigated for example via NMR-studies. To confirm the reactivity of the allyl-linker **44**, other drugs should be investigated in the olefin cross-metathesis linkage with a less complex surrounding of the allyl group.

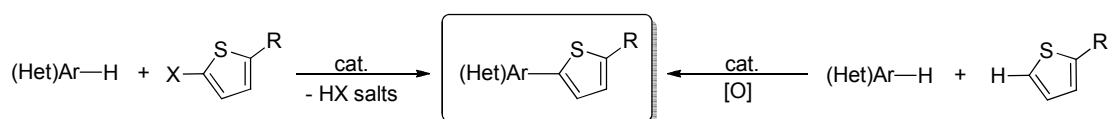
4.2.3 Thiophene-linkage strategy

This third linkage approach introduces the linker again in two steps. Since it is still very challenging to perform a C(sp²)-C(sp³) coupling for a broad range of substrates, our approach starts from coupling of a biologically active molecule, which consists of a heteroaromatic scaffold, with a functionalized thiophene derivative (scheme 48). This cross-coupling reaction is followed by reduction of the thiophene to the corresponding alkyl chain. With this approach it should be possible to form a C(sp²)-C(sp³) bond within two steps.



Scheme 48. Thiophene linkage scheme.

This linkage strategy would only be advantageous if the heteroaromatic scaffold of the biologically active molecule needs no modification prior to linkage. Because of that, transition metal catalyzed cross-couplings via organometallic (hetero)arenes, although they are well described in literature,^[45] should be excluded. Direct arylation might be an opportunity, if only the thiophene derivative carries the functionality, for example a halogen. In this coupling method, the (hetero)aromatic small molecule could be directly arylated via CH-activation.

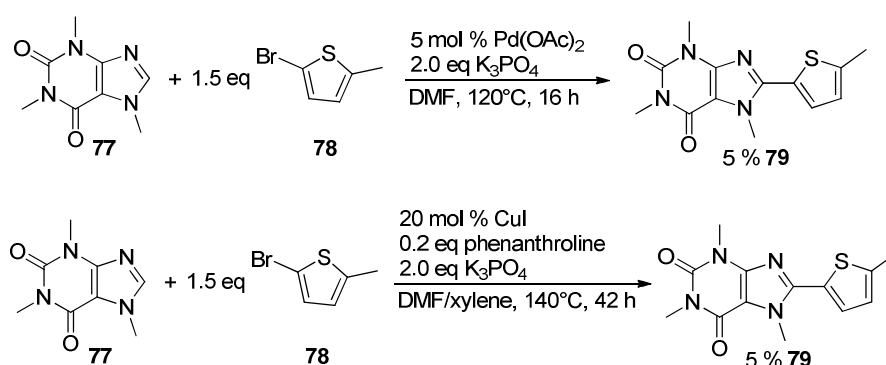


Scheme 49. Direct arylation versus tandem direct arylation.

But the more innovative cross-coupling method would be the tandem direct arylation via double CH-activation. Initial introduction of a good leaving group, such as a halogen, is not necessary anymore. However, an oxidizing agent in equimolar concentrations is required to recover the catalyst.

4.2.3.1 Cross-coupling

For our linkage approach we chose four promising cross-coupling reactions, either direct or tandem direct arylations (schemes 50, 51 and 53). As catalysts, Pd(II) or Cu(I) species were tested. The first two direct arylations were performed analogously to the cross-coupling reaction of caffeine (**77**) and 4-bromotoluene reported by *Zhao* and co-workers.^[46] As model substrate we also chose caffeine (**77**) as it is already well explored. 2-Bromo-5-methylthiophene (**78**) as one of the simplest thiophene derivatives was investigated to ensure no unintended side reactions due to thiophene substituents.



Scheme 50. Onefold direct arylation of caffeine (**77**) with 2-bromo-5-methylthiophene (**78**).

In both direct arylation reactions the cross product **79** was formed. The moderate yields were ascribed to the low conversion. Additionally, dimerization of the thiophene derivative **78** was favored over the cross-coupling in both catalytic systems. With the Cu(I) catalyst 47 % of the thiophene dimer **80** occurred whereas with Pd(II) catalyst 20 % were formed. By adding 0.1 eq pivalic acid to the Pd(II) catalysed reaction, the conversion could be increased considerably, but only the formation of homocoupling product **80** increased to 93 %. Dimerization of caffeine (**77**) did not occur at all.

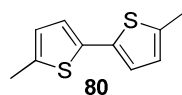
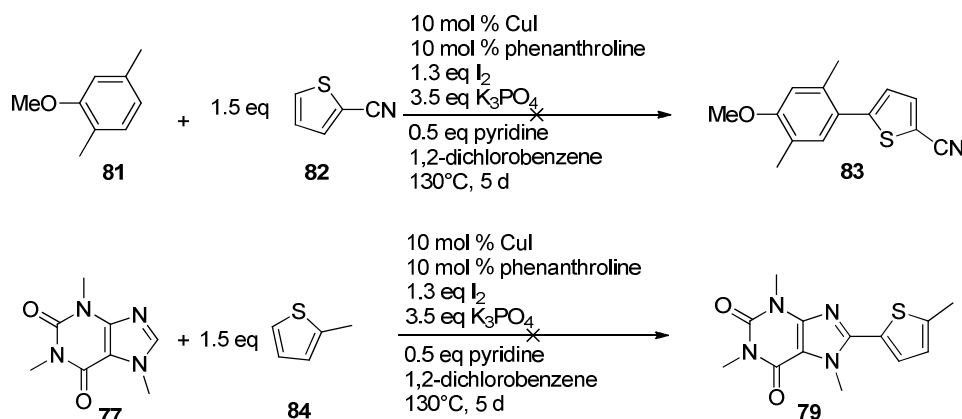


Figure 18. Main product of direct arylation reactions.

For the third cross-coupling reaction we chose substrates, catalytic system and reaction conditions reported by *Do* and *Daugulis* in 2009.^[60] At the first glance their reaction looks like a tandem direct arylation. But *Do* and *Daugulis* postulated an *in situ* activation of one arene via iodination followed by direct arylation of the second arene. In the cross-coupling reaction of 2,5-dimethylaniline (**81**) and 2-thiophenecarbonitrile

(**82**) they received a yield of 72 %.^[60] We tested their reaction conditions in the cross-coupling of caffeine (**77**) and 2-methylthiophene (**84**) as well.



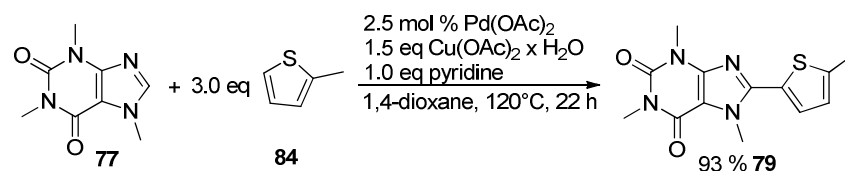
Scheme 51. Tandem direct arylation via *in situ* iodination following the procedure of *Do* and *Daugulius*.^[60]

Despite long reaction times, we did not observe any of the cross coupling products **83** and **79**. Nevertheless, selective iodination of one arene (**81** and **84**) in each reaction occurred, although not quantitatively. Even after 8 d of reaction time no cross-coupling took place.

Reaction time	81:85
1 d	54:46
5 d	44:56
8 d	35:65

Scheme 52. Iodination reaction via cross-coupling of *Do* and *Daugulius*, monitored by GC-MS. For reaction conditions see scheme 51. The conversion of 2-methylthiophene (**84**) could not be determined due to its low retention time that prevented detection with the chosen GC-MS method.

Xi et al reported a new catalytic system for the dehydrogenative twofold CH-activated arylation of heteroaromatic compounds including the cross-coupling of caffeine (**77**) with 2-methylthiophene (**84**), in which they obtained excellent 96 % yield.^[53] They used palladium acetate as catalytic Pd(II) species, copper(II) acetate for re-oxidation of the formed Pd(0) and presumably for its stabilization pyridine was added, which was supposed to reduce the formation of palladium black. Since we could reproduce their results, we chose their reaction conditions for our thiophene-linkage strategy.



Scheme 53. Tandem direct arylation of caffeine (**77**) with 2-methylthiophene (**84**).

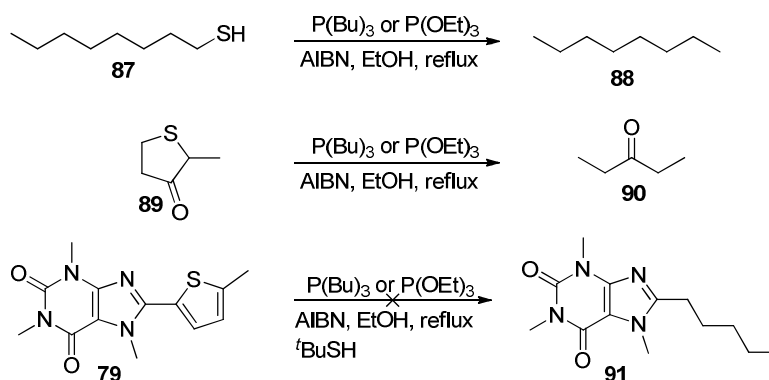
4.2.3.2 Desulfurization

For the desulfurization reaction, a metal-free version often applied for the removal of the HS-group of cysteines to form alanine in tailor-made peptides was tested. Since we wanted to desulfurize an aromatic substrate instead of a saturated, aliphatic one, high bond dissociation energies indicated that this will be difficult.

bond	dissociation energy [kJ/mol]
S-S	268
S-H	368
S-C	305
S=C	573

Table 7. Bond dissociation energies of the main sulfur containing bonds.^[85]

Nevertheless, the radical desulfurization of octanethiol (**87**) under exclusion of O₂ went smoothly (scheme 54). Although the desulfurized product **88** was not directly detectable via TLC or GC-MS, the conversion of octanethiol (**87**) could be monitored via consumption of the starting material **87** and in parallel by an increase of the sulfured phosphines or phosphites. Also the tetrahydrothiophene **89** was desulfurized successfully using the same reaction conditions. But the metal-free desulfurization of the unsaturated thiophene derivative **79** did not proceed. Even supporting the reaction by initiation using catalytic amounts of *tert*-BuSH as additive did not lead to any desulfurized product **91**. Since the S=C bond dissociation energy is nearly twice as big as that of a S-C bond, this result was somehow expected.



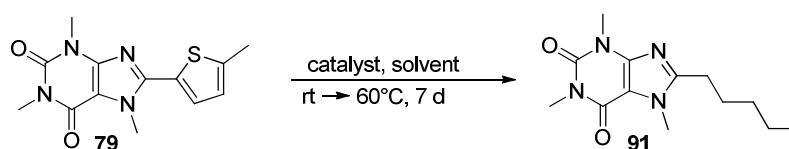
Scheme 54. Metal-free desulfurization reactions, monitored via GC-MS. Products **88** and **90** were not isolated.

Alternatively, we tested the metal catalyzed hydrodesulfurization. Due to safety reasons we began our screening with the less reactive Raney-Ni W-2 that was prepared according to the Organic Syntheses procedure by *Mozingo*, from NiAl alloy in aqueous sodium hydroxide.^[68b] The obtained ethanolic, black suspension could be stored for several months. Because of hydrogen emerging from the Raney-Ni synthesis, additional hydrogen sources were not necessary.



Scheme 55. Synthesis of Raney Nickel W-2.

We screened the hydrogenation of our cross-coupled thiophene **79** with Raney-Ni and different Pd catalysts in different solvents. Ethanol is a standard solvent for these kinds of hydrogenations. Our starting material **79** should be well soluble in chloroform. THF and 1,4-dioxane were chosen as more apolar alternatives. All reactions were monitored by GC-MS.

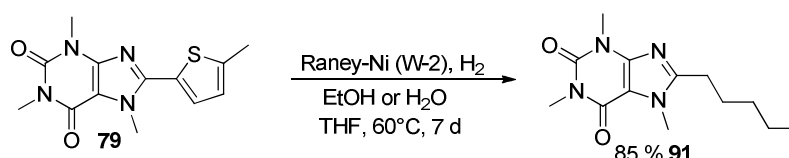


Catalyst	Solvent	Conversion
Raney-Ni*	THF	85 %**
Raney-Ni*	CHCl ₃	0 %
Raney-Ni*	dioxane	0 %
Raney-Ni	EtOH	0 %
Pd/Al ₂ O ₃	THF	0 %

Pd/Al ₂ O ₃	dioxane	1 %
Pd/BaSO ₄	THF	9 %
Pd/BaSO ₄	dioxane	2 %
Pd/C	THF	3 %
Pd/C	dioxane	12 %

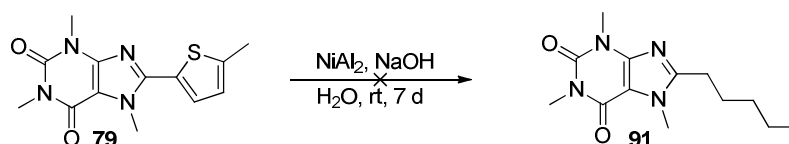
Table 8. Screening of catalysts and solvents in the hydrodesulfurization. Conversions were monitored by GC-MS. *The W-2 type Raney-Ni was applied as ethanolic suspension. **Isolated yield. 15 % of starting material **79** were reisolated.

Our screening indicated that this Raney-Ni hydrodesulfurization was extremely sensitive to different solvents. The reaction occurred only satisfactory in THF, despite the poor solubility of the starting material **79**. In all other solvents no reaction occurred. Heating up to 60°C had only little influence on the course of the reaction. Crucial was another hydrogen source, which is why we created a hydrogen atmosphere via an orsat balloon. Considering all this information, we achieved slow but nearly complete conversion (96 %) as indicated by GC-MS. But due to the poor solubility of the starting material **79**, GC-MS control produced incorrect data. Actually, 85 % conversion were received. 15 % of the cross-coupled thiophene **79** could be reisolated during purification by column chromatography. Usage of Pd catalysts in the desulfurization and hydrogenation reaction of our substrate resulted in a dramatically decreased conversion or resulted in no reaction.



Scheme 56. Hydrodesulfurization of the cross-coupled 2-methylthiophene **79** with Raney-Ni (W-2).

Also no influence on the course of the reaction had the exchange of our synthesized, ethanolic Raney-Ni suspension to activated Raney-Ni 2800 from Sigma-Aldrich, which is sold as aqueous suspension with a reactivity comparable to Raney-Ni (W-2). *In situ* synthesis of Raney-Ni with NiAl₂ and NaOH followed by hydrodesulfurization did not work at all.



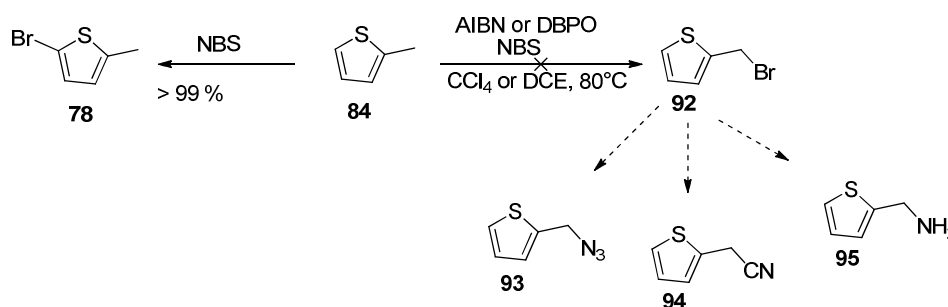
Scheme 57. Hydrodesulfurization via *in situ* synthesis of Raney-Ni.

4.2.3.3 Synthesis of thiophene derivatives

With these promising results in our hands, we started to synthesize several thiophene derivatives, which are supposed to result in a linker with a terminal amino or hydroxy group. Starting from 2-methylthiophene **84**, we wanted to brominate the methyl group selectively followed by substitution with different functional groups. We tested AIBN and DBPO as initiator and two solvents typical for this reaction (tetrachloromethane and dichloroethane). *N*-bromosuccinimide (NBS), applied as bromine source, was recrystallized from water before use. Furthermore, we tested different types of addition:

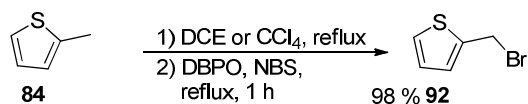
- i) thiophene **84**, NBS and initiator in one pot, followed by heating to reflux,
- ii) thiophene **84** heated to reflux, followed by fast or slow addition of initiator and NBS or
- iii) initiator and NBS heated to reflux, followed by addition of thiophene **84**.

In all reactions 2-methylthiophene (**84**) was converted quantitatively but not to the desired 2-bromomethylthiophene (**92**). Instead, 2-bromo-5-methylthiophene (**78**) was generated immediately. Side chain bromination of 2-methylthiophene (**84**) failed due to the extremely high reactivity of the aromatic C-2 carbon leading to S_EAr -products.



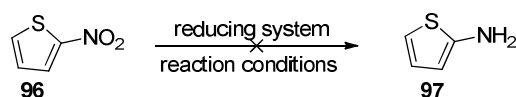
Scheme 58. Bromination of 2-methylthiophene (**84**) at the aromatic scaffold.

Our results are in contrast to the procedures reported by *Ngwendson et al.*^[86] or *Younes et al.*^[87] They converted 2-methylthiophene (**84**) nearly completely to the desired 2-bromomethylthiophene (**92**) using similar reaction conditions.



Scheme 59. Bromination of the methyl group by *Ngwendson* or *Younes* and co-workers.^[86,87]

An alternative route to the amino substituted thiophene **97** starts from 2-nitrothiophene (**96**). For its reduction several methods were screened varying mainly in reducing system and reaction conditions.

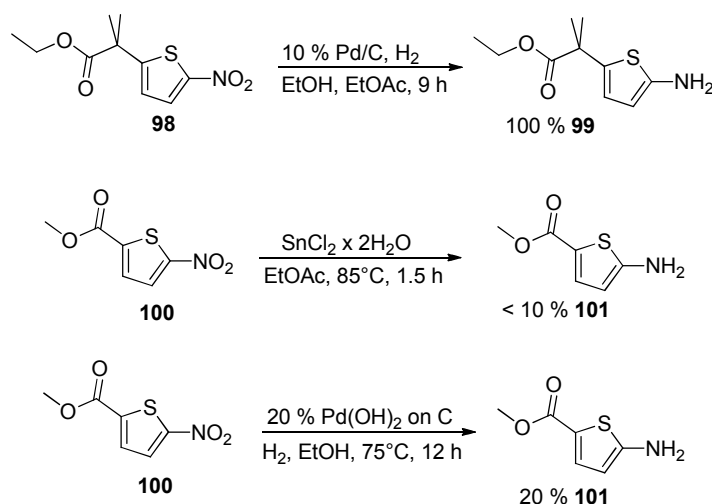


Entry	Reducing system	Reaction conditions	Consumption of 96
1	Fe, AcOH	100°C, 10 min	67 %
2	Fe, AcOH	100°C, 1 d	100 %
3	FeCl ₃ , charcoal, MeOH, N ₂ H ₄ × H ₂ O	80°C, 20 h	50 %
4	Raney-Ni, N ₂ H ₄ × HCOOH	rt, 22 h	20 %
5	NiCl ₂ , NaBH ₄ , MeOH	rt, 22 h	100 %
6	Pd/C, H ₂ , MeOH	rt, 23 h	95 %
7	Zn, CF ₃ SO ₃ H, ACN	rt, 17 h	0 %
8	Sn, AcOH	rt, 17 h	100 %

Table 9. Screening of reduction systems and reaction conditions for the reduction of 2-nitrothiophene. Consumption of starting material **96** was confirmed by NMR. Additionally, reactions were monitored by GC-MS and TLC.

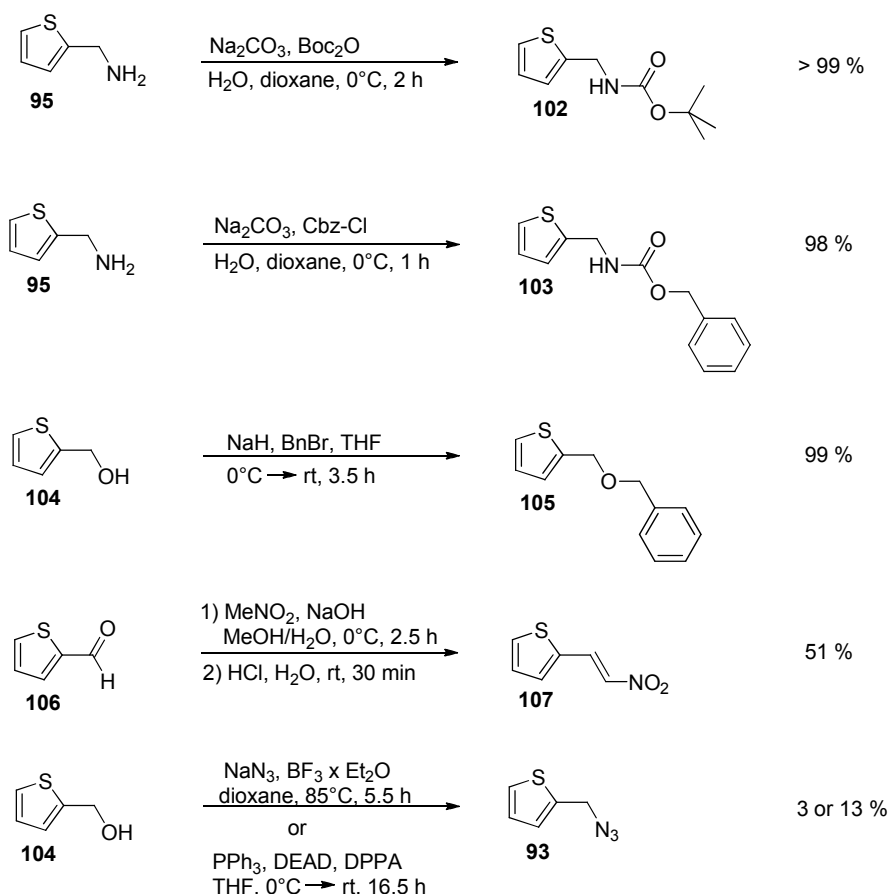
Also the reduction of 2-nitrothiophene (**96**) to 2-aminothiophene (**97**) failed. Nevertheless, consumption of 2-nitrothiophene (**96**) was acceptable, except in entries 4 and 7, where nearly no reaction occurred. Using the reaction conditions of entries 2, 5 or 8, 2-nitrothiophene (**96**) was even fully converted. But the desired 2-aminothiophene (**97**) could never be identified, although the reductions were monitored by TLC, GC-MS and NMR. Interestingly, during the reaction in entry 5, all aromatic protons in the ¹H-NMR spectra vanished completely, meaning that possibly a tetrahydrothiophene

derivative arose. But formation of the fully hydrogenated thiophene has not been proven. Despite, a few hydrogenation reactions of nitrothiophene derivatives **98** and **100** to form the corresponding aminothiophene derivatives **99** and **101** were reported, for example by *Arnould et al.*^[88] or *Chao et al.*^[89] The partially very low yields display the difficulties associated with the reduction of nitrothiophenes.



Scheme 60. Reported reductions of nitrothiophene derivatives **98** and **100**.

Not discouraged by these results, we synthesized a couple of interesting thiophene derivatives (scheme 61). 2-(Aminomethyl)thiophene (**95**) was Cbz- and Boc-protected in quantitative yield each, using standard reaction conditions. 2-Thiophenemethanol (**104**) was protected with a benzyl group and yielded 99 % of the benzyl protected 2-thiophenemethanol **105**. 51 % 2-((*E*)-2-nitrovinyl)thiophene (**107**) were obtained via Henry reaction of thiophene-2-carbaldehyde (**106**) with nitromethane following the synthesis procedure of *Trost and Müller* who reported 41 %.^[90] The synthesis of 2-(azidomethyl)thiophene (**93**) was more challenging. The 2-(azidomethyl)thiophene synthesis, reported by *Kumar* and co-workers,^[91] was described slightly imprecisely. Anyway, after a few optimization reactions we were able to obtain 2-(azidomethyl)thiophene (**93**) in 3 % yield. In parallel we tested the introduction of the azide by a Mitsunobu reaction to yield 13 % of the colorless liquid. Bulb-to-bulb distillation was used in both syntheses for purification. Obviously, 2-(azidomethyl)thiophene (**93**) is not stable under these conditions.



Scheme 61. Synthesized thiophene derivatives.

Five other thiophene derivatives were commercially available (figure 19). In total, we had nine different thiophene derivatives for our linker synthesis in our hand. 2-(Azidomethyl)thiophene (**93**) was not tested in the cross-coupling with caffeine (**77**) since it is thermally unstable and the cross-coupling reaction occurred at 120°C .

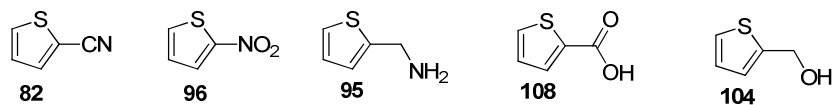
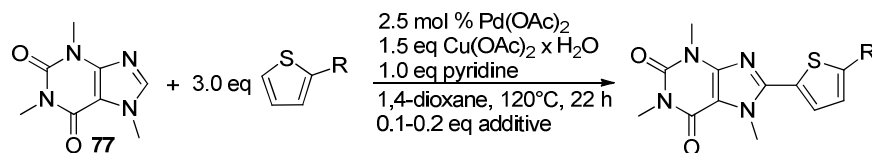


Figure 19. Thiophene derivatives that were applied from commercial sources.

4.2.3.4 Optimization and thiophene substrate screening

With all starting materials in our hands, we began to investigate the optimal conditions to receive high yields starting with the catalytic system developed by Xi and co-workers.^[53] We screened every substrate under the same reaction conditions as described, varying only the additives (1,10-phenanthroline, CuCl and CuBr or none). Xi and co-workers proposed an increased product formation using catalytic amounts of

CuCl for electron rich (hetero)arenes and CuBr for electron deficient (hetero)arenes. They postulate an improved catalytic efficiency and regioselectivity probably due to selective activation of heteroaryl CH-bonds by these Cu(I) salts.

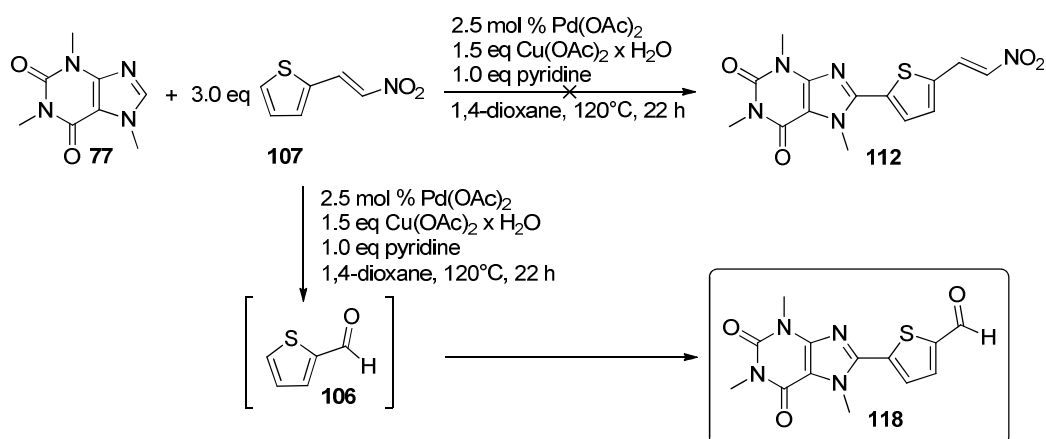


Entry	Thiophene	Additives	Yield	Product
		-	39 %	
1		CuBr	26 %	109
		CuCl	63 %	
		1,10-phenanthroline	11 %	
2		-	89 %	110
		CuBr, CuCl or 1,10-phenanthroline	14 %	
3		CuBr, CuCl, 1,10-phenanthroline or none	0 %	111
4		-	0 %	112
5		-	25 %	113
		CuBr	20 %	
6		-	50 %	114
7		CuBr, CuCl, 1,10-phenanthroline or none	< 1 %	115
8		CuBr, CuCl or none	15 %	116
		1,10-phenanthroline	87 %	
9		-	36 %	117
		CuBr	66 %	
		CuCl	> 99 %	

Table 10. Screening of thiophenes and additives in the dehydrogenative cross-coupling reaction with caffeine (77).

Interestingly, the additives influenced the cross-coupling with varying thiophene derivatives completely differently. The course of a cross-coupling reaction was not as predictable as described by Xi and co-workers by using the additives mentioned. The additives had no influence on the course of the reaction with 2-(aminomethyl)thiophene (**95**) (entry 7), thiophenyl carboxylic acid (**108**) (entry 3) and 2-nitrothiophene (**96**) (entry 5). Thiophenyl carboxylic acid (**108**) and 2-(aminomethyl)thiophene (**95**) might interfere through its reactive functional group with the catalytic system resulting in inhibition.

The cross-coupling reactions with 2-thiophenecarbonitrile (**82**) (entry 6) and 2-((E)-2-nitrovinyl)thiophene (**107**) (entry 4) were not investigated with different additives. Presumably, 2-((E)-2-nitrovinyl)thiophene (**107**) did not react at all. We have evidence that it was not stable under these reaction conditions and underwent aldol cleavage. The formed 2-thiophenecarbaldehyde (**106**) reacted in the cross-coupling to form the coupled thiophenecarbaldehyde **118**. This product was not isolated, but crude HPLC and NMR data correspond to the cross-coupled thiophenecarbaldehyde **118** reported by Xi and co-workers.^[53]



Scheme 62. Dehydrogenative cross-coupling of 2-thiophenecarbaldehyde **106**, formed *in situ* via nitro aldol cleavage.

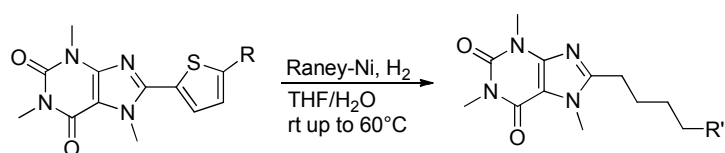
With 2-thiophenemethanol (**104**) (entry 1), for the first time a significant influence of the additives was observed. Without additive, 2-thiophenemethanol (**104**) yielded 39 % of its cross-coupled product **109**. By adding catalytic amounts of CuBr or 1,10-phenanthroline the yield even decreased. But upon the addition of CuCl acceptable 63 % of the cross-coupled product **109** were obtained after purification by column chromatography.

In the cross-coupling reaction with the benzyl-protected 2-thiophenemethanol **105** all additives tested influenced the course of reaction negatively. The product yields (14 %) were only moderate. In contrast, the reaction without additive yielded 89 % of cross-coupled, benzyl-protected 2-thiophenemethanol **110**, which precipitated from methanol.

The cross-coupling of the Cbz-protected amine **103** (entry 8) could also be influenced positively using additives. Without additive, 15 % of the cross-coupling product **116** were isolated. By addition of 0.1 eq 1,10-phenanthroline, we improved the reaction yield to 87 %. The copper salts had no influence on the course of this cross-coupling reaction.

In the cross-coupling reaction of Boc-protected amine **102** (entry 9) 36 % of the isolated product **117** were obtained. With 1,10-phenanthroline or CuBr the yield could be increased but was still not acceptable. Fortunately, 0.2 eq CuCl were necessary to obtain 99 % of the cross-coupled product **117**.

Subsequently, the hydrodesulfurization was performed with all cross-coupled thiophenes that were received in acceptable yields. The applied reaction conditions were obtained from the optimized desulfurization reaction of the cross-coupled 2-methylthiophene **79**. The results of the hydrodesulfurization reactions were shown in table 11.



Entry	Thiophene	Product	Yield
1	 109	 119	40 %
2	 110	 119	99 %

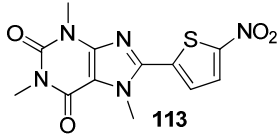
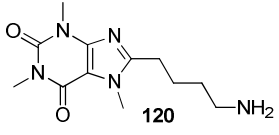
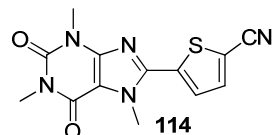
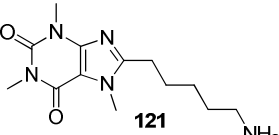
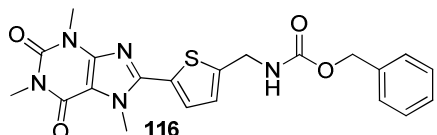
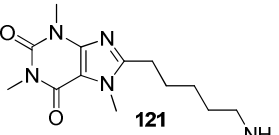
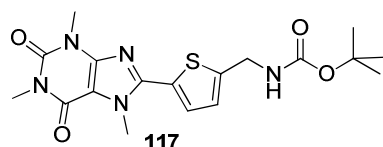
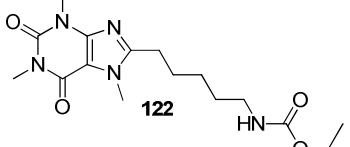
3			2 %
4			3 %
5			40 %
6			83 %

Table 11. Desulfurization of thiophenes with Raney Nickel. All amines were received as ammonium formates through purification by semi-preparative HPLC.

The reduction with Raney-Ni highly depended on the nature of the substrate to be reduced. In all reactions with nitrogen functionalities that were hydrogenated together with the thiophene ring to yield the amine (entries 3 and 4), several side products emerged. Therefore, the yields were rather low. Acceptable yields were obtained in the hydrodesulfurization of cross-coupled 2-thiophenemethanol **109** and cross-coupled Cbz-protected amine **116**. After preparative HPLC purification still 40 % of the alcohol **119** or the free amine **121** were isolated.

Interestingly, the hydrodesulfurization and deprotection of the benzyl protected, cross-coupled 2-thiophenemethanol **110** in one pot occurred in excellent 99 % yield. This high yield might be ascribed to the stepwise reduction process. Only when the selective hydrodesulfurization of the thiophene ring was completed, hydrogenolytic cleavage of the benzyl protecting group occurred. Hence, the hydroxyl group was never free for interference with Raney-Ni during the hydrodesulfurization.

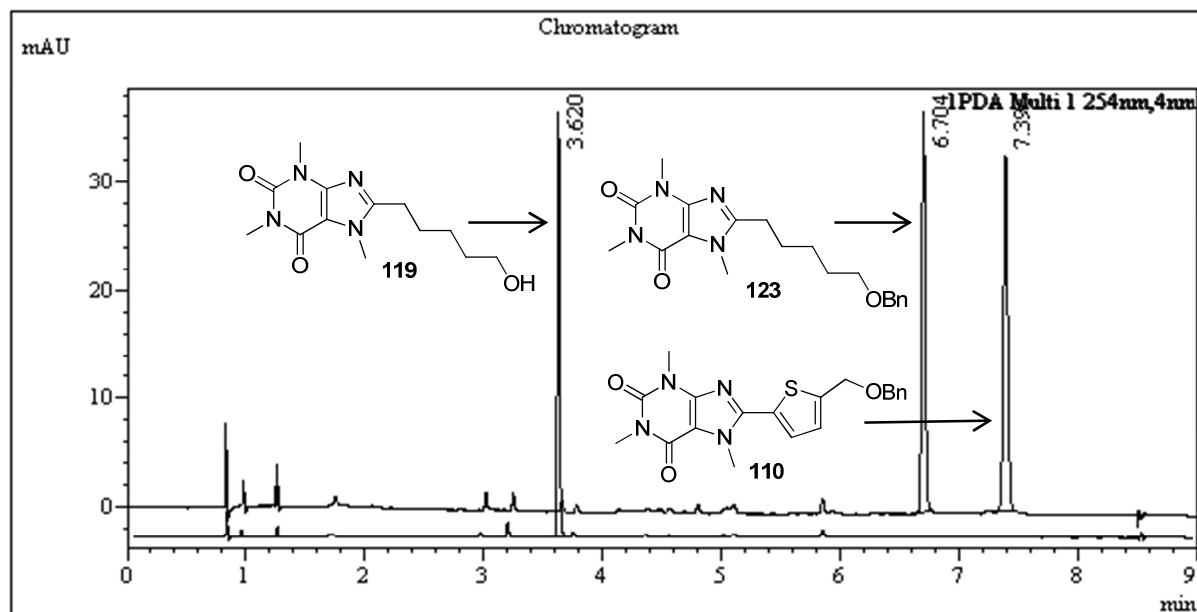
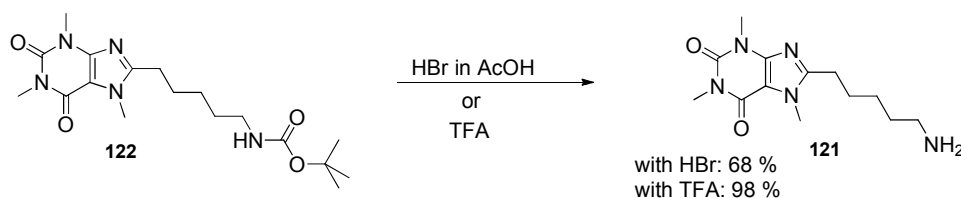


Figure 20. Overlaid chromatograms from HPLC monitoring of the reduction of the benzyl-protected, cross-coupled 2-thiophenemethanol **110**. Upper chromatogram after 3 d reaction time with 6 mL Raney-Ni. Lower chromatogram after 4 d reaction time with additional 4 mL Raney-Ni. HPLC-method G, 254 nm.

Furthermore, we were able to reduce the cross-coupled, Boc-protected amine **117** to the corresponding alkyl chain **122** with Raney-Ni in excellent 83 % yield. Due to the remaining protecting group, monitoring of the reaction was much easier. The product could be detected also by TLC in addition to LC-MS. Eventually, purification was also a lot easier because quick filtration through silica gel was sufficient instead of the more elaborate preparative HPLC. On the other hand, the deprotection as additional step was necessary.

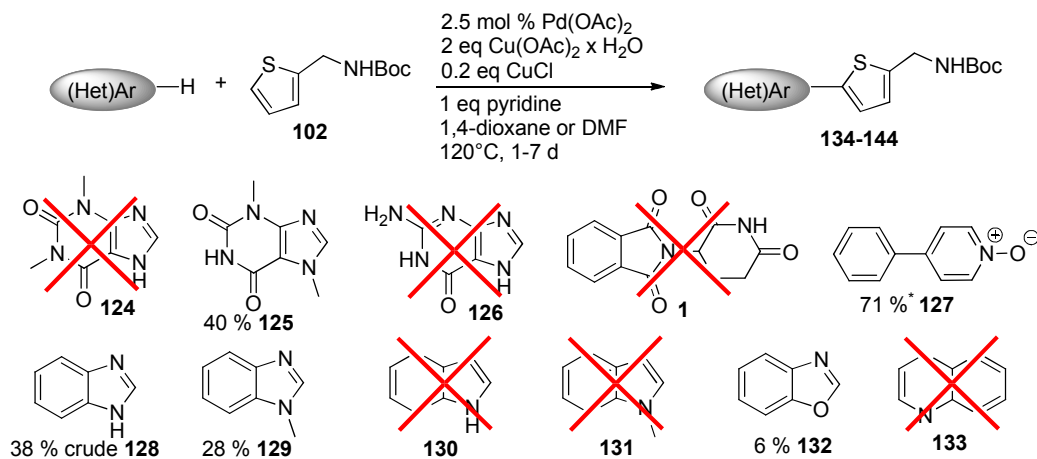
Deprotection was performed under acidic conditions with 33 % HBr in acetic acid or in the presence of an excess of trifluoroacetic acid in dichloromethane within 1 h to yield 68 % up to 98 % of the linked caffeine **121**. Only in the reaction mixture mentioned first, the deprotected product **121** precipitated as hydrobromide from acetonitrile in an ultrasonic bath. Unfortunately, it precipitated not quantitatively so the mother liquor had to be purified by preparative HPLC. The counterion depended on the acid used in the deprotection step. During preparative HPLC purification normally the formate was formed, due to the formic acid content in the aqueous eluent acidified with formic acid.



Scheme 63. Boc-deprotection of the linked caffeine using different acids.

4.2.3.5 Screening of heterocyclic substrates in the thiophene linkage

With our optimized thiophene-linkage strategy in hands we started to screen several small molecules to be linked for mimicking common drug scaffolds. We selected them considering the following aspects. Reactivity is supposed to be similar to caffeine (**77**) when only little changes in the structure of the small molecules were introduced. Free amines might disturb the reaction and therefore should not dominate the assortment of small molecules. *N*-protected amines should also be screened. To test the scope of the reaction, not only *N*-heterocyclic substrates but also other heteroarenes and aromatic systems without heteroatom were employed. For the first screening we finally chose 11 substrates to be investigated. All reactions were monitored via HPLC-MS and TLC.



Scheme 64. Cross-coupling of Boc-(aminomethyl)thiophene **102** with various small molecules. *Conversion is given, which was determined by HPLC. **127** was not isolated.

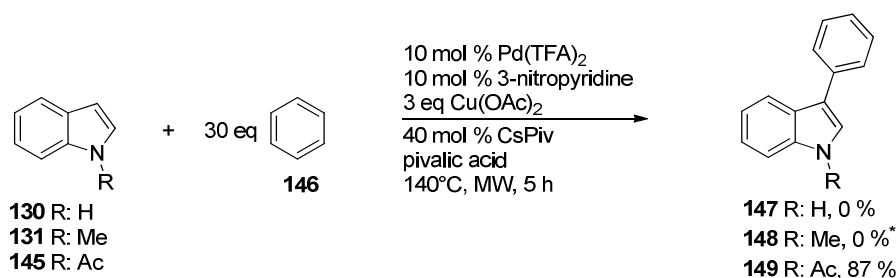
The first results of this screening with our optimized reaction conditions were sobering. First of all, not all investigated (hetero)arenes were soluble in 1,4-dioxane. Those substrates (**124**, **127** and **128**) were therefore dissolved in DMF. Despite, theobromine (**125**) and theophylline (**124**) remained undissolved. Interestingly, all cross-coupled thiophene derivatives possessed fluorescent activity by excitation of their solutions at

366 nm. This simplified their recovery for example during column chromatography because of easy detection.



Figure 21. Cross-coupled caffeine **117** in a dichloromethane/methanol mixture at visible light (left) and by excitation at 366 nm (right).

As we expected from former screenings, free NH₂-groups disturbed the dehydrogenative cross-coupling. This could be reconfirmed with guanine (**126**) as substrate. Quinoline (**133**) was also not consumed. Thalidomide (**1**), the only arene without heteroatom in our screening showed no conversion under these reaction conditions. Nevertheless, *Stuart* and *Fagnou* already cross-coupled heteroarenes with heteroatom-free arenes using Pd(II) trifluoroacetate and some other additives (scheme 65).^[51a] So, potential for this molecule class exists and the cross-coupling with thiophene derivatives might still be possible.



Scheme 65. Dehydrogenative cross-coupling of indoles **130**, **131** and **145** with benzene by *Stuart* and *Fagnou*. *Homodimerization of *N*-methylindole (**131**) occurred instead of the cross-coupling.

Under our optimized reaction conditions, indole (**130**) did not react in the dehydrogenative cross-coupling reaction, which corresponds to the results by *Stuart* and *Fagnou*. Also *N*-methylindole (**131**) did not undergo the cross-coupling, neither with our catalyst system nor with the one of *Stuart* and *Fagnou*. Only their *N*-acetylindole (**145**) derivatives were reactive, probably due to the *N*-acetyl residue, which seemed to be required for catalyst pre-coordination. If a heteroatom near the reacting CH-group is essential for catalyst pre-coordination, this would explain the lack of reactivity of

indoles **130** and **131**. Instead, benzimidazole derivatives **128** and **129**, both allow catalyst pre-coordination and indeed, they yielded 38 % of **139** and 28 % of cross-coupled *N*-methyl-indole **140**, respectively. The isolation of the cross-coupled benzimidazole **139** proved difficult. It could be enriched from the crude reaction mixture, but not purified completely. A significant impurity of the purified cross-coupled benzimidazole **139** was benzimidazole (**128**), the starting material. Due to nearly similar R_f -values separation via column chromatography was impossible. This problem was also observed in all other cross-coupling reactions. Therefore, full conversion was required to finally end up with pure products.

Surprisingly, theophylline (**124**) did not react so far, although it has close resemblance to caffeine (**77**) and benzimidazole (**128**), which both underwent the dehydrogenative cross-coupling. But theobromine (**125**) again yielded 40 % of its cross-coupling product **135** although it was only poorly soluble in 1,4-dioxane. In all other tested solvents, the solubility of theobromine (**125**) was even worse.

The cross-coupled benzoxazole **143** could be obtained in 6 % isolated yield. Electronic properties of benzoxazole (**132**) must closely resemble Boc-(aminomethyl)thiophene **102** because both homo-coupling products **150** and **151** emerged beside the desired cross-coupling product **143**. This was determined via HPLC-MS.

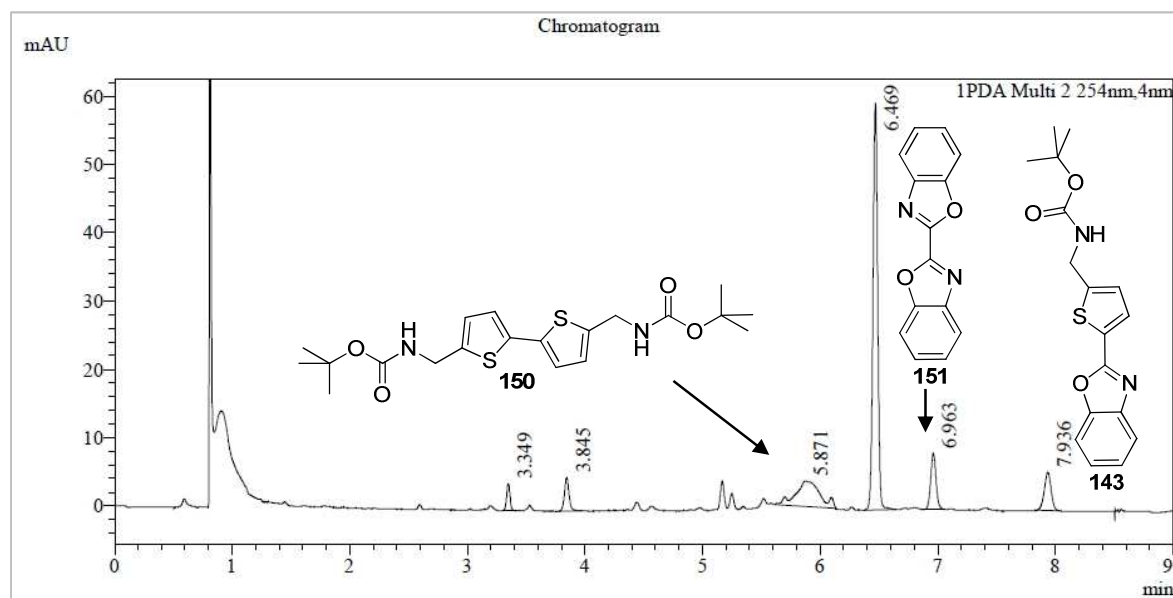
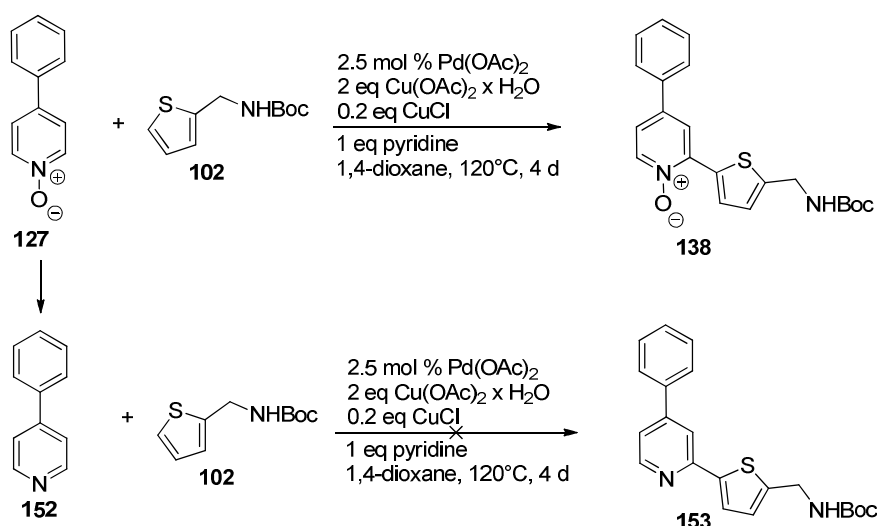


Figure 22. Chromatogram of the reaction mixture from cross-coupling of benzoxazole (**132**) with Boc-protected 2-(aminomethyl)thiophene **102** after 3 d reaction time. HPLC-method G, 254 nm.

Another interesting substance class were pyridines and derivatives that did not react in the dehydrogenative cross-coupling. But they could be easily transformed to *N*-oxides that were highly active in this reaction. This was proven by cross-coupling with 4-phenyl-pyridine-1-oxide (**127**), which was performed in 71 % conversion after 2 d reaction time. Purification of the cross-coupled *N*-oxide **138** by column chromatography or precipitation was difficult and could not be accomplished so far. The main side product occurred from the back-reaction of the *N*-oxide **127** to 4-phenyl-pyridine (**152**) in 20 % conversion (scheme 66), although cross-coupling was performed under oxidative reaction conditions. 4-Phenyl-pyridine (**152**) was inert to the cross-coupling under these reaction conditions.



Scheme 66. Cross-coupling of 4-phenyl-pyridine-1-oxide (**127**) with the Boc-protected 2-(aminomethyl)thiophene **102**.

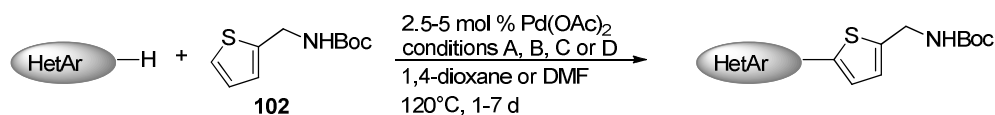
In this screening we gained much information about the required structure of the substrates for dehydrogenative cross-coupling and we identified several reacting structures. Since we were not able to reach excellent yields using our cross-coupling conditions (except for caffeine (**77**)), we optimized them again but now for each heteroarene individually. For these screenings only those heteroarenes were investigated that already reacted under the former conditions. Additionally, *N*-methylindole (**131**) was investigated in this screening. All cross-coupling reactions were monitored by HPLC-MS. The solvent used in the cross-coupling depended on the solubility of the heteroarenes and was chosen for each substrate individually. This solvent was then applied in the defined reaction conditions. Starting from our former optimized reaction conditions A, the following cross-coupling conditions were tested:

Conditions A: 1.5 eq $\text{Cu}(\text{OAc})_2 \times \text{H}_2\text{O}$, 0.2 eq CuCl , 1 eq pyridine,

Conditions B: 2 eq AgOAc , 0.2 eq CuCl , 1 eq pyridine,

Conditions C: 2 eq AgOAc , 0.2 eq AgF , 1 eq pyridine and

Conditions D: 2 eq $\text{Cu}(\text{OAc})_2 \times \text{H}_2\text{O}$, 1 eq Ag_2CO_3 , 1.5 eq PivOH .



Entry	Heteroarenes	HetAr:Product ratio			
		Conditions A	Conditions B	Conditions C	Conditions D
1		0:100	27:73	39:61	47:53
2		12:88	77:23	13:87	67:33
3		25:75	98:2	90:10	44:56
4		could not be determined reliably			
5		69:31	98:2	99:1	87:13
6		29:71	18:82	22:78	28:72

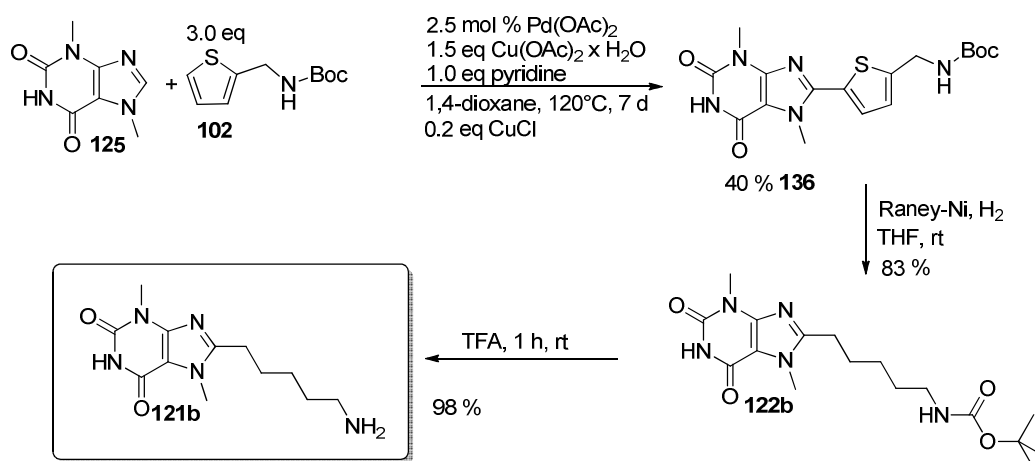
Table 12. Screening of heteroarenes for thiophene linkage with Boc-protected 2-(aminomethyl)thiophene **102**. HetAr:Product ratio was confirmed by HPLC-MS at 254 nm.

The screening of cross-coupling conditions A, B, C and D indicated that we already had the optimal reaction conditions A for theobromine (**125**). Whereas in the presence of $\text{Ag}(\text{I})$ salts, the consumption of theobromine (**125**) decreased. Due to the poor solubility of theobromine (**125**), these results have to be taken with caution. After workup, the conversion of theobromine (**125**) was sometimes inferior to the previous HPLC measurements.

Although the conversions of benzoxazole (**132**) (75 %) and benzimidazole (**128**) (31 %) were not satisfying, they were still higher under conditions A compared to B, C and D. Nearly no consumption of benzimidazole (**128**) was monitored in the presence of Ag(I). In contrast, the conversion of the *N*-oxide **127** (entry 6) could be improved by using Ag(I) as oxidant independently from the presence or absence of Cu-agents. For *N*-methylbenzimidazole (**129**) (entry 2) conversions with only Cu- or only Ag-agents in pyridine were similar. Under conditions B and D, which combined Ag- and Cu-agents, the consumption of *N*-methylbenzimidazole (**129**) decreased dramatically. The cross-coupled *N*-methylindole (**142**) could not be determined safely through the whole screening.

This screening of cross-coupling conditions confirmed the limitation of each reaction condition to a smaller set of compounds. Nevertheless, for five out of six heteroarenes tested we identified new conditions, which led to better conversions or we could confirm the optimal cross-coupling conditions from our former descriptions.

Making use of all experiences of the thiophene-linkage strategy so far, we were able to tether not only caffeine (**77**) but also theobromine (**125**) via dehydrogenative cross-coupling with Boc-protected 2-(aminomethyl)thiophene **102**, followed by hydrodesulfurization and Boc-deprotection in an overall yield of 33 %. Yield limiting still remains the dehydrogenative cross-coupling whose investigation must be continued.



Scheme 67. Tethering of theobromine (**125**) via thiophene linkage strategy with Boc-protected 2-(aminomethyl)thiophene **102**.

4.3 Isolation of an unknown cytotoxin

Recently, researchers at the Institute of Molecular Biosciences at the University of Graz discovered that a small organic molecule, produced and excreted by *K. oxytoca* wild type bacteria, caused antibiotic associated hemorrhagic colitis. To study its cytotoxic effect, this small molecule has to be isolated and its chemical structure must be clarified.

4.3.1 Preparation of the culture solution

Prof. Ellen Zechner and Georg Schneditz from the Institute of Molecular Biosciences at the University of Graz provided us with each 1 L culture solution of the cytotoxin positive wild type of *K. oxytoca* and the cytotoxin negative non-ribosomal synthesis mutant $\Delta npsA$. For this purpose, both strains were grown at 37°C in CASO medium with constant shaking. After 16 h of shaking, formation and excretion of the cytotoxin in the wild type reached a maximum. Longer or shorter growing times resulted in a considerably reduced cytotoxin concentration. The mutant $\Delta npsA$, which cannot produce the cytotoxin, was required for negative control. All bacteria were removed from the culture solution by centrifugation and sterile filtration.

4.3.2 Purification

Since the cytotoxin was supposed to be a small organic molecule, isolation was accomplished using methods typical in organic chemistry. Therefore, both culture solutions were divided and tested in the extraction with chloroform and *n*-butanol each. All aqueous layers were extracted three times and the organic layer was further washed with brine. After each extraction step samples of all layers were taken, concentrated and screened for toxic activity (figure 23 and 24). For this purpose Hep-2 cells were incubated for 2 days with the samples, which were diluted with buffer in advance. Afterwards, cell survival was determined in a MTT assay.^[92] Decreased cell viability indicated cytotoxic activity. For negative control the cytotoxin activity assay was performed with the $\Delta npsA$ extracts simultaneously.

With this method chloroform was recognized to be unsuitable for the isolation of the cytotoxin (figure 23). Since it could neither be found in any organic nor in any aqueous layer, the cytotoxin seemed to decompose. This might be due to traces of hydrochloric acid evolved in chloroform.

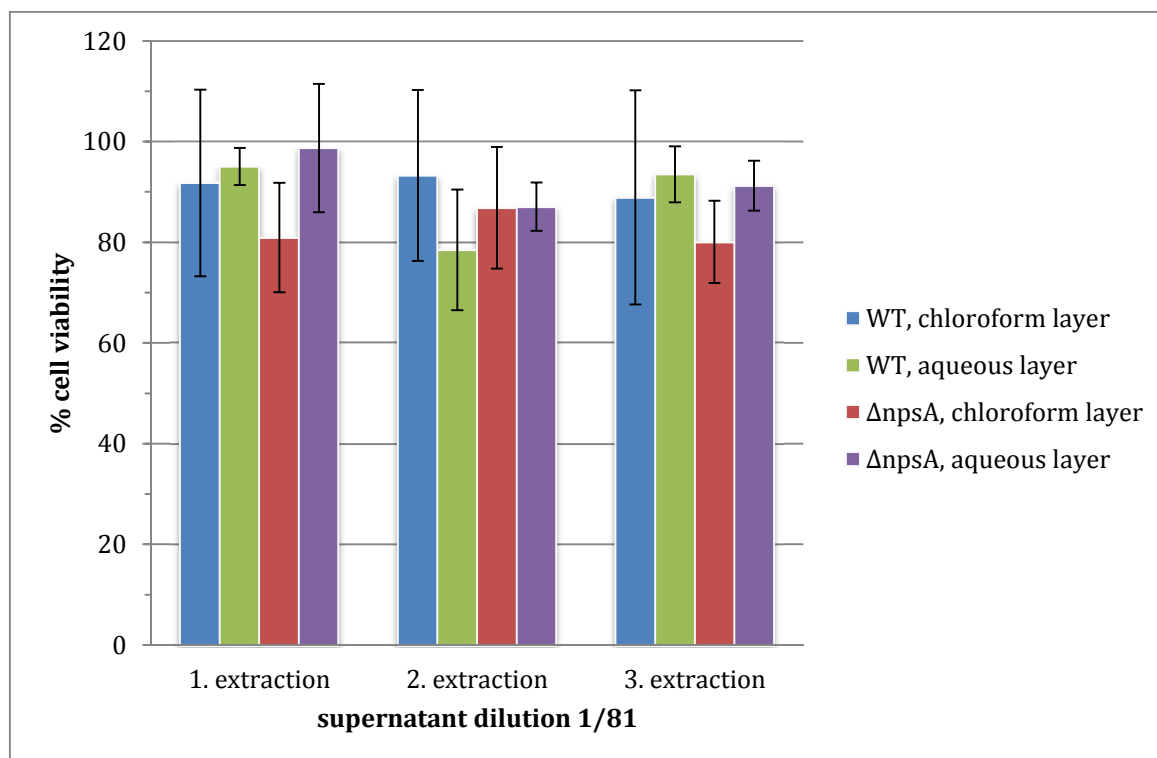


Figure 23. Toxicity screening of organic and aqueous chloroform extracts of the wild type and the mutant $\Delta npsA$.

In contrast, extraction with *n*-butanol was successful and the organic layer of the wild type contained nearly the whole amount of cytotoxin after the second extraction step (figure 24). A third extraction of the aqueous layer was not necessary. But washing of the *n*-butanol layer with brine could be used for pre-drying. All extracts of the mutant $\Delta npsA$ did not show any toxic activity.

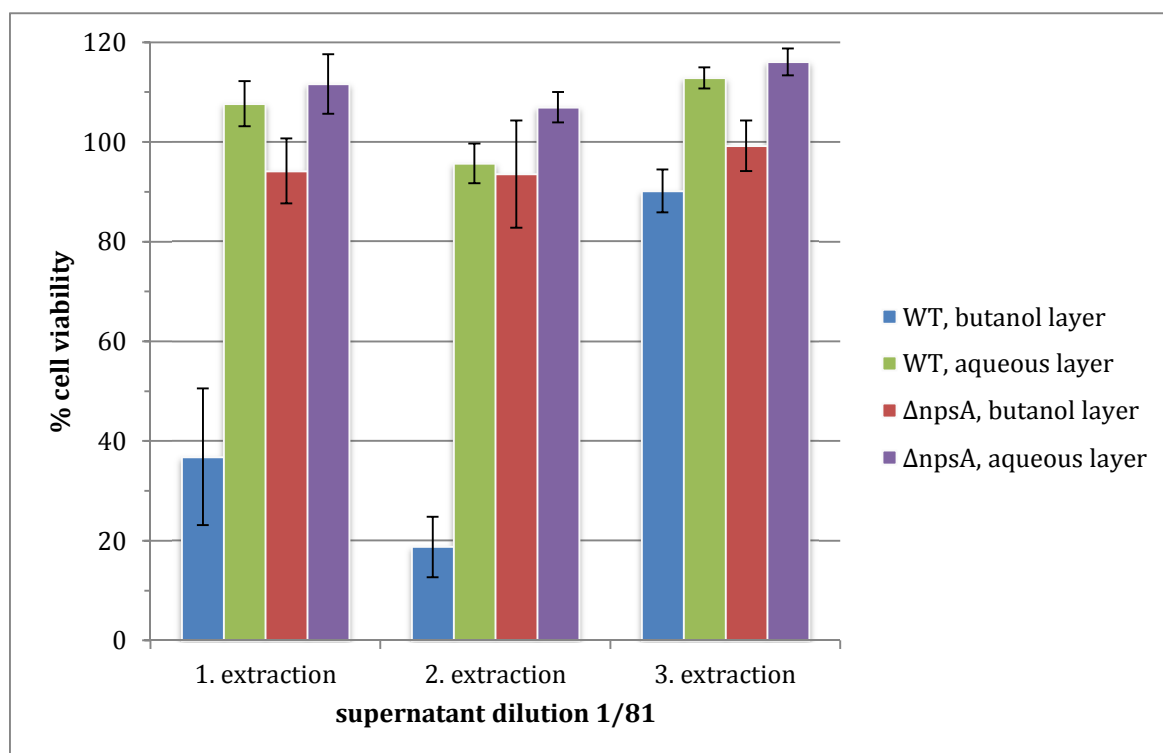


Figure 24. Toxicity screening of organic and aqueous *n*-butanol extracts of the wild type and the mutant $\Delta npsA$.

After drying of the combined butanol layers over sodium sulfate the crude extracts were concentrated under reduced pressure. Since the solubility of water in *n*-butanol is quite substantial, the aqueous layer could not be dried completely even with larger amounts of sodium sulfate. To retain cytotoxic activity rapid evaporation of the solvent under reduced pressure at a maximum temperature of 40°C was essential. Otherwise decomposition could be observed by decreasing cytotoxicity in the activity screening or by HPLC monitoring. After drying under high vacuum a pale yellow up to brown solid or sticky mass was obtained.

The crude product of the wild type and the mutant was then submitted to HPLC-MS analysis. Ideally the chromatograms of both extracts would be nearly identical and differ in only a single peak, which is supposed to be the cytotoxin. Surprisingly, such a pattern could be observed (figure 25). The only difference between these two chromatograms was the signal at 4.55 min with its most intense UV-activity at a wavelength of 221 nm.

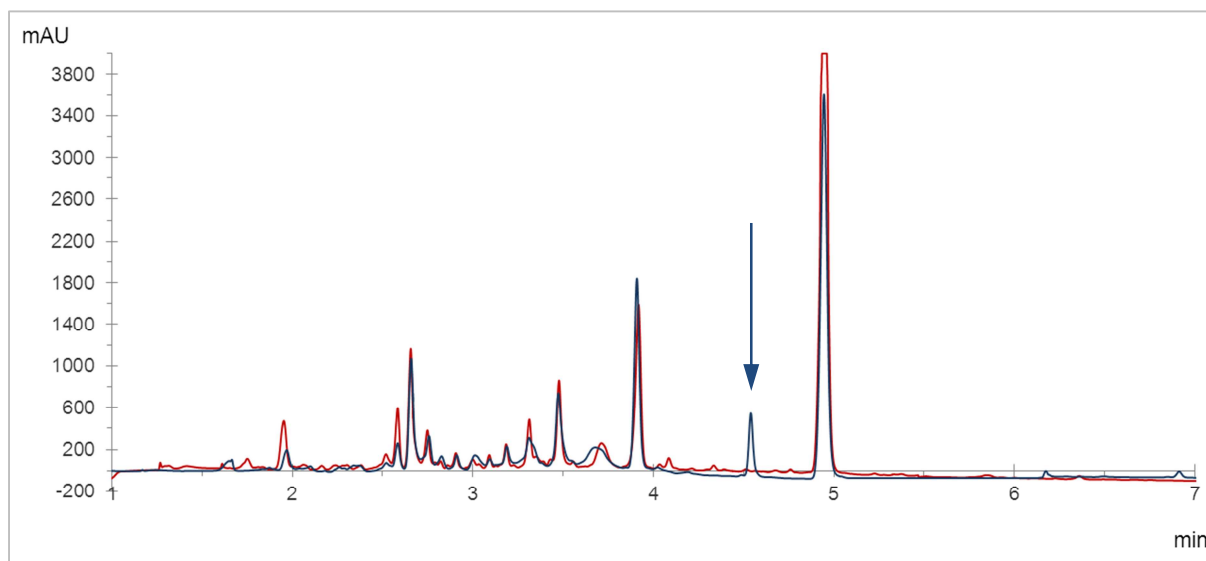


Figure 25. Overlaid chromatograms of the extracts from wild type (blue) and mutant (red) at 210 nm. Method: eluent A: 0.01 % HCOOH in H₂O, eluent B: acetonitrile, 0-6 min: 2-60 % B, 6-7 min: 60 % B, 0.7 mL/min, 40°C.

Luckily, this compound could be ionized with ESI positive and negative technique and its mass was defined as 333 Da. Subsequently, all parameters (stationary phase, eluents, gradient, time, flow and temperature) of the analytical HPLC method were optimized for the semi-preparative HPLC separation using the crude product of the mutant to identify the cytotoxin. Due to these optimization steps, we were able to shift the cytotoxin to a higher retention time, which simplified semi-preparative HPLC purification. The result of the numerous optimization steps is shown in figure 26.

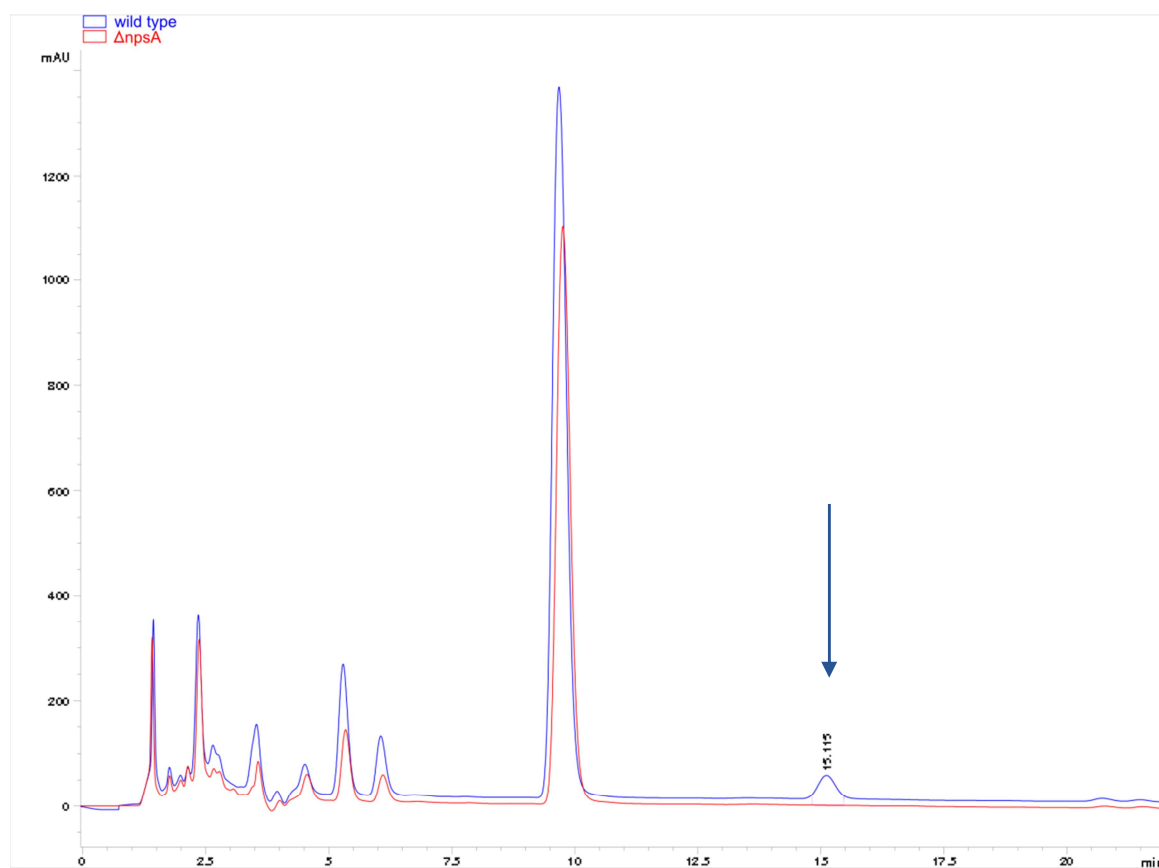


Figure 26. Optimized chromatogram of the wild type and the mutant at 220 nm. The supposed cytotoxin appeared after 15 min. Method: eluent A: H₂O, eluent B: methanol, 0-7 min: 50 % B, 7-17 min: 50-60% B, 17-21 min: 60 % B, 1.0 mL/min, 30°C.

The optimized HPLC method was applied for semi-preparative HPLC and had to be optimized again for the different HPLC instrument with increased dead volume and flow rate. Subsequently, the crude product of the wild type was purified by semi-preparative HPLC using a reversed phase C18 column. After evaporation of methanol and lyophilisation to remove residual water, a colorless solid was obtained (figure 27). This concentration of the cytotoxin again occurred carefully at a maximum temperature of 40°C as fast as possible. Toxicity tests of the purified substance confirmed the colorless solid to be the cytotoxin. Altogether, 41 mg of the cytotoxin were isolated from 1 L supernatant of *K. oxytoca*.



Figure 27. Purified cytotoxin.

4.3.3 Optimization attempts

When only a slow separation of the layers during extraction occurred, it could be accelerated by centrifugation. This was sometimes necessary to receive separated layers anyway.

To reduce the amount of major impurities in the crude product several filtration attempts were made. Filtration through a pad of silica gel resulted in decreased cytotoxic activity independently from the solvent used to rinse the cytotoxin although polar solvents were a little bit more efficient than middle up to apolar solvents. This confirmed the former results that the toxin is acid labile and starts to decompose in the presence of silica gel. However, washing the crude solid with water and rinsing it with methanol successfully reduced the amount of salts of the crude cytotoxin with only little loss in toxic activity.

When the crude product remained a sticky mass because of residual *n*-butanol, it was difficult to handle. Then it was dried under high vacuum by creating an azeotropic mixture with *n*-hexane, which vaporized easier. This azeotropic drying method was repeated several times until the crude product became a powdery solid.

Furthermore, reproducibility of the isolation procedure was not given all the time. The amount of toxin varied in the extracts. A reason for that could not be determined, but we speculate that varying time periods for extraction and concentration of the cytotoxin, in which it is supposed to decompose over time, might play a role.

By feeding the *K. oxytoca* bacteria instead of soya proteins with brain and heart proteins from pigs, we were able to increase the amount of cytotoxin in the extracts significantly.

4.3.4 Characterization and identification

The purified cytotoxin was submitted to gas chromatography with direct inlet coupled with high resolution mass spectrometry. With this analysis method its high resolution mass of 333.1493 Da was confirmed. Furthermore, two additional high resolution

fragments (264.0916 Da and 235.0893 Da) were obtained. The most stable fragment of the cytotoxin, the base peak, occurred at 117 Da and is characteristic for indole ions. The simple isotopic patterns of the molecular ion and its fragments exclude halogens and sulfur atoms from the cytotoxin structure, which would have characteristic isotopic patterns.

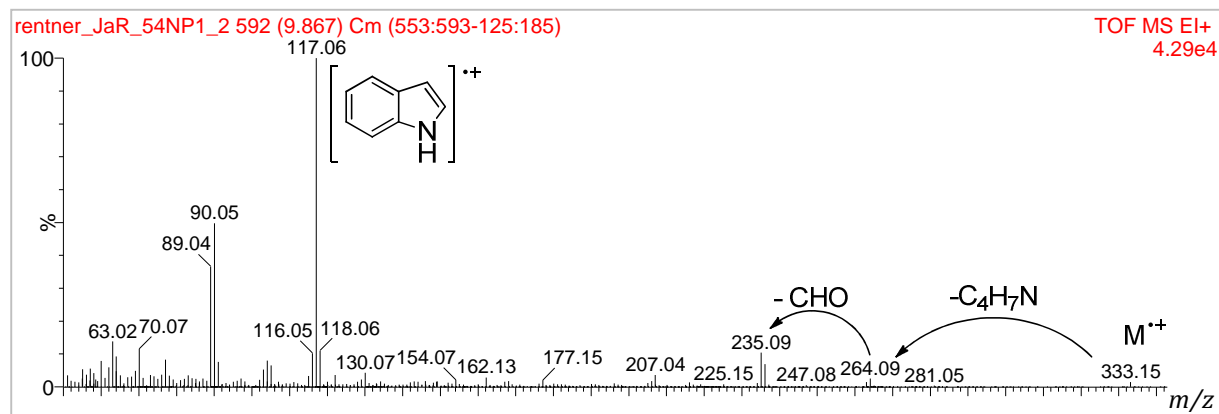


Figure 28. TOF EI MS of the cytotoxin.

Due to an odd molecular mass, the cytotoxin must contain an odd number of nitrogens. Considering this nitrogen-rule the molecular formula was calculated to be $C_{20}H_{19}N_3O_2$ and for the fragments 264 ($C_{16}H_{12}N_2O_2$) and 235 ($C_{15}H_{11}N_2O$) using a standard calculator for elemental composition. Results are shown in table 13.

Exp. Mass	Calc. Mass	Variance [ppm]	Formula
333.1493	333.1491	0.6	$C_{22}H_{21}O_6$
	333.1477	4.8	$C_{20}H_{19}N_3O_2$
	333.1517	-7.2	$C_{25}H_{19}N_1$
	333.1464	8.7	$C_{18}H_{17}N_6O_1$
	333.1523	-9.0	$C_{11}H_{21}N_6O_6$
263.0842	263.0861	-7.2	$C_{21}H_{11}$
	263.0821	8.0	$C_{16}H_{11}N_2O_2$
	263.0866	-9.1	$C_7H_{13}N_5O_6$
235.0893	235.0871	9.4	$C_{15}H_{11}N_2O_1$
	235.0917	-10.2	$C_6H_{13}N_5O_5$
	235.0858	14.9	$C_{13}H_9N_5$

Table 13. Calculation of the molecular formula of M^+ and two characteristic fragments. Tolerance: 25.0 ppm. Number of isotopic peaks used for i-FIT: 3. Elements used: C: 0-100, H: 0-1000, N: 0-6, O: 0-6.

With the molecular formula in our hands we were able to calculate the degree of unsaturation (DU) from the following general formula to be 13.

$$DU = \frac{2c - h + n - x + 2}{2} = \frac{40 - 19 + 3 - 0 + 2}{2} = 13$$

Formula 1. Degree of unsaturation of the unknown cytotoxin (C₂₀H₁₉N₃O₂) from the general formula C_cH_hO_oN_nX_x.

Measured IR-spectra gave some hints about structural elements such as aromatic substitution patterns and amide bonds. Also information about functional groups missing in the cytotoxin, such as triple bonds, halogens or cumulated dienes, was obtained from IR-spectra. To identify the structure of the cytotoxin over 50 one- and two-dimensional NMR-spectra were measured mainly in deuterated DMSO confirming the structural information from IR-spectra. Combining all this information, the cytotoxin could finally be identified as the structure **154** shown in figure 29. Stereochemistry was confirmed by NMR-spectroscopy. The main problem during NMR-characterization, beside stability of the cytotoxin **154** in deuterated solvents during long measurements, was its purity. Receiving the cytotoxin **154** in high purity was rather difficult since soluble parts of tubes or grease were found constantly in NMR-spectra. Nevertheless, by using Teflon-tubes and high-boiling grease these aliphatic signals could be reduced significantly.

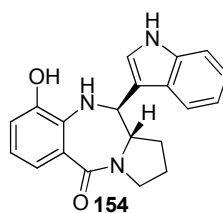


Figure 29. Structure of the cytotoxin **154**.

In 1982, *Mohr* and *Budzikiewicz* isolated 48 mg of a natural product from *K. pneumoniae* var. *oxytoca* from 360 L culture medium.^[15] The analytical data of our isolated cytotoxin **154** correspond to the analysis of their secondary metabolite, named tilivalline (**154**). Thus, our isolated cytotoxin **154** is already known as tilivalline (**154**). Studying their purification procedure, it is amazing that they isolated tilivalline (**154**) anyway. *Mohr* and *Budzikiewicz* extracted 360 L of the supernatant with ethyl acetate. But during our purification experiments we figured out that tilivalline (**154**) is only poorly soluble in solvents of middle polarity, such as ethyl acetate. Besides, they treated their ethyl

acetate extracts with 5 % aqueous HCl. From our experiments we know that tilivalline (**154**) is labile in the presence of acids even at traces. Furthermore, the concentrated extracts were purified by column chromatography using chloroform and methanol mixtures as eluent. Regarding our toxicity screening, tilivalline (**154**) decomposes in chloroform as well as on silica gel. Finally, *Mohr* and *Budzikiewicz* received the pure tilivalline (**154**) using reversed phase HPLC that succeeded also in our purification method. Nevertheless, with our modern bacteria growth and isolation method we clearly increased the efficiency of tilivalline production, isolation and purification.

Our recognized thermal instability of tilivalline (**154**) was also reported by *Minami* and co-workers.^[93] They determined the cytotoxic activity of tilivalline (**154**) in an aqueous buffer solution (Dulbecco's phosphate buffered saline) heated for 20 min to temperatures between 50-100°C (figure 30). At 70°C, the cytotoxic activity of tilivalline (**154**) decreased to 50 %. No cytotoxic activity remained after 20 min at 90°C.

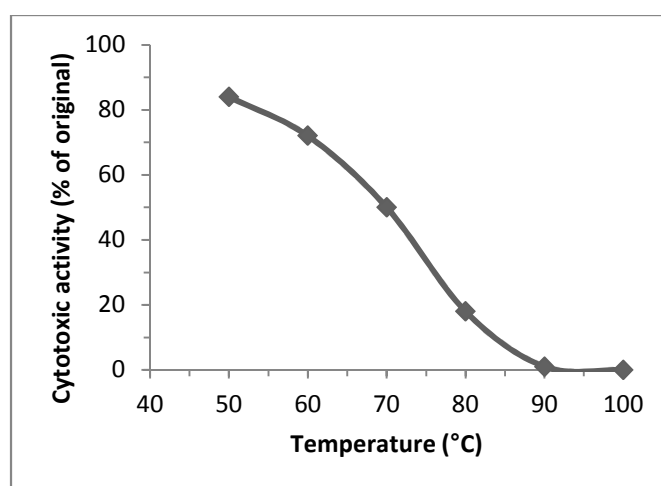
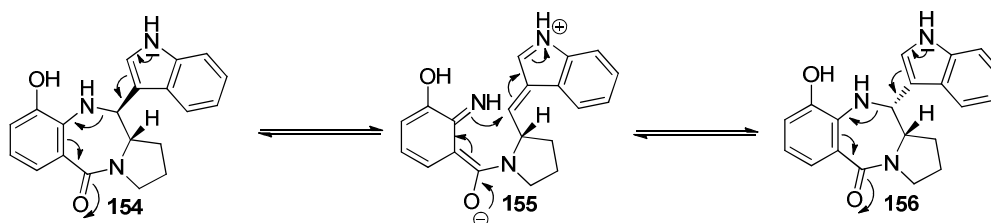


Figure 30. Diagram of tilivalline's activity in aqueous solution after treatment for 20 min at different temperatures.

The instability of tilivalline (**154**) in solution or under acidic conditions might result from its conjugated π -system that can stabilize the protonated form of tilivalline (**154**) through electron delocalization. This protonation-deprotonation process reminds a bit of the catalytic triade of enzymes. But exactly the protonated form **155** of tilivalline (**154**) might react unintended, which ends in decomposition. *Matsumoto* and co-workers made use of this effect and formed the epimer **156** of tilivalline (**154**) in the presence of lewis acids.^[94]



Scheme 68. Epimerization of tilivalline (**154**).

Furthermore, tilivalline (**154**) features one characteristic property, which has not been described in literature so far, i. e. fluorescence. Due to the indole scaffold, this effect could have been expected. Tilivalline's fluorescent activity can already be observed by irradiation of a tilivalline solution at a wavelength of $\lambda_{\text{exc}} = 366$ nm. From its UV-spectrum we knew the absorption maxima at a wavelength of $\lambda_{\text{ab}} = 221$ and 331 nm. Only excitation of tilivalline (**154**) in an aqueous solution at the latter wavelength resulted in an intensive emission of light with its maximum at $\lambda_{\text{em}} = 441$ nm. But yet this fluorescent activity of tilivalline (**154**) should be sufficient to enable studies of its interaction with biological macromolecules, such as proteins or DNA, without making use of additional fluorescent markers.



Figure 31. Tilivalline (**154**) in H₂O, irradiated at 366 nm.

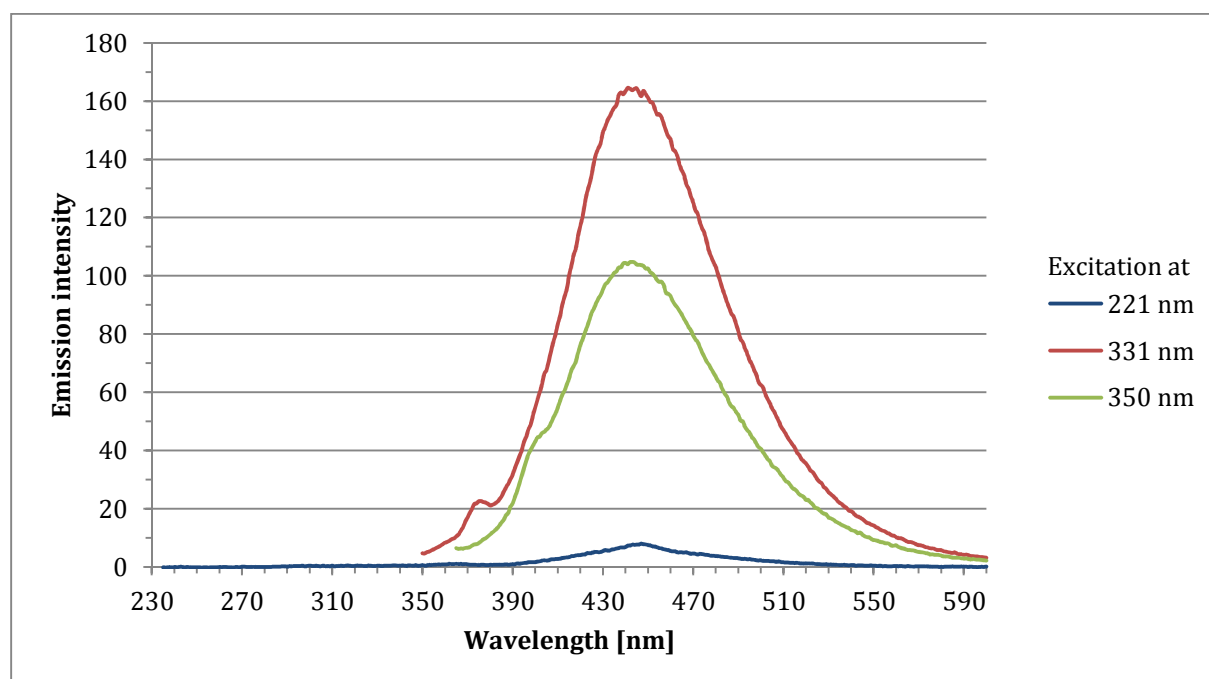


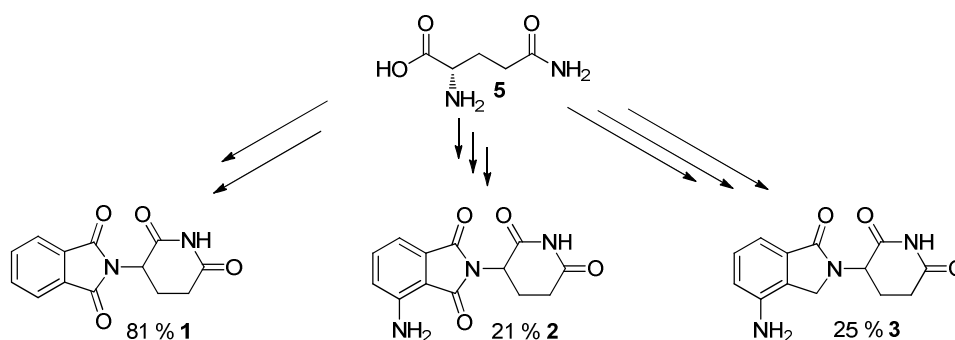
Figure 32. Fluorescence spectrum of tilivalline (**154**) ($c = 81 \mu\text{M}$ in H₂O). Excitation occurred at $\lambda_{\text{exc}} = 221, 331$ and 350 nm.

5. Summary and outlook

Even today, there is a great demand for a universal method to identify all types of protein targets and off-targets of an emerging drug. To simplify drug approval, compound-centric chemical proteomics was developed previously. In this proteomics approach biologically active molecules were tethered onto a solid support and screened for binding proteins. This enables studies about the entire protein target spectrum of a drug. State-of-the-art techniques provide the potential for a general protein target screening by compound-centric chemical proteomics. But for a universal application, general methods for tethering the drugs of interest to a solid support without diminishing their biological activity are required.

5.1 Drug syntheses

To identify the whole protein target spectrum of thalidomide (**1**), pomalidomide (**2**) and lenalidomide (**3**), these drugs were synthesized according to literature. Thalidomide (**1**) was synthesized in two steps with an overall yield of 81 %, whereas *Muller* and co-workers reached 61 %.^[74] The synthesis of pomalidomide (**2**) required one more step and yielded only 21 % of the product **2** following the procedure of *Ge* and co-workers who did not mention the yields in their patent.^[75] But the most challenging drug synthesis was the one of lenalidomide (**3**). Following the patent of *Muller* and co-workers was unrewarding.^[76] Intramolecular cyclization occurred in the very beginning of the synthesis sequence but was not mentioned. Nevertheless, lenalidomide (**3**) could be synthesized according to the patent of *Devarakonda* and co-workers, reported in 2009.^[82] By only little optimization studies we obtained lenalidomide (**3**) in overall 25 % yield within six steps.

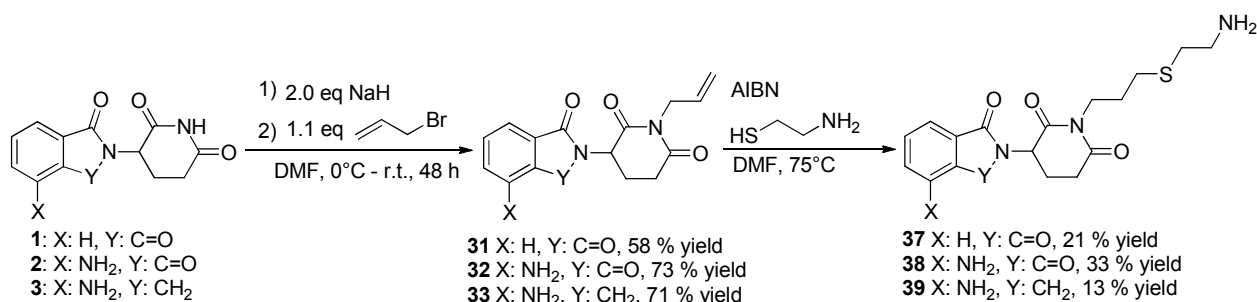


Scheme 69. Thalidomide, pomalidomide and lenalidomide.

5.2 Thiol-ene linkage

Two strategies for tethering the synthesized drugs thalidomide (**1**), pomalidomide (**2**) and lenalidomide (**3**) onto a solid support were developed. These strategies consist of two to three steps starting with the allylation of the drugs **1-3**, which occurred in 58-73 % yield (scheme 68). Because of the low solubility of the allylated drugs **31-33**, purification was difficult but could be achieved either by recrystallization or by preparative TLC.

The first linkage strategy, namely thiol-ene approach, was established with the former allylated drugs **31-33** by adding cysteamine hydrochloride (**35**), a linker type thiol. Starting this radical reaction with AIBN, 21 % of the linked thalidomide **37**, 33 % linked pomalidomide **38** and 13 % linked lenalidomide **39** could be isolated after preparative HPLC. The moderate yields might be ascribed to the very poor solubility of the linked substrates **37-39**. Surprisingly, the linked lenalidomide **39** was also labile and oxidized in the presence of air to the more stable linked pomalidomide **38**. Screening of the linked drugs **37-39** via compound-centric chemical proteomics was pursued. No binding proteins could be identified so far, possibly because of the sensitive cell extracts, whose proteins denatured over time.



Scheme 70. Thiol-ene linkage strategy.

Nevertheless, this strategy should be applicable to all dissolvable drugs with a functional group free for allylation. The thiol-ene reaction tolerates many types of functional groups except strong bases and reactive double bonds. For the future other interesting substrates should be linked with this thiol-ene approach and investigated in chemical proteomics studies. Some interesting drugs that might be suitable for thiol-ene linkage are listed in figure 33. These drugs were all withdrawn from the market within the last decades due to dramatic adverse effects.^[95,96] They might be investigated for the

identification of their entire protein target spectrum using compound-centric chemical proteomics. Tethering could occur at free NH-groups, hydroxy groups or carboxylic acids. Rapacuronium (**163**) already contains an allyl-group that might be used for linkage as long as this allyl group is not required for protein interaction.

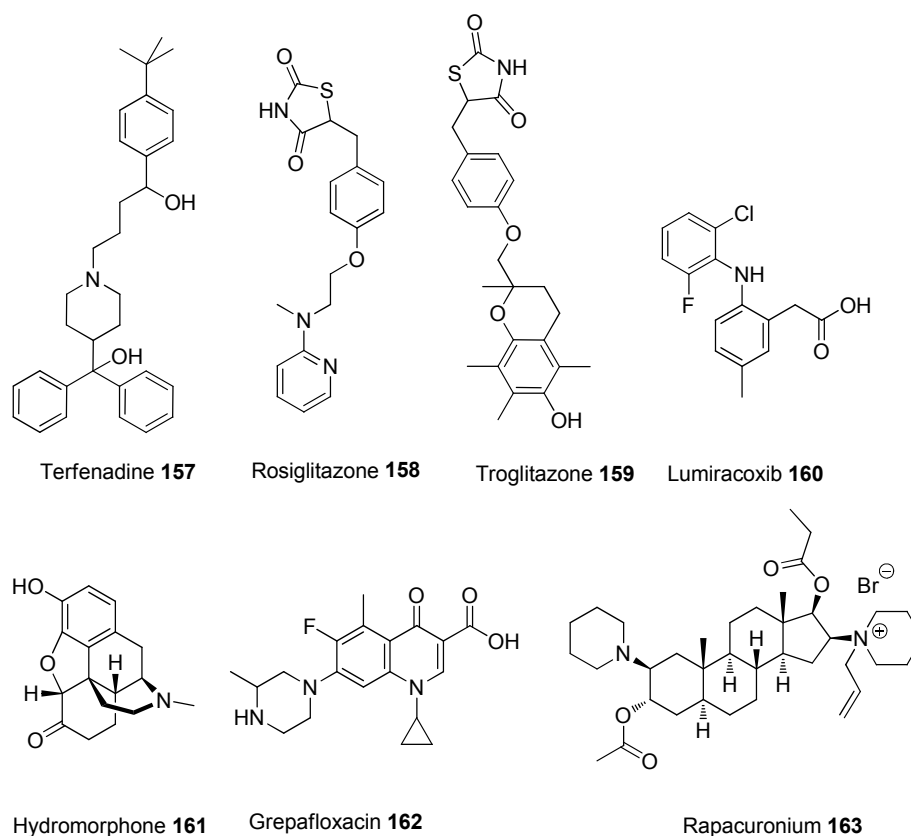
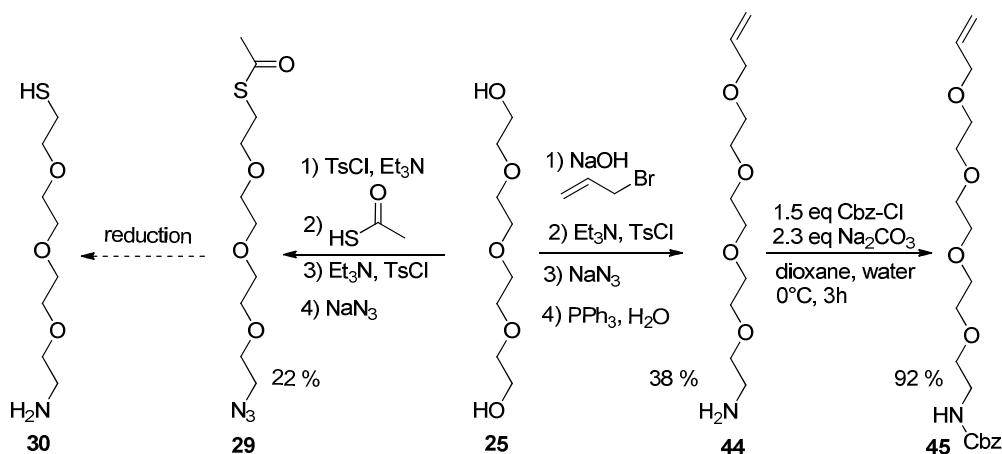


Figure 33. Possible candidate drugs for thiol-ene or cross-metathesis linkage following chemical proteomics.

5.3 Linker syntheses

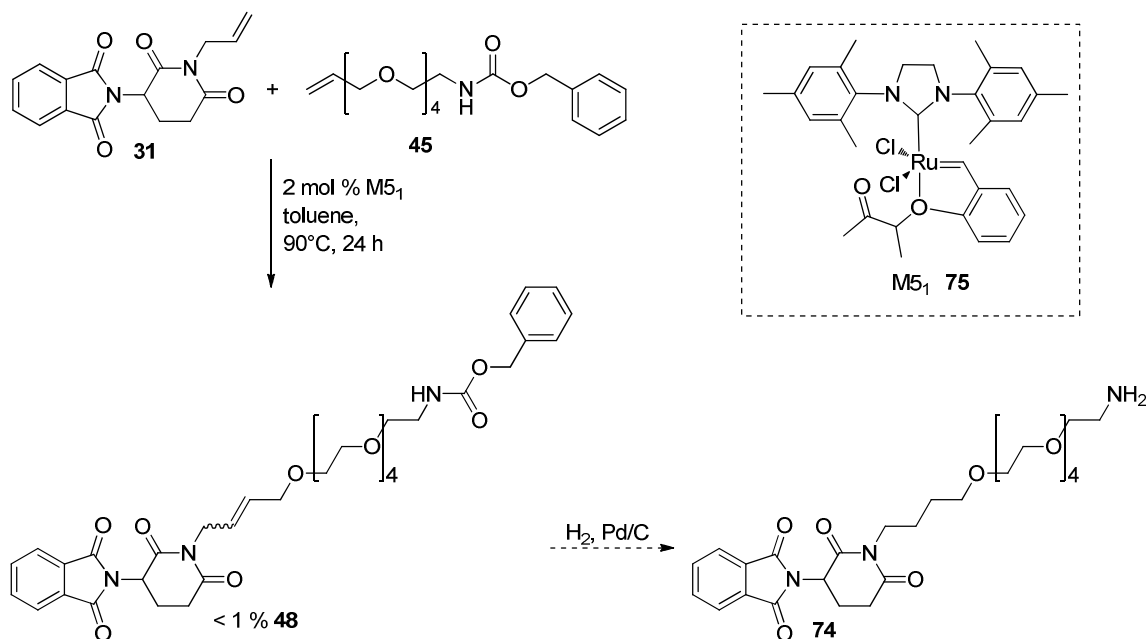
Furthermore, we started to synthesize a longer thiol linker according to the procedure of *Stefanko* and co-workers^[24] to increase the variety of possible linkers and therefore the applicability of this thiol-ene strategy. We chose tetraethylene glycol (**25**) as starting material and received 22 % yield for the pre-thiol-linker **29**, synthesized in four steps (scheme 71). The last step of the linker synthesis and its coupling with an allylated drug is still pending as the thiol is air sensitive and such a long thiol-linker **30** was not needed for tethering allylic thalidomide **31** and its derivatives **32** and **33**. But this should be investigated in the future. Analogously, the allyl-linker **44** for cross-metathesis was synthesized with an overall yield of 38 % in four steps. Also a Cbz-protected variant **45**

of the allyl-linker **44** was synthesized. Both allylic linkers **44** and **45** and the allylic azide **43** were tested simultaneously in the olefin cross-metathesis with allyl-thalidomide **31**.



5.4 Cross-metathesis linkage

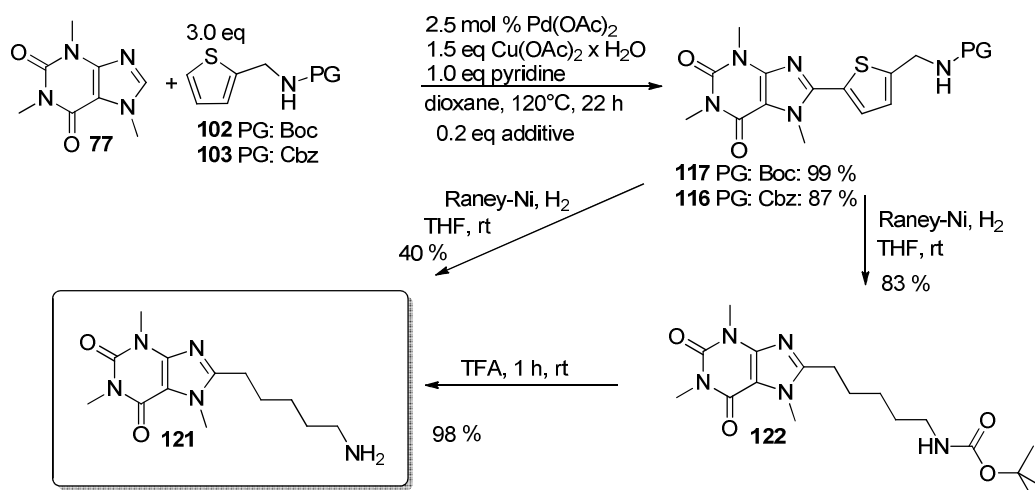
As a second linkage strategy we developed the cross-metathesis approach, in which an allyl type linker is coupled to an allylated drug. This approach required a third step, the hydrogenation of the produced double bond. We tested our linkage strategy with allyl-thalidomide **31** and allylated tetraethylene glycol derivatives **43-45**, synthesized before. In over 80 reactions we screened three different catalysts (Grubbs II, Grubbs-Hoveyda II and M5₁ (**75**)) and three different linkers (azide **43**, allyl-linker **44**, Cbz-protected allyl-linker **45**). We optimized the amount of catalyst, the equivalents of both alkenes, their order of addition, solvents and reaction temperature. Finally, we were able to link the allylated thalidomide **31** for the first time in a cross-metathesis reaction (scheme 72). This result was amazing since cross-metathesis reactions with allylic ethers are very rare. Unfortunately, conversion in this olefin cross-metathesis was below 1 %. Subsequent hydrogenation to the new linked thalidomide **74** was therefore not investigated. Consequently, allyl-thalidomide **31** is not a suitable olefin for cross-metathesis.



To establish the cross-metathesis linkage, less complex, allylated drugs must be investigated. Hydrogenation of these cross-metathesis products will accomplish this linkage approach. Drugs suitable in the thiol-ene linkage can also be taken into account for cross-metathesis linkage. This proof is still pending.

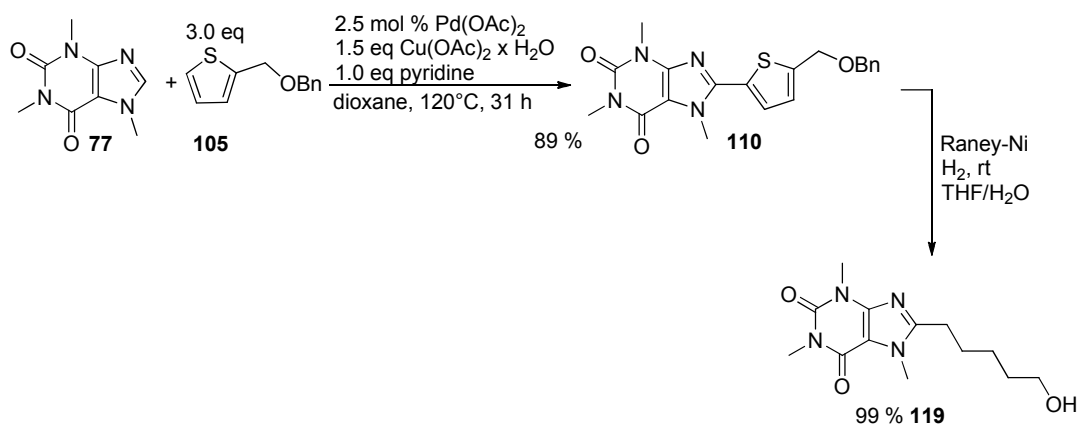
5.5 Thiophene linkage

The third linkage approach started again as a two step strategy that did not require a functional group at the drug anymore. Instead, a heteroaromatic compound was used. The drug-like molecule, in our case we used caffeine (**77**) as test substrate, was coupled in the first step to thiophene derivatives via dehydrogenative cross-coupling. Before, these thiophene derivatives were synthesized. The synthesis of the required thiophenes was often difficult probably due to the sulfur atom, which influenced the reactivity of thiophenes remarkably. Nevertheless, 5 thiophenes could be synthesized in addition to the commercially available thiophenes. After optimization of the cross-coupling conditions (4 different additives, 1 ligand, 3 oxidants) and screening of 9 different thiophenes excellent conversions of caffeine (**77**) with *N*-Boc-aminomethyl thiophene **102** and *N*-Cbz-aminomethyl thiophene **103** were achieved.



Scheme 73. Optimized thiophene linkage with caffeine (**77**) and *N*-protected aminomethyl thiophenes **102** and **103**. PG = Boc: 0.2 eq CuCl, PG = Cbz: 0.2 eq 1,10-phenanthroline.

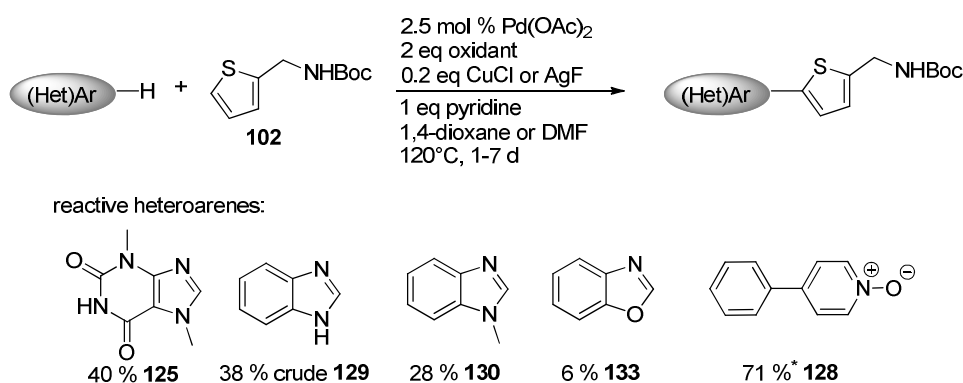
The second step of this linkage method was the desulfurization and hydrogenation of the cross-coupled thiophene derivatives resulting in the correspondingly functionalized alkyl chain **121** in 40 % yield starting from the Cbz-protected derivative **116** and 83 % yield of **122** starting from the Boc-protected thiophene **117**. To achieve this yield, 4 different catalysts in varying amounts, 5 solvents, several reaction temperatures and one metal-free reaction system were screened. Our best desulfurizing conditions were an excess of Raney Nickel (W-2, 2-3 mL Raney-Ni per 0.1 mmol substrate) in THF at rt under hydrogen atmosphere. All other cross-coupled thiophene derivatives with evolving amines during reduction reacted hardly. Using the Boc-protected derivative **117**, purification by flash chromatography instead of preparative HPLC was easy but required deprotection as a third step. Due to high yields and simple purification this third step can be accepted to receive the linked caffeine **121** via thiophene linkage strategy in 81 % overall yield.



Scheme 74. Optimized thiophene linkage with caffeine (**77**) and *O*-protected 2-thiophenemethanol **105**.

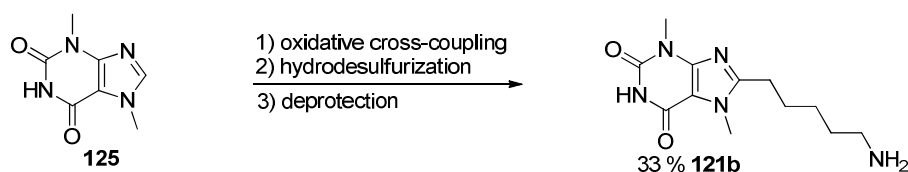
Using benzyl-protected 2-thiophenemethanol **105**, the cross-coupling product with caffeine **110** precipitated from methanol in 89 % yield. Hydrodesulfurization and benzyl deprotection occurred stepwise with Raney-Ni in a one-pot reaction resulting in the alkyl tethered caffeine **119** with a terminal hydroxyl group free for linkage with a solid support in 88 % overall yield (scheme 74). Considerable advantages of the thiophene linkage with benzyl-protected 2-thiophenemethanol **105** are the simple purification steps combined with excellent yields and simultaneous deprotection together with the hydrodesulfurization reaction.

Scope and limitations of our thiophene linkage strategy were verified by testing it under the optimized conditions with other heteroarenes differing in type and amount of heteroatoms, functional groups and electronical properties. Altogether 11 different arenes were screened with sobering results. None of these substrates showed similar reactivity compared to caffeine (**77**). Nevertheless, five heteroarenes reacted in the dehydrogenative cross-coupling (scheme 75). Optimizing the catalytic system for each compound individually must be continued to receive excellent yields. Purification of the cross-coupled substrates remains challenging. Subsequent hydrodesulfurization and Boc-deprotection is still outstanding and has to complete the linkage approach of these heteroarenes.



Scheme 75. Scope of cross-coupling in the thiophene linkage with *N*-Boc aminomethyl thiophene **102**. Oxidant was either copper(I) acetate monohydrate or silver acetate. *Conversion is given, which was determined by HPLC. **128** was not isolated.

Nevertheless, our developed thiophene-linkage strategy could be demonstrated with theobromine (**125**) as second heteroarene. The three-step approach was performed with *N*-Boc aminomethyl thiophene **102** and yielded the linked theobromine **121b** in 33 % overall yield.



Scheme 76. Tethering of theobromine via thiophene-linkage strategy.

Since new methods for cross-coupling of arenes or heteroarenes are published almost monthly, new, evolving catalytic systems can be tested soon and the range of valuable substrates can be increased by simultaneously optimized reaction yields. Drugs containing indole or imidazole structures also with free NH-groups or even arenes without heteroatom might be reactive in thiophene linkage soon. The drugs shown in figure 34 were all withdrawn from the market due to their dramatic adverse effects.^[95,96] Their protein targets still have to be identified, for example using our established thiophene-linkage strategy, to investigate their mode of action.

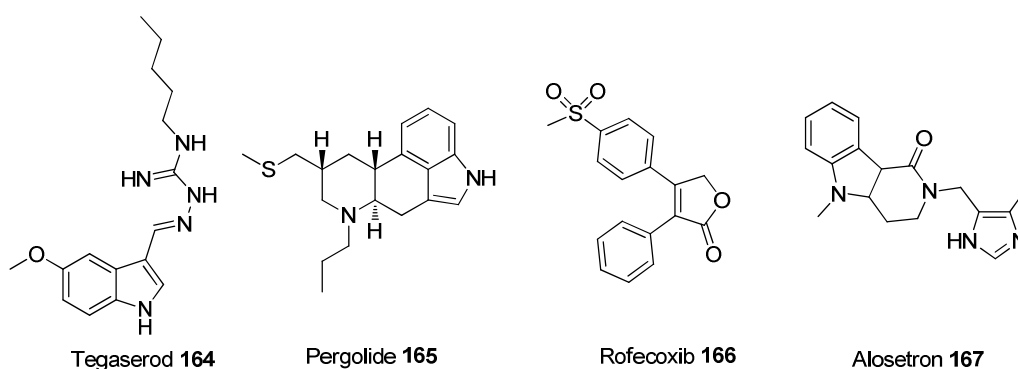


Figure 34. Possible candidate drugs for thiophene-linkage following chemical proteomics.

5.6 Isolation of an unknown cytotoxin

An unknown cytotoxin, which is produced and excreted by intestinal *K. oxytoca* wild type bacteria, was determined to cause antibiotic associated hemorrhagic colitis. To study its mode of action, this cytotoxin had to be identified in advance. Therefore, it was isolated by extraction of the supernatant of the *K. oxytoca* wild type bacteria with *n*-butanol followed by optimized semi-preparative reversed-phase HPLC purification. For negative control the non-ribosomal synthesis mutant Δ npsA underwent the same procedure simultaneously. From 1 L culture solution of the wild type we could successfully isolate 41 mg of the cytotoxin as colorless solid although reproducibility

was not given all the time. Nevertheless, we were able to characterize this cytotoxin using reversed phase HPLC-MS, HRMS, polarimetry, 1D- and 2D-NMR, FT-IR and fluorescence spectroscopy methods. Finally we identified this cytotoxin to be the previously described natural product tilivalline (**154**) with a molecular mass of 333.1493 Da and a molecular formula of C₁₉H₂₀N₃O₂.

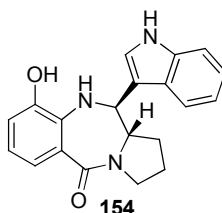


Figure 35. The cytotoxin of *K. oxytoca* was identified as tilivalline (**154**).

For future biological studies the identification of enzymes participating in the biosynthesis of tilivalline (**154**) would be reasonable. This might be accomplished by feeding *K. oxytoca* bacteria with tagged inhibitors that bind selectively to the enzymes responsible for tilivalline synthesis. This enzyme-inhibitor interaction may be determined using for example chemical proteomics techniques. Moreover, tilivalline's mode of action as intestinal cytotoxin must be clarified. Its toxic effect might be regulated by selective substitution of its functional groups. Since tilivalline (**154**) possesses fluorescent activity, the interaction of tilivalline (**154**) with biological macromolecules, such as DNA or proteins, may be monitored by fluorescence correlation spectroscopy.

6. Experimental part

6.1 General Aspects

6.1.1 Chemicals and solvents

All commercially available reagents and solvents were received from Sigma-Aldrich, Fisher Scientific, ABCR, Alfa Aesar, Roth, Lactan, Lancaster, VWR, TCI, Fluorochem or Acros Organics and were used without further purification except otherwise stated. When it was required, non-dry solvents were distilled before use. If reactions were performed under exclusion of water and oxygen, solvents and reagents were degassed and dried with common methods and stored under inert gas (Ar or N₂) over molecular sieves. Otherwise, solvents were already received dry. When high vacuum is mentioned in experimental procedures, typically a vacuum of 0.1-0.001 mbar was applied. All reactions were stirred with a magnetic stirring bar unless otherwise stated.

Small amounts of solvents (5 mL or less) were degassed by evacuation under high vacuum until the solvent started to boil. Then it was flushed with inert gas. This process was repeated at least three times depending on the amount of solvent to be degassed. Larger amounts of solvent were degassed by bubbling Ar from a balloon via cannula through the solvent during ultrasonification for about 30 min. If this was not possible, the solvent had to be frozen in liquid N₂ followed by evacuation under high vacuum. This procedure was repeated at least three times.

Before use, molecular sieves (beads with 8-12 mesh) were activated in a round-bottom flask with gas-inlet by heating them carefully with a heating mantle at level 1 under high vacuum for at least 2 d until complete dryness was obtained. Activated molecular sieves were stored at rt under Ar atmosphere.

The solvents and chemicals listed below were prepared according to the following procedures.

Non-dry **acetone** was carefully distilled using a rotary evaporator and stored in a dark bottle.

Acetonitrile (ACN) was purchased in dry quality without stabilizer and stored over 3 Å molecular sieves under Ar in a dark bottle.

N-Bromosuccinimide (25.8 g, 145 mmol) was recrystallized from 380 mL H₂O to yield 84 % colorless crystals before use. The purity was confirmed by NMR spectroscopy.

Non-dry **n-butanol** for toxin extraction was purchased from Alfa Aesar in 99 % purity containing 5 mg/L non-volatiles.

The second generation metathesis **catalysts** from Grubbs-Hoveyda and (1,3-bis(2,4,6-trimethylphenyl)-2-imidazolidinylidene)dichloro(2-(1-methylacetoxy)phenyl)methylen ruthenium(II) (**75**) (type M5₁) were kindly provided by Prof. C. Slugovc (Institute for Chemistry and Technology of Materials at the Graz University of Technology) and were used without further purification or characterization.

Non-dry **cyclohexane** was purchased in analytical grade or distilled through a 20 cm Vigreux column into a dark bottle before use.

Dichloromethane was dried in two steps. In the first step it was heated under reflux for one day over P₄O₁₀ and distilled through a 20 cm Vigreux column. Subsequently, the pre-dried dichloromethane was heated under reflux over calcium hydride for 2 or 3 d followed by distillation through a 20 cm Vigreux column into a dark Schlenk bottle and stored over 4 Å molecular sieves under Ar.

1,2-Dichloromethane was purchased in dry quality and stored under Ar in a dark bottle with AcroSeal®.

Non-dry **diethyl ether** was carefully distilled using a rotary evaporator and stored in a dark bottle over KOH before use. If dry diethyl ether was required, it was further heated under reflux over sodium until benzophenone indicated dryness of the solvent by turning the color of the solution from green into blue. The dry diethyl ether was distilled through a 20 cm Vigreux column into a Schlenk flask under Ar and was used immediately.

***N,N*-Dimethylacetamide** (DMA) was purchased in dry quality and stored over 3 Å molecular sieves under Ar in a dark Schlenk bottle.

***N,N*-Dimethylformamide** (DMF) was purchased in dry quality and stored over 3 Å molecular sieves under Ar in a dark Schlenk bottle.

1,4-Dioxane was purchased in dry quality and stored over 4 Å molecular sieves under Ar in a dark Schlenk bottle. Non-dry 1,4-dioxane was carefully distilled using a rotary evaporator and stored in a dark bottle over KOH before use.

Ethanol was dried by heating it carefully under reflux with sodium and diethyl phthalate for 2 h until hydrogen development decreased. Subsequently, the dried ethanol was distilled through a 10 cm Vigreux column under Ar and stored over 3 Å molecular sieves.

Non-dry **ethyl acetate** was purchased in analytical grade or distilled through a 20 cm Vigreux column into a dark bottle before use.

***n*-Hexane** was received dry and stored under Ar over 4 Å molecular sieves in a dark Schlenk bottle.

Methanol was heated under reflux over magnesium turnings for one day followed by distillation into a dark Schlenk bottle where it was stored over 3 Å molecular sieves under Ar.

1.0 g **palladium(II) acetate** was purchased from Sigma-Aldrich and recrystallized from 25 mL absolute acetic acid. The brown powder was stored in a Schlenk tube under inert gas at 4°C.

Pyridine was purchased with anhydrous quality and stored over molecular sieves in a dark bottle with AcroSeal® under Ar.

Raney Nickel as activated W-2 type catalyst was synthesized according to the procedure by *Mozingo* from 1941.^[68b] In an open Erlenmeyer flask with magnetic stirring bar, 760 mg (19 mmol, 2.7 eq) NaOH were dissolved in 3.0 mL water. The solution was cooled with an ice bath to keep the temperature of the reaction mixture below 25°C. Under vigorous stirring, 600 mg (7 mmol, 1.0 eq) NiAl alloy were added portionwise over 1 h. The black suspension was allowed to warm up to rt. Once the intensity of hydrogen release decreased, the reaction mixture was left for 14 h at rt without stirring. Subsequently, the mixture was heated carefully to 35°C, then 45°C, 55°C, 65°C, 75°C up to 85°C without stirring until hydrogen release stopped. After cooling to rt, the colorless solution was decanted and the black residue was washed with water (1x3 mL, 1x20 mL), NaOH solution (100 mg in 1 mL water, 1x1 mL), water (25x3 mL) until the pH of the supernatant reached 7, and finally with dry ethanol (6x3 mL). The activated Raney Nickel was stored in 3 mL dry ethanol under N₂ at rt until use. Alternatively, Raney-Nickel 2800 was purchased from Sigma Aldrich as black slurry in water, which is stated to be equivalent to the activated W-2 type catalyst.

Tetrahydrofuran (THF) was heated under reflux over sodium until benzophenone indicated dryness of the solvent by turning the color of the solution from green into blue. Then THF was distilled through a 20 cm Vigreux column into a dark bottle and stored under Ar over 4 Å molecular sieves. Alternatively, dry THF without inhibitor was purchased from Sigma Aldrich and stored over 4 Å molecular sieves under Ar in a dark Schlenk bottle. Non-dry THF was carefully distilled using a rotary evaporator and stored in a dark bottle over KOH before use.

Toluene was purchased in dry quality. Additionally, it was filtered through an Alox column (Pure Solv from Innovative Technology) right before use or dried dynamically by storage over 4 Å molecular sieves under Ar in a dark Schlenk bottle.

Triethylamine was dried in two steps. 1 L triethylamine were heated under reflux over 50 g KOH for 1 d and distilled into a dark bottle. Subsequently, the pre-dried triethylamine was heated under reflux over calcium hydride for 3 h. Afterwards, it was distilled into a dark Schlenk bottle, where it was stored over 3 Å molecular sieves under Ar.

Water used in reactions and workup was demineralized. Water for HPLC purpose was additionally filtrated through a 0.2 μm cellulose nitrate membrane filter. If necessary, 1 L of filtrated water was further acidified with 100 μL formic acid to obtain a 0.01 % formic acid solution in water (pH 3.40) right before use.

Workup of hydrogenation reactions:

After finishing a hydrogenation reaction, all pyrophoric catalyts were removed by filtration through a pad of celite or silica gel under an inert atmosphere (N_2 or Ar). The catalytic residue was immediately stored under water. This slurry was disposed of as hazardous waste.

6.1.2 Materials for chromatography

Reactions were monitored by *thin layer chromatography* (TLC) on commercial silica gel plates (TLC aluminum foil, Merck, 60 F₂₅₄). Detection was carried out under UV-light (254 or 366 nm) or by staining with one of the following staining solutions and development in the heat.

CAM: 5.0 g ammonium molybdate were dissolved in 100 mL H_2O . Under stirring, 6.3 mL sulfuric acid and 2.0 g $\text{Ce}(\text{SO}_4)_2$ were added.

Ninhydrin: 0.2 g ninhydrin were dissolved in 100 mL ethanol.

Vanillin: 0.5 g vanillin were dissolved in 80 mL conc. sulfuric acid and 20 mL ethanol.

KMnO₄: 0.3 g KMnO_4 and 20 g K_2CO_3 were dissolved in 300 mL H_2O . Under stirring, 5 mL 5 % aqueous NaOH were added.

For *preparative thin layer chromatography* (PTLC), PLC silica gel glass plates (60 F₂₅₄, 20x20 cm) from Merck with a layer thickness of 0.5, 1.0 or 2.0 mm, depending on the amount of crude product to be purified, were used. Product bands were detected by UV-light at 254 or 366 nm and marked with a pencil. Afterwards, the product band was

scraped off the glass, collected in a frit and rinsed with methanol until the product was completely removed from the silica gel. Concentration of the extract under reduced pressure yielded the purified product.

Flash chromatography was performed on silica gel 60 (particle size 35-70 μm) from Acros Organics at elevated pressure. Amounts of silica gel used, eluents and gradients were stated for each compound.

6.1.3 Equipment

If possible, reactions were monitored by *gas chromatography mass spectrometry* (GC-MS) using either a HP 6890 GC system (from Agilent Technologies) with the mass selective detector 5972 MSD (EI, 70 eV) or a HP 7890A GC system (from Agilent Technologies) with the mass selective detector 5975C MSD (EI, 70 eV). In both GC-MS instruments the samples were injected with a 7683B injector making use of the split mode. The components were separated on a capillary column HP-5MS, 30 m x 0.25 mm, layer thickness 0.25 μm with helium 5.0 as carrier gas. Temperature programmes for analysis of the samples depended on the nature of the components (polarity and boiling point). Two different methods were used:

JR_50_S: 1 min at 50°C, ramp 40°C/min linear to 300°C, hold for 5 min.

JR_100_L: 1 min at 100°C, ramp 40°C/min linear to 300°C, hold for 15 min.

The method used, the retention time t_R according to the GC chromatogram, the molecular peak including the relative intensity to the basis peak and the basis peak according to the mass spectrum are reported in each case. As no standards were used during the measurements, all data are relative values.

Nuclear magnetic resonance (NMR) spectra were recorded on a Bruker Avance III spectrometer (300.36 MHz for ^1H -NMR, 75.53 MHz for ^{13}C -NMR) with autosampler or a Varian Unity Inova NB high resolution spectrometer (499.90 MHz for ^1H -NMR, 125.71 MHz for ^{13}C -NMR). Tetramethylsilane or the residual solvent peak was set as internal standard. Chemical shifts (δ) are reported in parts per million (ppm) and the coupling

constants (J) are reported as absolute values in Hertz (Hz). Parts of the structure according to the signals are also mentioned. If necessary, APT spectra and additional 1D and 2D spectra (HSQC, HMBC, HMQC, COSY, TOCSY, NOESY) were measured to identify and confirm the structure.

High resolution mass spectrometry (HRMS) was performed using a Waters GCT premier micromass with electron impact ionization (EI) at 70 eV. The probes were submitted to HRMS either by direct inlet or by GC 7890A from Agilent Technologies with capillary column DB-5MS (30 m x 0.25 mm, film: 0.25 μ m). For molecules with a high molecular weight, a Micromass Tofspec 3E spectrometer with matrix assisted laser desorption ionisation (MALDI), α -cyano-4-hydroxycinnamic acid as matrix and a time of flight mass analyzer (TOF) was used.

Melting points were determined with a Mel-Temp[®] melting point apparatus with integrated microscopical support from Electrothermal in open capillary tubes and are uncorrected.

Infrared spectra were collected using a Bruker Tensor 37 FT-IR spectrophotometer (4000-600 cm^{-1}) with integrated ATR module. The background signal is air, which was subtracted automatically from each spectrum. The wavenumbers are reported in cm^{-1} and their intensities are given as w (weak), m (medium) or s (strong).

The *specific rotation* $[\alpha]_D^{20}$ was measured with a polarimeter 341 from Perkin Elmar at 20°C at a wavelength of 589 nm, which corresponds to the D-line of the sodium light source.

Fluorescence spectra were recorded on a RF-5301PC spectrofluorophotometer from Shimadzu at rt.

Analytical high performance liquid chromatography (HPLC) data were obtained on three different HPLC instruments. The first one is the high performance liquid chromatograph "1100 series" from Agilent technologies, consisting of a degasser G1322A, quat pump G1311A, ALS G1313A, column oven G1316A, RID G1362A and DAD G1315A. The second HPLC instrument belongs to the "1200 series" from Agilent with a degasser G1379B,

binary pump SL G1312B, High Performance Autosampler SL G1367C, FC/ALS thermostat G1330B, Thermostatted Column Compartment SL G1316B, 4-channel UV detector MWD SL G1365C and mass selective detector 6120 containing electro spray ionization (ESI positive or negative) and quadrupole analyzer. The third instrument is a Shimadzu Nexera HPLC-MS system with two Nexera LC-30AD pump modules, Nexera SIL-30AC auto sampler, CTO-20AC prominence column oven, SPD-M20A prominence diode array detector, CBM-20A prominence communications bus module, FCV-20AH₂ valve unit and LCMS-2020 quadrupole mass detector allowing for simultaneous collection of ESI signals in positive and negative mode.

Following columns were used for analytical HPLC and HPLC-MS:

Chromolith® Performance RP-18e 100x2 mm, Merck.

Nucleodur C18 ec 150/4, 100x5 mm, Macherey-Nagel.

Poroshell 120 EC-C18, 100x3 mm, 2.7 μm, Agilent.

Columns and methods for analytical purpose were selected and optimized depending on each separation problem. The method used, retention times (t_R) according to the HPLC chromatogram at a defined wavelength and the molecular peaks in the mass spectrum were reported in each case. Counterions were not detectable with this characterization method. The following methods were used for analytical HPLC-MS:

Method A: Chromolith, A: 0.01 % HCOOH in H₂O, B: MeOH, 25°C, 0.7 mL/min, 0-15 min: 25 % B, ESI⁺, λ = 254, 230, 210 nm.

Method B: Chromolith, A: 0.01 % HCOOH in H₂O, B: acetonitrile, 25°C, 0.7 mL/min, 0-5 min: 15 % B, 5.0-5.5 min: 100 % B constant, ESI⁺, λ = 260, 230, 210 nm.

Method C: Nucleodur, A: 0.01 % HCOOH in H₂O, B: MeOH, 25°C, 0.8 mL/min, 0-12 min: 15 % B constant, λ = 260, 230, 210 nm.

Method D: Chromolith, A: 0.01 % HCOOH in H₂O, B: MeOH, 25°C, 0.8 mL/min, 0-6 min: 25 % B constant, 6-12 min: 100 % B constant, λ = 260, 230, 210 nm.

Method E: Poroshell, A: 0.01 % HCOOH in H₂O, B: acetonitrile, 40°C, 0.7 mL/min, 0-8 min: 2-100 % B, 8-10 min: 100 % B constant, ESI⁺, λ = 254, 210 nm.

Method F: Nucleodur, A: 0.01 % HCOOH in H₂O, B: MeOH, 30°C, 0.7 mL/min, 0-7 min: 15 % B constant, 7-9 min: 15-100 % B, 9-14 min: 100 % B constant, λ = 254, 210 nm.

Method G: Poroshell, A: 0.01 % HCOOH in H₂O, B: acetonitrile, 40°C, 0.7 mL/min, 0-6 min: 2-60 % B, 6-8 min: 60 % B constant, ESI⁺, λ = 254, 210 nm.

Method H: Poroshell, A: 0.01 % HCOOH in H₂O, B: acetonitrile, 40°C, 0.7 mL/min, 0-8 min: 2-100 % B, 8-10 min: 100 % B constant, ESI⁺, λ = 254, 210 nm.

Semi-preparative high performance liquid chromatography (PHPLC) was performed on an instrument from Knauer Technologies consisting of a smartline pump 1000 V7603, smartline UV detector 2500 V7605 or smartline DAD UV detector 2600, smartline manager 5000 V7602, smartline autosampler 3800 V9759 or manual 6 port injection ventill, fraction collector Teledyne Isco Foxy Jr. FC100 and Knauer instrument control chromgate V3.1.7 V7057-65. The compounds were separated on a C18-reversed phase VP 125/21 Nucleodur 100-5 C18ec column from Macherey & Nagel with VP 20/16 Nucleodur C18ec pre-column and detected with a UV detector at one specific wavelength or a UV diode array detector in the wavelength range of 200-400 nm. For each separation problem, an optimized method was developed, which is reported with each synthesis procedure.

6.1.4 Biological preparations

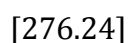
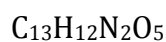
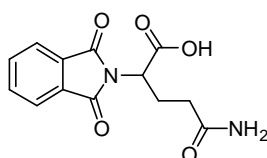
K. oxytoca strains were grown in CASO media or BHI broth at 37°C under constant shaking for 16 h. Afterwards, the conditioned medium was centrifugated at 4°C for 20 min (4000 rpm) and the supernatant was filtrated through a sterile 0.2 μ m cellulose acetate membrane filter. The resulting sterile supernatant was then tested in the cytotoxin activity assay and stored at -20°C until workup.

The cytotoxin activity assay was performed via modified MTT Cell Culture Assay.^[92] Therefore, eukaryotic Hep2 cells were seeded in 96 well tissue culture plates containing 1.5×10^4 cells per 100 μL minimal medium in each well. 50 μL conditioned medium per well, diluted with phosphate buffered saline (1:3, 1:9, 1:27 and 1:81) was added. After incubation of the 96 well plates for 2 days cell survival was determined qualitatively via Light Microscopy. For quantitative analysis the liquids were subsequently removed, 200 μL of phosphate buffered saline were added and the wells were incubated for another 2 h with 25 μL MTT reagent (5 mg/mL MTT in phosphate buffered saline). After media aspiration and dilution with 200 μL of a 1:25 mixture of 96 % acetic acid and 2-propanol the samples were quantified by threefold optical density measurements of each dilution at 595 nm. Samples treated with phosphate buffered saline only were used as reference for comparison.

6.2 Experimental procedures

6.2.1 Drug syntheses

α -(3-Amino-3-oxopropyl)-1,3-dihydro-1,3-dioxo-2H-isoindol-2-acetic acid (**6**)



To a solution of 1.39 g (9.5 mmol, 1.0 eq) L-glutamine (**5**) and 1.06 g (10.0 mmol, 1.1 eq) sodium carbonate in 24 mL H_2O in a 50 mL round-bottom flask were added 2.17 g (10.0 mmol, 1.1 eq) *N*-carbethoxyphthalimide (**4**). The resulting white suspension was stirred for 90 min at rt. Afterwards, the remaining *N*-carbethoxyphthalimide (**4**) was removed by filtration under reduced pressure. The resulting clear solution was slowly acidified with 6 N HCl to pH 1-2 until the product **6** precipitated (about 5 mL HCl). After stirring for another hour, the precipitate was collected by filtration under reduced

pressure and washed with H₂O (3x3 mL). The colorless solid was freeze dried. Because the crude product **6** still contained sodium chloride, it was treated with 4 mL H₂O. The resulting suspension was filtrated under reduced pressure. The solid was washed with ice cold H₂O (3x1 mL) and dried under high vacuum at 60°C.

Yield: 2.20 g (8.0 mmol, 85 %) colorless solid.

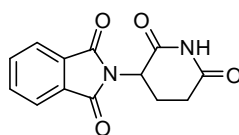
M.p. = 169°C. (lit. 169-171°C)^[74]

¹H-NMR (300 MHz, DMSO-d₆): δ = 13.20 (bs, 1H, COOH), 7.95-7.85 (m, 4H, 4x Ar-H), 7.20 (bs, 1H, CONH₂), 6.72 (bs, 1H, CONH₂), 4.75 (dd, ³J = 10.5 Hz, ³J = 4.5 Hz, 1H, CH-N), 2.42-2.18 (m, 2H, CH-CH₂), 2.09 (t, ³J = 7.2 Hz, 2H, CH₂-CONH₂).

¹³C-NMR (75 MHz, DMSO-d₆): δ = 173.01 (C_q, C=O), 170.36 (C_q, C=O), 167.33 (C_q, C=O), 134.72 (2x CH, 2x C_{Ar}), 131.16 (2x C_q, 2x C_{Ar}), 123.29 (2x CH, 2x C_{Ar}), 51.24 (CH-N), 31.29 (CH₂), 23.91 (CH₂).

GC-MS (The product is not stable. It cyclized to thalidomide (**1**) under GC-MS conditions).

2-(2,6-Dioxo-3-piperidiny)-1H-isoindol-1,3(2H)-dione (**1**)



C₁₃H₁₀N₂O₄

[258.23]

A 250 mL round-bottom flask, equipped with a reflux condenser, was charged with 15.2 g (54.3 mmol, 1.00 eq) α-(3-amino-3-oxopropyl)-1,3-dihydro-1,3-dioxo-2H-isoindol-2-acetic acid (**6**), 9.2 g (56.5 mmol, 1.04 eq) CDI and 24 mg (0.2 mmol, 0.004 eq) DMAP. The apparatus was flushed with Ar before 90 mL of dry THF were added and the reflux condenser was connected to a drying tube. The yellow mixture was carefully

heated under reflux for 15 h. After cooling to rt, the precipitate was collected by filtration under reduced pressure, washed with dichloromethane (4x30 mL) and dried under high vacuum at 60°C. The filtrate was concentrated and brought again to precipitation with 30 mL of dichloromethane. The precipitate was washed with dichloromethane (3x20 mL) and dried under high vacuum at 60°C.

Yield: 13.2 g (51.3 mmol, 95 %) colorless solid.

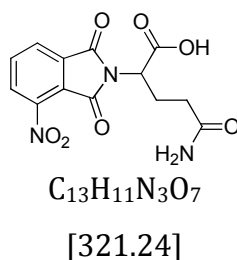
M.p. = 275°C. (lit. 274-276°C)^[74]

¹H-NMR (300 MHz, DMSO-d₆): δ = 11.14 (s, 1H, NH), 7.95-7.86 (m, 4H, 4x Ar-H), 5.16 (dd, ³J = 12.6 Hz, ³J = 5.1 Hz, 1H, CH-N), 2.98-2.02 (m, 4H, CH₂-CH₂).

¹³C-NMR (75 MHz, DMSO-d₆): δ = 172.68 (C_q, C=O), 169.77 (C_q, C=O), 167.07 (C_q, C=O), 134.80 (2x CH, 2x C_{Ar}), 131.15 (2x C_q, 2x C_{Ar}), 123.34 (2x CH, 2x C_{Ar}), 48.91 (CH-N), 30.86 (CH₂), 21.91 (CH₂).

GC-MS (JR_50_S): t_R = 7.74 min, m/z = 258 (22 %), 76 (100 %).

**α-(3-Amino-3-oxopropyl)-1,3-dihydro-4-nitro-1,3-dioxo-2H-isoindol-2-acetic acid
(8)**



In a 100 mL round-bottom flask, equipped with reflux condenser, 2.34 g (12.1 mmol, 1.02 eq) 4-nitroisobenzofuran-1,3-dione (**7**) and 1.74 g (11.9 mmol, 1.00 eq) L-glutamine (**5**) were dissolved in 21 mL dry DMF. After heating at 100°C for 24 h, the solvent was evaporated under high vacuum. To precipitate the product **8**, the yellow oil was stirred for 5.5 h after addition of 20 mL H₂O. Because no precipitate was formed, the aqueous layer was decanted and the remaining yellow oil was dissolved in 20 mL

acetone. Both layers were successively concentrated under reduced pressure. NMR-spectra indicated that both layers contain pure product **8**.

Yield: 1.56 g (4.8 mmol, 40 %) yellow solid.

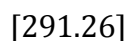
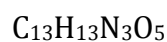
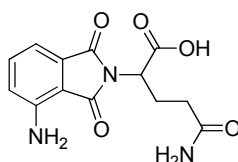
$R_f = 0.21$ (dichloromethane/methanol 2:1).

M.p. = 179°C. (lit. 180-182°C)^[75]

¹H-NMR (300 MHz, DMSO-d₆): $\delta = 13.33$ (bs, 1H, OH), 8.34 (d, ³J = 7.8 Hz, 1H, Ar-H), 8.23 (d, ³J = 6.9 Hz, 1H, Ar-H), 8.11 (t, ³J = 7.8 Hz, 1H, Ar-H), 7.18 (s, 1H, NH), 6.71 (s, 1H, NH), 4.80 (dd, ³J = 9.6 Hz, ³J = 3.9 Hz, 1H, CH-N), 2.41-2.05 (m, 4H, 2x CH₂).

¹³C-NMR (75 MHz, DMSO-d₆): $\delta = 173.09$ (C_q, C=O), 169.90 (C_q, C=O), 165.31 (C_q, C=O), 162.64 (C_q, C=O), 144.35 (C_q, C_{Ar}), 136.58 (CH, C_{Ar}), 132.89 (C_q, C_{Ar}), 128.70 (CH, C_{Ar}), 127.13 (CH, C_{Ar}), 122.42 (C_q, C_{Ar}), 51.81 (CH-N), 31.25 (CH₂), 23.80 (CH₂).

4-Amino- α -(3-amino-3-oxopropyl)-1,3-dihydro-1,3-dioxo-2H-isoindol-2-acetic acid (**9**)



A 100 mL three-necked round-bottom flask was heat dried under vacuum and flushed with Ar. Under Ar-counterflow, 7.20 g (22.4 mmol, 1.00 eq) α -(3-amino-3-oxopropyl)-1,3-dihydro-4-nitro-1,3-dioxo-2H-isoindol-2-acetic acid (**8**) were suspended in 68 mL dry methanol. Dry DMF was added dropwise until a clear yellow solution occurred (6 mL). Before and after addition of 0.19 g (0.7 mmol, 0.03 eq) palladium on activated charcoal (10 %), the black suspension was degassed with two vacuum-Ar cycles each. In three further vacuum-H₂ cycles the reaction mixture was flushed with H₂ and then stirred under H₂ from an orsat balloon at rt for 16 h. TLC indicated complete conversion.

The black suspension was filtrated through a pad of celite and rinsed with methanol until the eluate remained colorless (100 mL). Finally the solvent was evaporated and the product **9** was dried under high vacuum at 60°C.

Yield: 6.50 g (22.4 mmol, quantitative) yellow solid.

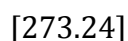
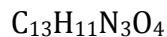
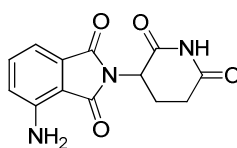
$R_f = 0.13$ (dichloromethane/methanol 2:1).

M.p. = 168°C. (lit. 177-179°C)^[75]

¹H-NMR (300 MHz, DMSO-*d*₆): $\delta = 7.45$ (t, $^3J = 7.5$ Hz, 1H, Ar-H), 7.21 (bs, 1H, NH-amide), 6.99 (dd, $^3J = 7.5$ Hz, $^3J = 6.3$ Hz, 2H, 2x Ar-H), 6.72 (bs, 1H, NH-amide) 6.50 (bs, 2H, Ar-NH₂), 4.61 (dd, $^3J = 10.8$ Hz, $^3J = 4.5$ Hz, 1H, CH-N) 2.41-2.10 (m, 2H, CH₂), 2.05 (t, $^3J = 7.2$ Hz, 2H, CH₂).

¹³C-NMR (75 MHz, DMSO-*d*₆): $\delta = 173.05$ (C_q, C=O), 170.70 (C_q, C=O), 168.88 (C_q, C=O), 167.60 (C_q, C=O), 146.56 (C_q, C_{Ar}), 135.24 (CH, C_{Ar}), 132.01 (C_q, C_{Ar}), 121.46 (CH, C_{Ar}), 110.75 (CH, C_{Ar}), 108.65 (C_q, C_{Ar}), 50.90 (CH-N), 31.41 (CH₂), 24.04 (CH₂).

4-Amino-2-(2,6-dioxo-3-piperidinyl)-1*H*-isoindol-1,3(2*H*)-dione (**2**)



In a 100 mL round-bottom flask, equipped with a reflux condenser and a CaCl₂ drying tube, 0.52 g (1.80 mmol, 1.0 eq) *N*-(3-aminophthaloyl)-glutamine **9** were dissolved in 20 mL dry acetonitrile. After stirring for 1 h at 40°C, 317 mg (2.00 mmol, 1.1 eq) CDI were added. The yellow solution was refluxed for 8 h. As TLC indicated incomplete conversion, another 59 mg (0.36 mmol, 0.2 eq) CDI were added to the reaction mixture and heating under reflux was continued for another 19 h until TLC showed complete conversion. The reaction mixture was allowed to cool to rt, where product **2**

precipitated from the red solution. The yellow solid was collected by filtration, washed with acetonitrile (4x5 mL) and dried under high vacuum.

Yield: 152 mg (55.8 mmol, 31 %) yellow solid.

$R_f = 0.66$ (ethyl acetate).

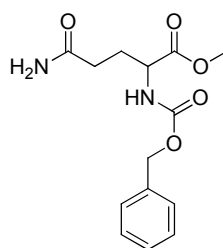
M.p. = 315°C. (lit. 309-310°C)^[75]

$^1\text{H-NMR}$ (300 MHz, DMSO-d_6): $\delta = 11.09$ (s, 1H, NH), 7.47 (t, $^3J = 7.5$ Hz, 1H, Ar-H), 7.00 (dd, $^3J = 8.1$ Hz, $^3J = 6.6$ Hz, 2H, 2x Ar-H), 6.53 (bs, 2H, NH_2), 5.04 (dd, $^3J = 12.6$ Hz, $^3J = 5.1$ Hz, 1H, CH-N), 2.98-1.95 (m, 4H, 2x CH_2).

$^{13}\text{C-NMR}$ (75 MHz, DMSO-d_6): $\delta = 172.72$ (C_q , C=O), 170.02 (C_q , C=O), 168.47 (C_q , C=O), 167.27 (C_q , C=O), 146.63 (C_q , C_{Ar}), 135.38 (CH, C_{Ar}), 131.91 (C_q , C_{Ar}), 121.62 (CH, C_{Ar}), 110.88 (CH, C_{Ar}), 108.43 (C_q , C_{Ar}), 48.39 (CH-N), 30.89 (CH_2), 22.06 (CH_2).

GC-MS (JR_100_L): $t_R = 8.65$ min, $m/z = 273$ (100 %).

***N*-(Benzyloxycarbonyl)glutamine methyl ester (16a)**



$\text{C}_{14}\text{H}_{18}\text{N}_2\text{O}_5$

[294.30]

In a 500 mL round-bottom flask, equipped with a reflux condenser, 21 g (75.0 mmol, 1.0 eq) *L-N*-Cbz-glutamine (**10a**) were dissolved in 250 mL dry methanol. To the colorless solution, 0.53 mL (7.5 mmol, 0.1 eq) acetyl chloride and 0.1 mL (0.79 mmol, 0.01 eq) TMSCl were added. The mixture was heated under reflux for 5 h. After

completion of the reaction, the solvent was removed *in vacuo* and the product **16a** was dried under high vacuum.

Yield: 22.6 g (75 mmol, quantitative) colorless solid.

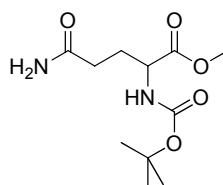
M.p. = 127°C. (lit. 135-137°C)^[97]

¹H-NMR (300 MHz, DMSO-d₆): δ = 7.75 (d, ³J = 7.8, 1H, NH), 7.42-7.23 (m, 6H, 5x Ar-H, 1x NH), 6.78 (bs, 1H, NH), 5.03 (s, 2H, O-CH₂), 4.12-3.98 (m, 1H, N-CH), 3.63 (s, 3H, O-CH₃), 2.15 (t, ³J = 7.5, 2H, C(O)-CH₂), 2.00-1.65 (m, 2H, CH-CH₂).

¹³C-NMR (75 MHz, DMSO-d₆): δ = 173.17 (C_q, C=O), 172.63 (C_q, C=O), 156.00 (C_q, C=O), 136.80 (C_q, C_{Ar}), 128.26 (2x CH, 2x C_{Ar}), 127.74 (CH, C_{Ar}), 127.63 (2x CH, C_{Ar}), 65.41 (CH₂-O), 53.40 (CH-N), 51.73 (CH₃), 30.97 (CH₂), 26.32 (CH₂).

GC-MS (JR_50_S): t_R = 6.57 min, m/z = 294 (3 %), 91 (100 %).

***N*-(*tert*-Butoxycarbonyl)glutamine methyl ester (**16b**)**



C₁₁H₂₀N₂O₅

[260.29]

8.20 g (33 mmol, 1.0 eq) L-*N*-Boc-glutamine (**10b**) were placed in a dry, Ar-filled Schlenk tube under Ar-counterflow and suspended in 85 mL dry diethyl ether. As the addition of 28 mL dry methanol did not result in a completely clear solution, another 8 mL diethyl ether and 2 mL methanol were added under dry conditions. TMS-diazomethane (2 M in diethyl ether) was added dropwise via syringe and septum over a period of 30 min until the colorless solution became slightly yellow. Since heat generation and gas formation (N₂) were observed, the flask was placed in an ice bath. After 21 mL (42 mmol, 1.3 eq) of TMS-diazomethane solution had been added, gas formation as well as heat generation

stopped and the reaction solution became yellow. TLC indicated complete conversion. The solvents were removed on a rotary evaporator and the product **16b** was dried under high vacuum.

Yield: 8.68 g (33 mmol, quantitative) highly viscous, reddish oil.

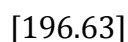
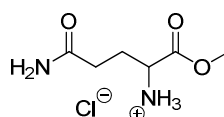
$R_f = 0.94$ (dichloromethane/methanol 3:2).

M.p. = 85-87°C. (lit. 86-89°C)^[97]

¹H-NMR (300 MHz, DMSO-d₆): $\delta = 7.31-7.22$ (m, 2H, NH₂), 6.78 (bs, 1H, NH), 4.00-3.85 (m, 1H, CH-N), 3.62 (s, 3H, O-CH₃), 2.12 (t, ³J = 7.2 Hz, 2H, C(O)-CH₂), 2.00-1.65 (m, 2H, CH-CH₂).

¹³C-NMR (75 MHz, DMSO-d₆): $\delta = 173.28$ (C_q, C=O), 172.93 (C_q, C=O), 155.45 (C_q, C=O), 78.13 (C_q, C(CH₃)₃), 53.07 (CH-N), 51.63 (CH₃-O), 31.10 (CH₂), 28.10 (3x CH₃, ^tBu), 26.28 (CH₂).

L-Glutamine methyl ester hydrochloride (**19**)



96.03 g (1.64 mol, 50 eq) NaCl were placed in a dry 500 mL two-necked round-bottom flask, equipped with magnetic stirring bar, septum and gas-outlet. 8.55 g (0.03 mol, 1 eq) L-N-Boc-glutamine methyl ester (**16b**) were dissolved in 120 mL CHCl₃, stabilized with amylene, in a second 250 mL two-necked round-bottom flask, equipped with a gas-inlet built by a modified syringe reaching into the solution and a gas-outlet. This orange solution was cooled to 0°C when HCl gas, which was formed by adding concentrated sulfuric acid dropwise to NaCl, was bubbled into the solution. After 21 mL (0.39 mol, 12 eq) of sulfuric acid had been added to the NaCl, the orange solution became colorless

and the product **19** started to precipitate. After 70 mL (1.31 mol, 40 eq) of sulfuric acid had been added, no additional precipitation could be observed and the HCl production was stopped. After stirring of the suspension for 2 h at 0°C, the product **19** was isolated by decantation. The crystals were washed with chloroform (3x50 mL) and methanol (3x50 mL) and dried under high vacuum.

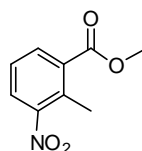
Yield: 8.22 g (30 mmol, 92%) colorless solid.

M.p. = 29-30°C.

¹H-NMR (300 MHz, DMSO-d₆): δ = 8.76 (bs, 3H, NH₃⁺), 7.71-7.38 + 7.09-6.76 (m, 2H, NH₂), 4.01-3.85 (m, 1H, CH-N), 3.71 (s, 3H, O-CH₃), 2.38-1.94 (m, 4H, 2x CH₂).

¹³C-NMR (75 MHz, DMSO-d₆): δ = 172.90 (C_q, C=O), 169.66 (C_q, C=O), 52.68 (CH-N), 51.48 (CH₃-O), 30.14 (CH₂), 25.78 (CH₂).

Methyl 2-methyl-3-nitrobenzoate (**22**)



C₉H₉NO₄

[195.17]

Method A:

In a 250 mL round-bottom flask, equipped with a reflux condenser and a CaCl₂ drying tube, 13.97 g (77.1 mmol, 1.0 eq) 2-methyl-3-nitrobenzoic acid (**21**) were dissolved in 175 mL dry methanol. After addition of 0.4 mL (7.1 mmol, 0.1 eq) concentrated sulfuric acid, the apparatus was flushed with Ar. The reaction mixture was heated under reflux for 17 h. Afterwards, the solvent was removed under reduced pressure and the yellow residue was suspended in 180 mL dichloromethane and 40 mL cyclohexane. The precipitated product **22** was collected by filtration, washed with 60 mL H₂O and dried under high vacuum at 40°C. The filtrate was concentrated to one half under reduced

pressure. At 0°C, further precipitated product **22** was again collected by filtration, washed with 40 mL H₂O and dried under high vacuum at 40°C. This procedure was repeated until no more precipitate was formed (2 times).

Yield: 5.27 g (27.0 mmol, 35 %) yellow solid (from the first fraction).

The mixed fractions (two and three) with starting material **21** and product **22** were used in method B.

Method B:

In a 250 mL round-bottom flask with a reflux condenser and a CaCl₂ drying tube, 7.90 g (43.60 mmol, 1.0 eq) 2-methyl-3-nitrobenzoic acid (**21**) (mixed fraction from method A, already containing some product **22**) were dissolved in 90 mL dry methanol. 0.31 mL (4.36 mmol, 0.1 eq) acetyl chloride and 0.1 mL (4.36 mmol, 0.1 eq) trimethylsilyl chloride were added to the solution and the mixture was stirred at 80°C for 2 d until GC-MS indicated full conversion. The product **22** was concentrated under reduced pressure and dried under high vacuum.

Yield: 8.50 g (43.6 mmol, quantitative) off-white solid.

R_f = 0.45 (cyclohexane/ethyl acetate 5:1).

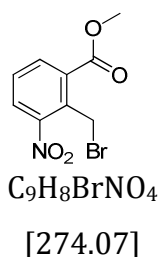
R_f = 0.49 (cyclohexane/ethyl acetate 5:1) starting material **21**.

M.p. = 65°C. (lit. 64-65°C) [98]

¹H-NMR (300 MHz, DMSO-d₆): δ = 8.01 (dd, ³J = 12.3 Hz, ³J = 12.0 Hz, 2H, 2x Ar-H), 7.58 (t, ³J = 8.1 Hz, 1H, Ar-H), 3.88 (s, 3H, CH₃-O), 2.49 (s, 3H, CH₃).

¹³C-NMR (75 MHz, DMSO-d₆): δ = 166.33 (C_q, C=O) 151.36 (C_q, C_{Ar}), 133.16 (CH, C_{Ar}), 133.05 (C_q, C_{Ar}), 131.04 (C_q, C_{Ar}), 127.19 (CH, C_{Ar}), 126.57 (CH, C_{Ar}), 52.54 (CH₃-O), 15.39 (CH₃).

GC-MS (JR_50_S): t_R = 5.90 min, m/z = 195 (100 %).

Methyl 2-(bromomethyl)-3-nitrobenzoate (12)

In a 250 mL round-bottom flask, equipped with a reflux condenser, 13.87 g (73.9 mmol, 1.00 eq) methyl 2-methyl-3-nitrobenzoate (**22**) were dissolved in 135 mL tetrachloromethane. 13.25 g (73.9 mmol, 1.04 eq) *N*-bromosuccinimide and 0.70 g (2.9 mmol, 0.40 eq) dibenzoyl peroxide were then added. The resulting solution was stirred at 80°C for 3.5 h followed by another addition of 0.35 g (1.5 mmol, 0.20 eq) dibenzoyl peroxide. After further heating at 80°C for 23 h, another 0.35 g (1.5 mmol, 0.20 eq) dibenzoyl peroxide and 1.0 g (4.1 mmol, 0.57 eq) *N*-bromosuccinimide were added. After altogether refluxing for 51 h the reaction mixture was cooled to 0°C in an ice bath, filtrated under reduced pressure and then the filtrate was concentrated. The crude solid was dissolved in 160 mL diethyl ether and washed with saturated sodium sulfite (1x50 mL), water (2x50 mL), 2.5 % aqueous NaOH solution (1x50 mL), H₂O (1x50 mL) and finally brine (1x50 mL). The combined organic layers were dried over Na₂SO₄, filtrated and then the solvent was removed under reduced pressure. The yellow solid was dried under high vacuum.

Yield: 14.36 g (52.4 mmol, 74 %) yellow solid.

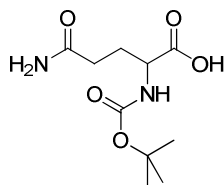
M.p. = 69°C. (lit. 69-72°C)^[99]

¹H-NMR (300 MHz, DMSO-d₆): δ = 8.15 (dd, ³J = 14.7 Hz, ³J = 14.4 Hz, 2H, 2x Ar-H) 7.74 (t, ³J = 7.6 Hz, 1H, Ar-H), 3.92 (s, 3H, CH₃), 2.49 (s, 2H, CH₂).

¹³C-NMR (75 MHz, DMSO-d₆): δ = 165.70 (C_q, C=O), 150.13 (C_q, C_{Ar}), 134.50 (C_q, C_{Ar}), 132.17 (C_q, C_{Ar}), 130.90 (CH, C_{Ar}), 130.22 (CH, C_{Ar}), 128.00 (CH, C_{Ar}), 53.06 (CH₃-O), 24.06 (CH₂-Br).

GC-MS (JR_50_S): $t_R = 6.75$ min, $m/z = 162$ (45 %), 63 (100 %).

N-tert-Butoxycarbonyl-L-glutamine (**10b**)



$C_{10}H_{18}N_2O_5$

[246.26]

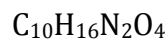
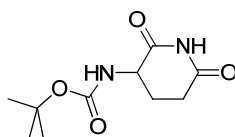
In a 250 mL round-bottom flask 8.04 g (55 mmol, 1.0 eq) L-glutamine (**5**) and 2.48 g (62 mmol, 1.1 eq) NaOH were dissolved in 53 mL H₂O. 36 mL acetonitrile were added and the mixture was cooled to 0°C. Then 12.03 g (55 mmol, 1.0 eq) Boc₂O were added carefully so that the temperature did not rise above 2°C. Afterwards, the mixture was stirred at rt for 18 h. After TLC indicated complete conversion, the mixture was acidified with saturated aqueous KHSO₄ solution to pH = 1.5 (83 mL) and then extracted with diethyl ether (6x25 mL). The combined organic layers were dried over Na₂SO₄, filtrated and the solvent evaporated under reduced pressure. The greenish crude product **10b** was recrystallized from 80 mL diethyl ether and 80 mL ethyl acetate.

Yield: 4.48 g (18 mmol, 33 %) colorless solid.

M.p. = 120°C. (lit. 118-120°C)^[100]

¹H-NMR (300 MHz, DMSO-d₆): $\delta = 12.47$ (bs, 1H, COOH), 7.27 (bs, 1H, C(O)NH), 7.08 (d, $^3J = 8.1$ Hz, 1H, NH-CH), 6.76 (bs, 1H, C(O)NH), 3.89-3.79 (m, 1H, CH-N), 2.17 (t, $^3J = 7.5$ Hz, 2H, CH₂-C(O)NH₂), 2.00-1.82 + 1.77-1.60 (m, 2H, CH₂-CH, diastereotopic), 1.37 (s, 9H, ^tBu).

¹³C-NMR (75 MHz, DMSO-d₆): $\delta = 173.98$ (C_q, C=O), 173.53 (C_q, C=O), 155.55 (C_q, C=O), 77.96 (C_q, C(CH₃)₃), 53.13 (CH-N), 31.42 (CH₂), 28.20 (^tBu), 26.51 (CH₂).

***N*-(2,6-Dioxo-3-piperidinyl)-1,1-dimethylethyl ester (168)**

[228.25]

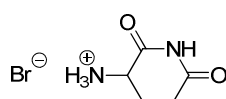
A 250 mL Schlenk flask was heat dried and flushed with N₂. 14.4 g (59 mmol, 1.0 eq) *N*-*tert*-butoxycarbonyl-L-glutamine (**10b**) were dissolved in 150 mL dry THF and then 11.2 g (69 mmol, 1.2 eq) CDI, 1.8 g (14 mmol, 0.3 eq) DMAP and 9.6 mL (69 mmol, 1.2 eq) triethylamine were sequentially added. After stirring for 15 h, the reaction mixture was evaporated under reduced pressure to about 1/3 of the volume and then diluted with 150 mL H₂O. The mixture was extracted with chloroform (3x50 mL). The combined organic layers were washed with 0.2 M HCl (1x200 mL) and brine (1x200 mL), dried over Na₂SO₄, filtrated and concentrated under reduced pressure. The crude product **168** was recrystallized from 400 mL chloroform and 500 mL diisopropyl ether.

Yield: 10.3 g (45 mmol, 78 %) colorless solid.

M.p. = 155-157°C. (lit. 153-155°C)^[101]

¹H-NMR (300 MHz, DMSO-d₆): δ = 10.75 (bs, 1H, NH), 7.14 (d, ³J = 8.7 Hz, 1H, Ar-H), 4.29-4.16 (m, 1H, CH-N), 2.80-1.82 (m, 4H, 2x CH₂), 1.39 (s, 9H, ^tBu-H).

¹³C-NMR (75 MHz, DMSO-d₆): δ = 172.92 (C_q, C=O), 172.46 (C_q, C=O), 155.33 (C_q, C=O), 78.09 (C_q, C(CH₃)₃), 50.32 (CH-N), 30.92 (CH₂), 28.11 (^tBu), 24.37 (CH₂).

3-Amino-2,6-piperidinedione hydrobromide (20)

[209.04]

In a 250 mL round-bottom flask 5.3 g (23 mmol, 1 eq) *N*-(2,6-dioxo-3-piperidiny)-1,1-dimethylethyl ester (**168**) were stirred at rt for 30 min in 50 mL HBr (33 % HBr in acetic acid). Precipitation of the product **20** from the yellow suspension was accomplished by addition of 150 mL ethyl acetate. The precipitate was collected by filtration, washed with ethyl acetate (5x10 mL) and dried under high vacuum.

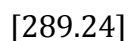
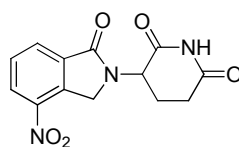
Yield: 4.85 g (23 mmol, quantitative), colorless solid.

M.p. = 264°C (decomposition). (lit. 274-277°C)^[102]

¹H-NMR (300 MHz, DMSO-d₆): δ = 11.27 (s, 1H, NH), 8.47 (s, 3H, NH₃), 4.26 (dd, ³J = 11.4 Hz, ³J = 3.3 Hz, 1H, CH), 2.81-2.53 (m, 2H, CH₂), 2.25-1.90 (m, 2H, CH₂).

¹³C-NMR (75 MHz, DMSO-d₆): δ = 172.17 (C_q, C=O), 170.20 (C_q, C=O), 48.96 (CH-N), 30.12 (CH₂), 22.07 (CH₂).

2-(2,6-Dioxo-3-piperidiny)-4-nitro-1*H*-isoindol-1,3(2*H*)-dione (**15**)



In a 1 L three-necked round-bottom flask, equipped with a reflux condenser and an Ar inlet and protected from light with aluminum foil, 5.90 g (21.5 mmol, 1 eq) methyl 2-(bromomethyl)-3-nitrobenzoate (**12**) were dissolved in 600 mL dry acetonitrile. After addition of 4.50 g (21.5 mmol, 1 eq) 3-amino-2,6-piperidinedione hydrobromide (**20**) and 6.0 mL (43.0 mmol, 2 eq) dry triethylamine, the yellow reaction mixture was stirred at 50°C for 19 h. TLC showed no complete conversion. After another addition of 0.6 mL (4.3 mmol, 0.2 eq) triethylamine the mixture was stirred for further 2 h and then cooled to rt. The reaction mixture was quenched with 150 mL H₂O and stirred at rt for another 2 h. The precipitate was collected by filtration with suction and washed with H₂O

(4x25 mL). The pale purple solid was dried under high vacuum at 45°C. Eventual additional precipitate formed was also collected by filtration, washed and dried.

Yield: 3.55 g (12.3 mmol, 57%), pale purple solid.

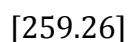
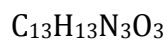
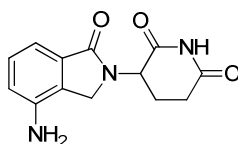
$R_f = 0.29$ (ethyl acetate).

M.p. = 288-289°C. (lit. 285°C)^[99]

$^1\text{H-NMR}$ (300 MHz, DMSO- d_6): $\delta = 11.04$ (s, 1H, NH), 8.47 (d, $^3J = 8.1$ Hz, 1H, Ar-H), 8.19 (d, $^3J = 7.2$ Hz, 1H, Ar-H), 7.84 (t, $^3J = 7.8$ Hz, 1H, Ar-H), 5.18 (dd, $^3J = 13.2$ Hz, $^3J = 4.8$ Hz, 1H, N-CH), 4.85 (q, $^3J = 19.2$ Hz, 2H, N-CH $_2$), 3.00-2.84 + 2.72-2.50 + 2.09-1.95 (m, 4H, CH $_2$ -CH $_2$).

$^{13}\text{C-NMR}$ (75 MHz, DMSO- d_6): $\delta = 172.70$ (C $_q$, C=O), 170.61 (C $_q$, C=O), 165.86 (C $_q$, C=O), 143.27 (C $_q$, C $_{Ar}$), 137.33 (C $_q$, C $_{Ar}$), 134.60 (C $_q$, C $_{Ar}$), 130.08 (CH, C $_{Ar}$), 129.53 (CH, C $_{Ar}$), 126.96 (CH, C $_{Ar}$), 51.75 (N-CH), 48.37 (N-CH $_2$), 31.08 (CH $_2$), 22.15 (CH $_2$).

4-Amino-2-(2,6-dioxo-3-piperidiny)-1*H*-isoindol-1,3(2*H*)-dione (**3**)



In a 15 mL Schlenk tube 83 mg (0.29 mmol, 1.0 eq) 2-(2,6-dioxo-3-piperidiny)-4-nitro-1*H*-isoindol-1,3(2*H*)-dione (**15**) were suspended in 1.7 mL methanol under Ar counterflow. 25 mg (0.3 eq) Pd on activated charcoal (10 %, contains 50 % water) were added. The mixture was degassed by three vacuum-Ar cycles and flushed with H $_2$ (three vacuum-H $_2$ cycles). The black suspension was stirred at rt for 19 h under H $_2$ from an orsat balloon, until TLC indicated complete conversion. The reaction mixture was filtrated through a pad of celite and rinsed with methanol (4x1 mL). The product **3** was dried first at the rotary evaporator and then under high vacuum.

Yield: 49 mg (0.19 mmol, 65%) off-white solid.

$R_f = 0.13$ (ethyl acetate).

M.p. = 268°C. (lit. 268°C)^[103]

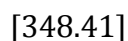
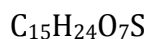
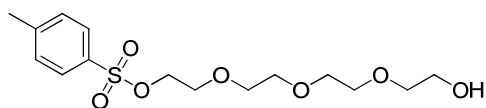
¹H-NMR (300 MHz, DMSO-*d*₆): $\delta = 10.98$ (bs, 1H, NH), 7.19 (t, ³*J* = 7.8 Hz, 1H, Ar-H), 6.90 (d, ³*J* = 7.2 Hz, 1H, Ar-H), 6.79 (d, ³*J* = 7.8 Hz, 1H, Ar-H), 5.42 (bs, 2H, NH₂), 5.10 (dd, ³*J* = 13.5 Hz, ³*J* = 5.1 Hz, 1H, N-CH), 4.28-4.02 (m, 2H, N-CH₂), 3.00-2.84 + 2.68-2.52 + 2.39-2.21 + 2.08-1.98 (m, 4H, CH₂-CH₂).

¹³C-NMR (75 MHz, DMSO-*d*₆): $\delta = 172.79$ (C_q, C=O), 171.13 (C_q, C=O), 168.78 (C_q, C=O), 143.52 (C_q, C_{Ar}), 132.15 (C_q, C_{Ar}), 128.72 (CH, C_{Ar}), 125.49 (C_q, C_{Ar}), 116.30 (CH, C_{Ar}), 110.32 (CH, C_{Ar}), 51.41 (N-CH), 45.50 (N-CH₂), 31.14 (CH₂), 22.68 (CH₂).

GC-MS (JR_50_S): $t_R = 10.70$ min, $m/z = 259$ (100 %).

6.2.2 Linker syntheses

Tetraethylene glycol monotosylate (**26**)



In a 500 mL Schlenk tube, heat dried and flushed with Ar, 64 mL (0.37 mol, 7.0 eq) tetraethylene glycol (**25**) and 8 mL (0.06 mol, 1.1 eq) triethylamine were dissolved in 50 mL dry dichloromethane. In a second 100 mL Schlenk flask, heat dried and flushed with Ar, 9.8 g (0.05 mol, 1.0 eq) *p*-toluenesulfonyl chloride were dissolved in 60 mL dry dichloromethane. Under vigorous stirring every hour 5 mL of *p*-toluenesulfonyl chloride solution were added dropwise to the basic slightly yellow solution over a period of 1 d.

Afterwards, the orange solution was stirred at rt for another day until TLC monitoring indicated complete conversion. The reaction mixture was quenched with 60 mL 1 M HCl, 60 mL H₂O and finally 70 mL brine. The aqueous layer was extracted with dichloromethane (3x40 mL). The combined organic layers were dried over MgSO₄, filtrated and the solvent was removed under reduced pressure. The crude orange oil was purified by flash chromatography (600 g silica gel, ethyl acetate).

Yield: 17.3 g (0.05 mol, 97 %) colorless oil.

R_f = 0.53 (ethyl acetate/methanol 3:1).

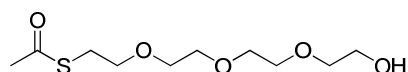
¹H-NMR (300 MHz, CDCl₃): δ = 7.79 (d, ³J = 8.1 Hz, 2H, 2x Ar-H) 7.34 (d, ³J = 8.1 Hz, 2H, 2x Ar-H), 4.16 (t, ³J = 4.8 Hz, 2H, CH₂), 3.73-3.55 (m, 14H, 7x CH₂), 2.44 (s, 3H, CH₃).

¹³C-NMR (75 MHz, CDCl₃): δ = 144.75 (C_q), 132.93 (C_q), 129.80 (CH, 2x C_{Ar}), 127.96 (CH, 2x C_{Ar}), 72.41 (CH₂), 70.68 (CH₂), 70.59 (CH₂), 70.41 (CH₂), 70.27 (CH₂), 69.19 (CH₂), 68.65 (CH₂), 61.67 (CH₂), 21.58 (CH₃).

IR (neat): ν_{max} = 3411 (w), 2872 (m), 1598 (w), 1453 (w), 1352 (s), 1175 (s), 1096 (s), 1013 (m), 918 (s), 816 (m), 774 (m), 663 (s).

GC-MS (JR_50_S): t_R = 6.39 min, m/z = 229 (5 %), 198 (10 %), 155 (100 %).

1-Hydroxy-3,6,9-trioxa-12-thiatetradecan-13-one (27)



C₁₀H₂₀O₅S

[252.33]

In a 500 mL Schlenk tube, evacuated under heat and flushed with Ar, 6.98 g (20 mmol, 1.0 eq) tetraethylene glycol monotosylate (**26**) were dissolved in 100 mL dry DMF. To the colorless solution, 8.56 g (75 mmol, 3.7 eq) potassium thioacetate powder was added under Ar counterflow. The black suspension was stirred at rt for 17 h until TLC

control indicated complete conversion. The reaction mixture was carefully quenched with 125 mL saturated, aqueous NH_4Cl solution, which caused heat development. After addition of 150 mL dichloromethane and 25 mL brine the mixture was vigorously stirred for 10 min. The aqueous layer was extracted with dichloromethane (4x80 mL) and the combined organic layers were dried over MgSO_4 , filtrated and then the solvent was evaporated. The crude black product was purified by flash chromatography (300 g silica gel, dichloromethane). Because of the high vapor pressure of the product **27**, parts of it disappeared during solvent evaporation and drying under high vacuum.

Yield: 3.20 g (13 mmol, 63 %) yellow oil.

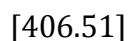
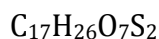
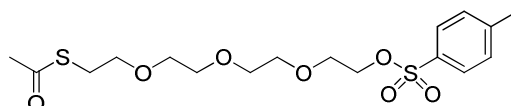
$R_f = 0.78$ (ethyl acetate/methanol 3:1).

$^1\text{H-NMR}$ (300 MHz, CDCl_3): $\delta = 3.73\text{-}3.57$ (m, 14H, 7x $\text{CH}_2\text{-O}$), 3.09 (t, $^3J = 6.6$ Hz, 2H, $\text{CH}_2\text{-OH}$), 2.33 (s, 3H, CH_3).

$^{13}\text{C-NMR}$ (75 MHz, CDCl_3): $\delta = 195.57$ (C_q , C=O), 72.47 ($\text{CH}_2\text{-O}$), 70.62 ($\text{CH}_2\text{-O}$), 70.45 ($\text{CH}_2\text{-O}$), 70.32 ($\text{CH}_2\text{-O}$), 70.24 ($\text{CH}_2\text{-O}$), 69.75 ($\text{CH}_2\text{-O}$), 61.73 ($\text{CH}_2\text{-OH}$), 30.54 (CH_3), 28.75 ($\text{CH}_2\text{-S}$).

GC-MS (JR_50_S): $t_R = 6.74$ min, $m/z = 252$ (25 %), 87 (100 %).

1-(((4-Methylbenzene)sulfonyl)oxy)-3,6,9-trioxa-12-thiatetradecan-13-one (**28**)



In a 10 mL Schlenk tube, evacuated under heat and flushed with Ar, 80 mg (0.32 mmol, 1.0 eq) 1-hydroxy-3,6,9-trioxa-12-thiatetradecan-13-one (**27**) were dissolved in 1.3 mL dry dichloromethane. To this greenish solution, 0.1 mL (0.73 mL, 2.3 eq) dry triethylamine and a solution of 85 mg (0.44 mmol, 1.4 eq) *para*-toluenesulfonyl chloride

in 1.0 mL dry dichloromethane were added. The brown solution was stirred at rt under Ar for 17 h until TLC indicated complete conversion. The reaction mixture was diluted with 0.85 mL dichloromethane and quenched with 1.4 mL aqueous HBr solution (48 %). After addition of 1.0 mL brine, the aqueous layer was extracted with dichloromethane (5x1 mL). The combined organic layers were dried over MgSO₄, filtrated and the solvent was evaporated under reduced pressure. The crude orange solid was purified by flash chromatography (15 g silica gel, 100 mL dichloromethane, then 200 mL dichloromethane/methanol 99:1, then 100 mL dichloromethane/methanol 98:2, then 100 mL dichloromethane/methanol 97:3, then 100 mL dichloromethane/methanol 95:5 and finally 100 mL dichloromethane/methanol 3:1).

Yield: 85 mg (21 mmol, 65 %) beige solid.

R_f = 0.40 (dichloromethane/methanol 99:1).

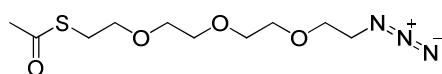
M.p. = 75°C.

¹H-NMR (300 MHz, CDCl₃): δ = 7.80 (d, ³J = 8.4 Hz, 2H, 2x Ar-H), 7.34 (d, ³J = 8.1 Hz, 2H, 2x Ar-H), 4.16 (t, ³J = 4.8 Hz, 2H, CH₂), 3.73-3.51 (m, 12H, 6x CH₂-O), 3.08 (t, ³J = 6.6 Hz, 2H, CH₂-O), 2.44 (s, 3H, CH₃), 2.32 (s, 3H, CH₃).

¹³C-NMR (75 MHz, CDCl₃): δ = 195.10 (C_q, C=O), 144.77 (C_q, C_{Ar}), 139.33 (C_q, C_{Ar}), 129.79 (CH, 2x C_{Ar}), 127.96 (CH, 2x C_{Ar}), 70.73 (CH₂), 70.55 (CH₂), 70.51 (CH₂), 70.26 (CH₂), 69.72 (CH₂), 69.21 (CH₂), 68.67 (CH₂), 30.56 (CH₃), 28.79 (CH₂), 21.63 (CH₃).

GC-MS (JR_50_S): t_R = 7.31 min, m/z = 287 (8 %), 155 (100 %).

1-Azido-3,6,9-trioxa-12-thiatetradecan-13-one (29)



C₁₀H₁₉N₃O₄S

[277.34]

In a 10 mL Schlenk flask, 70 mg (0.17 mmol, 1.0 eq) 1-(((4-methylbenzene)sulfonyl)oxy)-3,6,9-trioxa-12-thiatetradecan-13-one (**28**) were dissolved in 3.5 mL dry DMF under Ar counterflow. After addition of 13 mg (0.20 mmol, 1.2 eq) sodium azide, the orange solution was stirred at rt for 18 h. As TLC indicated incomplete conversion, another 13 mg (0.20 mmol, 1.2 eq) sodium azide were added to the reaction mixture. After another 22 h of stirring, TLC control indicated full conversion. DMF was removed under reduced pressure and the beige solid was purified by flash chromatography (6 g silica gel, 100 mL cyclohexane/ethyl acetate 9:1, then 100 mL cyclohexane/ethyl acetate 1:1, then 100 mL cyclohexane/ethyl acetate 1:9, then 100 mL ethyl acetate, then 100 mL ethyl acetate/methanol 9:1 and finally 100 mL methanol).

Yield: 27 mg (0.10 mmol, 57 %) colorless oil.

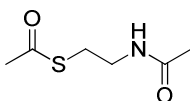
R_f = 0.81 (ethyl acetate/methanol 99:1).

$^1\text{H-NMR}$ (300 MHz, CDCl_3): δ = 3.71-3.61 (m, 12H, 6x $\text{CH}_2\text{-O}$), 3.39 (t, 3J = 5.1 Hz, 2H, $\text{CH}_2\text{-N}$), 3.09 (t, 3J = 6.6 Hz, 2H, $\text{CH}_2\text{-S}$), 2.33 (s, 3H, CH_3).

$^{13}\text{C-NMR}$ (75 MHz, CDCl_3): δ = 195.57 (C_q , C=O), 70.67 ($\text{CH}_2\text{-O}$), 70.57 ($\text{CH}_2\text{-O}$), 70.29 ($\text{CH}_2\text{-O}$), 70.02 ($\text{CH}_2\text{-O}$), 69.73 ($\text{CH}_2\text{-O}$), 67.05 ($\text{CH}_2\text{-O}$), 50.65 ($\text{CH}_2\text{-N}$), 30.54 (CH_3), 28.80 ($\text{CH}_2\text{-S}$).

IR (neat): ν_{max} = 2867 (m), 2100 (s), 1690 (s), 1442 (w), 1353 (w), 1287 (m), 1102 (s), 950 (w), 625 (s).

N-(2-(Acetylsulfanyl)ethyl)acetamide (**169**)



$\text{C}_6\text{H}_{11}\text{NO}_2\text{S}$

[161.22]

General Method:

In a 15 mL Schlenk tube 100 mg cysteamine (**36**) or cysteamine hydrochloride (**35**) were suspended in 0.5 mL dry pyridine under Ar counterflow. The yellow suspension was diluted with 0.3 mL dry dichloromethane. At 0°C 0.3 mL acetic anhydride were added dropwise. The yellow solution was allowed to warm up to rt and stirred for 30 min. Then the reaction mixture was quenched with 1.5 mL 5 % aqueous HCl and another 5 mL dichloromethane were added. The organic layer was washed with 5 % HCl (3x5 mL) and saturated aqueous NaHCO₃ (1x5 mL). The organic layer was dried over Na₂SO₄, filtrated and the solvent was evaporated under reduced pressure.

Approach A: 100 mg (1.30 mmol, 1.0 eq) cysteamine (**36**)

0.5 mL (6.13 mmol, 4.7 eq) dry pyridine

0.3 mL (3.24 mmol, 2.5 eq) acetic anhydride

Yield: 45 mg (0.28 mmol, 22 %), colorless liquid.

Approach B: 100 mg (0.88 mmol, 1.0 eq) cysteamine hydrochloride (**35**)

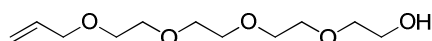
0.5 mL (6.13 mmol, 7.0 eq) dry pyridine

0.3 mL (3.24 mmol, 3.7 eq) acetic anhydride

Yield: 40 mg (0.25 mmol, 28 %), colorless liquid.

¹H-NMR (300 MHz, DMSO-d₆): δ = 8.07 (bs, 1H, NH), 3.15 (q, ³J = 6.6 Hz, 2H, CH₂-N), 2.88 (t, ³J = 6.6 Hz, 2H, CH₂-S), 2.33 (s, 3H, CH₃), 1.78 (s, 3H, CH₃).

GC-MS (JR_50_S): t_R = 5.47 min, m/z = 161 (1 %), 119 (100 %).

3,6,9,12-Tetraoxapentadec-14-en-1-ol (41)

C₁₁H₂₂O₅

[234.30]

In a 250 mL round-bottom flask, equipped with a magnetic stirring bar, 20.0 g (103 mmol, 1.0 eq) tetraethylene glycol (**25**) were dissolved in 25 mL (103 mmol, 1.0 eq

NaOH) 4 M aqueous NaOH solution at 0°C and 10 mL (116 mmol, 1.1 eq) allyl bromide were added. The colorless solution was stirred at rt for 20 h until TLC indicated complete conversion. The reaction mixture was extracted with dichloromethane (3x50 mL). The combined organic layers were dried over Na₂SO₄, filtrated and the solvent was evaporated under reduced pressure.

Yield: 18.66 g (80 mmol, 78 %) colorless oil.

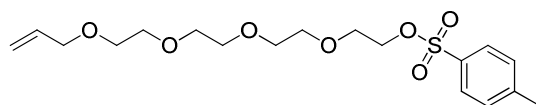
R_f = 0.52 (ethyl acetate/ethanol 9:1).

¹H-NMR (300 MHz, CDCl₃): δ = 5.97-5.82 (m, 1H, CH₂-CH=CH₂), 5.25 (dd, ³J = 17.1 Hz, ⁴J = 1.5 Hz, 1H, CH₂-CH=CH₂), 5.16 (dd, ³J = 10.2 Hz, ⁴J = 1.2 Hz, 1H, CH₂-CH=CH₂), 4.00 (t, ³J = 5.7 Hz, 2H, O-CH₂-CH=CH₂), 3.73-3.68 (m, 2H, CH₂-O), 3.68-3.61 (m, 10H, 5x CH₂-O), 3.61-3.55 (m, 4H, 2x CH₂-O), 2.82 (s, 1H, OH).

¹³C-NMR (75 MHz, CDCl₃): δ = 134.56 (CH, C-14), 117.26 (CH₂, C-15), 72.58 (CH₂, C-13), 70.56 (2x CH₂-O), 70.49 (4x CH₂-O), 70.21 (CH₂-O), 61.52 (CH₂-OH).

GC-MS (JR_100_L): t_R = 4.91 min, m/z = 207 (1 %), 163 (4 %), 89 (100 %).

3,6,9,12-Tetraoxapentadec-14-en-1-yl 4-methylbenzene-1-sulfonate (42)



C₁₈H₂₈O₇S

[388.48]

In a 250 mL Schlenk flask, evacuated under heat and flushed with N₂, 5.53 g (23.6 mmol, 1.0 eq) 3,6,9,12-tetraoxapentadec-14-en-1-ol (**41**) were dissolved with 25 mL dry dichloromethane. At 0°C, 8.4 mL (59.0 mmol, 2.5 eq) dry triethylamine, 20 mL dry dichloromethane and 6.96 g (35.4 mmol, 1.5 eq) *p*-toluenesulfonyl chloride were sequentially added. The reaction mixture was stirred at rt for 15 h. When TLC indicated complete conversion, the reaction mixture was diluted with 20 mL dichloromethane and

quenched with 8.5 mL 4 M aqueous HBr (48 %). After addition of 5 mL brine and 35 mL saturated aqueous NaHCO₃ solution, the aqueous layer was extracted with dichloromethane (3x20 mL). The combined organic layers were dried over Na₂SO₄, filtrated and the solvent was evaporated. The crude orange oil was purified by flash chromatography (400 g silica gel, cyclohexane/ethyl acetate 2:1).

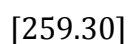
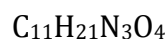
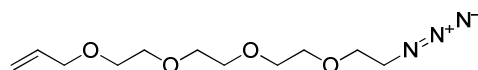
Yield: 7.06 g (18.2 mmol, 78 %) pale yellow oil.

R_f = 0.39 (cyclohexane/ethyl acetate 2:1).

¹H-NMR (300 MHz, CDCl₃): δ = 7.80 (d, ³J = 8.4 Hz, 2H, 2x Ar-H), 7.34 (d, ³J = 8.1 Hz, 2H, 2x Ar-H), 6.00-5.94 (m, 1H, CH₂-CH=CH₂), 5.29-5.15 (m, 2H, CH₂-CH=CH₂), 4.16 (t, ³J = 4.8 Hz, 2H, CH₂-O), 3.73-3.51 (m, 12H, 6x CH₂-O), 3.08 (t, ³J = 6.6 Hz, 2H, CH₂-O), 2.44 (s, 3H, CH₃).

GC-MS (JR_50_S): t_R = 9.49 min, m/z = 331 (1 %), 243 (5 %), 199 (100 %).

1-Azido-3,6,9,12-tetraoxapentadec-14-ene (43)



In a 250 mL round-bottom flask, equipped with a CaCl₂ drying tube, 2.36 g (6.97 mmol, 1.0 eq) 3,6,9,12-tetraoxapentadec-14-en-1-yl 4-methylbenzene-1-sulfonate (**42**) were dissolved in 27 mL dry DMF. After addition of 1.13 g (17.43 mmol, 2.5 eq) sodium azide and another 40 mL dry DMF, the mixture was stirred at rt for 16 h. When TLC indicated complete conversion, the solvent was evaporated under reduced pressure and the crude crystals were purified by flash chromatography (150 g silica gel, cyclohexane/ethyl acetate 2:1 up to 1:1).

Yield: 1.22 g (4.71 mmol, 68 %) colorless oil.

$R_f = 0.24$ (cyclohexane/ethyl acetate 2:1).

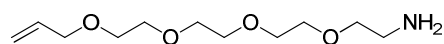
$^1\text{H-NMR}$ (300 MHz, CDCl_3): $\delta = 5.98\text{-}5.83$ (m, 1H, $\text{CH}_2\text{-CH}=\text{CH}_2$), 5.25 (dd, $^3J = 17.1$ Hz, $^4J = 1.5$ Hz, 1H, $\text{CH}_2\text{-CH}=\text{CH}_2$), 5.17 (dd, $^3J = 10.5$ Hz, $^4J = 1.5$ Hz, 1H, $\text{CH}_2\text{-CH}=\text{CH}_2$), 4.01 (dt, $^3J = 5.7$ Hz, $^4J = 1.2$ Hz, 2H, $\text{CH}_2\text{-CH}=\text{CH}_2$), 3.70-3.62 (m, 12H, 6x $\text{CH}_2\text{-O}$), 3.62-3.56 (m, 2H, $\text{CH}_2\text{-O}$), 3.38 (t, $^3J = 5.1$ Hz, 2H, $\text{CH}_2\text{-N}$).

$^{13}\text{C-NMR}$ (75 MHz, CDCl_3): $\delta = 134.74$ (CH, C-14), 117.07 (CH_2 , C-15), 72.21 ($\text{CH}_2\text{-O}$), 70.68 ($\text{CH}_2\text{-O}$), 70.67 ($\text{CH}_2\text{-O}$), 70.61 (3x $\text{CH}_2\text{-O}$), 70.01 ($\text{CH}_2\text{-O}$), 69.40 ($\text{CH}_2\text{-O}$), 50.67 ($\text{CH}_2\text{-N}$).

IR (neat): $\nu_{\text{max}} = 2867$ (m), 2102 (m), 1286 (w), 1100 (s), 928 (m), 732 (m).

GC-MS (JR_50_S): $t_R = 5.24$ min, $m/z = 231$ (4 %), 73 (100 %).

3,6,9,12-Tetraoxapentadec-14-en-1-amine (44)



$\text{C}_{11}\text{H}_{23}\text{NO}_4$

[233.30]

In a 10 mL Schlenk tube, heat dried under vacuum and flushed with Ar, 1.51 g (5.82 mmol, 1.0 eq) 1-azido-3,6,9,12-tetraoxapentadec-14-ene (**43**) were dissolved in 26 mL dry THF. After degassing by 10 vacuum-Ar cycles, 1.83 g (6.98 mmol, 1.2 eq) triphenylphosphine and 0.42 mL (23.28 mmol, 4.0 eq) H_2O were added. The reaction mixture was again degassed by 10 vacuum-Ar cycles and subsequently stirred at rt for 19 h. When TLC indicated complete conversion the solvents were evaporated under reduced pressure and the crude product was purified by flash chromatography (30 g silica gel, methanol/triethyl amine 99:1, second column: 30 g silica gel, dichloromethane/methanol 1:1).

Yield: 1.24 g (5.31 mmol, 92 %) dark yellow oil.

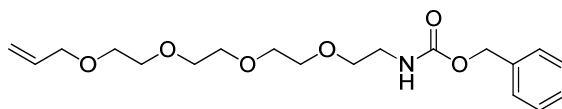
$R_f = 0.16$ (methanol).

$^1\text{H-NMR}$ (300 MHz, CDCl_3): $\delta = 5.98\text{-}5.82$ (m, 1H, $\text{CH}_2\text{-CH}=\text{CH}_2$), 5.25 (dq, $^3J = 17.1$ Hz, $^4J = 1.5$ Hz, 1H, $\text{CH}_2\text{-CH}=\text{CH}_2$), 5.17 (dd, $^3J = 10.5$ Hz, $^4J = 1.2$ Hz, 1H, $\text{CH}_2\text{-CH}=\text{CH}_2$), 4.01 (d, $^3J = 5.7$ Hz, 2H, $\text{CH}_2\text{-CH}=\text{CH}_2$), 3.68-3.56 (m, 12H, 6x $\text{CH}_2\text{-O}$), 3.50 (t, $^3J = 5.1$ Hz, 2H, $\text{CH}_2\text{-O}$), 2.85 (bs, 2H $\text{CH}_2\text{-N}$).

$^{13}\text{C-NMR}$ (75 MHz, CDCl_3): $\delta = 134.71$ (CH, C-14), 117.09 (CH_2 , C-15), 73.40 ($\text{CH}_2\text{-O}$), 72.20 ($\text{CH}_2\text{-O}$), 70.60 (2x $\text{CH}_2\text{-O}$), 70.58 ($\text{CH}_2\text{-O}$), 70.55 ($\text{CH}_2\text{-O}$), 70.27 ($\text{CH}_2\text{-O}$), 69.40 ($\text{CH}_2\text{-O}$), 41.76 ($\text{CH}_2\text{-N}$).

The amine **44** is not detectable via GC-MS.

Benzyl *N*-(3,6,9,12-tetraoxapentadec-14-en-1-yl)carbamate (**45**)



$\text{C}_{19}\text{H}_{29}\text{NO}_6$

[367.44]

A 10 mL round-bottom flask was charged with 63 mg (0.60 mmol, 2.2 eq) Na_2CO_3 in 1.3 mL H_2O and 62 mg (0.27 mmol, 1.0 eq) 3,6,9,12-tetraoxapentadec-14-en-1-amine (**44**). At 0°C , 1.3 mL 1,4-dioxane and 57 μL (0.40 mmol, 1.5 eq) Cbz-Cl were added and the mixture was stirred at rt for 1.5 h until TLC indicated complete conversion. After evaporation of 1,4-dioxane under reduced pressure, the aqueous layer was extracted with dichloromethane (3x10 mL). The combined organic layers were extracted with 0.1 M HCl (3x10 mL), dried over Na_2SO_4 , filtrated and the solvent was evaporated. Finally the product **45** was dried under high vacuum.

Yield: 90 mg (0.24 mmol, 92 %) colorless oil.

$R_f = 0.69$ (methanol).

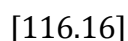
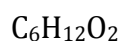
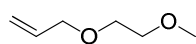
$^1\text{H-NMR}$ (300 MHz, CDCl_3): δ = 7.38-7.28 (m, 5H, 5x Ar-H), 5.98-5.82 (m, 1H, $\text{CH}_2\text{-CH}=\text{CH}_2$), 5.28 (dq, 3J = 17.1 Hz, 4J = 1.5 Hz, 1H, $\text{CH}_2\text{-CH}=\text{CH}_2$), 5.16 (dd, 3J = 10.5 Hz, 4J = 1.2 Hz, 1H, $\text{CH}_2\text{-CH}=\text{CH}_2$), 5.10 (s, 2H, $\text{CH}_2\text{-O}$), 4.00 (d, 3J = 5.7 Hz, 2H, $\text{CH}_2\text{-CH}=\text{CH}_2$), 3.67-3.54 (m, 14H, 7x $\text{CH}_2\text{-O}$), 3.38 (t, 3J = 5.1 Hz, 2H, $\text{CH}_2\text{-N}$), 2.03 (bs, 1H, NH).

$^{13}\text{C-NMR}$ (75 MHz, CDCl_3): δ = 156.45 (C_q , $\text{C}=\text{O}$), 140.91 (C_q , C_{Ar}), 134.69 (CH, $\text{CH}_2\text{-CH}=\text{CH}_2$), 128.50 (CH, C_{Ar}), 128.45 (CH, C_{Ar}), 128.05 (CH, C_{Ar}), 128.01 (CH, C_{Ar}), 127.58 (CH, C_{Ar}), 126.93 (CH, C_{Ar}), 117.08 (CH_2 , $\text{CH}_2\text{-CH}=\text{CH}_2$), 72.18 ($\text{O-CH}_2\text{-CH}=\text{CH}_2$), 70.56 (2x $\text{CH}_2\text{-O}$), 70.49 ($\text{CH}_2\text{-O}$), 70.25 ($\text{CH}_2\text{-O}$), 70.02 ($\text{CH}_2\text{-O}$), 69.36 ($\text{CH}_2\text{-O}$), 65.29 ($\text{CH}_2\text{-O}$), 40.88 ($\text{CH}_2\text{-N}$).

IR (neat): ν_{max} = 3342 (w), 2869 (w), 1719 (s), 1529 (m), 1455 (w), 1250 (s), 1096 (s), 1025 (m), 926 (m), 802 (w), 738 (m), 698 (s).

HPLC-ESI-MS (Method H): t_{R} = 8.35 min, $[\text{M}+\text{H}]^+$ = 368, $[\text{M}+\text{Na}]^+$ = 390.

1-Methoxy-2-(prop-2-en-1-yloxy)ethane (**62**)



In a 50 mL round-bottom flask, 504 mg (6.63 mmol, 2.9 eq) 2-methoxyethanol were dissolved in 250 μL (1.00 mmol, 0.4 eq) NaOH solution (4 M in water). At 0°C , 688 μL (7.95 mmol, 3.5 eq) allyl bromide were added and the reaction mixture was allowed to stir at rt for 20 h. As TLC indicated incomplete conversion, another 50 mg (1.25 mmol, 0.6 eq) NaOH were added. When 2-methoxyethanol was fully consumed (after another 2 h of stirring) the colorless solution was extracted with dichloromethane (3x10 mL). The combined organic layers were dried over Na_2SO_4 , filtrated and concentrated *in vacuo*. The crude product **62** was purified by flash chromatography (3 g silica gel, dichloromethane up to dichloromethane/methanol 10:1).

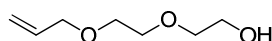
Yield: 145 mg (1.25 mmol, 56 %) colorless liquid.

$R_f = 0.74$ (ethyl acetate/ethanol 9:1).

$^1\text{H-NMR}$ (300 MHz, CDCl_3): $\delta = 5.98\text{-}5.84$ (m, 1H, $\text{CH}_2\text{-CH}=\text{CH}_2$), 5.27 (dq, $^3J = 17.1$ Hz, $^4J = 1.8$ Hz, 1H, $\text{CH}_2\text{-CH}=\text{CH}_2$), 5.17 (dd, $^3J = 10.5$ Hz, $^4J = 1.8$ Hz, 1H, $\text{CH}_2\text{-CH}=\text{CH}_2$), 4.02 (dt, $^3J = 5.7$ Hz, $^4J = 1.2$ Hz, 2H, $\text{O-CH}_2\text{-CH}=\text{CH}_2$), 3.63-3.53 (m, 4H, 2x $\text{CH}_2\text{-O}$), 3.38 (s, 3H, $\text{CH}_3\text{-O}$).

GC-MS (JR_50_S): $t_R = 4.22$ min, $m/z = 87$ (17 %), 59 (100 %).

2-(2-(Prop-2-en-1-yloxy)ethoxy)ethan-1-ol (**63**)



$\text{C}_7\text{H}_{14}\text{O}_3$

[146.18]

In a 50 mL round-bottom flask, 502 mg (4.72 mmol, 2.1 eq) diethylene glycol were dissolved in 250 μL (1.00 mmol, 0.4 eq) NaOH solution (4 M in water). At 0°C , 448 μL (5.18 mmol, 2.3 eq) allylic bromide were added and the reaction mixture was allowed to stir at rt for 20 h. As TLC indicated incomplete conversion, another 50 mg (1.25 mmol, 0.6 eq) sodium hydroxide were added. When diethylene glycol was fully consumed (after another 2 h of stirring) the colorless solution was extracted with dichloromethane (3x10 mL). The combined organic layers were dried over Na_2SO_4 , filtrated and concentrated *in vacuo*. The crude product **63** was purified by flash chromatography (8 g silica gel, dichloromethane up to dichloromethane/methanol 10:1).

Yield: 328 mg (2.25 mmol, quantitative) pale yellow oil.

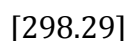
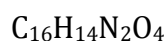
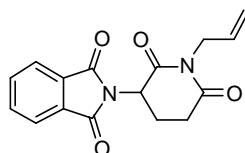
$R_f = 0.65$ (ethyl acetate/ethanol 9:1).

$^1\text{H-NMR}$ (300 MHz, CDCl_3): $\delta = 5.98\text{-}5.83$ (m, 1H, $\text{CH}_2\text{-CH}=\text{CH}_2$), 5.27 (d, $^3J = 17.4$ Hz, 1H, $\text{CH}_2\text{-CH}=\text{CH}_2$), 5.19 (dd, $^3J = 10.2$ Hz, $^4J = 1.2$ Hz, 1H, $\text{CH}_2\text{-CH}=\text{CH}_2$), 4.02 (d, $^3J = 5.4$ Hz, 2H, $\text{O-CH}_2\text{-CH}=\text{CH}_2$), 3.76-3.53 (m, 8H, 4x $\text{CH}_2\text{-O}$), 2.54 (bs, 1H, OH).

GC-MS (JR_50_S): $t_R = 4.22$ min, $m/z = 146$ (1 %), 73 (100 %).

6.2.3 Drug linkage

2-(2,6-Dioxo-1-(2-propen-1-yl)-3-piperidinyl)-1H-isoindol-1,3(2H)-dione (31)



A 15 mL Schlenk tube, equipped with a stirring bar, was heat dried under vacuum and flushed with N_2 before 170 mg (4.2 mmol, 2.3 eq) sodium hydride (60 % dispersion) were suspended in 6 mL dry DMF. The mixture was cooled to $0^\circ C$ and 500 mg (1.9 mmol, 1.0 eq) thalidomide (**1**) were added in portions. After 20 min of stirring, the light yellow suspension was allowed to warm up to rt and the mixture was stirred for additional 30 min. Subsequently, 200 μL (2.3 mmol, 1.2 eq) allylic bromide and 5 mL DMF were added and the yellow suspension stirred at rt for another 20 h. After GC-MS and TLC indicated full conversion, allyl-thalidomide **31** was isolated from the crude reaction mixture either by preparative TLC (20x20 cm, 2 mm thickness, cyclohexane/ethyl acetate 1:1) or by filtration through a pad of silica gel and subsequent elution with 10 mL ethyl acetate.

With the latter isolation method, a white precipitate (NaBr) was also removed by filtration. After concentration of the filtrate, 1.43 g of crude yellow oil was obtained. The crude product **31** was again dissolved in 50 mL ethyl acetate. A brown precipitate formed, was filtered off and the solution was again evaporated. The resulting yellow oil was then brought to precipitation with 30 mL ethyl acetate/cyclohexane (1:5).

When purified by preparative TLC, the product band was scraped off and stirred with 60 mL methanol. The mixture was filtrated and subsequently methanol was removed

under reduced pressure. In order to remove the last traces of DMF, toluene was added and the residue was dried under high vacuum.

Crystallization: Yield: 330 mg (1.10 mmol, 58 %) pale yellow solid.

PTLC: Yield: 249 mg (0.85 mmol, 43 %) colorless solid.

$R_f = 0.54$ (cyclohexane/ethyl acetate 1:1).

M.p. = 143-145°C.

$^1\text{H-NMR}$ (300 MHz, DMSO- d_6): $\delta = 7.93$ (s, 4H, 4x Ar-H), 5.80-5.69 (m, 1H, $\text{CH}_2\text{-CH}=\text{CH}_2$), 5.30 (dd, $^3J = 12.6$ Hz, $^3J = 4.5$ Hz, 1H, CH-N), 5.01 (dd, $^3J = 15.9$ Hz, $^3J = 8.4$ Hz, 2H, $\text{CH}_2\text{-CH}=\text{CH}_2$), 4.26 (s, 2H, $\text{CH}_2\text{-N}$), 3.11-2.05 (m, 4H, 2x CH_2).

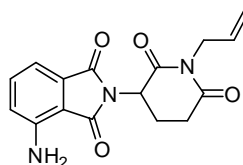
$^{13}\text{C-NMR}$ (75 MHz, DMSO- d_6): $\delta = 171.20$ (C_q , C=O), 169.10 (C_q , C=O), 167.12 (2x C_q , 2x C=O), 134.92 (2x CH, 2x C_{Ar}), 132.31 ($\text{CH}_2\text{-CH}=\text{CH}_2$), 131.21 (C_q , C_{Ar}), 123.45 (2x CH, 2x C_{Ar}), 115.79 ($\text{CH}_2\text{-CH}=\text{CH}_2$), 49.54 (CH-N), 41.49 ($\text{CH}_2\text{-N}$), 31.06 (CH_2), 21.20 (CH_2).

IR (neat): $\nu_{\text{max}} = 1713$ (s), 1676 (s), 1387 (m), 1333 (w), 1245 (w), 1174 (w), 1128 (m), 997 (m), 888 (w), 778 (w), 719 (s), 635 (m).

GC-MS (JR_50_S): $t_R = 8.56$ min, $m/z = 298$ (60 %), 173 (100 %).

HRMS (TOF MS EI $^+$): m/z calculated for $\text{C}_{16}\text{H}_{14}\text{N}_2\text{O}_4^+$ [M] $^+$: 298.0954, found 298.0970.

4-Amino-2-(2,6-dioxo-1-(2-propen-1-yl)-3-piperidiny)-1H-isoindol-1,3(2H)-dione (32)



$\text{C}_{16}\text{H}_{15}\text{N}_3\text{O}_4$

[313.31]

In a 15 mL Schlenk tube, heat dried under vacuum and flushed with Ar, 75 mg (1.83 mmol, 2.0 eq) sodium hydride (60 % dispersion) were suspended in 1.5 mL dry DMF. At 0°C, 249 mg (0.92 mmol, 1.0 eq) pomalidomide (**2**) were added portionwise. After 15 min of stirring at 0°C, the suspension was allowed to warm up to rt and was stirred for another hour. Then 95 μ L (1.10 mmol, 1.2 eq) allylic bromide were added. After 16 h at rt, GC-MS indicated complete conversion and the orange-brown solution was filtrated through a pad of silica gel and rinsed with ethyl acetate (4x2 mL). The ethyl acetate was evaporated and the crude yellow liquid was purified by PTLC (20x20 cm, 1 mm thickness, dichloromethane/methanol 99:1).

Yield: 104 mg (0.33 mmol, 36 %) yellow solid.

R_f = 0.83 (ethyl acetate).

R_f = 0.48 (dichloromethane/methanol 99:1).

M.p. = 180°C.

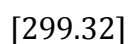
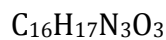
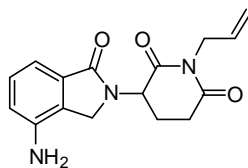
$^1\text{H-NMR}$ (300 MHz, DMSO- d_6): δ = 7.47 (dd, 3J = 7.2 Hz, 3J = 8.4 Hz, 1H, Ar-H), 7.01 (dd, 3J = 8.4 Hz, 3J = 6.6 Hz, 2H, 2x Ar-H), 6.53 (bs, 2H, NH₂), 5.81-5.65 (m, 1H, CH₂-CH=CH₂), 5.19 (dd, 3J = 5.4 Hz, 3J = 12.6 Hz, 1H, CH-N), 5.08 (ddd, 3J = 15.0 Hz, 3J = 9.0 Hz, 4J = 1.2 Hz, 2H, CH₂-CH=CH₂), 4.25 (d, 3J = 3.9 Hz, 2H, CH₂-N), 3.10-2.00 (m, 4H, 2x CH₂).

$^{13}\text{C-NMR}$ (75 MHz, DMSO- d_6): δ = 171.17 (C_q, C=O), 169.26 (C_q, C=O), 168.43 (C_q, C=O), 167.23 (C_q, C=O), 146.66 (C_q, C_{Ar}), 135.39 (CH, C_{Ar}), 132.27 (CH₂-CH=CH₂), 131.88 (C_q, C_{Ar}), 121.65 (CH, C_{Ar}), 115.72 (CH₂-CH=CH₂), 110.90 (CH, C_{Ar}), 108.38 (C_q, C_{Ar}), 48.96 (CH-N), 41.04 (CH₂-N), 31.04 (CH₂), 21.30 (CH₂).

IR (neat): ν_{max} = 3480 (w), 3377 (w), 1700 (s), 1670 (s), 1635 (s), 1483 (w), 1411 (m), 1335 (m), 1247 (w), 1170 (s), 1129 (w), 1011 (w), 990 (w), 925 (m), 820 (m), 748 (s), 619 (m).

GC-MS (JR_50_S): t_R = 10.27 min, m/z = 313 (100 %).

HRMS (TOF MS EI⁺): m/z calculated for C₁₆H₁₅N₃O₄⁺ [M]⁺: 313.1063, found 313.1070.

3-(4-Amino-1-oxo-1*H*-isoindol-1,3(2*H*)-2-yl)-1-(2-propen-1-yl)piperidine-2,6-dione (33)

A 15 mL Schlenk tube was heat dried under vacuum and flushed with Ar. 58 mg (1.46 mmol, 1.9 eq) sodium hydride (60 % dispersion) were suspended in 1.2 mL dry DMF and cooled in an ice bath to 0°C. After addition of 200 mg (0.77 mmol, 1.0 eq) lenalidomide (**3**), the dark grey suspension was allowed to warm up to rt followed by another 2 h of stirring. Afterwards, 76 μL (0.88 mmol, 1.1 eq) allylic bromide were added and the mixture was again stirred at rt for another 17 h. GC-MS control indicated 98 % conversion. The reaction mixture was quenched with 2 mL ethyl acetate, filtrated through 1 cm silica gel and rinsed with ethyl acetate (3x2mL). The solvents were removed under reduced pressure and the crude product **33** was dried under high vacuum at 45°C. The resulting orange-brown highly viscous oil was purified by preparative TLC (160 mg dissolved in 0.5 mL DMF, 20x20 cm TLC plate, 1 mm thickness, ethyl acetate).

Yield: 164 mg (0.55 mmol, 71 %) yellow solid.

R_f = 0.30 (ethyl acetate).

M.p. = 179°C.

$^1\text{H-NMR}$ (300 MHz, DMSO-d_6): δ = 7.19 (t, 3J = 7.8 Hz, 1H, Ar-H), 6.93 (d, 3J = 7.5 Hz, 1H, Ar-H), 6.80 (d, 3J = 7.8 Hz, 1H, Ar-H), 5.82-5.66 (m, 1H, $\text{CH}_2\text{-CH}=\text{CH}_2$), 5.41 (bs, 2H, NH_2), 5.18 (dd, 3J = 13.5 Hz, 3J = 5.1 Hz, 1H, N-CH), 5.11-5.01 (m, 2H, $\text{CH}_2\text{-CH}=\text{CH}_2$), 4.27-4.20 (m, 2H, N- $\text{CH}_2\text{-CH}=\text{CH}_2$), 4.20-4.01 (m, 2H, $\text{CH}_2\text{-N}$), 3.10-2.70 + 2.44-2.00 (m, 4H, $\text{CH}_2\text{-CH}_2$).

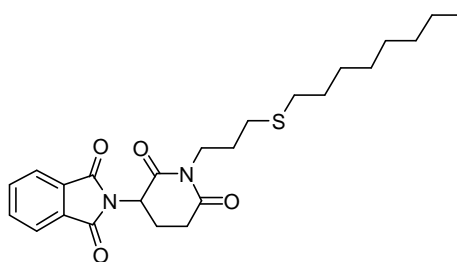
^{13}C -NMR (75 MHz, DMSO- d_6): δ = 171.50 (C_q , C=O), 170.28 (C_q , C=O), 169.11 (C_q , C=O), 143.48 (C_q , C_{Ar}), 132.53 (CH_2 - $\underline{\text{C}}\text{H}=\text{CH}_2$), 132.08 (C_q , C_{Ar}), 128.98 (CH , C_{Ar}), 125.53 (C_q , C_{Ar}), 116.59 (CH , C_{Ar}), 115.93 (CH_2 - $\text{CH}=\underline{\text{C}}\text{H}_2$), 110.59 (CH , C_{Ar}), 52.15 (N-CH), 45.67 (N-CH_2), 41.56 ($\text{N-}\underline{\text{C}}\text{H}_2$ - $\text{CH}=\text{CH}_2$), 31.33 (CH_2), 21.89 (CH_2).

IR (neat): ν_{max} = 3485 (w), 3364 (m), 1671 (s), 1630 (s), 1490 (m), 1417 (w), 1366 (w), 1324 (m), 1291 (w), 1232 (w), 1182 (m), 1127 (m), 993 (m), 939 (m), 805 (w), 750 (s), 615 (m).

GC-MS (JR_50_S): t_{R} = 11.16 min, m/z = 299 (100 %).

HRMS (TOF MS EI $^+$): m/z calculated for $\text{C}_{16}\text{H}_{17}\text{N}_3\text{O}_3^+$ [M] $^+$: 299.1270, found 299.1283.

2-(1-(3-(Octylsulfanyl)propyl)-2,6-dioxopiperidin-3-yl)-1H-isoindol-1,3(2H)-dione (34)



$\text{C}_{24}\text{H}_{32}\text{N}_2\text{O}_4\text{S}$

[444.59]

A 5 mL Schlenk tube was heat dried under vacuum and flushed with N_2 . 50 mg (0.16 mmol, 1 eq) allyl-thalidomide **31** were dissolved in 0.5 mL dry DMF and the solution was degassed by four vacuum- N_2 cycles. After addition of 5 mg (0.03 mmol, 0.2 eq) azobisisobutyronitrile, the mixture was again degassed by two vacuum- N_2 cycles. 36 mg (0.25 mmol, 1.5 eq) octanethiol (**87**) were added and three degassing cycles were applied. Afterwards, the reaction mixture was stirred at 75°C for 19 h. After full conversion of allyl-thalidomide **31** was proven by TLC, the solvent was removed under high vacuum.

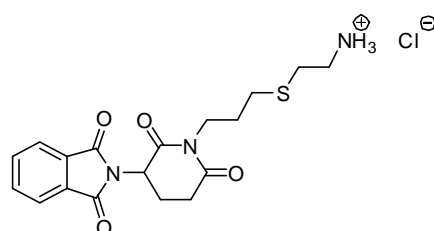
Yield: 71 mg (0.16 mmol, quantitative) grey solid.

$R_f = 0.55$ (cyclohexane/ethyl acetate 1:1).

$^1\text{H-NMR}$ (300 MHz, DMSO-d_6): $\delta = 8.00\text{-}7.91$ (m, 4x Ar-H), 5.30 (dd, $^3J = 12.9$ Hz, $^3J = 5.4$ Hz, 1H, CH-N), 3.79 (t, $^3J = 6.9$ Hz, 2H, $\text{CH}_2\text{-N}$), 3.10-2.05 (m, 4H, 2x CH_2 cyclic), 1.73 (t, $^3J = 7.2$ Hz, 2H, $\text{CH}_2\text{-S}$), 1.60-1.45 (m, 2H, $\text{CH}_2\text{-S}$), 1.26 (bs, 12H, 6x CH_2), 0.87 (t, $^3J = 6.9$ Hz, 3H, CH_3).

$^{13}\text{C-NMR}$ (75 MHz, DMSO-d_6): $\delta = 171.42$ (C_q , C=O), 169.27 (C_q , C=O), 166.99 (C_q , C=O), 134.76 (2x CH, 2x C_{Ar}), 131.13 (C_q , C_{Ar}), 123.30 (2x CH, 2x C_{Ar}), 49.47 (CH-N), 38.74 ($\text{CH}_2\text{-N}$), 31.13 ($\text{CH}_2\text{-S}$), 31.06 ($\text{CH}_2\text{-ring}$), 30.82 ($\text{CH}_2\text{-S}$), 28.95 (CH_2), 28.52 (CH_2), 28.48 (CH_2), 28.34 (CH_2), 28.14 (CH_2), 27.39 (CH_2), 21.97 (CH_2), 21.20 ($\text{CH}_2\text{-ring}$), 13.81 (CH_3).

2-((3-(3-(1,3-Dioxo-1*H*-isoindol-1,3(2*H*)-2-yl)-2,6-dioxopiperidin-1-yl)propyl)sulfanyl)ethyl-1-amine hydrochloride (37)



$\text{C}_{18}\text{H}_{22}\text{ClN}_3\text{O}_4\text{S}$

[411.90]

A 15 mL Schlenk tube, equipped with a stirring bar, was heat dried under vacuum and flushed with Ar. 100 mg (0.34 mmol, 1.0 eq) allyl-thalidomide **31** were dissolved in 1 mL dry DMF. The colorless solution was degassed by three vacuum-Ar cycles before 22 mg (0.14 mmol, 0.4 eq) azobisisobutyronitrile and 76 mg (0.67 mmol, 2.0 eq) cysteamine hydrochloride (**35**) were added. After additional degassing by three vacuum-Ar cycles, the yellow solution was stirred at 75°C for 18 h. LC-MS control indicated product formation and stirring was continued at 75°C for another 5 h. Afterwards, the yellow solution was cooled to rt and DMF was removed under high vacuum. Finally the crude product **37** was purified by preparative HPLC and freeze dried using a lyophilisator.

Yield: 30 mg (0.07 mmol, 21 %) colorless solid.

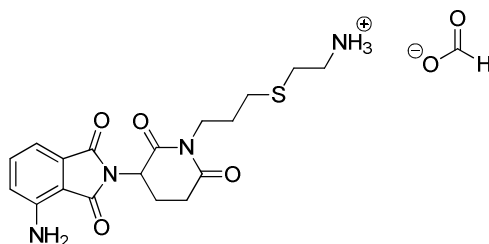
$^1\text{H-NMR}$ (300 MHz, DMSO-d_6): δ = 8.38 (s, 1H, HCOO^-), 8.00-7.85 (m, 4H, 4x Ar-H), 5.25 (dd, 3J = 12.9 Hz, 3J = 5.1 Hz, 1H, CH-N), 3.75 (t, 3J = 7.2 Hz, 2H, $\text{CH}_2\text{-N}$), 3.11-2.05 (10H, m, 5x CH_2), 1.69 (t, 3J = 6.9 Hz, 3H, CH_3).

$^{13}\text{C-NMR}$ (75 MHz, DMSO-d_6): δ = 171.56 (C_q , C=O), 169.42 (C_q , C=O), 167.07 (C_q , C=O), 134.86 (2x CH, 2x C_{Ar}), 131.14 (C_q , C_{Ar}), 123.41 (2x CH, 2x C_{Ar}), 49.49 (CH-N), 38.72 (CH_2), 38.63 (CH_2), 31.07 ($\text{CH}_2\text{-ring}$), 29.17 (CH_2), 28.05 (CH_2), 27.23 (CH_2), 21.21 ($\text{CH}_2\text{-ring}$).

PHPLC (TD_HCOOH_MeOH_15_nucleodur): A: 0.01 % HCOOH in H_2O , B: MeOH, rt, 17 mL/min, 0-15 min: 16 % B constant, λ = 254 nm. t_R = 9.8 min.

HPLC-ESI-MS (Method A): t_R = 6.82 min, $[\text{M}+\text{H}]^+$ = 376, $[\text{M}+\text{Na}]^+$ = 395, $[\text{M}+\text{K}]^+$ = 411.

4-Amino-2-((3-(3-(1,3-dioxo-1*H*-isoindol-1,3(2*H*)-2-yl)-2,6-dioxopiperidin-1-yl)propyl)sulfanyl)ethan-1-aminium formate (38)



$\text{C}_{19}\text{H}_{24}\text{N}_4\text{O}_6\text{S}$

[436.48]

A 15 mL Schlenk tube containing a stirring bar was heat dried under vacuum and flushed with Ar. 400 mg (1.28 mmol, 1.0 eq) allyl-pomalidomide **32** and 290 mg (2.55 mmol, 2.0 eq) cysteamine hydrochloride (**35**) were dissolved in 1.8 mL dry DMF. The yellow solution was degassed by four vacuum-Ar cycles before 84 mg (0.51 mmol, 0.4 eq) azobisisobutyronitrile were added. After additional degassing by two vacuum-Ar cycles, the yellow solution was stirred at 75°C for 27 h. TLC indicated nearly complete conversion. Afterwards, the yellow solution was cooled to rt and DMF was removed

under high vacuum. Finally the crude product **38** was purified by preparative HPLC and lyophilized.

Yield: 183 mg (0.43 mmol, 33 %) yellow solid.

M.p. > 360°C.

$^1\text{H-NMR}$ (300 MHz, D_2O): δ = 8.45 (s, 1H, HCOO^-), 7.50 (dd, $^3J = 8.1$ Hz, $^3J = 7.5$ Hz, 1H, Ar-H), 7.13 (d, $^3J = 6.9$ Hz, 1H, Ar-H), 7.05 (d, $^3J = 8.4$ Hz, 1H, Ar-H), 5.13 (dd, $^3J = 12.9$ Hz, $^3J = 5.7$ Hz, 1H, CH-N), 3.87 (t, $^3J = 6.9$ Hz, 2H, $\text{CH}_2\text{-N}$), 3.21 (t, $^3J = 6.6$ Hz, 2H, CH_2), 2.98-2.89 (m, 2H, $\text{CH}_2\text{-ring}$), 2.85 (t, $^3J = 6.6$ Hz, 2H, CH_2), 2.68-2.50 (m, 3H, $\text{CH}_2\text{-ring}$, CH_2), 2.23-2.11 (m, 1H, $\text{CH}_2\text{-ring}$), 1.82 (p, $^3J = 6.9$ Hz, 2H, CH_2).

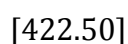
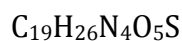
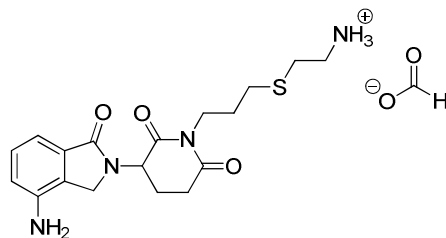
$^{13}\text{C-NMR}$ (75 MHz, D_2O): δ = 174.68 (C_q , C=O), 171.72 (C_q , C=O), 171.04 (C_q , C=O), 169.67 (C_q , C=O), 169.56 (C_q , C=O), 146.33 (C_q , C_{Ar}), 136.10 (CH, C_{Ar}), 131.58 (C_q , C_{Ar}), 123.02 (CH, C_{Ar}), 113.38 (CH, C_{Ar}), 109.75 (C_q , C_{Ar}), 49.66 (CH-N), 48.91 (CH_2), 39.44 (CH_2), 38.34 (CH_2), 31.27 ($\text{CH}_2\text{-ring}$), 28.18 (CH_2), 28.13 (CH_2), 26.61 (CH_2), 21.32 ($\text{CH}_2\text{-ring}$).

IR (neat): ν_{max} = 2924 (w), 1698 (s), 1675 (s), 1633 (m), 1482 (w), 1409 (m), 1396 (s), 1257 (w), 1148 (s), 1026 (m), 748 (m), 610 (s).

PHPLC: A: 0.01 % HCOOH in H_2O , B: MeOH , rt, 15 mL/min, 0-21.5 min: 15 % B constant, 21.5-30.0 min: 100 % B constant, $\lambda = 260$ nm. $t_{\text{R}} = 24$ min.

HPLC-ESI-MS (Method B): $t_{\text{R}} = 1.75$ min, $[\text{M}+\text{H}]^+ = 391$, $[\text{M}+\text{Na}]^+ = 413$.

2-((3-(3-(4-Amino-1-oxo-1*H*-isoindol-1,3(2*H*)-2-yl)-2,6-dioxopiperidin-1-yl)propyl)sulfanyl)ethan-1-aminium formate (39)



A 10 mL Schlenk tube was heat dried under vacuum and flushed with N₂. 100 mg (0.33 mmol, 1.0 eq) allyl-lenalidomide **33** were dissolved in 0.5 mL dry DMF. This yellow solution was degassed by four vacuum-N₂ cycles. 76 mg (0.67 mmol, 2.0 eq) cysteamine hydrochloride (**35**) and 22 mg (0.13 mmol, 0.4 eq) azobisisobutyronitrile were added followed by three vacuum-N₂ cycles. The resulting solution was stirred at 75°C for 18 h. TLC indicated complete conversion of allyl-lenalidomide **33**. The crude product **39**, still dissolved in DMF, was purified by preparative HPLC. Due to product instability during purification, the linked pomalidomide **38** was formed and identified according to its characterization above.

Yield: Fraction A: 10 mg (0.02 mmol, 7 %), yellow solid (90 % pure from HPLC-MS).

Fraction B: 8 mg (0.02 mmol, 6 %), colorless solid (50 % pure from HPLC-MS).

Fraction C: 60 mg (0.14 mmol, 41 %), yellow solid (pure, identified as linked pomalidomide **38**).

All impurities of the linked lenalidomide **39** were the monooxidized linked lenalidomide **40** or the linked pomalidomide **38**.

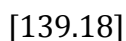
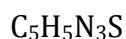
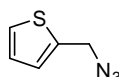
PHPLC: A: 0.01 % HCOOH in H₂O, B: MeOH, rt, 15 mL/min, 0-14 min: 10 % B constant, 14-25 min: 100 % B constant, $\lambda = 260$ nm. $t_R = 8.5$ min ($t_R = 17.0$ min linked pomalidomide **38**).

HPLC-ESI-MS (Method C): $t_R = 5.81$ min, $[M+H]^+ = 377$, $[M+Na]^+ = 399$. $t_R = 2.99$ min, $[M+H]^+ = 393$, $[M+Na]^+ = 415$ (monooxidized linked lenalidomide **40**).

HPLC-ESI-MS (Method D): $t_R = 3.89$ min, $[M+H]^+ = 377$, $[M+Na]^+ = 399$. $t_R = 6.75$ min, $[M+H]^+ = 391$, $[M+Na]^+ = 413$ (linked pomalidomide **38**).

6.2.4 Thiophene derivatives

2-(Azidomethyl)thiophene (**93**)



Method A:

In a 15 mL Schlenk tube, heat dried under vacuum and flushed with N_2 , 0.30 g (4.61 mmol, 1.03 eq) sodium azide and 0.42 mL (4.38 mmol, 1.00eq) 2-thiophenemethanol (**104**) were suspended in 3 mL dry 1,4-dioxane. After 1 h of stirring at $80^\circ C$, 0.81 mL (6.55 mmol, 1.50eq) $BF_3 \times Et_2O$ were added dropwise within 90 min. The brownish suspension was stirred at $85^\circ C$ for another 3 h until GC-MS monitoring indicated complete conversion. The reaction mixture was poured into 25 mL ice cold H_2O followed by extraction with dichloromethane (2x30 mL). The combined organic layers were washed with brine (2x25 mL), dried over Na_2SO_4 , filtrated and the solvent was removed under reduced pressure. The brownish viscous liquid was purified by bulb-to-bulb distillation (0.091 mbar, $90^\circ C$).

Yield: 20 mg (0.143 mmol, 3 %) pale yellow liquid.

Method B:

In a 50 mL Schlenk tube, heat dried under vacuum and flushed with N_2 , 42 mL (4.38 mmol, 1.0 eq) 2-thiophenemethanol (**104**) were dissolved in 10 mL of dry THF. At $0^\circ C$, 1.15 g (4.38 g, 1.0 eq) PPh_3 and 0.68 mL (4.38 mmol, 1.0 eq) DEAD were added. After stirring for 20 min a solution of 0.94 mL (4.38 mmol, 1.0 eq) DPPA in 3 mL dry THF was added portionwise followed by stirring at $0^\circ C$ for 1 h. Subsequently, the yellow

solution was allowed to warm up to rt and stirred for another 15 h until GC-MS control indicated complete conversion. The solvent of the greenish solution was evaporated under reduced pressure and the residue was purified by bulb-to-bulb distillation (0.087 mbar, 80-85°C).

Yield: 76 mg (0.546 mmol, 13 %), pale yellow liquid.

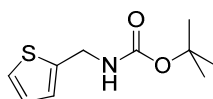
R_f = 0.41 (cyclohexane).

B.p. = 80°C (0.087 mbar).

$^1\text{H-NMR}$ (300 MHz, CDCl_3): δ = 7.32 (dd, 3J = 4.8 Hz, 4J = 1.2 Hz, 1H, CH-S), 7.08-7.00 (m, 2H, 2x CH_{Ar}), 4.50 (s, 2H, CH_2).

GC-MS (JR_50_S): t_R = 4.32 min, m/z = 139 (10 %), 110 (100 %).

***tert*-Butyl *N*-(thiophen-2-ylmethyl)carbamate (102)**



$\text{C}_{10}\text{H}_{15}\text{NO}_2\text{S}$

[213.30]

In a 50 mL round-bottom flask 237 mg (2.24 mmol, 2.5 eq) sodium carbonate were dissolved in 2 mL H_2O and 92 μL (0.89 mmol, 1.0 eq) 2-aminomethylthiophene (**95**) were added. At 0°C, 2 mL 1,4-dioxane and 314 mg (1.44 mmol, 1.6 eq) di-*tert*-butyl-dicarbonate were added to the reaction mixture and it was stirred for 2 h until TLC indicated complete conversion. The crude product was concentrated under reduced pressure. The residue was diluted with 10 mL dichloromethane and 10 mL H_2O and the aqueous layer was extracted with dichloromethane (3x10 mL). The combined organic layers were extracted with 1 M HCl (3x10 mL), dried over Na_2SO_4 , filtrated and the solvent was evaporated under reduced pressure. The crude colorless oil was purified by flash chromatography (20 g silica gel, cyclohexane/ethyl acetate 4:1).

Yield: 187 mg (0.46 mmol, 98 %) colorless solid.

R_f = 0.43 (cyclohexane/ethyl acetate 4:1).

M.p. = 47°C.

$^1\text{H-NMR}$ (300 MHz, CDCl_3): δ = 7.21 (dd, 3J = 4.2 Hz, 3J = 6.3 Hz, 1H, Ar-H), 6.98-6.91 (m, 2H, 2x Ar-H), 4.88 (bs, 1H, NH), 4.48 (d, 3J = 3.3 Hz, 2H, $\text{CH}_2\text{-N}$), 1.46 (s, 9H, ^tBu).

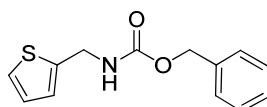
$^{13}\text{C-NMR}$ (75 MHz, CDCl_3): δ = 155.49 (C_q , C=O), 141.90 (C_q , C_{Ar}), 126.77 (CH, C_{Ar}), 125.44 (CH, C_{Ar}), 124.91 (CH, C_{Ar}), 79.73 (C_q , ^tBu), 39.56 ($\text{CH}_2\text{-N}$), 28.37 (3x CH_3 , ^tBu).

IR (neat): ν_{max} = 3320 (m), 2983 (w), 2938 (w), 1680 (s), 1533 (s), 1363 (m), 1291 (s), 1251 (s), 1167 (s), 1128 (m), 914 (m), 850 (m), 710 (s), 694 (s), 686 (s), 644 (s).

GC-MS (JR_50_S): t_R = 5.82 min, m/z = 213 (2 %), 97 (100 %).

HPLC-ESI-MS (Method G): t_R = 6.47 min. The product **102** did not ionize in HPLC-MS neither in ESI positive mode nor in ESI negative mode.

Benzyl *N*-(thiophen-2-ylmethyl)carbamate (**103**)



$\text{C}_{13}\text{H}_{13}\text{NO}_2\text{S}$

[247.31]

In a 50 mL round-bottom flask 3.93 g (36 mmol, 2.3 eq) sodium carbonate were dissolved in 92 mL H_2O and 2.0 mL (16 mmol, 1.0 eq) 2-aminomethylthiophene (**95**) were added. At 0°C, 91 mL 1,4-dioxane and 4.8 mL (23 mmol, 1.4 eq) benzyl chloroformate were added to the reaction mixture and it was stirred for 1 h until TLC indicated complete conversion. The solvents were evaporated and the residue was

diluted with 60 mL dichloromethane and 60 mL H₂O. The aqueous layer was extracted with dichloromethane (3x15 mL). The combined organic layers were extracted with 1 M HCl (3x15 mL), dried over Na₂SO₄, filtrated and the product **103** was concentrated under reduced pressure.

Yield: 4.79 g (19 mmol, quantitative) colorless solid.

R_f = 0.64 (cyclohexane/ethyl acetate 2:1).

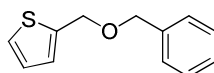
M.p. = 33-36°C.

¹H-NMR (300 MHz, CDCl₃): δ = 7.30-7.22 (m, 5H, 5x Ar-H), 7.13 (dd, ³J = 4.5 Hz, ³J = 4.8 Hz, 1H, Ar-H), 6.90-6.81 (m, 2H, 2x Ar-H), 5.19 (bs, 1H, NH), 5.04 (s, 2H, CH₂-O), 4.44 (d, ³J = 5.7 Hz, 2H, CH₂-N).

¹³C-NMR (75 MHz, CDCl₃): δ = 156.03 (C_q, C=O), 141.16 (C_q, C_{Ar}), 136.27 (C_q, C_{Ar}), 128.42 (CH, C_{Ar}), 128.06 (CH, C_{Ar}), 128.02 (CH, C_{Ar}), 126.77 (CH, C_{Ar}), 125.67 (CH, C_{Ar}), 125.02 (CH, C_{Ar}), 66.83 (CH₂-O), 39.81 (CH₂-N).

GC-MS (JR_50_S): t_R = 7.38 min, m/z = 156 (100 %).

2-((Benzyloxy)methyl)thiophene (**105**)



C₁₂H₁₂OS

[204.29]

In a 50 mL Schlenk tube, heat dried under vacuum and flushed with N₂, 1.21 mL (11.4 mmol, 1.0 eq) 2-thiophenemethanol (**104**) were dissolved in 9 mL dry THF. At 0°C, 688 mg (17.2 mmol, 1.5 eq) sodium hydride (60 % dispersion) were added portionwise. The yellow suspension was allowed to warm up to rt under stirring for 20 min. Subsequently, 4.2 mL (17.1 mmol, 1.5 eq) benzyl bromide were added dropwise at 0°C

followed by stirring at rt for 3 h. As GC-MS control indicated full conversion 10 mL methanol were added to the white suspension. After evaporation of the solvents under reduced pressure the residue was diluted with 15 mL dichloromethane, 15 mL H₂O and 2 mL saturated aqueous NaHCO₃ solution and extracted with dichloromethane (3x7 mL). The combined organic layers were dried over Na₂SO₄, filtrated and the product **105** was concentrated under reduced pressure. The crude yellow oil was purified by flash chromatography (100 g silica gel, cyclohexane, then cyclohexane/ethyl acetate 50:1).

Yield: 2.31 g (11.3 mmol, 99 %) colorless liquid.

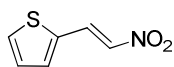
R_f = 0.25 (cyclohexane/ethyl acetate 50:1).

¹H-NMR (300 MHz, CDCl₃): δ = 7.40-7.34 (m, 4H, 4x Ar-H), 7.33-7.27 (m, 2H, 2x Ar-H), 7.03-6.96 (m, 2H, 2x Ar-H), 4.72 (s, 2H, CH₂), 4.57 (s, 2H, CH₂).

¹³C-NMR (75MHz, CDCl₃): δ = 141.02 (C_q), 137.94 (C_q), 128.42 (2x CH), 127.71 (2x CH), 126.63 (CH), 126.47 (CH), 125.84 (CH), 71.67 (CH₂), 66.45 (CH₂).

GC-MS (JR_50_S): t_R = 6.21 min, m/z = 204 (2 %), 97 (100 %).

2-((E)-2-Nitroethenyl)thiophene (**107**)



C₆H₅NO₂S

[155.17]

In a 250 mL two-necked round-bottom flask, heat dried under vacuum and flushed with N₂, 2.0 mL (22.3 mmol, 1.0 eq) 2-thiophencarbaldehyde (**106**) and 1.2 mL (22.3 mmol, 1.0 eq) nitromethane were dissolved in 5 mL methanol. To the colorless solution 1.09 g (26.8 mmol, 1.2 eq) NaOH, dissolved in 1.5 mL H₂O, were added dropwise at 0°C. The yellow solution was diluted with 2.5 mL methanol and stirred at 0°C for 2.5 h. TLC control was difficult due to nearly similar R_f-values. After the reaction seemed to be complete according to TLC analysis, the yellow solution was diluted with 15 mL H₂O and

the reaction mixture (pH 12) was poured into a solution of 10 mL HCl conc. in 15 mL H₂O (pH 1) and stirred for 30 min. Subsequently, this mixture was extracted with dichloromethane (3x10 mL), dried over MgSO₄, filtrated and the solvent was evaporated under reduced pressure. The brown solid was recrystallized from 5 mL ethanol.

Yield: 1.76 g (11.4 mmol, 51 %) brownish crystals.

R_f = 0.77 (cyclohexane/ethyl acetate 2:1).

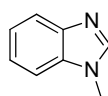
M.p. = 70°C. (lit. 78-79°C) [90]

¹H-NMR (300 MHz, CDCl₃): δ = 8.15 (d, ³J = 13.2 Hz, 1H, CH=CH-NO₂), 7.57 (d, ³J = 5.1 Hz, 1H, Ar-H), 7.52-7.43 (m, 2H, 1x Ar-H, 1x CH-NO₂), 7.15 (dd, ³J = 5.1 Hz, ³J = 5.1 Hz, 1H, Ar-H).

¹³C-NMR (75 MHz, CDCl₃): δ = 135.38 (CH-db), 134.57 (CH-db), 133.77 (C_q, C_{Ar}), 132.05 (CH, C_{Ar}), 131.57 (CH, C_{Ar}), 128.85 (CH, C_{Ar}).

6.2.5 Other heteroarenes

1-Methyl-1H-1,3-benzodiazole (129)



[132.16]

In a 15 mL Schlenk tube, heat dried under vacuum and flushed with N₂, 1.17 g (9.91 mmol, 1.00 eq) benzimidazole (**128**) were dissolved in 4 mL of dry THF. While stirring at 0°C, 608 mg (15.21 mmol, 1.53 eq) sodium hydride (60 % dispersion) were added carefully and the suspension was allowed to warm up to rt within 30 min. Again at 0°C, 0.90 mL (14.39 mmol, 1.45 eq) methyl iodide were added dropwise. After stirring the white suspension at rt for 3 h TLC indicated complete conversion. The reaction mixture was poured into ice cold water in one portion. The mixture was extracted with

ethyl acetate (3x30 mL). The combined organic layers were washed with brine (3x50 mL), dried over Na₂SO₄, filtrated and then the solvent was removed under reduced pressure. The crude product **129** was purified by flash chromatography (35 g silica gel, cyclohexane/ethyl acetate 3:1, 2:1, 1:1, then ethyl acetate).

Yield: 1.11 g (8.40 mmol, 85 %) beige solid.

R_f = 0.09 (ethyl acetate).

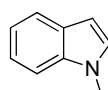
M.p. = 50°C. (lit. 57-60°C)^[105]

¹H-NMR (300 MHz, CDCl₃): δ = 7.89 (bs, 1H, Ar-H), 7.80 (dd, ³J = 6.0 Hz, ⁴J = 1.8 Hz, 1H, Ar-H), 7.40 (dd, ³J = 6.3 Hz, ⁴J = 2.1 Hz, 1H, Ar-H), 7.36-7.28 (m, 2H, 2x Ar-H), 3.84 (s, 3H, CH₃).

¹³C-NMR (75 MHz, CDCl₃): δ = 143.58 (C_q, C_{Ar}), 143.50 (CH, C_{Ar}), 134.53 (C_q, C_{Ar}), 123.00 (CH, C_{Ar}), 122.17 (CH, C_{Ar}), 120.25 (CH, C_{Ar}), 109.37 (CH, C_{Ar}), 31.05 (CH₃-N).

GC-MS (JR_50_S): t_R = 5.50 min, m/z = 132 (100 %).

1-Methyl-1H-indole (132)



C₉H₉N

[131.17]

In a 15 mL Schlenk tube, heat dried under vacuum and flushed with N₂, 1.17 g (10.02 mmol, 1.00 eq) indole (**131**) were dissolved in 3 mL dry THF. At 0°C, 606 mg (15.16 mmol, 1.52 eq) sodium hydride (60 % dispersion) were added carefully under stirring. The white suspension was stirred at rt for 20 min followed by dropwise addition of 0.90 mL (14.39 mmol, 1.44 eq) methyl iodide at 0°C. The white suspension was stirred at rt for 4 h followed by addition of another 2 mL dry THF. After stirring for

24 h, TLC and GC-MS control indicated complete conversion. The white suspension was poured onto ice cold H₂O in one portion. The mixture was extracted with ethyl acetate (4x30 mL). The combined organic layers were washed with brine (2x50 mL), dried over Na₂SO₄, filtrated and the crude product **132** was concentrated under reduced pressure. Purification was accomplished by flash chromatography (28 g silica gel, cyclohexane/ethyl acetate 4:1).

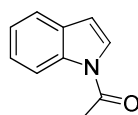
Yield: 860 mg (6.56 mmol, 66 %) orange liquid.

R_f = 0.89 (cyclohexane/ethyl acetate 4:1).

¹H-NMR (300 MHz, CDCl₃): δ = 7.66 (d, ³J = 7.8 Hz, 1H, Ar-H), 7.35 (d, ³J = 8.1 Hz, 1H, Ar-H), 7.25 (dt, ³J = 6.9 Hz, ⁴J = 0.9 Hz, 1H, Ar-H), 7.14 (t, ³J = 6.9 Hz, 1H, Ar-H), 7.07 (d, ³J = 2.7 Hz, 1H, Ar-H), 6.51 (d, ³J = 3.0 Hz, 1H, Ar-H), 3.81 (s, 3H, CH₃).

GC-MS (JR_50_S): t_R = 4.96 min, m/z = 131 (100 %).

1-Acetyl-1H-indole (170)



C₁₀H₉NO

[159.18]

In a 500 mL Schlenk tube, heat dried under vacuum and flushed with N₂, 1.02 g (8.7 mmol, 1.0 eq) indole (**130**) and 203 mg (1.7 mmol, 0.2 eq) DMAP were dissolved in 20 mL dry 1,2-dichloroethane. Subsequently, 1.80 mL (12.9 mmol, 1.5 eq) dry triethylamine and 1.60 mL (16.9 mmol, 1.9 eq) acetic anhydride were added and the yellow solution was stirred at 80°C for 12 h. When GC-MS control indicated complete conversion, the reaction mixture was diluted with ethyl acetate (50 mL) and saturated, aqueous ammonium chloride (40 mL). The aqueous layer was extracted with ethyl acetate (3x20 mL). The combined organic layers were dried over MgSO₄, filtrated and

the crude product **170** was concentrated under reduced pressure. Purification was accomplished by flash chromatography (60 g silica gel, cyclohexane/ethyl acetate 9:1).

Yield: 1.38 g (8.7 mmol, quantitative) pale yellow liquid.

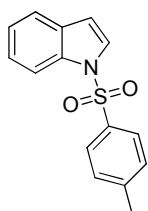
R_f = 0.32 (cyclohexane/ethyl acetate 85:15).

$^1\text{H-NMR}$ (300 MHz, CDCl_3): δ = 8.36 (d, 3J = 8.1 Hz, 1H, Ar-H), 7.49 (d, 3J = 7.8 Hz, 1H, Ar-H), 7.34 (d, 3J = 3.6 Hz, 1H, Ar-H), 7.28 (dt, 3J = 7.2 Hz, 4J = 1.2 Hz, 1H, Ar-H), 7.19 (dt, 3J = 7.5 Hz, 4J = 0.9 Hz, 1H, Ar-H), 6.56 (d, 3J = 3.6 Hz, 1H, Ar-H), 3.56 (s, 3H, CH_3).

$^{13}\text{C-NMR}$ (75 MHz, CDCl_3): δ = 168.83 (C_q , C=O), 135.75 (C_q , C_{Ar}), 130.62 (C_q , C_{Ar}), 125.42 (CH , C_{Ar}), 125.32 (CH , C_{Ar}), 123.56 (CH , C_{Ar}), 121.04 (CH , C_{Ar}), 116.74 (CH , C_{Ar}), 109.36 (CH , C_{Ar}), 24.17 (CH_3).

GC-MS (JR_50_S): t_R = 5.78 min, m/z = 159 (30 %), 117 (100 %).

1-((4-Methylphenyl)sulfonyl)-1H-indole (**171**)



$\text{C}_{15}\text{H}_{13}\text{NO}_2\text{S}$

[271.33]

In a 500 mL Schlenk tube, heat dried under vacuum and flushed with N_2 , 1.02 g (8.7 mmol, 1.0 eq) indole (**130**) and 214 mg (1.7 mmol, 0.2 eq) DMAP were dissolved in 20 mL dry dichloromethane. Subsequently, 2.5 mL (18.3 mmol, 2.1 eq) dry triethylamine and 1.71 g (12.9 mmol, 1.5 eq) *para*-toluenesulfonyl chloride were added and the yellow solution was stirred at rt for 18 h. When GC-MS control indicated full conversion, the reaction mixture was diluted with ethyl acetate (50 mL) and saturated, aqueous ammonium chloride solution (40 mL). The aqueous layer was extracted with ethyl acetate (3x20 mL). The combined organic layers were dried over MgSO_4 , filtrated and

the crude product **171** was concentrated under reduced pressure. Purification was accomplished by flash chromatography (30 g silica gel, cyclohexane/ethyl acetate 99:1).

Yield: 2.18 g (8.0 mmol, 92 %) colorless solid.

R_f = 0.41 (cyclohexane/ethyl acetate 9:1).

M.p. = 82-83°C. (lit. 85-86°C)^[104]

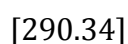
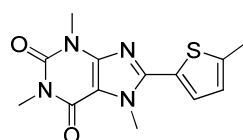
¹H-NMR (300 MHz, CDCl₃): δ = 7.97 (d, 3J = 8.1 Hz, 1H, Ar-H), 7.74 (d, 3J = 8.4 Hz, 1H, Ar-H), 7.55 (d, 3J = 3.9 Hz, 1H, Ar-H), 7.50 (d, 3J = 7.8 Hz, 1H, Ar-H), 7.29 (dt, 3J = 7.2 Hz, 4J = 0.9 Hz, 1H, Ar-H), 7.24-7.15 (m, 4H, 4x Ar-H), 6.63 (d, 3J = 3.3 Hz, 1H, Ar-H), 2.31 (s, 3H, CH₃).

¹³C-NMR (75 MHz, CDCl₃): δ = 145.11 (C_q, C_{Ar}), 135.54 (C_q, C_{Ar}), 135.03 (C_q, C_{Ar}), 130.95 (C_q, C_{Ar}), 130.06 (CH, 2x C_{Ar}), 127.01 (CH, 2x C_{Ar}), 126.54 (CH, C_{Ar}), 124.74 (CH, C_{Ar}), 123.46 (CH, C_{Ar}), 121.56 (CH, C_{Ar}), 113.74 (CH, C_{Ar}), 109.22 (CH, C_{Ar}), 21.75 (CH₃).

GC-MS (JR_50_S): t_R = 7.80 min, m/z = 271 (47 %), 91 (100 %).

6.2.6 Cross-coupling

1,3,7-Trimethyl-8-(5-methylthiophen-2-yl)-2,3,6,7-tetrahydro-1H-purine-2,6-dione (**79**)



In a 20 mL Schlenk tube, heat dried under vacuum and flushed with N₂, 2.8 mg (0.0125 mmol, 0.025 eq) palladium acetate, 150 mg (0.75 mmol, 1.50 eq) copper acetate monohydrate and 97.1 mg (0.50 mmol, 1.00 eq) caffeine (**77**) were suspended in 0.6 mL

dry 1,4-dioxane. After addition of 40.8 μL (0.50 mmol, 1.00 eq) pyridine the blue suspension was degassed in three vacuum- N_2 cycles. 145 μL (1.50 mmol, 3.00 eq) 2-methylthiophene (**84**) were added and the reaction mixture was heated at 120°C for 24 h until GC-MS control indicated complete conversion. The green-black suspension was filtrated through a pad of celite and a pad of silica gel and rinsed with dichloromethane (17 mL). After evaporation of the solvent under reduced pressure the light green solid was purified by flash chromatography (6 g silica gel, dichloromethane/acetone 30:1).

Yield: 133 mg (0.46 mmol, 92 %) light yellow powder.

R_f = 0.29 (dichloromethane/acetone 30:1).

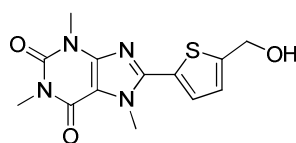
M.p. = 188-190°C. (lit. 185-188°C)^[53]

$^1\text{H-NMR}$ (300 MHz, CDCl_3): δ = 7.38 (d, 3J = 3.6 Hz, 1H, Ar-H), 6.84 (dd, 3J = 3.6 Hz, 4J = 0.9 Hz, 1H, Ar-H), 4.16 (s, 3H, CH_3), 3.60 (s, 3H, CH_3), 3.41 (s, 3H, CH_3), 2.56 (s, 3H, CH_3).

$^{13}\text{C-NMR}$ (75 MHz, CDCl_3): δ = 155.30 (C_q , C=O), 151.60 (C_q , C=O), 148.22 (C_q), 146.82 (C_q), 144.61 (C_q), 128.91 (CH, C_{Ar}), 128.14 (C_q), 126.49 (CH, C_{Ar}), 108.13 (C_q), 33.64 (CH_3 -N), 29.79 (CH_3 -N), 27.86 (CH_3 -N), 15.30 (CH_3).

GC-MS (JR_50_S): t_R = 9.47 min, m/z = 290 (100 %).

8-(5-(Hydroxymethyl)thiophen-2-yl)-1,3,7-trimethyl-2,3,6,7-tetrahydro-1H-purine-2,6-dione (109)



[306.34]

$\text{C}_{13}\text{H}_{14}\text{N}_4\text{O}_3\text{S}$

In a 10 mL Schlenk tube, heat dried under vacuum and flushed with N₂, 50.3 mg (0.259 mmol, 1.00 eq) caffeine (**77**), 5.5 mg (0.056 mmol, 0.22 eq) CuCl, 1.5 mg (0.006 mmol, 0.02 eq) palladium acetate and 77.8 mg (0.389 mmol, 1.50 eq) copper acetate monohydrate were suspended in 0.45 mL dry 1,4-dioxane and 20 μ L (0.259 mmol, 1.00 eq) pyridine. After 10 min stirring at rt 0.11 mL (0.770 mmol, 2.97 eq) 2-thiophenemethanol (**104**) were added and the green suspension was stirred at 120°C for 19 h. As HPLC-MS indicated complete conversion the reaction mixture was deluted with 30 mL dichloromethane, filtrated through a pad of celite and rinsed with dichloromethane (4x25 mL). After evaporation of the solvent the crude product **109** was purified by flash chromatography (26 g silica gel, dichloromethane).

Yield: 50 mg (0.163 mmol, 63 %) colorless solid.

R_f = 0.62 (dichloromethane/acetone 2:1).

M.p. = 220°C.

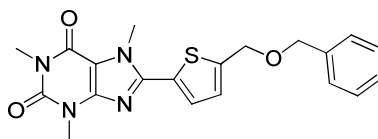
¹H-NMR (300 MHz, CDCl₃): δ = 7.49 (d, ³J = 3.9 Hz, 1H, Ar-H), 7.08 (d, ³J = 3.9 Hz, 1H, Ar-H), 4.91 (s, 2H, CH₂), 4.20 (s, 3H, CH₃-N), 3.62 (s, 3H, CH₃-N), 3.43 (s, 3H, CH₃-N).

IR (neat): ν_{\max} = 3405 (w), 2925 (w), 1684 (m), 1647 (s), 1538 (m), 1505 (w), 1452 (m), 1414 (w), 1359 (m), 1224 (m), 1164 (m), 1048 (m), 1029 (s), 1006 (m), 973 (m), 827 (w), 758 (s), 744 (s), 680 (m).

HPLC-ESI-MS (Method G): t_R = 4.07 min, [M+H]⁺ = 307.

HRMS (TOF MS LD⁺): *m/z* calculated for C₁₃H₁₅N₄O₃S⁺[M+H]⁺: 307.0865, found 307.0884.

8-(5-((Benzyloxy)methyl)thiophen-2-yl)-1,3,7-trimethyl-2,3,6,7-tetrahydro-1H-purine-2,6-dione (110)



C₂₀H₂₀N₄O₃S

[396.46]

In a 10 mL Schlenk tube, heat dried under vacuum and flushed with N₂, 202 mg (1.040 mmol, 1.00 eq) caffeine (**77**), 5.2 mg (0.023 mmol, 0.02 eq) palladium acetate and 311 mg (1.555 mmol, 1.50 eq) copper acetate monohydrate were suspended in 2.0 mL dry 1,4-dioxane and 80 μ L (1.040 mmol, 1.00 eq) pyridine. After stirring at rt for 10 min 637 mg (3.117 mmol, 3.00 eq) 2-((benzyloxy)methyl)thiophene (**105**) were added and the dark green suspension was stirred at 120°C for 1 d. After HPLC-MS control indicated full conversion the mixture was filtrated through a pad of celite and rinsed with methanol (8x20 mL). The precipitating product **110** was collected from the blue filtrate by filtration under reduced pressure and washed with methanol (3x5 mL). The colorless solid was dried under high vacuum.

Yield: 367 mg (0.926 mmol, 89 %) colorless solid.

R_f = 0.27 (dichloromethane/acetone 5:1).

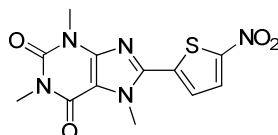
M.p. = 142-143°C.

¹H-NMR (300 MHz, CDCl₃): δ = 7.44 (d, ³J = 3.6 Hz, 1H, Ar-H), 7.40-7.25 (m, 5H, 5x Ar-H), 7.04 (d, ³J = 3.6 Hz, 1H, Ar-H), 4.72 (s, 2H, CH₂-O), 4.59 (s, 2H, CH₂-O), 4.17 (s, 3H, CH₃-N), 3.59 (s, 3H, CH₃-N), 3.40 (s, 3H, CH₃-N).

¹³C-NMR (75 MHz, CDCl₃): δ = 155.57 (C_q, C=O), 151.83 (C_q, C=O), 148.34 (C_q), 146.65 (C_q), 145.90 (C_q), 137.69 (C_q, C_{Ar}), 130.65 (C_q, C_{Ar}), 128.73 (2x CH, 2x C_{Ar}), 128.70 (CH, C_{Ar}), 128.14 (CH, C_{Ar}), 128.06 (2x CH, 2x C_{Ar}), 126.97 (CH, C_{Ar}), 108.52 (C_q), 72.44 (CH₂-O), 66.58 (CH₂-O), 33.84 (CH₃-N), 30.03 (CH₃-N), 28.18 (CH₃-N).

HPLC-ESI-MS (Method G): $t_R = 6.85$ min, $[M+H]^+ = 397$, $[M+Na]^+ = 419$, $[M+K]^+ = 435$.

1,3,7-Trimethyl-8-(5-nitrothiophen-2-yl)-2,3,6,7-tetrahydro-1H-purine-2,6-dione (113)



[321.31]

In a 20 mL Schlenk tube, heat dried under vacuum and flushed with N_2 , 11.2 mg (0.05 mmol, 0.025 eq) palladium acetate, 600 mg (3.00 mmol, 1.50 eq) copper acetate monohydrate and 389 mg (2.00 mmol, 1.00 eq) caffeine (**77**) were suspended in 2.4 mL dry 1,4-dioxane. After addition of 0.16 mL (2.00 mmol, 1.00 eq) pyridine the blue suspension was degassed in five vacuum- N_2 cycles. 775 mg (6.00 mmol, 3.00 eq) 2-nitrothiophene (**96**) (85 % pure, contains 15 % 3-nitrothiophene) were added and the reaction mixture was heated at $120^\circ C$ for 19 h. GC-MS control was not sufficient as the product **113** was not detectable on GC-MS. TLC indicated incomplete conversion. Therefore, the black suspension was stirred at $120^\circ C$ for further 6 d. Since TLC control still indicated incomplete conversion and a metal mirror on the Schlenk tube wall already occurred, the reaction mixture was filtrated through a pad of celite and flushed with dichloromethane (15x5 mL). After evaporation of the solvent, the black solid was purified by flash chromatography (80 g silica gel, dichloromethane/acetone 9:1).

Yield: 160 mg (0.50 mmol, 25 %) red-brownish powder.

$R_f = 0.53$ (dichloromethane/acetone 9:1).

M.p. = $287^\circ C$.

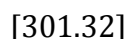
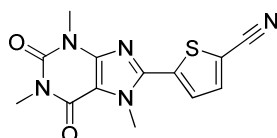
1H -NMR (300 MHz, $DMSO-d_6$): $\delta = 8.24$ (d, $^3J = 4.2$ Hz, 1H, Ar-H), 7.81 (d, $^3J = 4.5$ Hz, 1H, Ar-H), 4.21 (s, 3H, CH_3-N), 3.45 (s, 3H, CH_3-N), 3.25 (s, 3H, CH_3-N).

At rt the product **113** was only poorly soluble in CDCl_3 , CD_3CN , acetone- d_6 and DMSO- d_6 . Therefore, no ^{13}C -NMR could be measured. The product **113** was also not detectable via GC-MS.

HPLC-ESI-MS (Method G): $t_R = 5.90$ min, $[\text{M}+\text{H}]^+ = 322$.

HRMS (TOF MS LD^+): m/z calculated for $\text{C}_{12}\text{H}_{12}\text{N}_5\text{O}_4\text{S}^+$ $[\text{M}+\text{H}]^+$: 322.0610, found 322.0632.

5-(1,3,7-Trimethyl-2,6-dioxo-2,3,6,7-tetrahydro-1H-purin-8-yl)thiophene-2-carbonitrile (**114**)



In a 10 mL Schlenk tube, heat dried under vacuum and flushed with N_2 , 1.6 mg (0.006 mmol, 0.01 eq) palladium acetate, 154 mg (0.772 mmol, 1.50 eq) copper acetate monohydrate and 101 mg (0.516 mmol, 1.00 eq) caffeine (**77**) were suspended in 1.0 mL dry 1,4-dioxane. After addition of 42 μL (0.516 mmol, 1.00 eq) pyridine the blue suspension was degassed in three vacuum- N_2 cycles. 143 μL (1.545 mmol, 3.00 eq) 2-thiophencarbonitrile (**82**) were added and the reaction mixture was stirred at 120°C for 20 h. Although TLC indicated incomplete conversion, the greenish solution was filtrated through a pad of celite and flushed with dichloromethane (5x5 mL). After evaporation of the solvent under reduced pressure the green solid was purified by flash chromatography (18 g silica gel, dichloromethane/acetone 15:1).

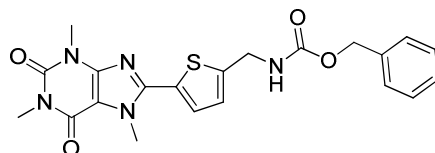
Yield: 79 mg (0.26 mmol, 50 %) yellow solid.

$R_f = 0.56$ (dichloromethane/acetone 15:1).

M.p. = 268°C . (lit. $298\text{-}301^\circ\text{C}$)^[53]

$^1\text{H-NMR}$ (300 MHz, DMSO-d_6): δ = 7.67 (d, 3J = 4.2 Hz, 1H, Ar-H), 7.54 (d, 3J = 4.2 Hz, 1H, Ar-H), 4.24 (s, 3H, $\text{CH}_3\text{-N}$), 3.60 (s, 3H, $\text{CH}_3\text{-N}$), 3.42 (s, 3H, $\text{CH}_3\text{-N}$).

Benzyl *N*-((5-(1,3,7-trimethyl-2,6-dioxo-2,3,6,7-tetrahydro-1*H*-purin-8-yl)thiophen-2-yl)methyl)carbamate (116)



$\text{C}_{21}\text{H}_{21}\text{N}_5\text{O}_4\text{S}$

[439.49]

In a 50 mL Schlenk tube, heat dried under vacuum and flushed with N_2 , 30 mg (0.14 mmol, 0.02 eq) palladium acetate, 1.70 g (8.51 mmol, 1.50 eq) copper acetate monohydrate, 0.10 g (0.55 mmol, 0.1 eq) 1,10-phenanthroline and 1.10 g (5.66 mmol, 1.00 eq) caffeine (**77**) were suspended in 8 mL dry 1,4-dioxane. After addition of 0.5 mL (6.19 mmol, 1.00 eq) pyridine the blue suspension was degassed in three vacuum- N_2 cycles. 4.25 g (17.18 mmol, 3.00 eq) benzyl (thiophen-2-ylmethyl)carbamate (**103**) were added and the reaction mixture was stirred at 120°C for 20 h until TLC control indicated complete conversion. The suspension was filtrated through a pad of celite and rinsed with dichloromethane (40 mL). After evaporation of the solvent under reduced pressure, the green solid was purified by flash chromatography (400 g silica gel, cyclohexane/ethyl acetate 1:2 up to ethyl acetate/methanol 2:1).

Yield: 2.16 g (4.92 mmol, 87 %) pale yellow solid.

R_f = 0.65 (cyclohexane/ethyl acetate 2:1).

M.p. = $140\text{-}142^\circ\text{C}$.

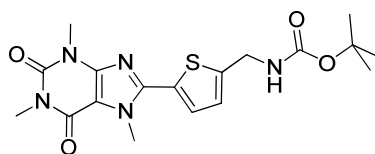
$^1\text{H-NMR}$ (300 MHz, CDCl_3): δ = 7.41 (d, 3J = 3.6 Hz, 1H, Ar-H), 7.39-7.32 (m, 5H, 5x Ar-H), 7.04 (d, 3J = 5.1 Hz, 1H, Ar-H), 5.26 (bs, 1H, NH), 5.15 (s, 2H, $\text{CH}_2\text{-O}$), 4.59 (d, 3J = 6.0 Hz, 2H, $\text{CH}_2\text{-N}$), 4.16 (s, 3H, $\text{CH}_3\text{-N}$), 3.60 (s, 3H, $\text{CH}_3\text{-N}$), 3.42 (s, 3H, $\text{CH}_3\text{-N}$).

^{13}C -NMR (75 MHz, CDCl_3): δ = 156.21 (C_q , C=O), 155.35 (C_q , C=O), 151.61 (C_q , C=O), 148.12 (C_q), 146.26 (C_q), 145.96 (C_q), 136.14 (C_q , C_{Ar}), 130.07 (C_q , C_{Ar}), 128.56 (2x CH, 2x C_{Ar}), 128.48 (CH, C_{Ar}), 128.28 (CH, C_{Ar}), 128.18 (2x CH, 2x C_{Ar}), 126.46 (CH, C_{Ar}), 108.33 (C_q), 67.20 ($\text{CH}_2\text{-O}$), 39.98 ($\text{CH}_2\text{-N}$), 33.61 ($\text{CH}_3\text{-N}$), 29.79 ($\text{CH}_3\text{-N}$), 27.98 ($\text{CH}_3\text{-N}$).

HPLC-ESI-MS (Method G): t_{R} = 6.31 min, $[\text{M}+\text{H}]^+$ = 440, $[\text{M}+\text{Na}]^+$ = 462.

HRMS (TOF MS LD^+): m/z calculated for $\text{C}_{21}\text{H}_{22}\text{N}_5\text{O}_4\text{S}^+$ $[\text{M}+\text{H}]^+$: 440.1393, found 440.1384.

***tert*-Butyl *N*-((5-(1,3,7-trimethyl-2,6-dioxo-2,3,6,7-tetrahydro-1*H*-purin-8-yl)thiophen-2-yl)methyl)carbamate (117)**



$\text{C}_{18}\text{H}_{23}\text{N}_5\text{O}_4\text{S}$

[405.47]

In a 15 mL Schlenk tube, heat dried under vacuum and flushed with N_2 , 7 mg (0.03 mmol, 0.03 eq) palladium acetate, 385 mg (1.93 mmol, 1.51 eq) copper acetate monohydrate, 25 mg (0.26 mmol, 0.20 eq) CuCl and 249 mg (1.28 mmol, 1.00 eq) caffeine (**77**) were suspended in 2.2 mL dry 1,4-dioxane. After addition of 100 μL (1.30 mmol, 1.02 eq) pyridine the blue suspension was degassed in three vacuum- N_2 cycles. 822 mg (3.85 mmol, 3.00 eq) *tert*-butyl (thiophen-2-ylmethyl)carbamate (**102**) were added and the reaction mixture was stirred at 120°C for 20 h until TLC control indicated complete conversion. The suspension was diluted with 50 mL dichloromethane, filtrated through a pad of celite and rinsed with dichloromethane (4x20 mL). After evaporation of the solvent under reduced pressure the green solid was purified by filtration through a 2 cm pad of silica gel (dichloromethane/acetone 15:1).

Yield: 514 mg (1.27 mmol, 99 %) colorless solid.

$R_f = 0.13$ (dichloromethane/acetone 15:1).

M.p. = 169-170°C.

$^1\text{H-NMR}$ (300 MHz, CDCl_3): $\delta = 7.41$ (d, $^3J = 3.6$ Hz, 1H, Ar-H), 7.02 (d, $^3J = 3.6$ Hz, 1H, Ar-H), 5.00 (bs, 1H, NH), 4.52 (d, $^3J = 5.7$ Hz, 2H, $\text{CH}_2\text{-N}$), 4.17 (s, 3H, $\text{CH}_3\text{-N}$), 3.61 (s, 3H, $\text{CH}_3\text{-N}$), 3.42 (s, 3H, $\text{CH}_3\text{-N}$), 1.47 (s, 9H, ^tBu).

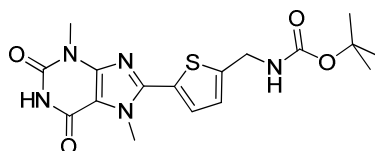
$^{13}\text{C-NMR}$ (75 MHz, CDCl_3): $\delta = 155.50$ (C_q , C=O, Boc), 155.36 (C_q , C=O, caffeine), 151.62 (C_q , C=O, caffeine), 148.12 (C_q , C_{Ar}), 146.81 (C_q , C_{Ar}), 146.38 (C_q , C_{Ar}), 129.74 (C_q , C_{Ar}), 128.57 (CH, C_{Ar}), 126.15 (CH, C_{Ar}), 108.32 (C_q , C_{Ar}), 80.18 (C_q , $\text{C}(\text{CH}_3)_3$), 39.61 ($\text{CH}_2\text{-N}$), 33.62 ($\text{CH}_3\text{-N}$), 29.82 ($\text{CH}_3\text{-N}$), 28.36 (3x CH_3 , ^tBu), 27.98 ($\text{CH}_3\text{-N}$).

IR (neat): $\nu_{\text{max}} = 3320$ (w), 2980 (w), 1694 (s), 1652 (s), 1537 (m), 1503 (m), 1450 (m), 1248 (m), 1163 (s), 745 (s).

HPLC-ESI-MS (Method G): $t_R = 6.53$ min, $[\text{M}+\text{H}]^+ = 406$, $[\text{M}+\text{Na}]^+ = 428$, $[\text{M}+\text{K}]^+ = 444$.

HRMS (TOF MS LD^+): m/z calculated for $\text{C}_{18}\text{H}_{24}\text{N}_5\text{O}_4\text{S}^+$ $[\text{M}+\text{H}]^+$: 406.1549, found 406.1559.

***tert*-Butyl *N*-((5-(3,7-dimethyl-2,6-dioxo-2,3,6,7-tetrahydro-1*H*-purin-8-yl)thiophen-2-yl)methyl)carbamate (135)**



$\text{C}_{17}\text{H}_{21}\text{N}_5\text{O}_4\text{S}$

[391.44]

In a 10 mL Schlenk tube, heat dried under vacuum and flushed with N_2 , 1.6 mg (0.006 mmol, 0.03 eq) palladium acetate, 77.0 mg (0.39 mmol, 1.50 eq) copper acetate monohydrate, 5.2 mg (0.05 mmol, 0.20 eq) CuCl and 47.5 mg (0.26 mmol, 1.00 eq) theobromine (**125**) were suspended in 0.5 mL dry 1,4-dioxane. After addition of 21 μL

(0.29 mmol, 1.00 eq) pyridine the blue suspension was degassed in three vacuum-N₂ cycles. 168 mg (0.79 mmol, 3.05 eq) *tert*-butyl (thiophen-2-ylmethyl)carbamate (**102**) were added and the reaction mixture was stirred at 120°C for 6 d until HPLC control indicated no further conversion. The suspension was filtrated through a pad of celite and rinsed with methanol (100 mL) and acetonitrile (50 mL). After evaporation of the solvent the green solid was purified by flash chromatography (5 g silica gel, dichloromethane/acetone 4:1).

Yield: 40 mg (0.10 mmol, 40 %) pale yellow solid.

R_f = 0.27 (dichloromethane/acetone 4:1).

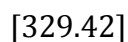
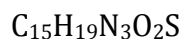
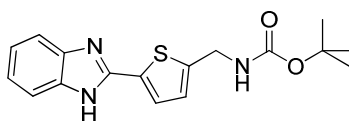
M.p. = 305°C (decomposition).

¹H-NMR (300 MHz, CDCl₃): δ = 7.76 (bs, 1H, NH), 7.42 (d, ³J = 3.9 Hz 1H, Ar-H), 7.03 (d, ³J = 3.9 Hz 1H, Ar-H), 4.99 (bs, 1H, NH), 4.52 (d, ³J = 5.4 Hz, 2H, CH₂), 4.15 (s, 3H, CH₃-N), 3.56 (s, 3H, CH₃-N), 1.48 (s, 9H, 3xCH₃).

¹³C-NMR (75 MHz, DMSO-d₆): δ = 155.64 (C_q), 154.87 (C_q), 150.78 (C_q), 149.05 (C_q), 147.90 (C_q, N-C_{Ar}-N), 145.70 (C_q, C_{Ar}), 128.97 (C_q, C_{thio}), 128.43 (CH, C_{thio}), 126.01 (CH, C_{thio}), 108.00 (C_q, C_{Ar}), 78.26 (C_q), 78.24 (CH₂), 39.50 (CH₃-N), 28.46 (CH₃-N), 28.20 (3xCH₃).

HPLC-ESI-MS (Method G): t_R = 5.36 min, [M+H]⁺ = 392, [M+Na]⁺ = 414, [M+K]⁺ = 430.

HRMS (TOF MS LD⁺): *m/z* calculated for C₁₇H₂₂N₅O₄S⁺ [M+H]⁺: 392.1393, found 392.1423.

***tert*-Butyl *N*-((5-(1*H*-1,3-benzodiazol-2-yl)thiophen-2-yl)methyl)carbamate (**139**)**

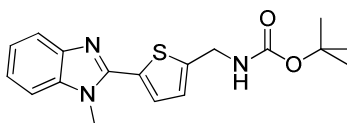
In a 10 mL Schlenk tube, heat dried under vacuum and flushed with N_2 , 30.6 mg (0.259 mmol, 1.00 eq) benzimidazole (**128**) were dissolved in 0.2 mL dry 1,4-dioxane. 1.4 mg (0.006 mmol, 0.02 eq) palladium acetate, 77.4 mg (0.388 mmol, 1.50 eq) copper acetate monohydrate, 5.6 mg (0.056 mmol, 0.22 eq) CuCl , 0.2 mL 1,4-dioxane and 20 μL (0.259 mmol, 1.00 eq) pyridine were added. After 30 min of stirring at rt, 165.4 mg (0.776 mmol, 3.00 eq) *tert*-butyl (thiophen-2-ylmethyl)carbamate (**102**) were added and the red suspension stirred at 120°C for 7 d. When HPLC-MS control showed no further conversion 0.40 mL DMF were added to the reaction mixture. After another 5 d of stirring at 120°C HPLC-MS monitoring indicated no further conversion. So the mixture was filtrated through a pad of celite and rinsed with dichloromethane (4x20 mL). After evaporation of the solvents under reduced pressure, the green residue was purified by flash chromatography (14 g silica gel, cyclohexane/ethyl acetate 3:1).

Yield: 11.7 mg (0.137 mmol, 38 %; 30 % pure from HPLC-MS) yellow liquid.

R_f = 0.17 (dichloromethane/acetone 9:1).

HPLC-ESI-MS (Method G): t_R = 5.53 min, $[\text{M}+\text{H}]^+$ = 330, $[\text{M}+\text{Na}]^+$ = 352, $[\text{M}+\text{K}]^+$ = 368.

Impurities: t_R = 3.36 min (51 %), 3.22 min (14 %), 2.63 min (5 %). No masses were detectable in ESI positive or negative mode.

***tert*-Butyl *N*-((5-(1-methyl-1*H*-1,3-benzodiazol-2-yl)thiophen-2-yl)methyl) carbamate (**140**)**C₁₈H₂₁N₃O₂S

[343.14]

In a 10 mL Schlenk tube, heat dried under vacuum and flushed with N₂, 34.8 mg (0.263 mmol, 1.00 eq) 1-methyl-benzimidazole (**129**) were dissolved in 0.2 mL dry 1,4-dioxane. 1.3 mg (0.006 mmol, 0.02 eq) palladium acetate, 77.8 mg (0.391 mmol, 1.49 eq) copper acetate monohydrate, 5.0 mg (0.050 mmol, 0.19 eq) CuCl, 0.2 mL 1,4-dioxane and 20 μL (0.263 mmol, 1.00 eq) pyridine were added. After stirring at rt for 30 min, 165.5 mg (0.776 mmol, 2.73 eq) *tert*-butyl (thiophen-2-ylmethyl)carbamate (**102**) were added and the blue suspension was stirred at 120°C for 5 d. As HPLC-MS control indicated nearly no consumption of 1-methyl-benzimidazole (**129**), 9.5 mg (0.053 mmol, 0.20 eq) 1,10-phenanthroline were added to the reaction mixture and it was stirred at 120°C for another 5 d. Because no further conversion occurred the brown reaction mixture was filtrated through a pad of celite and rinsed with dichloromethane (4x20 mL). After evaporation of the solvent under reduced pressure, the crude product was purified by flash chromatography (13 g silica gel, cyclohexane/ethyl acetate 20:1 up to 1:1).

Yield: 22.8 mg (0.066 mmol, 28 %) yellow solid.

R_f = 0.38 (cyclohexane/ethyl acetate 20:1).

M.p. = 125°C.

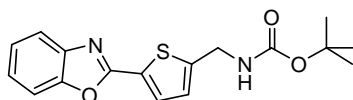
¹H-NMR (300 MHz, CDCl₃): δ = 7.80-7.75 (m, 1H, Ar-H), 7.44 (d, ³J = 3.6 Hz, 1H, Ar-H), 7.37-7.27 (m, 2H, 2x Ar-H), 7.02 (d, ³J = 3.3 Hz, 1H, Ar-H), 6.96-6.92 (m, 1H, Ar-H), 5.10 (bs, 1H, NH), 4.59 (d, ³J = 5.4 Hz, 2H, CH₂), 3.96 (s, 3H, CH₃-N), 1.47 (s, 9H, ^tBu).

^{13}C -NMR (75 MHz, CDCl_3): δ = 146.13 (C_q , C_{Ar}), 144.03 (C_q , C_{Ar}), 141.54 (C_q , C_{Ar}), 136.29 (C_q , C_{Ar}), 131.61 (C_q , C_{Ar}), 128.82 (CH , C_{Ar}), 126.42 (CH , C_{Ar}), 126.37 (CH , C_{Ar}), 124.02 (CH , C_{Ar}), 121.04 (CH , C_{Ar}), 109.81 (CH , C_{Ar}), 78.98 ($\text{C}(\text{CH}_3)_3$), 40.01 (CH_2), 31.82 (CH_3), 28.75 (^tBu).

HPLC-ESI-MS (Method G): t_{R} = 5.93 min, $[\text{M}+\text{H}]^+$ = 344, $[\text{M}+\text{Na}]^+$ = 366, $[\text{M}+\text{K}]^+$ = 382.

HRMS (TOF MS LD^+): m/z calculated for $\text{C}_{18}\text{H}_{22}\text{N}_3\text{O}_2\text{S}^+$ $[\text{M}+\text{H}]^+$: 344.1433, found 344.1417.

***tert*-Butyl *N*-((5-(1,3-benzoxazol-2-yl)thiophen-2-yl)methyl)carbamate (**143**)**



$\text{C}_{17}\text{H}_{18}\text{N}_2\text{O}_3\text{S}$

[330.40]

In a 10 mL Schlenk tube, heat dried under vacuum and flushed with N_2 , 77.8 mg (0.389 mmol, 1.51 eq) copper acetate monohydrate, 1.5 mg (0.006 mmol, 0.03 eq) palladium acetate, 29.5 mg (0.258 mmol, 1.00 eq) benzoxazole (**132**), 5.3 mg (0.052 mmol, 0.20 eq) CuCl and 21 μL (0.257 mmol, 1.00 eq) dry pyridine were suspended in 0.45 mL dry 1,4-dioxane. This suspension was stirred at rt for 10 min until 167 mg (0.783 mmol, 3.02 eq) *tert*-butyl (thiophen-2-ylmethyl)carbamate (**102**) were added. The blue suspension was stirred at 120°C for 6 d until HPLC control indicated no further conversion. The reaction mixture was allowed to cool down to rt. Subsequently, it was diluted with 15 mL methanol, filtrated through a pad of celite and rinsed with methanol (2x40 mL) and acetonitrile (2x5 mL). After evaporation of the solvents under reduced pressure, the green residue was purified by flash chromatography (7 g silica gel, cyclohexane/ethyl acetate 4:1).

Yield: 5 mg (0.015 mmol, 6 %), pale yellow solid.

R_f = 0.28 (cyclohexane/ethyl acetate 4:1).

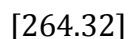
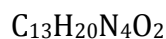
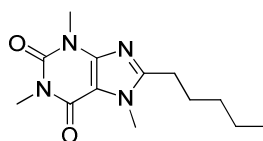
$^1\text{H-NMR}$ (300 MHz, CDCl_3): δ = 7.78-7.70 (m, 2H, 2x Ar- $\text{H}_{\text{benzoxazole}}$), 7.56-7.51 (m, 1H, Ar- H_{thio}) 7.36-7.31 (m, 2H, 2x Ar- $\text{H}_{\text{benzoxazole}}$), 7.02 (d, 3J = 3.6 Hz, 1H, Ar- H_{thio}), 5.01 (bs, 1H, NH), 4.54 (d, 3J = 5.7 Hz, $\text{CH}_2\text{-N}$), 1.48 (s, 9H, $t\text{Bu}$).

$^{13}\text{C-NMR}$ (75 MHz, CDCl_3): δ = 158.07 (C=O), 149.80 (C_q , C_{Ar}), 149.66 (C_q , C_{Ar}), 141.30 (2x C_q , C_{Ar}), 129.64 (C_q , C_{Ar}), 126.82 (CH, C_{Ar}), 125.69 (CH, C_{Ar}), 124.75 (CH, C_{Ar}), 124.41 (CH, C_{Ar}), 119.02 (CH), 110.17 (CH), 78.73 ($\text{C}(\text{CH}_3)_3$), 39.52 ($\text{CH}_2\text{-N}$), 27.98 ($t\text{Bu}$).

HPLC-ESI-MS (Method G): t_{R} = 7.94 min, $[\text{M}+\text{H}]^+$ = 331, $[\text{M}+\text{Na}]^+$ = 353, $[\text{M}+\text{K}]^+$ = 369.

6.2.7 Desulfurization and deprotection

1,3,7-Trimethyl-8-pentyl-2,3,6,7-tetrahydro-1H-purine-2,6-dione (91)



In a 10 mL Schlenk tube, heat dried under vacuum and flushed with N_2 , 116 mg (0.40 mmol, 1.0 eq) 1,3,7-trimethyl-8-(5-methylthiophen-2-yl)-1H-purine-2,6(3H,7H)-dione (**79**) were suspended in 2.0 mL dry THF. The yellow suspension was degassed in eight vacuum- N_2 cycles. An ethanolic black suspension of Raney-Ni (0.5 mL) was added to the reaction mixture, which was then flushed with H_2 in five vacuum- H_2 cycles and stirred under H_2 from an orsat balloon at rt. After 15 h, GC-MS indicated $\sim 1/3$ conversion. Therefore, further 0.5 mL Raney-Ni were added, the grey suspension underwent three vacuum- H_2 cycles and was then stirred at rt for 17 h. As GC-MS indicated $2/3$ conversion another 0.5 mL Raney-Ni were added, the grey suspension was again flushed with H_2 and then stirred at rt for 18 h. As GC-MS now indicated nearly complete conversion the reaction mixture was filtrated through a pad of celite, rinsed with methanol (6x10 mL) and the solvents were evaporated under reduced pressure.

The crude, green solid was purified by flash chromatography (60 g silica gel, dichloromethane/acetone 98:2 up to 94:6).

Yield: 90 mg (0.34 mmol, 85 %) pale yellow solid.

17 mg (0.06 mmol, 15 %) starting material (pale yellow solid) could be reisolated (as it was not completely dissolved in the reaction mixture).

$R_f = 0.18$ (dichloromethane/acetone 30:1).

M.p. = 79-80°C.

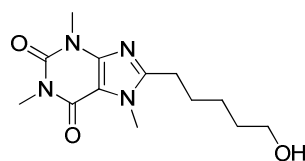
$^1\text{H-NMR}$ (300 MHz, CDCl_3): $\delta = 3.92$ (s, 3H, $\text{CH}_3\text{-N}$), 3.57 (s, 3H, $\text{CH}_3\text{-N}$), 3.40 (s, 3H, $\text{CH}_3\text{-N}$), 2.73 (t, $^3J = 7.5$ Hz, 2H, CH_2), 1.81-1.67 (m, 2H, CH_2), 1.41-1.32 (m, 4H, 2x CH_2), 0.91 (t, $^3J = 6.6$ Hz, 3H, CH_3).

$^{13}\text{C-NMR}$ (75 MHz, CDCl_3): $\delta = 155.32$ (C_q , C=O), 154.50 (C_q , C=O), 151.70 (C_q , C_{Ar}), 147.94 (C_q , C_{Ar}), 107.25 (C_q , C_{Ar}), 31.70 ($\text{CH}_3\text{-N}$), 31.45 (CH_2), 29.72 ($\text{CH}_3\text{-N}$), 27.84 ($\text{CH}_3\text{-N}$), 27.32 (CH_2), 26.80 (CH_2), 22.31 (CH_2), 13.90 (CH_3).

GC-MS (JR_50_S): $t_R = 7.93$ min, $m/z = 264$ (60 %), 208 (100 %).

HRMS (TOF MS EI^+): m/z calculated for $\text{C}_{13}\text{H}_{20}\text{N}_4\text{O}_2^+$ $[\text{M}]^+$: 264.1586, found 264.1602.

8-(5-Hydroxypentyl)-1,3,7-trimethyl-2,3,6,7-tetrahydro-1H-purine-2,6-dione (119)



$\text{C}_{13}\text{H}_{20}\text{N}_4\text{O}_3$

[280.32]

From 8-(5-(hydroxymethyl)thiophen-2-yl)-1,3,7-trimethyl-2,3,6,7-tetrahydro-1H-purine-2,6-dione (109):

In a 15 mL Schlenk tube, heat dried under vacuum and flushed with N₂, 35.7 mg (0.116 mmol, 1.0 eq) 8-(5-(hydroxymethyl)thiophen-2-yl)-1,3,7-trimethyl-2,3,6,7-tetrahydro-1H-purine-2,6-dione (**109**) were dissolved in 3 mL dry THF. After degassing in three vacuum-N₂ cycles, 2 mL Raney-Ni suspension in water were added and the Schlenk tube was flushed with H₂ in three vacuum-H₂ cycles. The black suspension was stirred under H₂ from an orsat balloon at rt for 1 d until TLC indicated full consumption of the starting material **109**. The reaction mixture was filtrated through a pad of celite and rinsed with methanol (2x30 mL) and dichloromethane (2x30 mL). After evaporation of the solvents under reduced pressure, the crude product was purified by silica gel filtration (20 g silica gel, dichloromethane).

Yield: 12.8 mg (0.046 mmol, 40 %) colorless solid.

From 8-(5-((benzyloxy)methyl)thiophen-2-yl)-1,3,7-trimethyl-2,3,6,7-tetrahydro-1H-purine-2,6-dione (110):

In a 15 mL Schlenk tube, heat dried under vacuum and flushed with N₂, 119 mg (0.30 mmol, 1.0 eq) 8-(5-((benzyloxy)methyl)thiophen-2-yl)-1,3,7-trimethyl-2,3,6,7-tetrahydro-1H-purine-2,6-dione (**110**) were dissolved in 5 mL dry THF. After degassing in three vacuum-N₂ cycles, 6 mL Raney-Ni suspension in water were added and the Schlenk tube was flushed with H₂ in four vacuum-H₂ cycles. The black suspension was stirred under H₂ from an orsat balloon at rt for 3 d. Since HPLC-MS indicated incomplete conversion, another 4 mL aqueous Raney-Ni suspension were added. After additional four vacuum-H₂ cycles the black suspension was stirred at rt for another day until full conversion could be monitored. The reaction mixture was filtrated through a pad of celite and rinsed with methanol (4x25 mL) and dichloromethane (1x30 mL). After evaporation of the solvents under reduced pressure, the crude product **119** was purified by silica gel filtration (3 g silica gel, dichloromethane).

Yield: 83 mg (0.30 mmol, 99 %) colorless solid.

R_f = 0.31 (dichloromethane/acetone 9:1).

M.p. = 119-120°C.

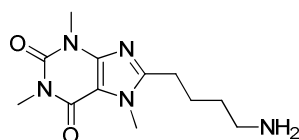
¹H-NMR (300 MHz, CD₃OD): δ = 3.90 (s, 3H, CH₃-N), 3.56 (t, ³J = 6.3 Hz, 2H, CH₂-O), 3.49 (s, 3H, CH₃-N), 3.30 (s, 3H, CH₃-N), 2.80 (t, ³J = 7.5 Hz, 2H, CH₂-N), 1.85-1.71 (m, 2H, CH₂), 1.64-1.40 (m, 4H, 2x CH₂).

¹³C-NMR (75 MHz, CD₃OD): δ = 156.67 (C_q, C=O), 156.63 (C_q, C=O), 153.28 (C_q), 149.32 (C_q), 108.59 (C_q), 62.83 (CH₂-O), 33.39 (CH₂), 32.37 (CH₃-N), 30.24 (CH₃-N), 28.45 (CH₃-N), 28.33 (CH₂), 27.53 (CH₂), 26.75 (CH₂).

IR (neat): ν_{max} = 3456 (m), 2936 (m), 1694 (s), 1655 (s), 1541 (m), 1497 (w), 1460 (s), 1411 (m), 1335 (w), 1282 (m), 1220 (m), 1049 (s), 1037 (m), 1007 (m), 978 (m), 761 (m), 746 (s).

HPLC-ESI-MS (Method G): t_R = 3.57 min, [M+H]⁺ = 281, [M+Na]⁺ = 303, [M+K]⁺ = 319.

8-(4-Aminobutyl)-1,3,7-trimethyl-2,3,6,7-tetrahydro-1H-purine-2,6-dione (**120**)



C₁₂H₁₉N₅O₂

[265.31]

In a 10 mL Schlenk tube, equipped with reflux condenser, heat dried under vacuum and flushed with N₂, 100 mg (0.31 mmol, 1.00 eq) 1,3,7-trimethyl-8-(5-nitrothiophen-2-yl)-1H-purine-2,6(3H,7H)-dione (**113**) were suspended in 2 mL THF. After degassing of the reaction mixture in three vacuum-N₂ cycles, 6 mL aqueous Raney-Ni suspension were added. In three vacuum-H₂ cycles the mixture was flushed with H₂. The reaction mixture was stirred at 60°C for 22 h under H₂ from an orsat balloon. When TLC indicated complete conversion the mixture was filtrated through a pad of celite and rinsed with methanol (15 mL). After evaporation of the organic solvents under reduced pressure, the product **120** was freeze dried at the lyophilisator. Finally the crude solid was purified by preparative HPLC.

Yield: 1.6 mg (0.006 mmol, 2 %) colorless solid.

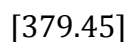
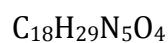
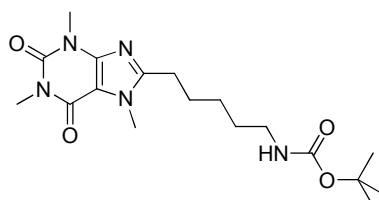
$^1\text{H-NMR}$ (300 MHz, CD_3OD): δ = 8.44 (bs, 2H, NH_2), 3.93 (s, 3H, $\text{CH}_3\text{-N}$), 3.53 (s, 3H, $\text{CH}_3\text{-N}$), 3.35 (s, 3H, $\text{CH}_3\text{-N}$), 2.98 (t, 3J = 7.5 Hz, 2H, CH_2), 2.87 (t, 3J = 6.9 Hz, 2H, CH_2), 1.95-1.72 (m, 4H, 2x CH_2).

$^{13}\text{C-NMR}$ (75 MHz, CD_3OD): δ = 156.76 (C_q , C=O), 155.69 (C_q , C=O), 153.96 (C_q), 149.35 (C_q), 101.55 (C_q), 40.52 ($\text{CH}_2\text{-N}$), 32.35 ($\text{CH}_3\text{-N}$), 30.24 ($\text{CH}_3\text{-N}$), 28.36 (CH_2), 28.26 ($\text{CH}_3\text{-N}$), 26.79 (CH_2), 25.09 (CH_2).

PHPLC: A: 0.01 % HCOOH in H_2O , B: MeOH , rt, 16 mL/min, 0-7 min: 12 % B constant, 7-9 min: 12-100 % B, 9-14 min: 100 % B constant. λ = 254 nm. t_R = 5.6 min.

HPLC-ESI-MS (Method F): t_R = 6.44 min, $[\text{M}+\text{H}]^+$ = 266.

***tert*-Butyl *N*-(5-(1,3,7-trimethyl-2,6-dioxo-2,3,6,7-tetrahydro-1*H*-purin-8-yl)pentyl)carbamate (122)**



In a 50 mL Schlenk tube, heat dried under vacuum and flushed with N_2 , 140 mg (0.345 mmol, 1.00 eq) *tert*-butyl *N*-((5-(1,3,7-trimethyl-2,6-dioxo-2,3,6,7-tetrahydro-1*H*-purin-8-yl)thiophen-2-yl)methyl)carbamate (**117**) were suspended in 5 mL THF. After degassing of the reaction mixture in three vacuum- N_2 cycles, 4 mL aqueous Raney-Ni suspension were added. In three vacuum- H_2 cycles the mixture was flushed with H_2 . Afterwards, the mixture was stirred at rt for 24 h under H_2 from an orsat balloon until another 1 mL of Raney-Ni suspension was added. After further 24 h stirring under H_2 atmosphere, TLC indicated complete conversion. The mixture was filtrated through a

pad of celite and rinsed with methanol (30 mL) and dichloromethane (30 mL). After concentration of the crude product **122** under reduced pressure, it was purified by filtration through 3 cm silica gel (eluent methanol).

Yield: 109 mg (0.287 mmol, 83 %) colorless solid.

$R_f = 0.25$ (dichloromethane/acetone 9:1).

M.p. = 106°C.

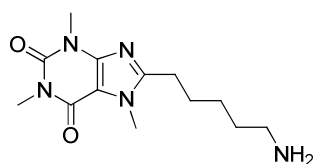
$^1\text{H-NMR}$ (300 MHz, CDCl_3): $\delta = 4.55$ (bs, 1H, NH), 3.91 (s, 3H, $\text{CH}_3\text{-N}$), 3.57 (s, 3H, $\text{CH}_3\text{-N}$), 3.40 (s, 3H, $\text{CH}_3\text{-N}$), 3.15 (q, $^3J = 4.5$ Hz, 2H, $\text{CH}_2\text{-N}$), 2.73 (t, $^3J = 7.5$ Hz, 2H, $\text{CH}_2\text{-C}(\text{sp}^2)$), 1.78 (p, $^3J = 7.2$ Hz, 2H, CH_2), 1.68-1.50 (m, 4H, 2x CH_2), 1.43 (s, 9H, ^tBu).

$^{13}\text{C-NMR}$ (75 MHz, DMSO-d_6): $\delta = 155.60$ (C_q , C=O), 154.26 (C_q , C=O), 150.86 (C_q , C_{Ar}), 147.28 (C_q , C=O), 106.50 (C_q , C_{Ar}), 77.31 ($\text{C}(\text{CH}_3)_3$), 40.39 ($\text{CH}_2\text{-N}$), 31.36 ($\text{CH}_3\text{-N}$), 29.62 ($\text{CH}_3\text{-N}$), 28.50 (CH_2), 28.23 (^tBu), 27.44 ($\text{CH}_3\text{-N}$), 26.43 (CH_2), 26.09 (2x CH_2).

IR (neat): $\nu_{\text{max}} = 3320$ (w), 2931 (m), 1698 (s), 1651 (s), 1542 (m), 1441 (m), 1405 (w), 1276 (m), 1220 (m), 1169 (s), 1037 (m), 977 (m), 748 (m).

HPLC-ESI-MS (Method G): $t_R = 5.59$ min, $[\text{M}+\text{H}]^+ = 380$, $[\text{M}+\text{Na}]^+ = 402$, $[\text{M}+\text{K}]^+ = 418$.

**5-(1,3,7-Trimethyl-2,6-dioxo-2,3,6,7-tetrahydro-1H-purin-8-yl)pentan-1-amine
(121)**



$\text{C}_{13}\text{H}_{21}\text{N}_5\text{O}_2$

[279.34]

Via reduction with Raney-Nickel (general procedure):

In a Schlenk tube equipped with reflux condenser, heat dried under vacuum and flushed with N₂, 1.00 eq of starting material was suspended in THF. After degassing of the reaction mixture in three vacuum-N₂ cycles an aqueous Raney-Ni suspension was added. In three vacuum-H₂ cycles the mixture was flushed with H₂. The mixture was stirred at 60°C for 22 h under H₂ from an orsat balloon. When TLC indicated complete conversion the reaction mixture was filtrated through a pad of celite and rinsed with methanol (15 mL). After evaporation of the organic solvents under reduced pressure the product **121** was freeze dried at the lyophilisator. Finally, the crude solid was purified by preparative HPLC to yield the product as formate.

From **114**: 60 mg (0.20 mmol) 5-(1,3,7-trimethyl-2,6-dioxo-2,3,6,7-tetrahydro-1*H*-purin-8-yl)thiophene-2-carbonitrile (**114**); 4 mL aqueous Raney-Ni; 1.5 mL THF
Yield: 1.5 mg (0.005 mmol, 3 %) colorless solid.

From **116**: 200 mg (0.46 mmol) benzyl ((5-(1,3,7-trimethyl-2,6-dioxo-2,3,6,7-tetrahydro-1*H*-purin-8-yl)thiophen-2-yl) methyl)carbamate (**116**); 10 mL aqueous Raney-Ni; 4 mL THF
Yield: 51 mg (0.18 mmol, 40 %) colorless solid.

Via Boc-deprotection (Method A):

In a 25 mL round-bottom flask with magnetic stirring bar 50 mg (0.13 mmol, 1 eq) *tert*-butyl (5-(1,3,7-trimethyl-2,6-dioxo-2,3,6,7-tetrahydro-1*H*-purin-8-yl)pentyl) carbamate (**122**) were dissolved in 0.5 mL (7.42 mmol, 56 eq) HBr (33 % in acetic acid) and stirred at rt for 1 h. When TLC indicated complete conversion the solvent of the orange solution was evaporated in an open flask under N₂ flow. The product **121** precipitated as hydrobromide in the ultrasonic bath by addition of 3 mL acetonitrile or was purified by preparative HPLC to obtain the formate.

Yield: 33 mg (0.090 mmol, 68 %) colorless solid (formate).

Via Boc-deprotection (Method B):

In a 25 mL round-bottom flask with magnetic stirring bar 16.4 mg (0.045 mmol, 1 eq) *tert*-butyl (5-(1,3,7-trimethyl-2,6-dioxo-2,3,6,7-tetrahydro-1*H*-purin-8-yl)pentyl) carbamate (**122**) were dissolved in 0.5 mL dichloromethane. After addition of 200 μ L (2.250 mmol, 50 eq) TFA, the slightly yellow solution was stirred at rt for 1 h. When TLC and HPLC indicated complete conversion, the product **121** was concentrated under N₂ flow. The crude sticky residue was purified by preparative HPLC to obtain the pure product as trifluoroacetate.

Yield: 14.3 mg (0.044 mmol, 98 %) colorless solid.

M.p. = 252-254°C.

¹H-NMR (300 MHz, CD₃OD): δ = 8.46 (s, 1H, HCOO⁻), 3.86 (s, 3H, CH₃), 3.44 (s, 3H, CH₃), 3.25 (s, 3H, CH₃), 2.90 (t, ³*J* = 7.5 Hz, 2H, CH₂), 2.78 (t, ³*J* = 7.5 Hz, 2H, CH₂), 1.84-1.61 (m, 4H, 2x CH₂), 1.53-1.41 (m, 2H, CH₂).

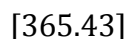
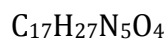
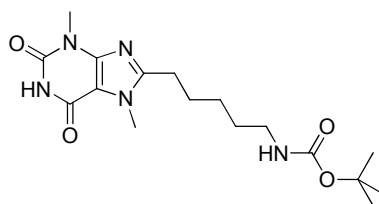
¹³C-NMR (75 MHz, CD₃OD): δ = 170.30 (HCOO⁻), 156.48 (C_q, C=O), 156.10 (C_q, C=O), 153.11 (C_q), 149.15 (C_q), 108.48 (C_q), 40.53 (CH₂-N), 32.27 (CH₃), 30.14 (CH₃), 28.34 (CH₂), 28.25 (CH₃), 27.81 (CH₂), 27.11 (CH₂), 27.01 (CH₂).

PHPLC: A: 0.01 % HCOOH in H₂O, B: MeOH, rt, 16 mL/min, 0-7 min: 17 % B constant, 7-9 min: 17-100 % B, 9-14 min: 100 % B constant, λ = 254 nm. *t_R* = 4.8 min.

HPLC-ESI-MS (Method G): *t_R* = 2.58 min, [M+H]⁺ = 280, [M+K]⁺ = 318.

HRMS (TOF MS LD⁺): *m/z* calculated for C₁₃H₂₂N₅O₂⁺ [M+H]⁺: 280.1773, found 280.1782.

***tert*-Butyl *N*-(5-(3,7-dimethyl-2,6-dioxo-2,3,6,7-tetrahydro-1*H*-purin-8-yl)pentyl) carbamate (122b)**



In a 50 mL Schlenk tube, heat dried under vacuum and flushed with N_2 , 105 mg (0.268 mmol, 1.00 eq) *tert*-butyl *N*-((5-(3,7-dimethyl-2,6-dioxo-2,3,6,7-tetrahydro-1*H*-purin-8-yl)thiophen-2-yl)methyl)carbamate (**136**) were suspended in 5 mL THF. After degassing of the reaction mixture in three vacuum- N_2 cycles, 8 mL aqueous Raney-Ni suspension were added. In four vacuum- H_2 cycles the mixture was flushed with H_2 . Afterwards, the mixture was stirred at rt for 24 h under H_2 from an orsat balloon until HPLC indicated complete conversion. The mixture was filtrated through a pad of celite and rinsed with methanol (120 mL) and dichloromethane (30 mL). The product **122b** was concentrated under reduced pressure and lyophilized to dryness.

Yield: 55 mg (0.151 mmol, 56 %) colorless solid.

R_f = 0.53 (dichloromethane/acetone 4:1).

M.p. = 156-158°C.

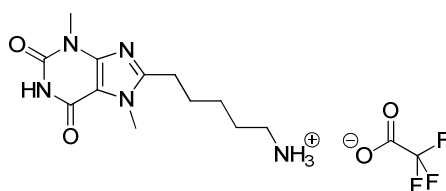
$^1\text{H-NMR}$ (300 MHz, DMSO-d_6): δ = 10.98 (bs, 1H, NH), 6.78 (bs, 1H, NH), 3.80 (s, 3H, $\text{CH}_3\text{-N}$), 3.31 (s, 3H, $\text{CH}_3\text{-N}$), 2.90 (q, 3J = 6.0 Hz, 2H, $\text{CH}_2\text{-N}$), 2.70 (t, 3J = 7.5 Hz, 2H, $\text{CH}_2\text{-C}(\text{sp}^2)$), 1.70-1.50 (m, 4H, 2x CH_2), 1.45-1.37 (m, 2H, CH_2), 1.36 (s, 9H, ^tBu).

$^{13}\text{C-NMR}$ (75 MHz, DMSO-d_6): δ = 155.57 (C_q , C=O), 155.33 (C_q , C=O), 153.98 (C_q , C_{Ar}), 148.94 (C_q , C=O), 106.85 (C_q , C_{Ar}), 77.26 ($\underline{\text{C}}(\text{CH}_3)_3$), 37.81 ($\text{CH}_2\text{-N}$), 31.24 ($\text{CH}_3\text{-N}$), 28.92 (CH_2), 28.36 ($\text{CH}_3\text{-N}$), 28.23 (^tBu), 26.44 (CH_2), 25.81 (CH_2), 25.75 (CH_2).

IR (neat): ν_{\max} = 3420 (w), 2971 (w), 1685 (s), 1550 (w), 1511 (m), 1441 (s), 1426 (s), 1406 (s), 1365 (m), 1161 (s), 751 (m), 621 (m).

HPLC-ESI-MS (Method G): t_R = 5.00 min, $[M+H]^+$ = 366, $[M+Na]^+$ = 388, $[M+K]^+$ = 404.

5-(3,7-Dimethyl-2,6-dioxo-2,3,6,7-tetrahydro-1H-purin-8-yl)pentan-1-aminium trifluoroacetate (121b)



$C_{14}H_{20}F_3N_5O_4$

[379.33]

A 25 mL round-bottom flask with magnetic stirring bar was charged with 11.0 mg (0.030 mmol, 1 eq) *tert*-butyl *N*-(5-(3,7-dimethyl-2,6-dioxo-2,3,6,7-tetrahydro-1H-purin-8-yl)pentyl) carbamate (**122b**). After addition of 150 μ L (1.505 mmol, 50 eq) TFA, the yellow solution was stirred at rt for 1 h. When TLC and HPLC indicated complete conversion, the product **121b** was concentrated under N_2 -flow and dried under high vacuum.

Yield: 11.4 mg (0.030 mmol, quantitative) colorless solid.

M.p. = 149-150°C.

1H -NMR (300 MHz, CD_3OD): δ = 3.90 (s, 3H, CH_3-N), 3.46 (s, 3H, CH_3-N), 2.95 (t, 3J = 7.5 Hz, 2H, CH_2-N), 2.82 (t, 3J = 7.5 Hz, 2H, $CH_2-C(sp^2)$), 1.90-1.65 (m, 4H, 2x CH_2), 1.55-1.45 (m, 2H, CH_2).

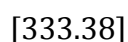
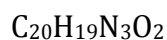
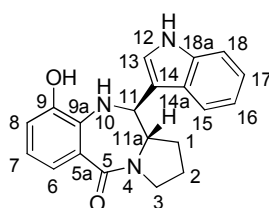
^{13}C -NMR (75 MHz, CD_3OD): δ = 161.19 (C_q , C=O), 156.47 (C_q , C=O), 153.19 (C_q , C_{Ar}), 151.04 (C_q , C=O), 115.57 (CF_3), 109.06 (C_q , C_{Ar}), 40.68 (CH_2-N), 32.36 (CH_3-N), 29.33 (CH_3-N), 28.37 (CH_2), 27.89 (CH_2), 27.14 (CH_2), 27.05 (CH_2).

IR (neat): ν_{\max} = 2360 (w), 1373 (s), 1431 (w), 1177 (s), 1128 (s), 839 (m), 800 (m), 723 (m), 677 (w), 638 (w), 617 (w).

HPLC-ESI-MS (Method G): t_R = 2.25 min, $[M+H]^+$ = 266, $[M+Na]^+$ = 288, $[M+K]^+$ = 304.

6.2.8 Isolation and characterisation of a cytotoxin of *K. oxytoca*

1 L of a brownish supernatant from *K. oxytoca* was extracted with *n*-butanol (2x800 mL). For a better separation of the layers brine (2x200 mL) and additional *n*-butanol (2x200 mL) were added. Ultimately, layer separation was accomplished by centrifugation (25 min, 10000 rpm, 4°C). The combined organic layers were dried over Na_2SO_4 , filtrated and the solvent was evaporated at exactly 40°C under reduced pressure yielding a yellow solid. When the crude product did not become solid, it was dried under high vacuum at rt. Therefore, the crude product was suspended in *n*-hexane (1 mL) for 5 min in the ultrasonic bath to guarantee mixing of the *n*-butanol traces with *n*-hexane. The resulting suspension was dried under high vacuum. This process was repeated until the crude product became powdery (up to 8 times). Now the crude yellow solid was stable and could be stored for weeks at rt in the presence of air and light. The crude powder was purified by preparative reversed phase HPLC to yield 41 mg of a colorless solid, identified as (1*S*,11*aS*)-1,2,3,10,11,11*a*-hexahydro-9-hydroxy-11-(1*H*-indol-3-yl)-5*H*-pyrrolo[2,1-*c*][1,4]benzo-diazepin-5-one (**154**).



R_f = 0.76 (methanol).

M.p. = 181-185°C. (lit. 180-185°C)^[106]

$^1\text{H-NMR}$ (500 MHz, DMSO-d_6): δ = 11.13 (bs, 1H, NH), 7.45-7.35 (m, 3H, H-13, H-15, H-18), 7.16 (d, 3J = 7.5 Hz, 1H, H-6), 7.09 (t, 3J = 7.5 Hz, 1H, H-17), 6.94 (t, 3J = 7.5 Hz, 1H, H-16), 6.77 (d, 3J = 7.5 Hz, 1H, H-8), 6.54 (t, 3J = 7.5 Hz, 1H, H-7), 5.09 (bs, 1H, OH), 4.73 (d, 3J = 9.5 Hz, 1H, H-11), 4.22-4.13 (m, 1H, H-11a), 3.74-3.65 (m, 1H, H-3, diastereotopic), 3.58-3.53 (m, 1H, H-3, diastereotopic), 1.92-1.83 (m, 1H, H-2, diastereotopic), 1.73-1.65 (m, 2H, H-2, H-1, diastereotopic), 1.57-1.50 (m, 1H, H-1, diastereotopic).

$^{13}\text{C-NMR}$ (125 MHz, DMSO-d_6): δ = 166.58 (C_q , C-5), 146.97 (C_q , C-9), 136.50 (C_q , C-18a), 134.94 (C_q , C-9a), 125.11 (C_q , C-14a), 123.72 (CH, C-13), 121.33 (CH, C-17), 121.13 (CH, C-6), 119.86 (CH, C-16), 118.95 (CH, C-15), 118.88 (C_q , C-14), 116.41 (CH, C-7), 116.25 (C_q , C-5a), 114.85 (CH, C-8), 111.77 (CH, C-18), 60.94 (CH, C-11), 59.56 (CH, C-11a), 47.49 (CH_2 , C-3), 30.26 (CH_2 , C-1), 22.06 (CH_2 , C-2).

IR (neat): ν_{max} = 3254 (w), 1613 (m), 1433 (m), 1203 (m), 742 (s).

PHPLC: A: H_2O , B: MeOH, rt, 14 mL/min, 0-9 min: 40 % B constant, 9-26 min: 40-50 % B, 26-32 min: 50 % B constant, λ_{max} = 221, 331 nm. t_{R} = 27 min.

HPLC-ESI-MS (Method G): t_{R} = 4.55 min, $[\text{M}+\text{H}]^+$ = 334, $[\text{M}+\text{Na}]^+$ = 356, $[\text{M}+\text{K}]^+$ = 372, $[\text{M}-\text{H}]^-$ = 332.

HRMS (TOF MS EI^+): m/z calculated for $\text{C}_{20}\text{H}_{19}\text{N}_3\text{O}_2^+$ $[\text{M}]^+$: 333.1477, found 333.1493.

$[\alpha]_{\text{D}}^{20}$ = 59 (c = 0.29 in methanol). (lit. $[\alpha]_{\text{D}}^{23}$ = 210, c = 1.01 in methanol)^[106]

7. References

- [1] a) J. Drews, *Science* **2000**, *287*, 1960-1964. b) C. Tsinopoulos, I. McCarthy, *An evolutionary classification of the strategies for drug discovery*, Manufacturing Complexity Network Conference, Cambridge, **2002**, pp. 373-385, available at: http://www.ifm.eng.cam.ac.uk/mcn/pdf_files/part7_2.pdf. Accessed on March **2012**.
- [2] a) K. C. Nicolaou, J. S. Chen, D. J. Edmonds, A. A. Estrada, *Angew. Chem. Int. Ed.* **2009**, *48*, 660-719. b) M. A. Fischbach, C. T. Walsh, *Science* **2009**, *325*, 1089-1093. c) S. Meinert, E. John, *Chem. Unserer Zeit* **2009**, *43*, 296-306.
- [3] M. M. Joainig, G. Gorkiewicz, E. Leitner, P. Weberhofer, I. Zollner-Schwetz, I. Lippe, G. Feierl, R. Krause, T. Hinterleitner, E. L. Zechner, C. Högenauer, *J. Clin. Microbiol.* **2010**, *48*, 817-824.
- [4] a) K. Roth, *Chem. Unserer Zeit* **2005**, *39*, 212-217. b) H. Bischoff, *Die Contergan-Tragödie*, Sonderdruck, Grüenthal GmbH, Aachen, **2007**.
- [5] N. Kuhnert, *Chem. Unserer Zeit* **1999**, *33*, 213-220.
- [6] R. v. Moos, R. Stolz, T. Cerny, S. Gillessen, *Swiss Med Wkly* **2003**, *133*, 77-87.
- [7] S. D. Patterson, R. H. Aebersold, *Nat. Genet. Supplement* **2003**, *33*, 311-323.
- [8] a) L. Beaugerie, M. Metz, F. Barbut, G. Bellaiche, *Clin. Gastroenterol. Hepatol.* **2003**, *1*, 70-76. b) J. E. Degener, A. C. W. Smit, M. F. Michel, H. A. Valkenburg, L. Muller, *J. Med. Microbiol.* **1983**, *16*, 139-145. c) C. Högenauer, C. Langner, E. Beubler, I. T. Lippe, R. Schicho, G. Gorkiewicz, R. Krause, N. Gerstgrasser, G. J. Krejs, T. A. Hinterleitner, *N. Engl. J. Med.* **2006**, *355*, 2418-2426.
- [9] O. Umeh, L. B. Berkowitz: "Klebsiella infections", <http://emedicine.medscape.com/article/219907-overview#showall>. Accessed on March **2012**.
- [10] I. Zollner-Schwetz, C. Högenauer, M. Joainig, P. Weberhofer, G. Gorkiewicz, T. Valentin, T. A. Hinterleitner, R. Krause, *Clin. Infect. Dis.* **2008**, *47*, e74-e78.
- [11] G. Schneditz, E. L. Zechner, *unpublished data* **2012**.
- [12] J. Minami, A. Okabe, J. Shiode, H. Hayashi, *Microbial Pathogenesis* **1989**, *7*, 203-211.
- [13] a) S. Fotso, *Mini-Reviews in Organic Chemistry* **2010**, *7*, 68-74. b) L. Rahbaek, J. Breinholt, *J. Nat. Prod.* **1999**, *62*, 904-905.
- [14] M. P. López-Gresa, M. C. González, J. Primo, P. Moya, V. Romero, E. Estornell, *J. Antibiot.* **2005**, *58*, 416-419.
- [15] N. Mohr, H. Budzikiewicz, *Tetrahedron* **1982**, *38*, 147-152.

- [16] T. Hadjivassileva, D. E. Thurston, P. W. Taylor, *J. Antimicrob. Chemother.* **2005**, *56*, 513-518.
- [17] a) W. Leimgruber, V. Stefanović, F. Schenker, A. Karr, J. Berger, *J. Am. Chem. Soc.* **1965**, *87*, 5791-5793. b) M. G. Brazhnikova, N. V. Konstantinova, A. S. Mesentsev, *J. Antibiot.* **1972**, *25*, 668-673.
- [18] H. Quach, D. Ritchie, A. K. Stewart, P. Neeson, S. Harrison, M. J. Smyth, H. M. Prince, *Leukemia* **2010**, *24*, 22-32.
- [19] N. Vargesson, *Bioessays* **2009**, *31*, 1327-1336.
- [20] a) C. Therapontos, L. Erskine, E. R. Gardner, W. D. Figg, N. Vargesson, *Proc. Natl. Acad. Sci.* **2009**, *106*, 8573-8578. b) T. Christoffersen, T. K. Guren, K.-L. Garm Spindler, O. Dahl, P. E. Lønning, B. T. Gjertsen, *Eur. J. Pharmacol.* **2009**, *625*, 6-22.
- [21] T. Ito, H. Ando, T. Suzuki, T. Ogura, K. Hotta, Y. Imamura, Y. Yamaguchi, H. Handa, *Science* **2010**, *327*, 1345-1350.
- [22] a) U. Rix, G. Superti-Furga, *Nat. Chem. Biol.* **2009**, *5*, 616-624. b) J. M. P. Ferreira de Oliveira, L. H. De Graaff, *Appl. Microbiol. Biotechnol.* **2011**, *89*, 225-237. c) B. Fang, E. B. Haura, K. S. Smalley, S. A. Eschrich, J. M. Koomen, *Biochem. Pharmacol.* **2010**, *80*, 739-747. d) B. Lomenick, R. W. Olsen, J. Huang, *ACS Chem. Biol.* **2011**, *6*, 34-46. e) M. Bantscheff, A. Scholten, A. J. R. Heck, *Drug Discovery Today* **2009**, *14*, 1021-1029. f) L. Sleno, A. Emili, *Curr. Opin. Chem. Biol.* **2008**, *12*, 46-54. g) M. Uttamchandani, C. H. S. Lu, S. Q. Yao, *Acc. Chem. Res.* **2009**, *42*, 1183-1192.
- [23] T. Shiyama, M. Furuya, A. Yamazaki, T. Terada, A. Tanaka, *Bioorg. Med. Chem.* **2004**, *12*, 2831-2841.
- [24] M. J. Stefanko, Y. K. Gun'ko, D. K. Rai, P. Evans, *Tetrahedron* **2008**, *64*, 10132-10139.
- [25] a) I. Olmedo, A. R. Guerrero, E. Araya, M. J. Kogan in *The Power of Functional Resins in Organic Synthesis* (Eds.: J. Tulla-Puche, F. Albericio), VCH, Weinheim, **2008**, pp. 45-82. b) R. Haag, A. Hebel, J.-F. Stumbé in *Handbook of Combinatorial Chemistry, Vol. 1* (Eds.: K. C. Nicolaou, R. Hanco, W. Hartwig), VCH, Weinheim, **2002**, pp. 46-58.
- [26] a) P. Seneci, *Solid-Phase Synthesis and Combinatorial Technologies*, John Wiley & Sons, New York, **2000**, pp. 1-8. b) R. Haag, A. Hebel, J.-F. Stumbé in *Handbook of Combinatorial Chemistry, Vol. 1* (Eds.: K. C. Nicolaou, R. Hanco, W. Hartwig), VCH, Weinheim, **2002**, pp. 24-45. c) F. Albericio, J. Tulla-Puche in *The Power of Functional Resins in Organic Synthesis* (Eds.: J. Tulla-Puche, F. Albericio), VCH, Weinheim, **2008**, pp. 3-14, 495-499.

- [27] a) J. M. Bevington, P. G. Needam, K. C. Verrill, R. F. Collaco, V. Basrur, J. P. Trempe, *Virology* **2007**, *357*, 102-113. b) C. Catuogno, M. N. Jones, *Int. J. Pharm.* **2003**, *257*, 125-140.
- [28] K. Nishio, Y. Masaike, M. Ikeda, H. Narimatsu, N. Gokon, S. Tsubouchi, M. Hatakeyama, S. Sakamoto, N. Hanyu, A. Sandhu, H. Kawaguchi, M. Abe, H. Handa, *Colloids Surf., B* **2008**, *64*, 162-169.
- [29] S. Raddatz, J. Mueller-Ibeler, J. Kluge, L. Wäß, G. Burdinski, J. R. Havens, T. J. Onofrey, D. Wang, M. Schweitzer, *Nucleic Acids Res.* **2002**, *30*, 4793-4802.
- [30] M. B. Biskup, J. U. Müller, R. Weingart, R. R. Schmidt, *ChemBioChem* **2005**, *6*, 1007-1015.
- [31] a) G. MacBeath, S. L. Schreiber, *Science* **2000**, *289*, 1760-1763. b) H. Zhu, M. Bilgin, R. Bangham, D. Hall, A. Casamyor, P. Bertone, N. Lan, R. Jansen, S. Bidlingmaier, T. Houfek, T. Mitchell, P. Miller, R. A. Dean, M. Gerstein, M. Snyder, *Science* **2001**, *293*, 2101-2105.
- [32] H. Zhu, J. F. Klemic, S. Chang, P. Bertone, A. Casamyor, K. G. Klemic, D. Smith, M. Gerstein, M. A. Reed, M. Snyder, *Nat. Genet.* **2000**, *26*, 283-289.
- [33] a) B. L. Nilsson, R. J. Hondal, M. B. Soellner, R. T. Raines, *J. Am. Chem. Soc.* **2003**, *125*, 5268-5269. b) R. David, M. P.O. Richter, A. G. Beck-Sickinger, *Eur. J. Biochem.* **2004**, *271*, 663-677.
- [34] B. L. Nilsson, R. J. Hondal, M. B. Soellner, R. T. Raines, *J. Am. Chem. Soc.* **2003**, *125*, 5268-5269.
- [35] M. Köhn, *PhD thesis* **2005**, University of Dortmund.
- [36] R. Breinbauer, M. Köhn, *ChemBioChem* **2003**, *4*, 1147-1149.
- [37] Y.-X. Chen, G. Triola, H. Waldmann, *Acc. Chem. Res.* **2011**, *44*, 762-773.
- [38] A. E. Speers, G. C. Adam, B. F. Cravatt, *J. Am. Chem. Soc.* **2003**, *125*, 4686-4687.
- [39] Y. G. Gololobov, L. F. Kasukhin, *Tetrahedron* **1992**, *48*, 1353-1406.
- [40] a) E. M. Sletten, C. R. Bertozzi, *Acc. Chem. Res.* **2011**, *44*, 666-676. b) J. A. Prescher, C. R. Bertozzi, *Nat. Chem. Biol.* **2005**, *433*, 13-21.
- [41] a) M. Köhn, R. Wacker, C. Peters, H. Schröder, L. Soulère, R. Breinbauer, C. M. Niemeyer, H. Waldmann, *Angew. Chem. Int. Ed.* **2003**, *42*, 5830-5834. b) M. Köhn, *J. Pept. Sci.* **2009**, *15*, 393-397.
- [42] T. M. Roper, C. A. Guymon, E. S. Jönsson, C. E. Hoyle, *J. Polym. Sci., Part A: Polym. Chem.* **2004**, *42*, 6283-6298.

- [43] P. Jonkheijm, D. Weinrich, M. Köhn, H. Engelkamp, P. C. M. Christianen, J. Kuhlmann, J. C. Maan, D. Nüsse, H. Schroeder, R. Wacker, R. Breinbauer, C. M. Niemeyer, H. Waldmann, *Angew. Chem. Int. Ed.* **2008**, *47*, 4421-4424.
- [44] S. Hiki, K. Kataoka, *Bioconjugate Chem.* **2007**, *18*, 2191-2196.
- [45] a) X.-F. Wu, P. Anbarasan, H. Neumann, M. Beller, *Angew. Chem. Int. Ed.* **2010**, *49*, 9047-9050. b) C. S. Yeung, V. M. Dong, *Chem. Rev.* **2011**, *111*, 1215-1292. c) K. C. Nicolaou, P. G. Bulger, D. Sarlah, *Angew. Chem. Int. Ed.* **2005**, *44*, 4442-4489.
- [46] a) D. Zhao, W. Wang, F. Yang, J. Lan, L. Yang, G. Gao, J. You, *Angew. Chem. Int. Ed.* **2009**, *48*, 3296-3300. b) D. Zhao, W. Wang, S. Lian, F. Yang, J. Lan, J. You, *Chem. Eur. J.* **2009**, *15*, 1337-1340.
- [47] H. A. Chiong, O. Daugulis, *Org. Lett.* **2007**, *9*, 1449-1451.
- [48] K. Muto, J. Yamaguchi, K. Itami, *J. Am. Chem. Soc.* **2012**, *134*, 169-172.
- [49] M. Wang, D. Li, W. Zhou, L. Wang, *Tetrahedron* **2012**, *68*, 1926-1930.
- [50] L. Ackermann, A. Althammer, S. Fenner, *Angew. Chem. Int. Ed.* **2009**, *48*, 201-204.
- [51] a) D. R. Stuart, K. Fagnou, *Science* **2007**, *316*, 1172-1175. b) X. Bugaut, F. Glorius, *Angew. Chem.* **2011**, *123*, 7618-7620.
- [52] a) C. Verrier, P. Lassalas, L. Théveau, G. Quéguiner, F. Trécourt, F. Marsais, C. Hoarau, *Beilstein J. Org. Chem.* **2011**, *7*, 1584-1601. b) S. H. Cho, J. Y. Kim, J. Kwak, S. Chang, *Chem. Soc. Rev.* **2011**, *40*, 5068-5083.
- [53] P. Xi, F. Yang, S. Qin, D. Zhao, J. Lan, G. Gao, C. Hu, J. You, *J. Am. Chem. Soc.* **2010**, *132*, 1822-1824.
- [54] Y. Wei, W. Su, *J. Am. Chem. Soc.* **2010**, *132*, 16377-16379.
- [55] C. C. Malakar, D. Schmidt, J. Conrad, U. Beifuss, *Org. Lett.* **2011**, *13*, 1379-1381.
- [56] W. Han, P. Mayer, A. R. Ofial, *Angew. Chem. Int. Ed.* **2011**, *50*, 2178-2182.
- [57] A. D. Yamaguchi, D. Mandal, J. Yamaguchi, K. Itami, *Chem. Lett.* **2011**, *40*, 555-557.
- [58] Z. Wang, K. Li, D. Zhao, J. Lan, J. You, *Angew. Chem. Int. Ed.* **2011**, *50*, 5365-5369.
- [59] C.-Y. He, Q.-Q. Min, X. Zhang, *Organometallics* **2012**, *31*, 1335-1340.
- [60] H.-Q. Do, O. Daugulis, *J. Am. Chem. Soc.* **2011**, *133*, 13577-13586.
- [61] Z. Ismagilov, S. Yashnik, M. Kerzhentsev, V. Parmon, A. Bourane, F. M. Al-Shahrani, A. A. Hajji, O. R. Koseoglu, *Catal. Rev. – Sci. Eng.* **2011**, *53*, 199-255.
- [62] a) Q. Wan, S. J. Danishefsky, *Angew. Chem. Int. Ed.* **2007**, *119*, 9408-9412. b) H. Rohde, O. Seitz, *Peptide Science* **2010**, *94*, 551-559. c) C. Walling, R. Rabinowitz, *J. Am. Chem. Soc.* **1957**, *79*, 5326.

- [63] a) L. Z. Yan, P. E. Dawson, *J. Am. Chem. Soc.* **2001**, *123*, 526-533. b) F. Mittendorfer, J. Hafner, *Surf. Sci.* **2001**, *492*, 27-33. c) H. Orita, N. Itho, *Surf. Sci.* **2004**, *550*, 177-184.
- [64] H. Zhu, W. Guo, M. Li, L. Zhao, S. Li, Y. Li, X. Lu, H. Shan, *ACS Catal.* **2011**, *1*, 1498-1510.
- [65] C. Morin, A. Eichler, R. Hirschl, P. Sautet, J. Hafner, *Surf. Sci.* **2003**, *540*, 474-490.
- [66] Ya. L. Gol'dfarb, B. P. Fabrichnyĭ, I. F. Shalavina, *Tetrahedron* **1961**, *18*, 21-36.
- [67] S.-y. Hayashi, Y. Inokuma, S. Easwaramoorthi, K. S. Kim, D. Kim, A. Osuka, *Angew. Chem. Int. Ed.* **2010**, *49*, 321-324.
- [68] a) L. W. Covert, H. Adkins, *J. Am. Chem. Soc.* **1932**, *54*, 4116-4117. b) R. Mozingo, *Org. Synth.* **1941**, *21*, 15. *Org. Synth. Coll. Vol. 3* **1955**, 181. c) H. Adkins, A. A. Pavlic, *J. Am. Chem. Soc.* **1947**, *69*, 3039-3041. d) H. Adkins, H. R. Billica, *J. Am. Chem. Soc.* **1948**, *70*, 695-698.
- [69] M. Raney, U.S. Patent 1628190, **1927**.
- [70] a) A. Fürstner, *Angew. Chem. Int. Ed.* **2000**, *39*, 3012-3043. b) S. J. Connon, S. Blechert, *Angew. Chem. Int. Ed.* **2003**, *42*, 1900-1923.
- [71] a) A. K. Chatterjee, R. H. Grubbs, *Angew. Chem. Int. Ed.* **2002**, *41*, 3171-3174. b) A. K. Chatterjee, *PhD thesis* **2002**, University of California. c) V. Thiel, M. Hendann, K.-J. Wannowius, H. Plenio, *J. Am. Chem. Soc.* **2012**, *134*, 1104-1114.
- [72] a) A. K. Chatterjee, T.-L. Choi, D. P. Sanders, R. H. Grubbs, *J. Am. Chem. Soc.* **2003**, *125*, 11360-11370. b) M. L. Macnaughtan, J. B. Gary, D. L. Gerlach, M. J. A. Johnson, J. W. Kampf, *Organometallics* **2009**, *28*, 2880-2887.
- [73] S. H. Hong, D. P. Sanders, C. W. Lee, R. H. Grubbs, *J. Am. Chem. Soc.* **2005**, *127*, 17160-17161.
- [74] G. W. Muller, W. E. Konnecke, A. M. Smith, V. D. Khetani, *Org. Pro. Res. & Dev.* **1999**, *3*, 139-140.
- [75] C. Ge, G. W. Muller, R. Chen, M. T. Saindane, Patent Application Publication, US2007/0004920 A1, **2007**.
- [76] G. W. Muller, R. Chen, M. T. Saindane, C. Ge, Patent US 2006/0052609A1, **2006**.
- [77] R. Castonguay, C. L. Herbet, J. W. Keillor, *Bioorg. Med. Chem.* **2002**, *10*, 4185-4191.
- [78] E. Kuehnel, D. D. P. Laffan, G. C. Lloyd-Jones, T. Martínez del Campo, I. R. Shepperson, J. L. Slaughter, *Angew. Chem.* **2007**, *119*, 7205-7208.
- [79] T. Nakamura, T. Noguchi, H. Kobayashi, H. Miyachi, Y. Hashimoto, *Chem. Pharm. Bull.* **2006**, *54*, 1709-1714.

- [80] S. G. Stewart, D. Spagnolo, M. E. Polomska, M. Sin, M. Karimi, L. J. Abraham, *Bioorg. Med. Chem. Lett.* **2007**, *17*, 5819-5824.
- [81] S. Keller, W. E. Keller, G. Van Look, G. Wersin, *Org. Synth. Coll. Vol. 7 1990*, 70-76; *Org. Synth.* **1985**, *63*, 160-166.
- [82] S. N. Devarakonda, S. R. Yarraguntla, V. K. Mudapaka, R. Kadaboina, V. Murki, A. Manda, V. R. Badisa, N. Vemula, R. S. R. Pulla, V. Nalivela, WO2009/114601 A2, PCT/US2009/036773, **2009**.
- [83] R. Rodebaugh, B. Fraser-Reid, H. M. Geysen, *Tetrahedron Lett.* **1997**, *38*, 7653-7656.
- [84] S. BouzBouz, R. Simmons, J. Cossy, *Org. Lett.* **2004**, *6*, 3465-3467.
- [85] J. A. Dean, *Lange's Handbook of Chemistry, 14th ed.*, McGraw-Hill, New York, **1992**.
- [86] J. N. Ngwendson, W. N. Atemnkeng, C. M. Schultze, A. Banerjee, *Org. Lett.* **2006**, *8*, 4085-4088.
- [87] A. H. Younes, L. Zhang, R. J. Clark, M. W. Davidson, L. Zhu, *Org. Biomol. Chem.* **2010**, *8*, 5431-5441.
- [88] J. C. Arnould, B. Delouvrié, P. Boutron, A. G. Dossetter, K. M. Foote, A. Hamon, U. Hancox, C. S. Harris, M. Hutton, M. Lamorlette, Z. Matusiak, *Bioorg. Med. Chem. Lett.* **2007**, *17*, 6448-6454.
- [89] J. Chao, A. G. Taveras, C. J. Aki, *Tetrahedron Lett.* **2009**, *50*, 5005-5008.
- [90] B. Trost, C. Müller, *J. Am. Chem. Soc.* **2008**, *130*, 2438-2439.
- [91] H. M. S. Kumar, B. V. S. Reddy, S. Anjaneyulu, J. S. Yadav, *Tetrahedron Lett.* **1998**, *39*, 7385-7388.
- [92] T. Mosmann, *J. Immunol. Methods* **1983**, *65*, 55-63.
- [93] J. Minami, S. Saito, T. Yoshida, T. Uemura, A. Okabe, *J. Gen. Microbiol.* **1992**, *138*, 1921-1927.
- [94] a) T. Matsumoto, N. Matsunaga, A. Kanai, T. Aoyama, T. Shioiri, E. Ōsawa, *Tetrahedron* **1994**, *50*, 9781-9788. b) T. Matsumoto, T. Aoyama, T. Shioiri, *Tetrahedron* **1996**, *52*, 13521-13524. c) T. Matsumoto, T. Aoyama, T. Shioiri, E. Ōsawa, *Tetrahedron*, **1994**, *50*, 9775-9780.
- [95] U.S. Department of Health and Human Services, Food and Drug Administration, Center for Drug Evaluation and Research, *Report to the Nation 2005 – Improving public health through human drugs*, Rockville, **2005**. Available at: <http://www.fda.gov/downloads/AboutFDA/CentersOffices/CDER/WhatWeDo/UCM078935.pdf>. Accessed on April **2012**.

- [96] Department of Economic and Social Affairs, *Consolidated List of Products Whose Consumption and/or Sale Have Been Banned, Withdrawn, Severely Restricted or not Approved by Governments*, 14. Issue, United Nations, New York, **2009**. Available at: <http://apps.who.int/medicinedocs/documents/s16779e/s16779e.pdf>. Accessed on April **2012**.
- [97] Y. Matsumura, Y. Satoh, K. Shirai, O. Onomura, T. Maki, *J. Chem. Soc., Perkin Transactions 1: Organic and Bio-Organic Chemistry* **1999**, *15*, 2057-2060.
- [98] M. Somei, Y. Karasawa, T. Shoda, C. Kaneko, *Chem. Pharm. Bull.* **1981**, *29*, 249-253.
- [99] a) J. V. Hay, G. Levitt, US 4,678,500, **1987**. b) G. W. Muller, D. I. Stirling, R. S.-C. Chen, Patent US 2002/0045643 A1, **2002**.
- [100] E. Schnabel, J. Stoltefuß, H. A. Offe, E. Klauke, *Liebigs Ann. Chem.* **1971**, *743*, 57-68.
- [101] J.-S. Kong, S. Venkatraman, K. Furness, S. Nimkar, T. A. Shepherd, Q. M. Wang, J. Aubé, R. P. Hanzlik, *J. Med. Chem.* **1998**, *41*, 2579-2587.
- [102] T. P. Johnston, C. L. Kussner, R. L. Carter, J. L. Frye, N. R. Lomax, J. Plowman, V. L. Narayanan, *J. Med. Chem.* **1984**, *27*, 1422-1426.
- [103] J. B. Zeldis, Patent US 2009/0163548 A1, **2009**.
- [104] A. García-Rubia, B. Urones, R. G. Arrayás, J. C. Carretero, *Chem. Eur. J.* **2010**, *16*, 9676.
- [105] J. Bergman, P. Sand, *Tetrahedron Lett.* **1984**, *25*, 1957-1960.
- [106] T. Nagasaka, Y. Koseki, *J. Org. Chem.* **1998**, *63*, 6797-6801.

8. Abbreviations

(Het)Ar	heteroarene or arene
$[\alpha]_{\text{D}}^{20}$	specific rotation at 589 nm and 20°C
Δ npsA	non-ribosomal synthesis mutant
AAHC	antibiotic associated hemorrhagic colitis
ab	absorption
ABPP	activity based protein profiling
Ac	acetyl
ACIB	Austrian Centre of Industrial Biotechnology
ACN	acetonitrile
Ad	adamantyl
AER	apical ectodermal ridge
AHC-6	antibiotic hemorrhagic colitis 6
AIBN	azobisisobutyronitrile
Amp	ampicillin
APT	attached proton test
Ar	aryl
BHI	brain heart infusion
Bn	benzyl
b.p.	boiling point
Boc	<i>tert</i> -butyloxycarbonyl
Boc ₂ O	di- <i>tert</i> -butyl dicarbonate
brine	saturated aqueous NaCl solution
bs	broad singulett (NMR)
Bu	butyl
c	concentration
calc.	calculated
CAM	cerammonium molybdate
CASO	Casein-Soja-Pepton-Agar
cat.	catalyst catalytic
Cbz	benzyloxycarbonyl

CCCP	compound-centric chemical proteomics
CDI	carbonyldiimidazol
CeMM	Research Center for Molecular Medicine
CM	cross-metathesis
cod	1,5-cyclooctadiene
conc	concentrated
COSY	correlated spectroscopy
CRBN	cereblon
Cul4	cullin 4
Cy	cyclohexyl
D	dimensional
d	day/s
	doublet (NMR)
D ₂ O	deuterated water
Da	dalton
DAD	diode array detector
db	double bond
DBPO	dibenzoylperoxide
DCC	<i>N,N'</i> -dicyclohexylcarbodiimide
DCE	dichloroethane
DCM	dichloromethane
dcype	1,2-bis-(dicyclohexylphosphino)ethane
dd	double doublet (NMR)
DDB 1	damage DNA binding protein 1
DEAD	diethylazodicarboxylate
dist.	distilled
DMA	<i>N,N</i> -dimethylformamide
DMAP	4-dimethylaminopyridine
DMF	dimethyl formamide
DMSO	dimethyl sulfoxide
DMSO-d ₆	fully deuterated dimethylsulfoxide
DNA	deoxyribonucleic acid
DPPA	diphenyl phosphorazidates

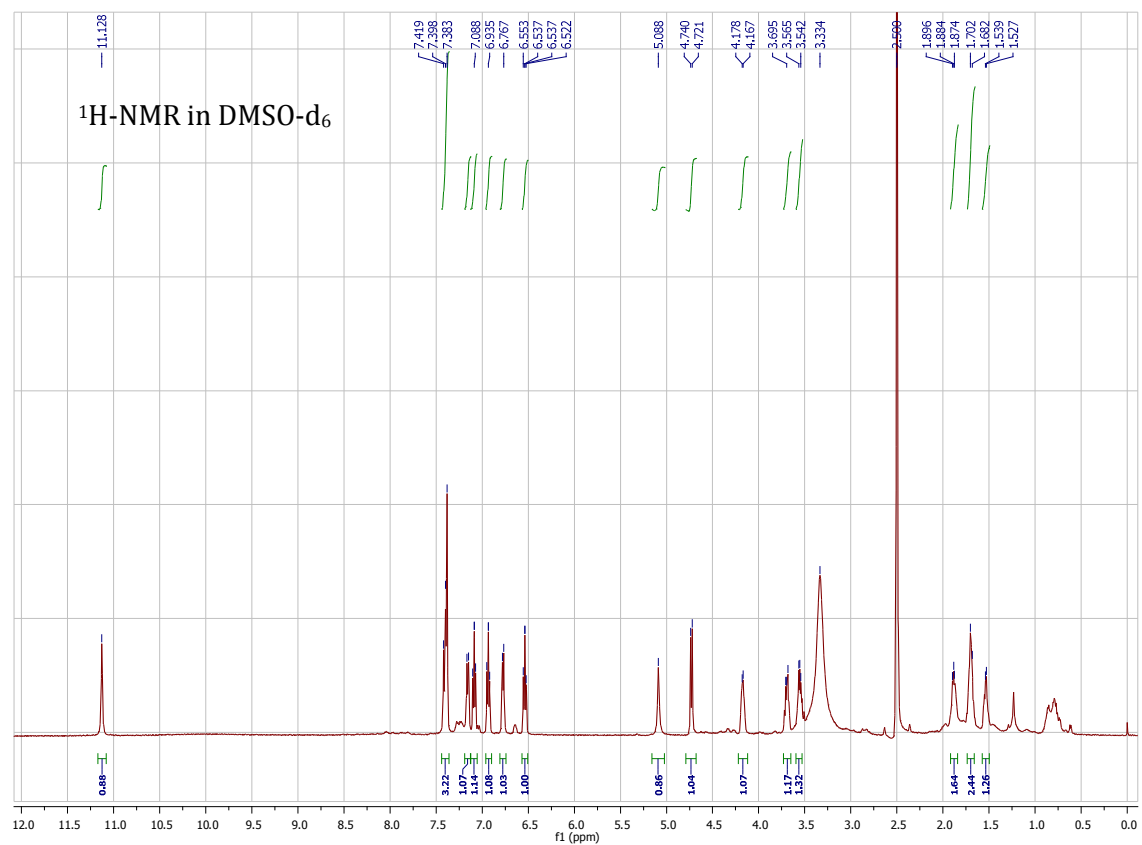
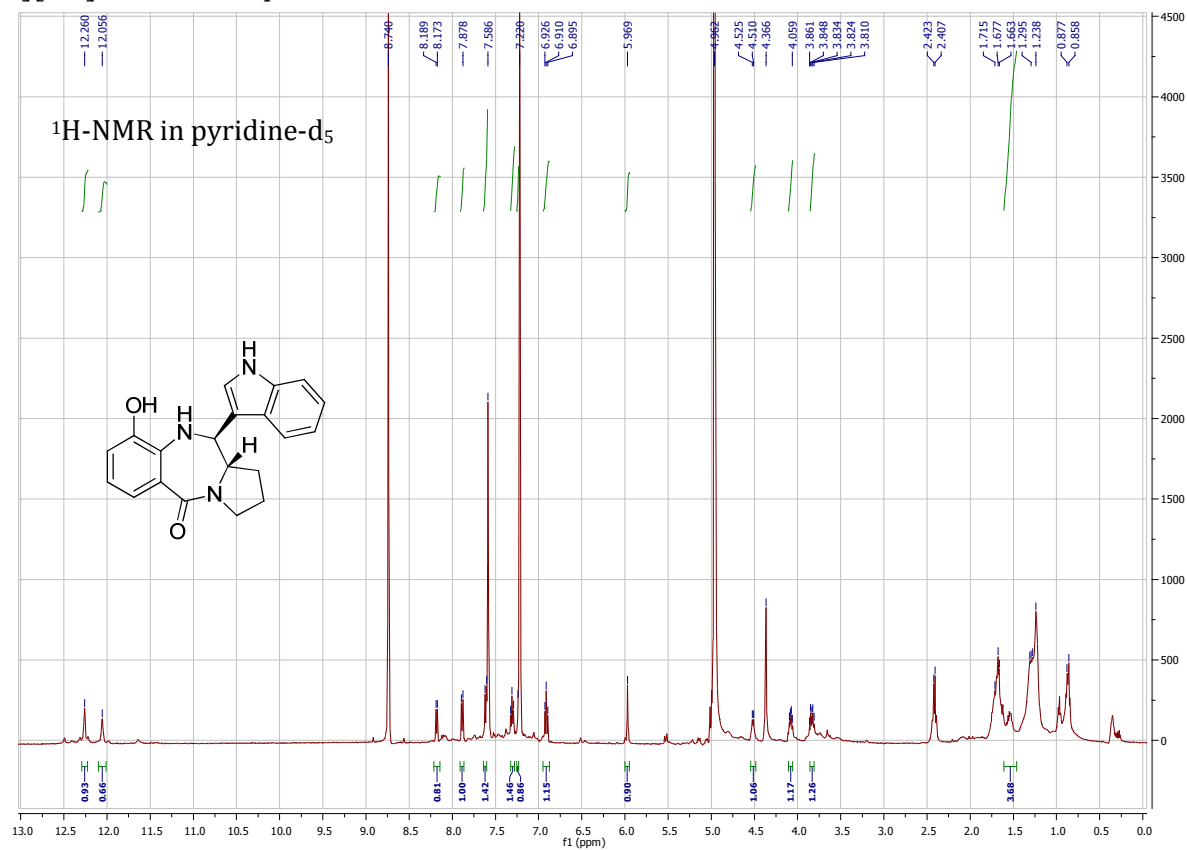
dppf	1,1'-bis(diphenylphosphino)ferrocene
DU	degree of unsaturation
<i>E</i>	orientation of substituents on the other side
e. g.	exempli gratia (for example)
EDC	1-ethyl-3-(3-dimethylaminopropyl)carbodiimide
EI	electron impact
em	emission
eq	equivalent/s
ESI	electrospray ionization
Et	ethyl
<i>et al</i>	<i>at alii</i> (and others)
exc	excitation
exp.	experimental
FG	functional group
FGF8	fibroblast growth factor 8
FT-IR	fourier-transform infrared spectroscopy
G	guanine
GC	gaschromatography
GMA	glycidyl methacrylate
h	hour/s Planck constant
HeLa	Henrietta Lacks cell line
HetAr	heteroarene
HMBC	heteronuclear multiple-bond correlation
HMQC	heteronuclear multiple quantum coherence
HOBt	hydroxy-benzotriazole
HPLC	high performance liquid chromatography
HRMS	high resolution mass spectrometry
HSQC	heteronuclear single-quantum correlation
i. e.	id est (that is)
i-FIT	isotopic fit
Ind	indometacin
IR	infrared

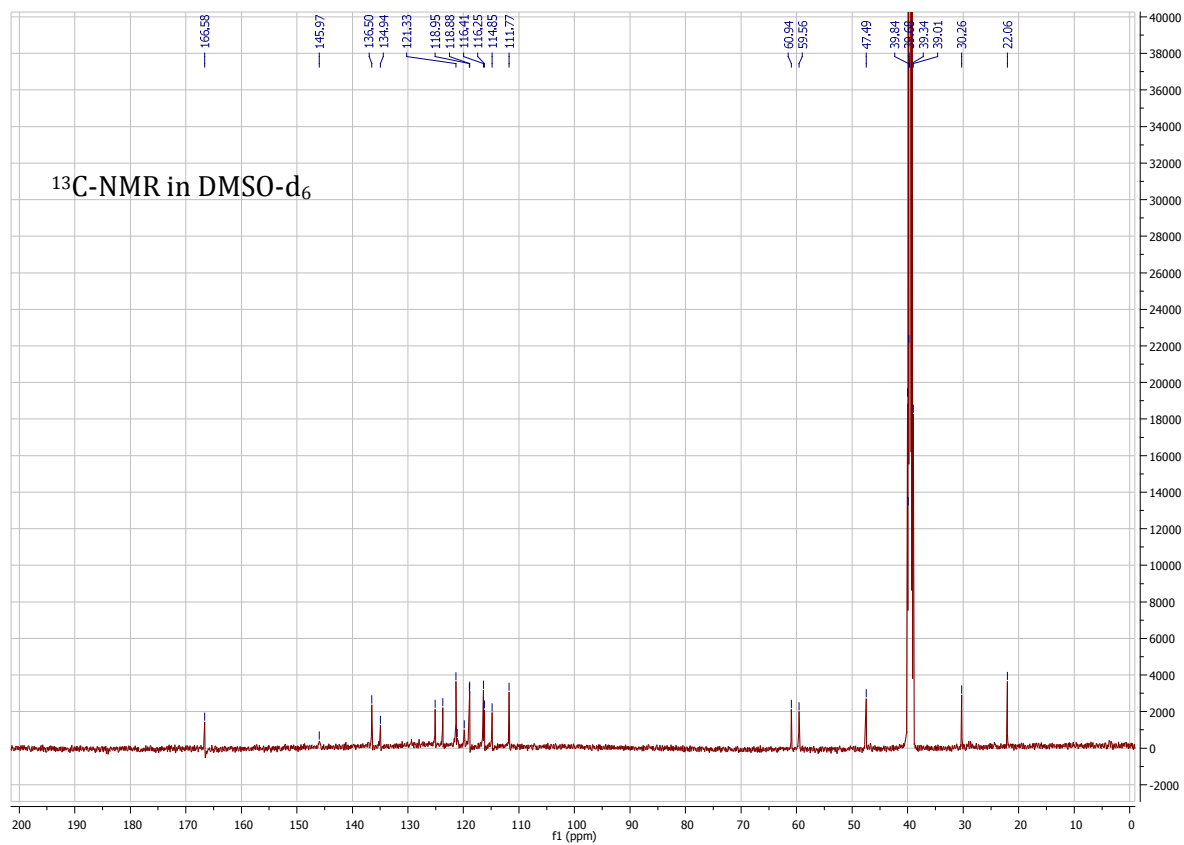
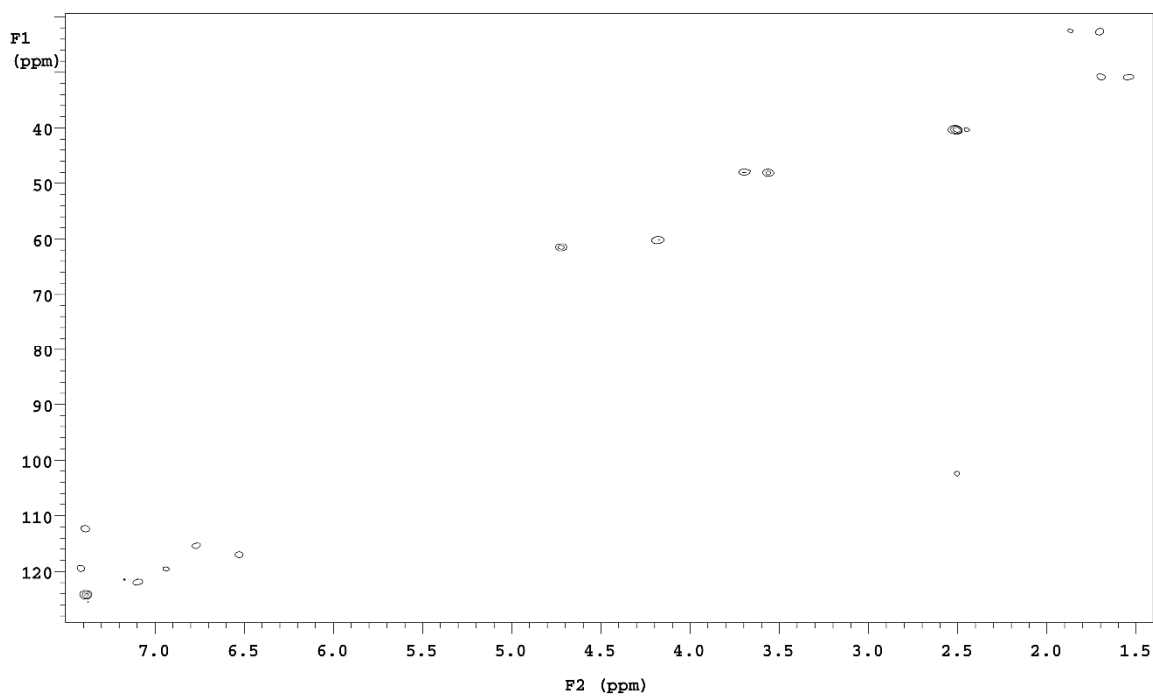
<i>J</i>	coupling constant
<i>K.</i>	<i>Klebsiella</i>
kbp	kilo-base pair
LC	liquid chromatography
lit.	literature
M	metal
	molar
	molecular mass
m	middle (IR)
	multiplet (NMR)
M.p.	melting point
<i>m/z</i>	mass-to-charge ratio
MS ₁	(1,3-bis(2,4,6-trimethylphenyl)-2-imidazolidinylidene)dichloro(2-(1-methylacetoxy)phenyl) methylenruthenium(II)
MALDI	matrix assisted laser desorption ionization
max	maximum
Me	methyl
min	minutes
MS	mass spectrometry
	molecular sieves
Ms	methanesulfonyl
MS/MS	tandem mass spectrometry
MSD	mass selective detector
MTT	(3-(4,5-dimethylthiazol-2-yl)-2,5-diphenyltetrazolium bromide
MW	microwaves
<i>n</i>	normal, straight-chain
NADH	nicotinamide adenine dinucleotide, reduced
NBS	<i>N</i> -bromosuccinimide
NMP	<i>N</i> -methyl-2-pyrrolidone
NMR	nuclear magnetic resonance
NOESY	nuclear overhauser effect spectroscopy
NRPS	nonribosomal peptide synthesis
O	oxidant

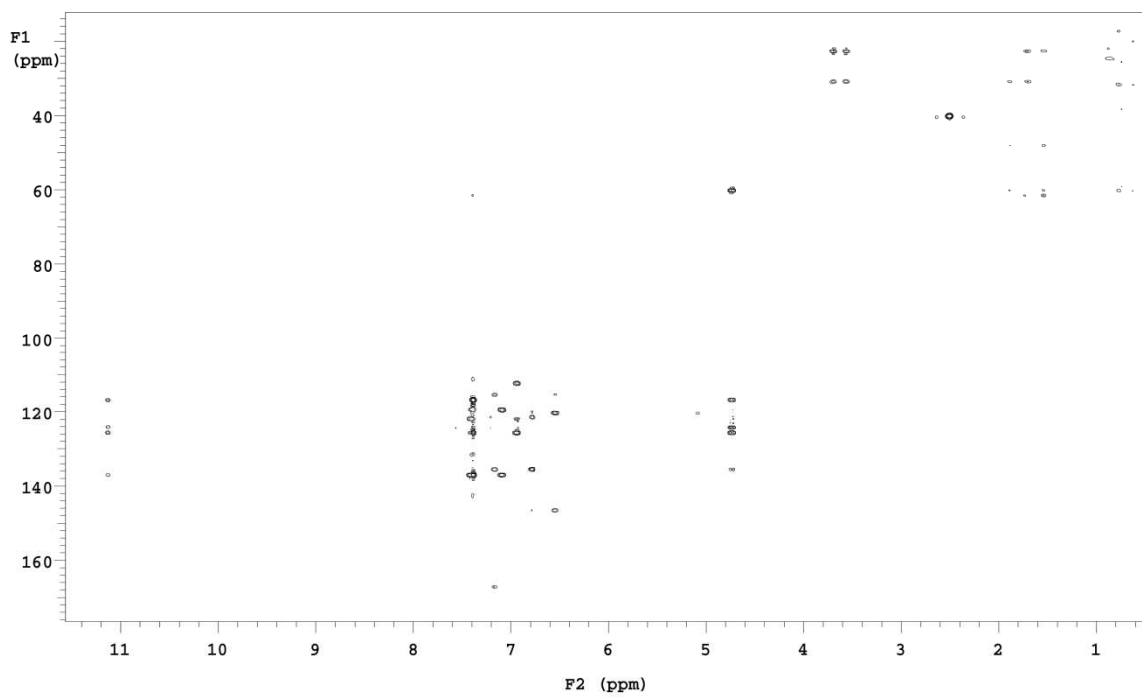
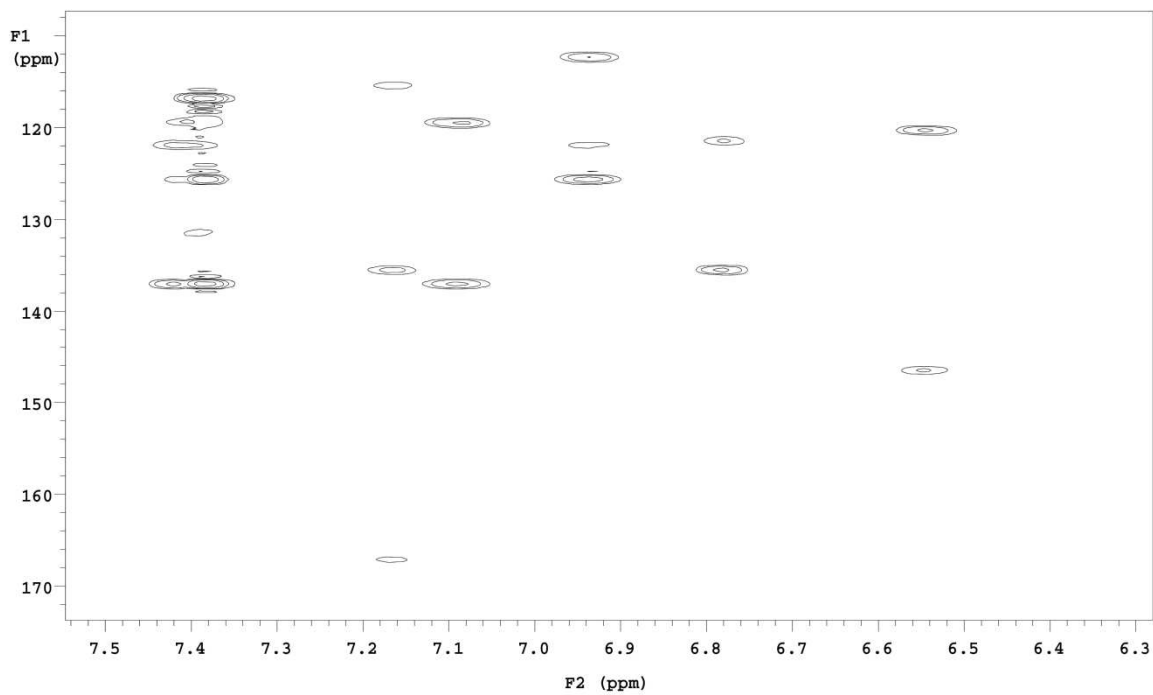
<i>o</i>	<i>ortho</i>
OPM-2	multiple myeloma cell line
p	pentet (NMR)
PBD	pyrrolobenzodiazepine
Pd/C	palladium on activated charcoal
PEG	polyethylene glycol
PG	protecting group
pH	negative logarithm of the molar concentration of hydronium ions
PHPLC	preparative high performance liquid chromatography
PivOH	pivalic acid
pK _a	logarithmic acid dissociation constant
PPh ₃	triphenyl phosphine
ppm	parts per million
psi	pound-force per square inch
PTLC	preparative thin layer chromatography
q	quadruplet (NMR)
R	residue
Raney-Ni	Raney Nickel
R _f	retardation factor
Roc1	regulator of cullins 1
rpm	rounds per minute
rt	room temperature
s	singlet (NMR) strong (IR)
S _E Ar	electrophilic aromatic substitution
Shh	sonic hedgehog homolog
SIM	single ion mode
<i>sp.</i>	<i>species</i>
t	time triplet (NMR)
<i>t</i>	<i>tertiary</i>
TCEP	tris(carboxyethyl)phosphine
TDM	thousand Deutschmark

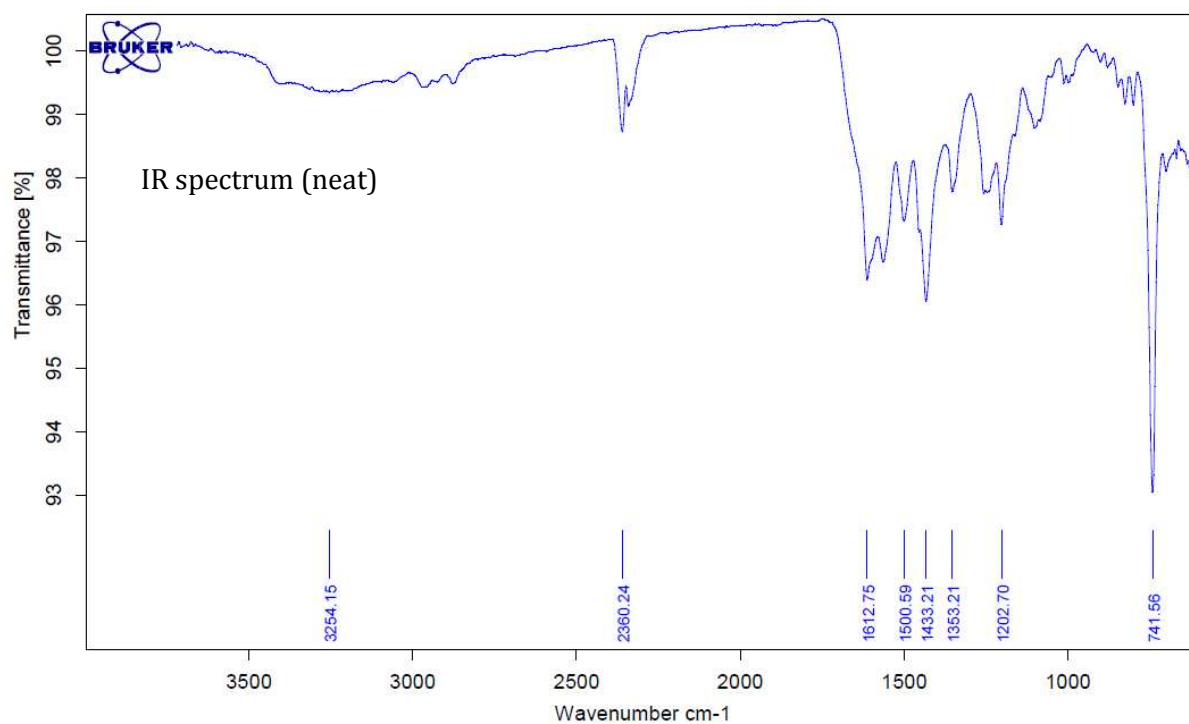
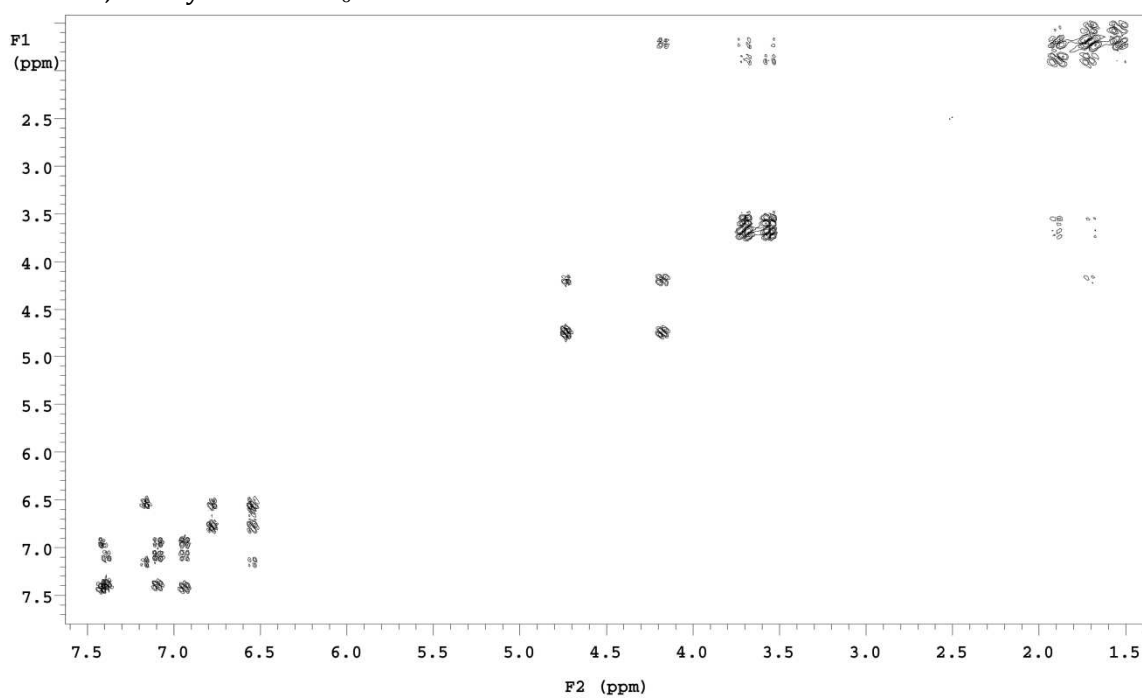
<i>tert</i>	<i>tertiary</i>
TFA	trifluoroacetic acid
THF	tetrahydrofuran
TLC	thin layer chromatography
TMS	trimethylsilyl
TOCSY	total correlation spectroscopy
TOF	time of flight
t_R	retention time
TsCl	<i>para</i> -toluenesulfonyl chloride
Ub	ubiquitin
UV	ultraviolet
V-50	2,2'-azobis(2-methylpropionamide) dihydrochloride
VA-044	2,2'-azobis(2-(2-imidazolin-2-yl)propan) dihydrochloride
var.	variety
w	weak (IR)
WT	wild type
X	halogen
X-Phos	2-dicyclohexylphosphino-2',4',6'-triisopropylbiphenyl
Z	orientation of substituents on the same side
ZPA	zone of polarizing activity
δ	chemical shift
λ	wavelength
ν	wavenumber

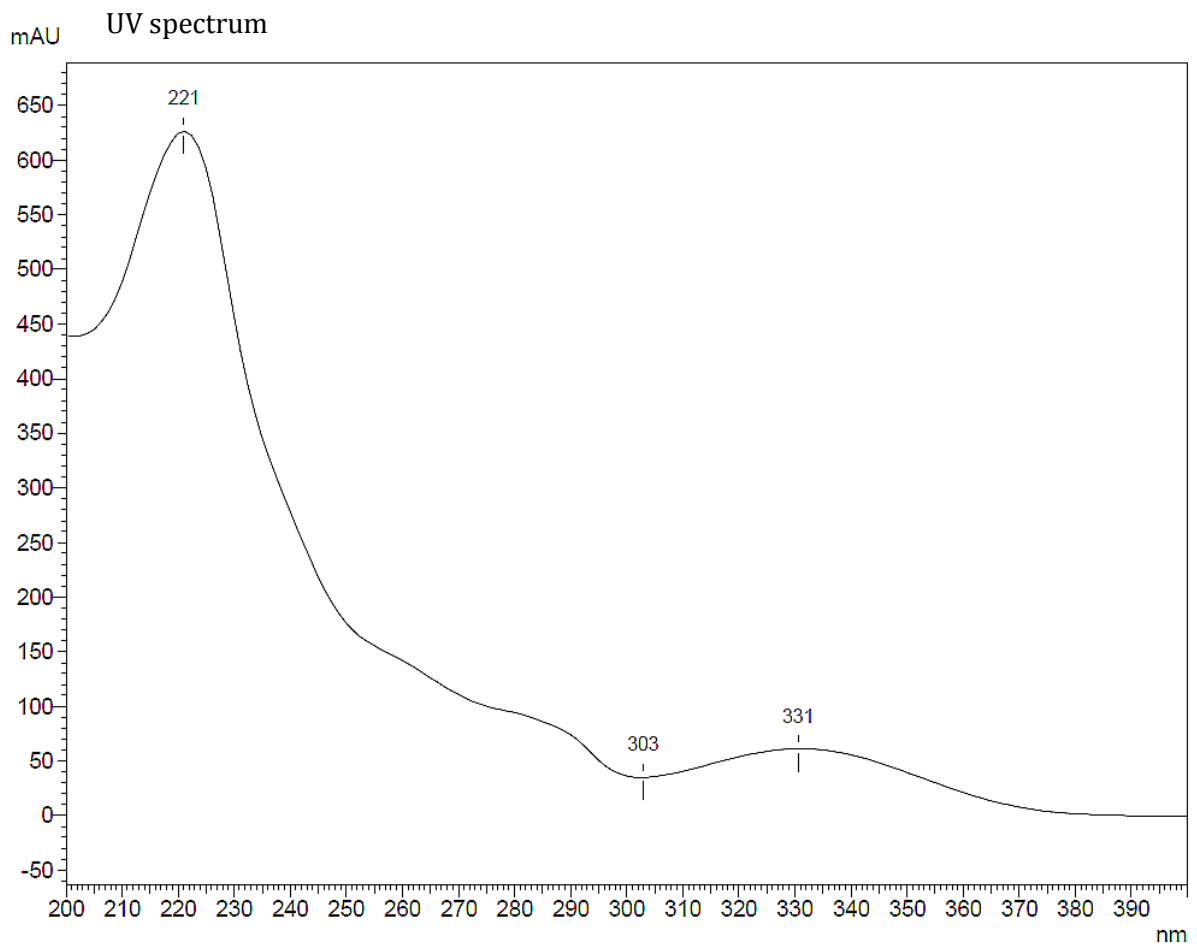
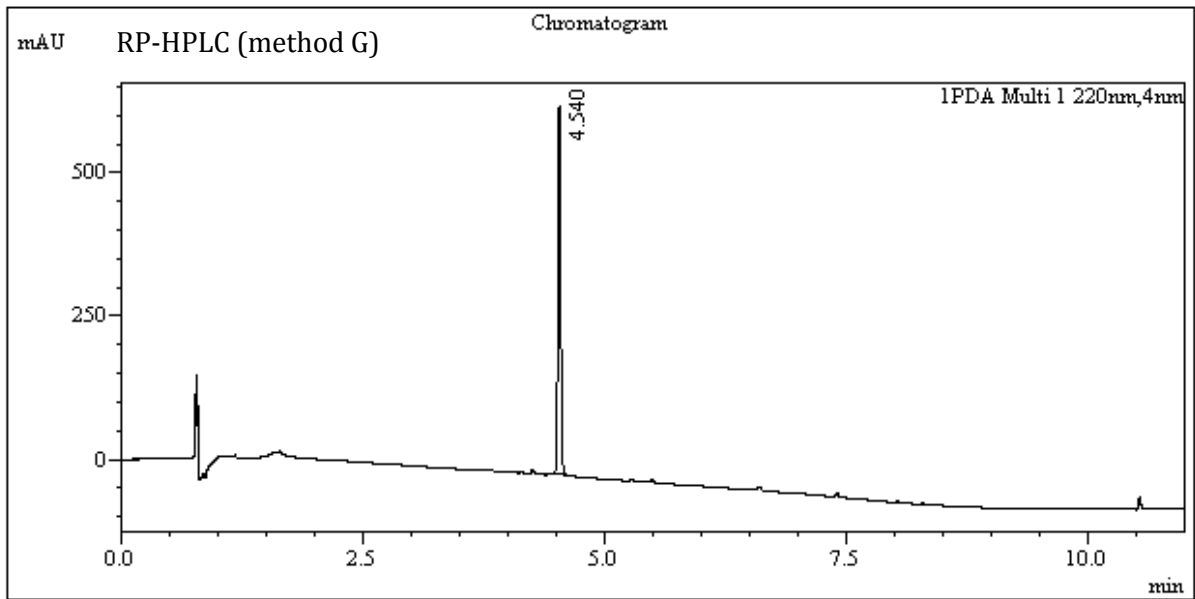
9. Appendix

(1*S*,11*aS*)-1,2,3,10,11,11*a*-Hexahydro-9-hydroxy-11-(1*H*-indol-3-yl)-5*H*-pyrrolo[2,1-*c*][1,4]benzo-diazepin-5-one **154**

HMQC in DMSO-d_6 

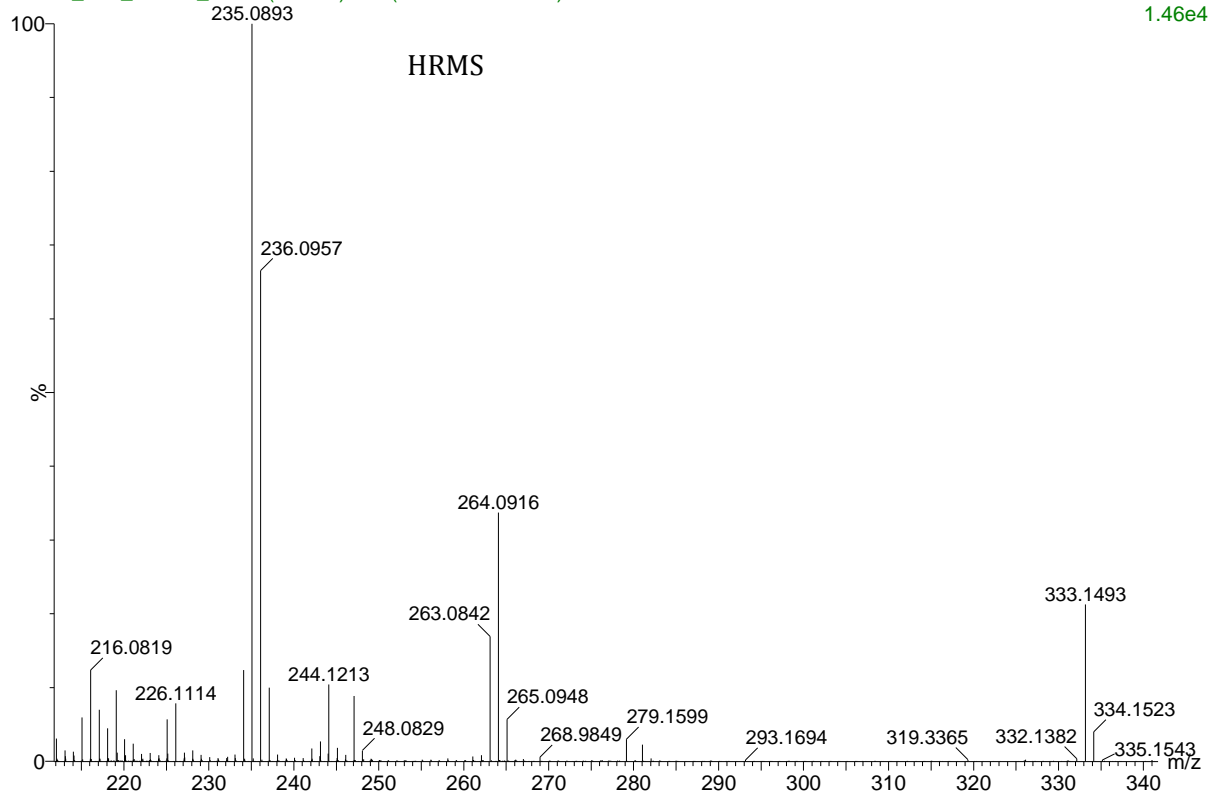
HMBC in DMSO-d₆HMBC in DMSO-d₆, aromatic region

H,H-Cosy in DMSO-d₆



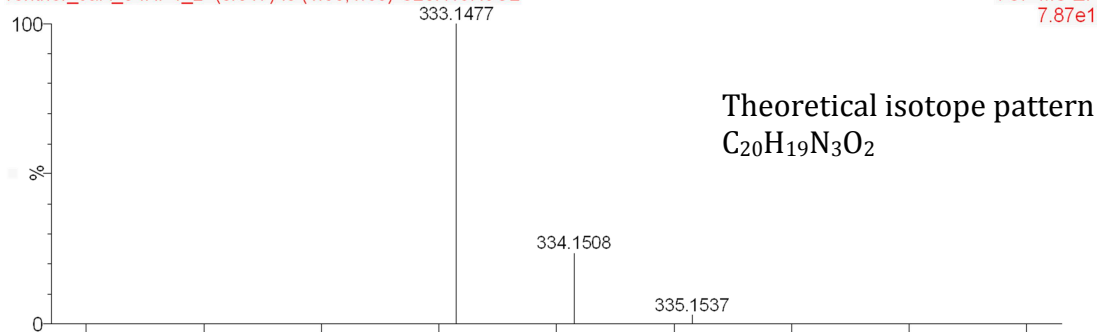
rentner_JaR_54NP1_2 730 (12.167) Cm (694:744-125:190)

TOF MS EI+
1.46e4



rentner_JaR_54NP1_2 (0.017) Is (1.00,1.00) C₂₀H₁₉N₃O₂

TOF MS EI+
7.87e12



rentner_JaR_54NP1_2 730 (12.167) Cm (694:744-125:190)

TOF MS EI+
3.10e3

